University of Greenwich
School of Science
Department of Pharmaceutical, Chemical and Environmental Sciences

Development of Novel Formulations for Mucosal Delivery of Protein Based Drugs

By

Isaac Ayensu
{BPharm, MSc (Pharmaceutical Analysis and quality control)}

Supervised by:

Dr. Joshua Boateng
Prof. John Mitchell

Thesis report presented in partial fulfilment of the requirement for the award of Doctor of Philosophy.

October, 2012

DECLARATION

"I certify that this work has not been accepted in substance for any degree, and is not concurrently being submitted for any degree other than that of Pharmaceutical sciences being studied at the University of Greenwich. I also declare that this work is the result of my own investigations except where otherwise identified by references and that I have not plagiarised the work of others".

……	……
ISAAC AYENSU (STUDENT)	DR. JOSHUA BOATENG (SUPERVISOR)
DATE:…….	DATE:…….....

ACKNOWLEDGEMENTS

First and foremost, I would like to take this opportunity to thank the almighty God for His loving kindness and faithfulness in sustaining my life all these years. I am nothing without you my Lord and saviour Jesus Christ. I love you with my heart, mind and soul.

Thanks to Dr. Joshua Boateng for your patience, understanding and guidance, not just as a supervisor but as a brother. You always knew what I needed and when. You understood the tension between family and school and never faltered. Thanks Boss. Prof. J. Mitchell, I greatly appreciate the fatherly manner you have guided me through my PhD experience. Thank you for being there when it mattered most. A big thank you to my research group members; Dr. Farnoosh Kianfar, Dr. Concetta Giovino and Mr. Harshavardhan Pawar for all your guidance and support. Harsh, thank you for your selfless help during the latter parts of my work. I am also grateful to Dr. Ian Slipper for all the SEM and XRPD techniques.

Thanks and love to Olivia my wife for representing constant love and support for the last 8 years of my life. I love you. Thanks to Irene and Kezia for your smiles and understanding of what it means when ‘daddy has to do his passion’ and for giving me the good reasons to stop when it was time to read the Bible, your story books and to listen to your readings. I have cherished every moment we’ve shared together as a family. You all deserve this PhD award and I therefore dedicate this piece of work to you; Olivia, Irene, Kezia and to our unborn child (Little Olivia).

I would want to thank my family and that of my wife for the inspiration and belief. I cannot fail to mention the spiritual support of friends at Kingdom Exchange Ministries. Pastor Emmanuel Oladipo and family, Dr. Bernasko and family, Mr. Josiah Reindorf and Family, Mr Kwarshie-Annang and Family, Mr. Emmanuel Asiedu, Mr. David Larkai and Miss Jemima Wiafe -thank you all for your care and encouragement.

Finally I would like to thank the Commonwealth Scholarships Commission for fully sponsoring the entire doctoral studies in addition to paying my stipend and family allowances. I am also grateful to the School of Science, University of Greenwich for the top-up bursary during the latter stages of my studies and KNUST for the study leave.

ABBREVIATIONS

ATR-FT-IR (attenuated total reflection-Fourier transform infra-red);

APR (aprotinin);

BSA (bovine serum albumin);

CD (circular dichroism);

DSC (differential scanning calorimetry);

DTT (dithiothreitol);

EDAC (N-(3-Dimethylaminopropyl)-N-ethyl carbodiimide hydrochloride);

EI (enzyme inhibitor);

GPC (gel permeation chromatography);

GSH (reduced glutathione);

HPLC (high-performance liquid chromatography);

ICH (International Conference on Harmonisation);

INS (insulin)

NaAc (sodium acetate);

NMR (nuclear magnetic resonance);

PAF (peak adhesive force);

PBS (phosphate buffered saline);

PE (permeation enhancer);

RH (relative humidity);

SEM (scanning electron microscopy);

TA (texture analyser);

TGA (thermo-gravimetric analysis);

TG (thioglycolic acid);

TWA (total work of adhesion);

XRPD (X-ray powder diffraction)

ABSTRACT

Stable mucoadhesive lyophilised chitosan and thiolated chitosan xerogels have been developed for potential delivery of proteins via the buccal mucosa. Membrane dialysis to eliminate sodium acetate (NaAc) and annealing during lyophilisation cycle (developed by differential scanning calorimetry; DSC) were critical for obtaining optimised porous xerogels. Based on characteristic performance and structural integrity, xerogels containing 10 % (per polymer weight) each of plasticizer (glycerol) and cryoprotectant (D-mannitol) were loaded with bovine serum albumin (BSA) and insulin (INS) as model drugs for further development. The optimised xerogels were loaded with enzyme inhibitor (EI) and permeation enhancer (PE) to enhance permeability of the buccal mucosa and backed with impervious ethylcellulose (EC) laminate to ensure unidirectional release. Characterisation of xerogels using ^{1}HNMR and ATR-FT-IR spectroscopy confirmed the functional groups in chitosan and TG-chitosan. The amount of thiol groups on TG-chitosan was quantified by Ellman's reaction with polymer molecular weight monitoring by gel permeation chromatography (GPC). The stability of the secondary structures of BSA and INS were by ATR-FT-IR and circular dichroism (CD) while xerogel crystallinity was examined by XRPD. SEM micrographs showed highly porous xerogels due to annealing which allowed for high drug loading and hydration capacities of the dialysed and annealed xerogels which also exhibited optimal moisture content for maintaining protein stability. Disulphide bond formation in thiolated xerogels however limited the hydration capacity. Storage at 25 °C/ 60 % RH for six months led to protein instability while storage at 5 °C maintained protein stability. 2% mucin concentration was found optimum for mucoadhesion studies of the chitosan based xerogels. EI (glutathione; GSH and aprotinin; APR) effect on mucoadhesion was concentration dependent and inhibitor specific. *In vitro* BSA release profiles from annealed xerogels were similar and significantly higher than non-annealed xerogels but were not affected by thiolation. Crystalline NaAc in the undialysed xerogel led to a three-fold reduction in BSA release. Significant reductions in BSA and INS release were also observed with the addition of EIs to TG-chitosan-BSA and TG-chitosan-INS xerogel respectively. The drug dissolution data from xerogels fitted best with model dependent First order, Hixson-Crowell and Korsmeyer-Peppas equations. Permeation studies' using EpiOral^{TM} showed 12- to 14-fold increase in BSA permeation but was reduced by GSH for both BSA and INS loaded xerogels. APR containing xerogel enhanced INS permeation through sheep buccal membrane and demonstrated a good linear correlation with EpiOral^{TM}. These results demonstrate the potential application of lyophilised chitosan and thiolated chitosan xerogels for buccal mucosa delivery of proteins with improved mucoadhesion, penetration enhancing and enzyme inhibition characteristics.

CONTENTS

TABLES

FIGURES

CHAPTER ONE

INTRODUCTION AND LITERATURE REVIEW

1.1 Overview

The buccal mucosa has received increased attention in recent years for the delivery of proteins and peptides as an alternative to the currently used parenteral route (Sudhakar *et al*., 2006). Although the buccal mucosa is limited by drug molecular size, hydrophobicity and low membrane permeability, chitosan and its thiolated derivatives have been identified to deliver proteins and peptides via this route because of their mucoadhesive, penetration enhancing and peptidase inhibition properties. Chitosan is a weak cationic polyaminosaccharide derived from deacetylation of the native polymer chitin (Wu *et al*., 2009), present in shellfish and was discovered 200 years ago (Muzzarelli *et al*., 2012). Chitosan is composed mainly of (1, 4) linked 2-amino-2- deoxy-β-D-glucan (Xu *et al*., 2007), and has been developed as a suitable matrix for the controlled release of protein or peptide drugs over the last two decades (Janes *et al*., 2001). Formulations with bioadhesive properties have been reported to offer certain advantages for mucosal drug delivery including prolonged residence time, ease of application (Lawlor *et al*., 1999; Jones *et al*., 2003) and controlled release of loaded drug.

The concept of mucoadhesion has gained significant interest in pharmaceutical technology over the past two decades and might provide opportunities for novel dosage forms, particularly useful for buccal drug delivery (Thanou *et al*., 2001). Chitosan exhibits mucoadhesive properties and is often used to enhance the residence time of drugs in the mucosal membrane thereby increasing drug bioavailability. The presence of hydrophilicity, functional amino groups, and a net cationic charge has made chitosan a suitable polymer for the ‘intelligent’ delivery of macromolecular compounds, such as proteins and genes. Large changes in functional properties such as swelling in response to small changes in environmental stimuli such as temperature, ionic strength, pH or light explain the intelligent properties of polymers. The ability of a polymer to respond to surrounding environment makes it attractive for use in controlling parameters such as mechanical properties, drug delivery and permeability (Martins *et al*., 2010).

Such intelligent properties of chitosan have been studied by Wu et al., (2006) when they developed a novel hydrogel composed of *N*-[(2-hydroxy-3-trimethylammonium) propyl] chitosan chloride (HTCC) and glycerophosphate (GP) with a thermo- sensitive sol-gel transition property at body temperature. The chitosan derivative incorporated drug as a stable solution at room temperature but transformed to a transparent hydrogel at body temperature

with pH-dependent swelling and drug release characteristics. At low pH, chitosan containing HTCC/GP hydrogel displayed increased hydrophilicity leading to polymer dissolution and consequent release of the entrapped drug. Furthermore, it has been shown that polymers (e.g. chitosan) with thiol groups (thiomers) exhibit much higher adhesive properties than other known mucoadhesive polymers. Sulfhydryl bearing agents can be covalently attached to their primary amino group via the formation of amide bonds where the carboxylic acid group of the ligand, such as thioglycolic acid (TGA) is conjugated with chitosan via the primary amino group, mediated by a water soluble carbodiimide (Kast & Bernkop-Schnürch, 2001). The improved mucoadhesive properties of thiolated chitosans are explained by the formation of stronger covalent bonds between thiol groups of the polymer and cysteine rich sub-domains of glycoproteins present in the mucus layer (Snyder *et al*., 1983; Leitner *et al*., 2003). Various factors that can alter the interaction between the polymer and the mucosal layer can affect the mucoadhesive property of a polymer. These include polymer molecular weight (Andrew *et al*., 2009; Tiwari *et al*., 1999), polymer concentration (Solomonidou *et al*., 2001) and method of drying.

Lyophilisation (freeze-drying) as a method of drying is preferred over others as it overcomes most of the limitations associated with formulation of protein-based products. Freeze-drying of formulations offers stable products, extends shelf-life, allows storage of products at room temperature instead of - 20 °C, avoids the complications of cold chain supply management, facilitates transportation of the products and increases patient compliance (Bunte *et al*., 2010). During freezing, or even storage however, a number of small molecule drugs and excipients tend to undergo incomplete or delayed crystallization resulting in the formation of mixtures of different polymorphic forms or vial breakage as in the case of the cryoprotectant mannitol (Kim *et al*., 1998; Liao *et al*., 2007). Such processes may cause reproducibility and product characterization problems. It is therefore critically important that the selection of conditions during the freezing step in a lyophilisation cycle be informed by knowledge from investigating potential for freeze induced damage, product characteristics and the attainment of product stability. Annealing as a process step may be employed to maintain samples at a particular temperature below the equilibrium freezing point but above the glass transition temperature for a specified period of time. The goal is to facilitate crystallization of the active ingredients and the cryoprotectant and to improve the pore size distribution of ice crystals as in Ostwald ripening (Schwegman, 2009a). Jiang *et al*., (2007) observed that mannitol based formulations sometimes caused vial breakage during early primary drying due mainly to moderate to fast freezing rates (when the mannitol remains amorphous), high fill volume and high total solid content of mannitol in the formulation. The

freezing rate at the start of a lyophilisation cycle can be critical with respect to phase separation and concentration gradients in the mould because it can yield more dense layers at the top of the cake, forming a barrier for water transport. However, fast freezing does result in significant morphological changes such as smaller pore diameter and altered surface structure of the cake (Seales, 2000; Gieseler, 2004) and could impose higher resistance to mass flow during primary drying of samples. In addition, knowledge of such properties is of value in predicting the final properties of the formulation including physical appearance and drug release characteristics.

This thesis reports on the formulation design, optimisation and characterisation of the physico-chemical properties of freeze dried chitosan and thiolated chitosan xerogels as potential protein drug delivery systems to the buccal mucosa membrane. Background to mucosal drug delivery and their advantages and challenges as well as the prospects of protein delivery via the buccal route has been critically reviewed. The weight average molecular weights (MW) of natural (chitosan) and synthesized (TG-chitosan) polymers were monitored with gel permeation chromatography (GPC) and chemical structures confirmed with proton nuclear magnetic resonance (^{1}HNMR) and attenuated total reflection Fourier transform-infrared spectroscopy (ATR-FT-IR). Differential scanning calorimetry (DSC) has been used in the preliminary formulation studies to develop an appropriate lyophilisation cycle incorporating an annealing step. The physical characterisation data obtained were used to compare formulations containing different amounts of glycerol (GLY) (plasticizer) and mannitol (MANN) (cryoprotectant) and also to select the most appropriate formulation for further development. The optimised xerogels have been characterised for moisture content, drug loading capacity, mucoadhesion properties, crystallinity and microscopic structure using thermo-gravimetric analysis, Bradford's assay, texture analysis, x-ray powder diffraction (XRPD) and scanning electron microscopy (SEM) respectively. The effect of the process of annealing on the hydration capacity, mucoadhesion properties, microscopic structure and the release profile of Bovine serum albumin (BSA) loaded in the optimised freeze-dried chitosan and thiolated chitosan formulations were studied. The effect of membrane dialysis on the characteristics of chitosan based lyophilised xerogels, as well as the hydration capacity with or without a reducing agent dithiothreitol, was investigated. In addition, the effect of different enzyme inhibitors as well as a permeation enhancer on xerogel characteristics was studied. Permeability and accelerated/real -time stability profile of BSA were studied with Epi-oral^{TM} tissue construct and UV spectrophometry respectively. Furthermore the optimised novel delivery system was loaded with human insulin (INS) as a model therapeutic protein, an enzyme inhibitor and permeation enhancer and characterised for *in vitro* release and *ex vivo*

permeability using sheep buccal tissue which was correlated with Epi-oral™ characterisation. Accelerated and real-time stability evaluation of the INS containing xerogels was determined by high-performance liquid chromatography (HPLC). The conformational stability of the protein drugs was studied with circular dichroism (CD) and attenuated total reflection Fourier transform infrared (ATR-FT-IR) spectrophotometry.

1.2 Protein structure and aggregation

Every protein molecule has a characteristic three-dimensional shape (Jankowska *et al*., 2012), or conformation. For example, fibrous proteins, such as collagen and keratin, consist of polypeptide chains arranged in roughly parallel fashion along a single linear axis, thus forming tough, usually water-insoluble, fibres or sheets. Because the physiological activity of most proteins is closely linked to their three-dimensional architecture, specific terms are used to refer to different aspects of protein structure. The term primary structure denotes the precise linear sequence of amino acids that constitutes the polypeptide chain of the protein molecule. The physical interaction of sequential amino-acid subunits results in a so-called secondary structure (Song *et al*., 2012), which can either be a twisting of the polypeptide chain approximating a linear helix (α-configuration), or a zigzag pattern (β-configuration). Most globular proteins also undergo extensive folding of the chain into a complex three-dimensional geometry designated as tertiary structure (Eyrich *et al*., 1999). Two or more polypeptide chains that behave in many ways as a single structural and functional entity are said to exhibit quaternary structure. The separate chains are not linked through covalent chemical bonds but by weak forces of association. The native state describes the precise three-dimensional structure of a protein molecule and appears, in almost all cases, to be required for proper biological function. If the tertiary or quaternary structure of a protein is altered, e.g., by such physical factors as extremes of temperature, changes in *p*H, or variations in salt concentration, the protein is said to be denatured and usually exhibits reduction or loss of biological activity.

Aggregation is a general term that encompasses several types of interactions or characteristics (Cromwell *et al*., 2006). Protein aggregates can arise from several mechanisms and may be classified in numerous ways, including soluble/insoluble, covalent/noncovalent, reversible/irreversible, and native/denatured. For protein therapeutics, the presence of aggregates of any type is considered to be undesirable because of concerns that such

aggregates may lead to an immunogenic reaction (small aggregates) or may cause adverse events on administration (Cromwell *et al*., 2006). There are clear guidelines and limitations on the number of particles ≥ 10 μm and ≤ 25 μm in size that may be present in pharmaceutical preparations (US Pharmacopeia, 2006). However, the levels of soluble aggregates such as dimers and trimers that are acceptable are not well defined. There are many types of interactions and environmental factors that can lead to protein aggregation, (Chi *et al*., 2003). Solution conditions such as temperature, protein concentration, pH, and ionic strength may affect the amount of aggregates observed. In addition, the presence of certain ligands, including specific ions such as calcium and magnesium (Zhu & Damodaran, 1994) may enhance aggregation. Further, stresses to the protein such as freezing, exposure to air, or interactions with metallic surfaces and mechanical stresses may result in surface denaturation which then leads to the formation of aggregates. Each of these environmental factors is typically encountered during bio-processing and formulation. Wang, (2000) observed that stresses associated with freezing can damage sensitive molecules including proteins. It is therefore critically important that the thermal treatment during a freeze drying cycle should be understood by preliminary investigations to determine the potential for freeze induced damage.

1.2.1 Use of proteins as therapeutic agents

The high prevalence of chronic non communicable diseases such as cardiovascular related conditions, diabetes, cancer and the rising number of ageing adults in the population have resulted in significant increase in protein therapeutics due to their important role in the development of current treatment options. Consequently, protein based pharmaceuticals has attracted many large and small biopharmaceutical and biotechnological industries, making protein therapeutics one of the fastest growing global emerging markets. According to the Global Protein Therapeutics Market Analysis, for 2011-2013, the pharmaceutical biotechnology market is expected to grow at an astounding Compound Annual Growth Rate (CAGR) of about 12 % (Szlachcic, *et al*., 2011) as a result of improved investment, production and subsequent marketing of novel protein therapeutics. Furthermore, the expiration of patents of many top biotech industries will strengthen the growth of the global protein market as they would now turn to the expected large number of generic biotech products, estimated to be a multi-billion dollar market.

1.2.2 Model protein drugs

Two model drugs representing small to medium sized endogenous proteins naturally present in the body were selected for this research; the well-studied and characterised albumin and insulin, one of the first biotechnologically derived protein therapeutic drugs and commonly used clinically.

1.2.2.1 Bovine serum albumin (BSA)

Serum albumins are the most abundant blood plasma proteins, corresponding to a concentration of 4.2 % $^{w}/_{v}$ and accounts for up to 60 % of the body's total protein. Albumins also provide approximately 80 % of the blood's osmotic pressure (Carter & Ho, 1994 cited in Gelamo *et al*., 2002). A number of diverse biochemical, biophysical and physicochemical studies have employed albumins as model proteins due to their ability to bind to a variety of hydrophobic substrates including anaesthetics, bilirubin, lysolecithin, steroids, tryptophan and several dyes (Curry *et al*.,1998; Narazaki *et al.*, 1997; Chadborn *et al*., 1999; Reynolds *et al*., cited in Gelamo *et al*., 2002). A single chain of about 580 amino acid residues constitute the primary structure while the secondary structure is composed of 67 % α-helix with 6 turns and 17 disulphide bridges which are located nearly exclusively between the helical segments (Carter & Ho., 1994; Narazaki *et al*., 1997, cited in Gelamo *et al*., 2002).

These disulphide bonds are inaccessible to reducing agents in the pH range of 5-7, but become progressively available at lower or higher pH. The three-dimensional structure of serum albumin is composed of three homologous domains namely; I, II and III based on crystallographic determination, conferring a heart shaped molecular form to the protein (He & Carter, 1992, cited in Gelamo *et al*., 2002). The domains are further divided into sub-domains: IAB, IC; IIAB, IIC; IIIAB and IIIC respectively (Figure. 1.1).

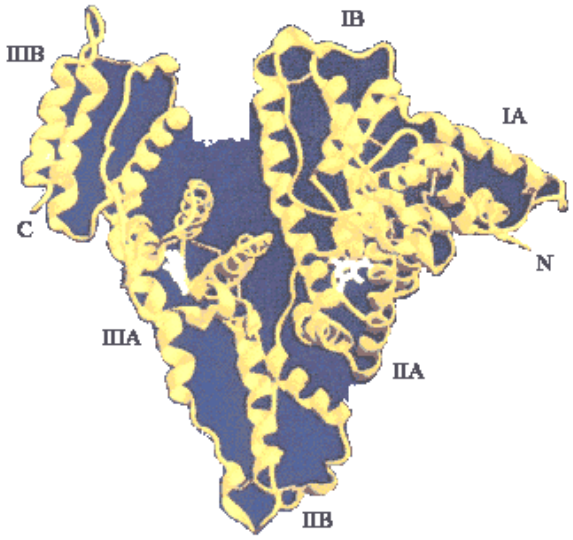

Figure 1.1: Molecular model of serum albumin. Available at <http://www.friedli.com/research/PhD/bsa/fig53.gif> [Accessed; 25/04/12]

A number of features such as basic amino acid residues, hydrophobic phase and proline residues at the tips of the loops, are shared by the sub-domains, however, each sub-domain is unique and may show a certain degree of specificity. Bovine serum albumin (BSA) shares 76 % sequence identity and same molecular weight (67 kDa) with human serum albumin (HSA) (Peters, 1985; Carter & Ho, 1994, cited in Gelamo *et al*., 2002). Two tryptophan residues (W131 and W214) are found in BSA while only one (W124) is found in HSA. Spectroscopically, the additional tryptophan has been proposed to lie close to the surface of the α-helix of the first domain of the BSA molecule (Carter & Ho, 1994, cited in Gelamo *et al*., 2002). Changes in pH result in reversible conformational isomerization as summarised in Table 1.1 below.

Table 1.1: Relationship of isomeric forms of bovine serum albumin (Forster, 1977).

	E	<---->	F	<---->	N	<---->	B	<---->	A
pH of transition		2.7		4.3		8		10	
Name	Expanded		Fast		Normal		Basic		Aged
% helix	35		45		55		48		48

<----> shows the transition from one isomeric form of BSA to the other based on pH.

BSA foams by diffusing into the air-water interface in solution with subsequent reduction in surface tension. Partial unfolding and association occurs resulting in an intermolecular cohesive film. Improvement in foam expansion and stability is achieved by BSA interaction with clupeine (Poole *et al*., 1984). Gelation of the protein follows a two step process of initial unfolding or dissociation and a subsequent aggregation step resulting in gel formation under suitable conditions. The heating of BSA results in the formation of soluble aggregates, through non-covalent and disulphide bonds, which leads to the formation of a gel. Albumin binds reversibly with a wide range of ligands serving as the principal carrier for insoluble fatty acids in plasma circulation. Oxidation of approximately 30 % of free sulphydryl Cys-34 in circulating plasma is by glutathione and cysteine (Peters, 1985).

1.2.2.2 Insulin (INS)

Insulin (INS) is a polypeptide hormone which regulates carbohydrate metabolism and produced in the Islets of Langerhans in the pancreas. As a primary effector in carbohydrate homeostasis, INS also partakes in fat and protein metabolism. Clinically, INS is used in some forms of diabetes mellitus. While Type 1 diabetes mellitus patients depend on injected exogenous INS for survival, Type 2 diabetes patients occasionally require INS administration in addition to adequate medication to control blood glucose level.

Chemical structure: The chemical structure of INS varies slightly between species however, porcine INS is similar in composition to human INS. The empirical formula of the protein is $C_{254}H_{377}N_{65}O_{75}S_6$ with a molecular weight of approximately 6,000. INS is synthesised from a single chain precursor, proinsulin. Proteolysis removes 4 basic amino acids and the remaining connector or C peptide to convert human proinsulin to INS which consists of two chains of A (acidic, consisting of 21 amino acids with glycine at the amino terminal residue) and B (basic, consisting of 30 amino acids with phenylalanine at the amino terminus) amino acids linked together by two disulphide bonds (Figure 1.2 (i) and (ii)). INS may exist as a monomer (biologically active), dimer or hexamer. The hexamer has two molecules of coordinated Zn^{2+} and is stored as granules in the beta cell. Porcine INS differs from that of humans only by the substitution of threonine by alanine residue in the B chain at the carboxyl terminus. Bovine INS, however, differs by three amino acid residues, making it more antigenic.

One of the greatest milestones in medical history was the discovery of INS which has revolutionised proteins and peptides as useful therapeutic agents. Until the recent breakthrough in biotechnology for the production of human INS in satisfactory quantities, INS products from different animal sources such as bovine and porcine were used for over six decades.

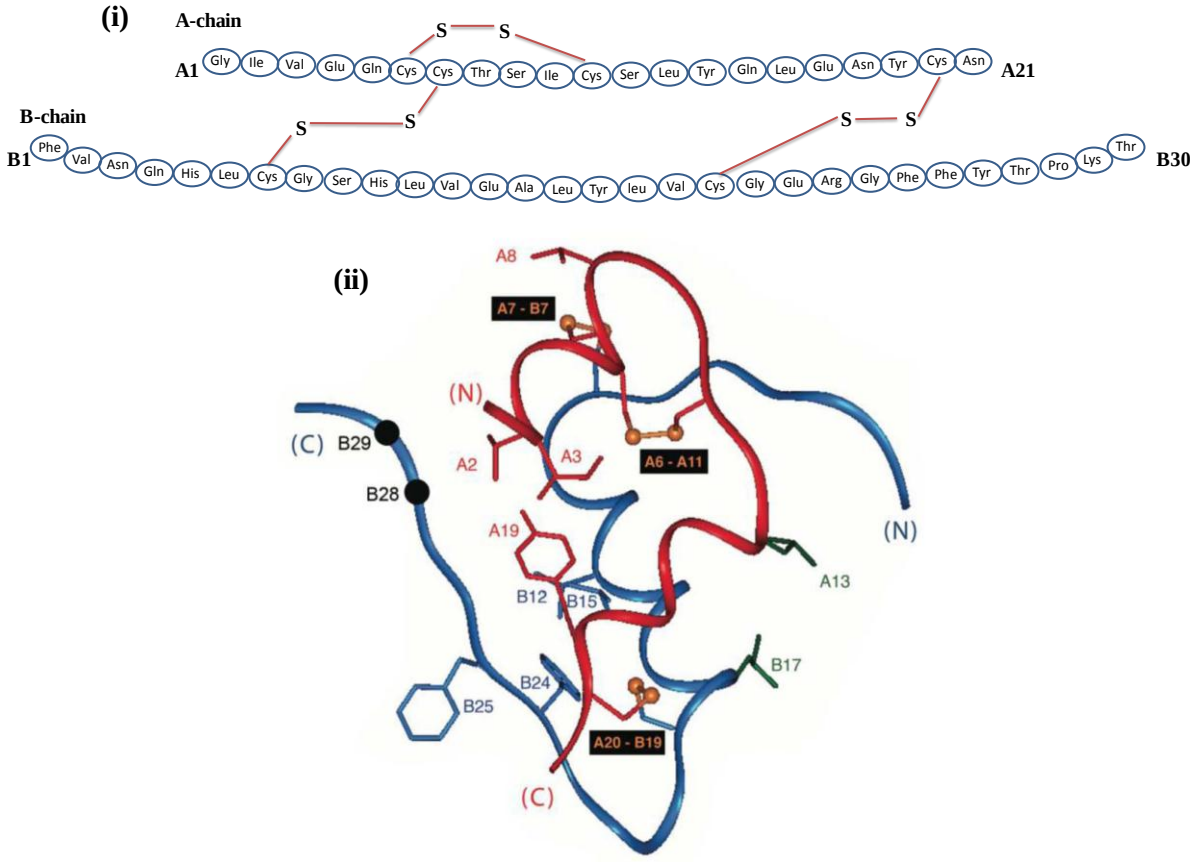

Figure 1.2: Structure and amino acid sequence of INS; **(i)** Sequence of human insulin with the A chain above and the B chain beneath. Cysteines forming disulphide linkages are indicated with bars. **(ii)** Ribbon model of INS. The A-chain is indicated in red, and the B-chain with blue. Disulphide bridges are shown by gold spheres (sulphur atoms); pairings are indicated in black boxes. Black spheres show Cα carbons of the residues (Adapted from T-state protomer; Protein Data bank access ion code 4 INS; Baker *et al*., 1988, cited in Hua *et al*., 2011).

Currently, research is focussed on developing non-invasive INS delivery systems with various technologies (see Table 1.2) at different stages of development. With over 22,000 published articles and 300 patents on non-invasive INS delivery, clinical application still remains an elusive goal despite the exploration of different approaches (Mukhopadhyay *et al*.,

2012). Treatment and management of diabetics using INS still relies on subcutaneous injections with the added complexities of needles, syringes and vial system that hinder patient compliance.

Table 1.2: Transmucosal routes of insulin delivery systems. Adapted from Khafagy *et al*., (2007).

Administration route	Delivery system	Model	Results
Buccal	Insulin solution/lysalbinic acid	Hamster cheek pouch	Significantly increased insulin permeability
	Deformable lipid vesicles	Rabbits	BR was 19.78 %
Nasal	Nasal powder formulation	Rabbits	BA was 11.1 %–22.4 %
	Insulin–chitosan powder	Sheep	BR was 17 %
	Chitosan–TBA–insulin microparticles	Rats	BA was 7.24 %
Pulmonary	Insulin microcrystals/Zn^2+	Rats	17 % reduction in blood glucose levels
	Insulin PLGA nanospheres	Guinea pigs	Long-lasting hypoglycaemic response
Ocular	Insulin solution/alkylglucosides	Rats	Significantly stimulated systemic insulin absorption
	Gelfoam® ocular device	Rabbits	60 % reduction in blood glucose levels over 8h
Rectal	Insulin suppositories/Witepsol W35, SDC, SC, STDC or STC	Dogs	PA was 50 %
	Insulin glycerol–gelatin suppositories/snail mucin	Rats	44 % reduction in blood glucose levels within 2h

Abbreviations: BR, relative bioavailability; BA, absolute bioavailability; SDC, sodium deoxycholate; chitosan–TBA–insulin, chitosan–4-thiobutylamidine insulin conjugate; PA, pharmacological availability; PLGA, poly(lactide-co-glycolide); STC, sodium taurocholate; SC, sodium cholate; STDC, sodium taurodeoxycholate

Delivery systems such as liposomes, liquid emulsions, pro-drugs, polymer-inhibitor conjugates and nanocapsules have been investigated for non-invasive INS delivery with

limited success. INS released in a pulsatile manner in response to blood glucose levels from intelligent stimuli-responsive delivery systems such as hydrogels have also been investigated. The development of poly(methacrylic acid-*g*-ethylene glycol) hydrogels with Ca^{2+} deprivation ability, mucoadhesive characteristics and sensitve pH-dependent (Wood *et al*., 2010) release led to approximately 10% pharmacological availability of orally administered INS (Morishita *et al*., 2006).

Insulin delivery via the buccal mucosa is an interesting approach that will be explored in this research, where the drug delivery system has been designed to achieve increased mucoadhesion, permeation enhancement and enzyme inhibition using chitosan and thiolated chitosan lyophilised xerogels, to overcome the limitations of protein transport across the buccal mucosa.

1.2.3 Protein delivery and challenges

The parenteral route (injection) has for decades been the major means for the systemic delivery of protein and peptide drugs but is limited by the problem of pain associated with injections. Although current technological advancements has led to the use of micro-needles that are virtually pain-free, there still remains the challenge of high injection frequency, site reactions (irritiations) (Kenndy, 1991, cited in Khafagy *et al*., 2007) and consequent patient non-compliance. These have necessitated the need to focus research on alternative non-invasive routes for the delivery of protein and peptide drugs (Figure 1.3).

However, these potential routes are fraught with their own challenges. Most proteins and peptides have shown poor bioavailability of the order of less than 1 % when delivered via the nasal route (Deurloo *et al.,* 1989). Limiting factors such as enzymatic inhibition in the GIT and at mucosal sites, hepatic first pass metabolism, size exclusion at epithelial barriers and cellular transport pathways are still a huge challenge for the pharmaceutical industry. In addition, these hydrophilic biopharmaceuticals may also be unstable and prone to modification or degradation due to extreme changes in the pH of the local environment as encountered in nasal delivery (Lee, 1988). In developing alternative protein/peptide delivery systems with high bioavailability, modification of the physicochemical properties of macromolecules, addition of novel functions to these macromolecules and the use of improved delivery carriers have been found essential for the maintenance of the biological activity of the proteins (Morishita & Peppas 2006).

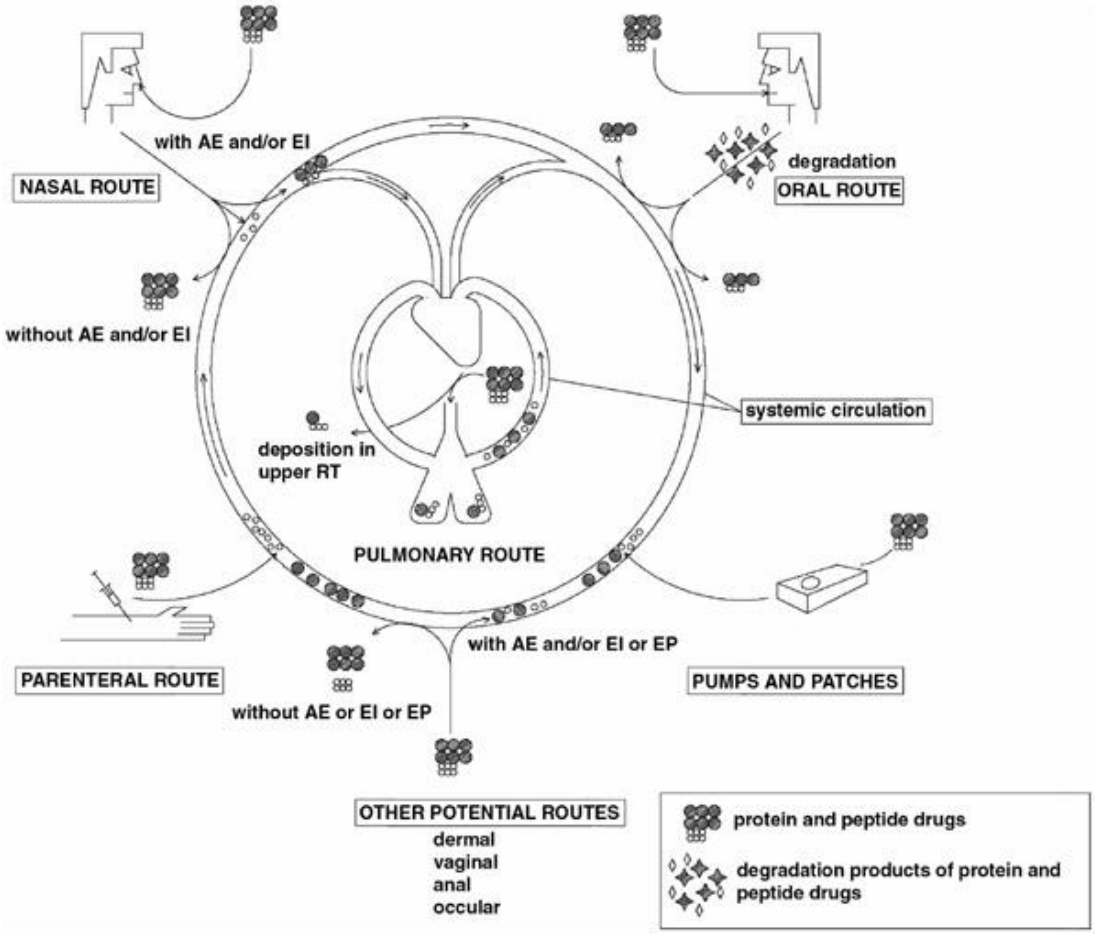

Figure 1.3: A schematic diagram showing clinical and potential protein delivery routes Abbreviation: absorption enhancers (AE) enzyme inhibitors (EI) and electroporation (EP), Adapted from Agu *et al*., 2001.

1.3 Improving protein absorption

The use of permeation enhancers (PE), enzyme inhibitors (EI) and the exploitation of bioadhesive delivery systems have been investigated to overcome protein delivery challenges.

1.3.1 Permeation enhancers

Permeation enhancers have been extensively studied to overcome the barriers to buccal protein and peptide delivery. Penetration enhancers act on the epithelium and increase the permeability of the membrane by either the paracellular or the transcellular pathway. Other mechanisms proposed for the improvement of mucosal peptide absorption by penetration enhancers include reduction of mucus layer elasticity and/or viscosity and increasing the thermodynamic activity of protein drugs which may be affected by the

composition of the delivery system with subsequent influence on micellization and solubility and by degree of drug and enhancer ion-pair formation (Veuillez *et al.,* 2001). Examples of this class of compounds include surfactants, fatty acids, bile salts, and chelators such as ethylene diamine tetra acetate (EDTA). Many gel-forming polymers such as polycarbophil, chitosan and thiolated chitosans also act as permeation enhancers by binding to the extracellular Ca^{2+}. Fatty acids, bile salts and surfactants mostly enhance permeability by increasing the fluidity of the lipid bilayer of the cell membranes. Local toxicity to the epithelium in the gastrointestinal tract is a major concern in using these systems in pharmaceutical products. Intracellular Ca^{2+} plays an important role in regulating the permeability of the tight junction (Kan & Coleman, 1988). Thus, compounds such as EDTA that can bind the extracellular Ca^{2+}, lowering the intracellular Ca^{2+} concentration, can act as permeation enhancers by rendering the paracellular pathway more permeable (Khafagy *et al*., 2007). Some of these enhancers, however, can cause local damage to the mucosal membrane and even enter the systemic circulation, leading to systemic toxic effects. The potential damage to the epithelium and changes in the mucosal morphology, especially in long term multi-dosing regimen, as would be required in diabetes treatment, are major concerns in the clinical use of these agents. Another disadvantage of these compounds is their non-specificity in permeation enhancement. Increased permeability of the epithelium may also allow toxins and microbial pathogens in the buccal cavity to pass more easily into the systemic circulation, an event which negates the very function of the buccal mucosa (Sudhakar *et al*., 2006). Factors such as characteristics of permeant, composition of the delivery system and the previous treatment of tissue with or without enhancer, affect the degree of enhancement. Enhancers may therefore be selected based on safety, chemical and biological inertness, effectiveness and rapid but reversible effect (Nicolazzo *et al*., 2005).

1.3.2 Enzyme inhibitors

The stability of protein and peptide drugs may be improved by the addition of enzyme inhibitors to formulations intended for absorption through the buccal mucosa (Khafagy *et al*., 2007). Concomitant administration of INS with aprotinin and soybean trypsin inhibitors has been shown to induce better hypoglycemic effect (Bernkop-Schnürch, 1998; Morishita, 1993). Polyacrylates such as Carbopol 934P and polycarbophil, which are typically used as bioadhesives, are also known to inhibit the activity of trypsin and chymotrypsin in a calcium-dependent manner (Madsen & Peppas, 1999; Lueben *et al*., 1997). Bai *et al*., (1996) showed that in-situ absorption of INS was improved by carbomer polymers and also induced a

significant decline in blood glucose levels. However, these enzyme inhibitors (Figure 1.4) have a toxic potential caused by the inhibition of digestive enzymes, which can further cause incomplete digestion of the nutrient proteins. In addition, the inhibitory action can cause increased secretion of these enzymes by a feed-back regulatory mechanism (Bernkop-Schnürch, 1998; Reseland *et al.*, 1996). Studies have shown that this feed-back regulation leads to both hypertrophy and hyperplasia of the pancreas and prolonged administration of soybean trypsin inhibitor may lead to invasive carcinoma (Bernkop-Schnürch, 1998). One of the recent additions to the class of absorption enhancers is zonula occludens toxin (Zot), a protein secreted by *Vibrio cholerae* (Baudry *et al.*, 1992). This toxin induces modifications of cytoskeletal organization, specifically at the actin filament of the zonula occludens which leads to opening of the tight junctions causing increased permeability. This increase in permeability is reversible, time and dose-dependent and is restricted to the jejunal and ileal sections of the small intestine owing to the presence of receptors for the protein in those sections (Fasano & Uzzau, 1997).

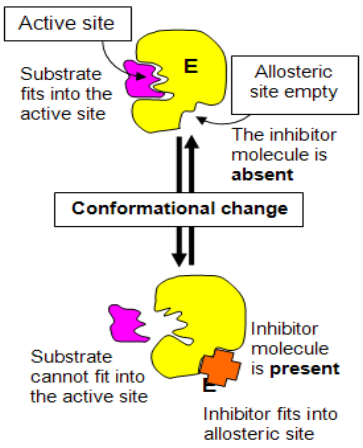

Figure 1.4: Schematic diagram showing the mechanism of enzyme inhibition. Available at <http://www.saburchill.com/IBbiology/chapters01/034.html> [Accessed; 20/03/2011]

Studies with diabetic animals have shown that INS administered with 5 μg Zot and $NaHCO_3$ to neutralize the gastric acidity, induced a hypoglycaemic effect comparable to that caused by subcutaneously administered INS. This is a promising approach to improving oral bioavailability of INS, but it suffers from the same safety and specificity issues that limit the use of permeation enhancers discussed above. Thus, attempts to increase the oral

bioavailability of proteins using permeation enhancers and protease inhibitors have not resulted in an acceptable delivery system as the potential side effects of these approaches have limited clinical application (Lee *et al*., 1991).

1.3.3 Mucoadhesive delivery systems

Application of mucosal drug delivery systems has increased exponentially for every conceivable route of administration because of the potential therapeutic benefits this delivery technology brings, particularly in the area of protein therapeutics. These include less frequent dosing, site-specific targeting and maintaining effective plasma concentrations without increased consumption.

Bioadhesive polymers can be broadly classified into two groups, namely specific and non-specific (Woodley, 2001). Specific bioadhesive polymers such as lectins and fimbrin have the ability to adhere to particular chemical structures within biological molecules while the nonspecific bioadhesive polymers such as polyacrylic acid, cyanoacrylates, chitosan and chitosan derivatives, have the ability to bind with both the cell surfaces and the mucosal layer (Sudhakar *et al*., 2006). A polymer will exhibit sufficient mucoadhesive property if it can form strong intermolecular hydrogen bonds with the mucosal layer, penetrate the mucus network or tissue crevices, easily wetted by the mucosal layer and the polymer chain has a high molecular weight.

The ideal characteristics of a mucoadhesive polymer matrix include (Sudhakar *et al*., 2006)

- rapid adherence to the mucosal layer without any change in the physical property of the delivery matrix,
- minimum interference with the release of the active agent,
- biodegradable without producing any toxic by-products,
- inhibit the enzymes present at the delivery site and
- enhance the penetration of the active agent (if the active agent is meant to be absorbed from the delivery site).

1.3.3.1 Theories of mucoadhesion

Many theories have been proposed to explain the complex mechanism involved with the phenomenon of bioadhesion. However, these six recently proposed theories enhance the understanding of the phenomenon of adhesion which might also be extended to explain the

mechanism of bioadhesion. The theories include: (a) the electronic theory; which proposes transfer of electrons among the surfaces resulting in the formation of an electrical double layer thereby giving rise to attractive forces; (b) the wetting theory; postulates that if the contact angle of liquids on the substrate surface is lower, then there is a greater affinity of the liquid to the substrate surface. If two such substrate surfaces are brought into contact with each other in the presence of the liquid, the liquid may act as an adhesive between the substrate surfaces; (c) the adsorption theory; proposes that the presence of intermolecular forces (hydrogen bonding and van der waal's forces), serve as adhesive interaction between the substrate surfaces; (d) the diffusion theory; which assumes the diffusion of the polymer chains present on the substrate surfaces, across the adhesive interface thereby forming a networked structure; (e) the mechanical theory; explains the diffusion of the liquid adhesives into the micro-cracks and irregularities present on the substrate surface thereby forming an interlocked structure which gives rise to adhesion and (f) the cohesive theory; proposes that the phenomena of bioadhesion is mainly due to the intermolecular interactions between like-molecules (Smart, 2005; Andrew *et al.*, 2009).

Based on these theories, the process of bioadhesion can be generally classified into two subsets, namely chemical (electronic and adsorption theories) and physical (wetting, diffusion and cohesive theory) methods (Hubbell, 1995; Peppas & Sahlin 1996). Two stages may be involved in the process of muco-adhesion. During the first stage (also known as contact stage), wetting of the mucoadhesive polymer and mucous membrane occurs followed by the consolidation stage (Figure 1.5), where the physicochemical interactions prevail (Wu, 1982; Smart, 1999).

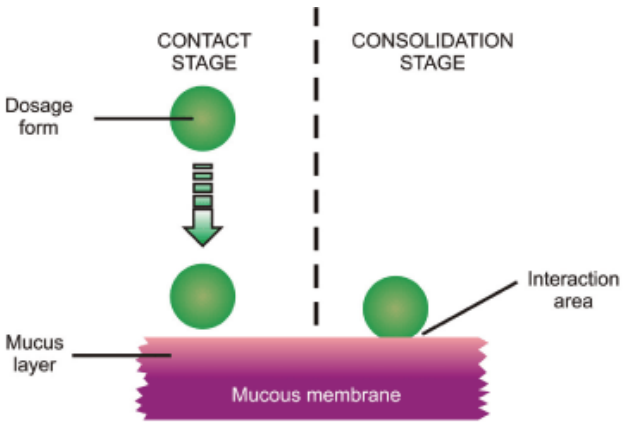

Figure 1.5: Mechanism of dosage form and mucosal layer interaction (Carvalho *et al.*, 2010)

1.3.3.2 Factors affecting mucoadhesion

A number of variables which have the capacity to alter the interaction between the polymer and the mucosal layer can affect the mucoadhesive property of a polymer and are discussed below. These include;

(a) *Molecular weight*; an increase in molecular weight (MW) of a polymer has been found to have a direct correlation with increasing muco-adhesivity of the polymer. Polymers with MW greater than 100,000 generally exhibit sufficient mucoadhesive properties for biomedical applications. A classical example is demonstrated by the negligible mucoadhesiveness of PEG 20,000, enhanced mucoadhesiveness of PEG 200,000 and the excellent mucoadhesiveness of PEG 400,000 (Middleton, 1990). Likewise, Dextrans of 200,000 MW, poly(acrylic) acid of ~750,000 MW and polyethylene oxide of 4,000,000 MW have demonstrated good bioadhesive properties with polyoxyethylene of 7,000,000 MW exhibiting excellent mucoadhesive properties in addition to being a candidate for buccal delivery system development (Andrew *et al*., 2009; Tiwari *et al*., 1999).

(b) *Hydrogen bonding;* formation of strong hydrogen bonds between polymeric functional groups such as hydroxyl, carboxyl and amino groups and the mucosal layer leads to stronger adhesion. In addition, the presence of these functional groups within the polymer structure may result in the polymer chains behaving as polyelectrolytes. The functional groups in the polymer chain have a marked effect on the strength of bioadhesion via hydrogen bonding between nonionised carboxylic acid and mucin (Sudhakar, 2006). Poly(vinyl alcohol), acrylic derivatives, celluloses (Lee *et al*., 2000) and chitosan have the ability to form hydrogen bonds.

(c) *Polymer concentration*; the process of mucoadhesion is significantly affected by the concentration of the polymer. An unstable and insufficient interaction occurs between the polymer and the mucosal layer at low polymer chain concentration which results in poor mucoadhesive properties. For biomedical applications, polymer concentration in the range of 1-2.5 % w/w exhibit adequate mucoadhesive properties (Roy *et al*., 2009). There is however a limited interpenetration of polymer and mucin chains at very high concentrations for polymers such as poly(vinyl pyrrolidone) and poly(vinyl alcohol) which subsequently results in a reduction of mucoadhesive property. These occur due to a decrease in solvent diffusion into the polymer network at very high polymer concentration as highly coiled structures are formed (Solomonidou *et al*., 2001).

(d) *pH of environment*; the pH of the external environment influences the ionization of the functional group(s), affecting the charge distribution on the polymer chains. As discussed earlier, mucoadhesion property depends on the presence of these functional groups and therefore a change in the pH of the external environment may impact on the mucoadhesive property. A typical example is the excellent mucoadhesive property of chitosan (cationic polyelectrolyte) in alkaline or neutral environment (Park *et al*., 1989)

(e) *Method of drying*; apart from the above factors, Grabovac *et al*., (2005) found that the method of drying is an important factor influencing the mucoadhesive potential of polymeric formulations. Lyophilisation of thiolated chitosan polymers at pH 3 produced greater mucoadhesion than other polymers that were dried by casting from organic solvents and air dried. On the other hand, polyacrylates showed improved mucoadhesion when precipitated in neutral sodium salts.

1.3.3.3 Mucin

The protein based material, mucin, is the main component of mucus and plays a significant role in the mucoadhesive characteristics of chitosan and chitosan derivatives (Fefelova *et al*., 2007; Sogias *et al*., 2008). The mucosa layer is made up of mucus secreted by the goblet cells (glandular columnar epithelial cells) and is a viscoelastic fluid. It lines the visceral organs, which are exposed to the external environment, including the alimentary canal/ gastrointestinal (oral cavity, stomach and intestines), respiratory and genitourinary tracts. The main components constituting the mucosa are water and mucin, which together constitute > 99 % of the total composition of the mucus and of this greater than 95 % is water (Roy *et al*., 2009). The other components present in mucus include proteins, lipids and mucopolysaccharides. The gel-like structure of the mucus can be attributed to the intermolecular entanglements of the mucin glycoproteins along with the non-covalent interactions (e.g. hydrogen, electrostatic and hydrophobic bonds) which results in the formation of a hydrated gel-like structure and explains the viscoelastic nature of the mucus (Andrew *et al.,* 2009).

Mucins (Figure 1.6) are a family of high molecular weight (anionic polyelectrolytes), heavily glycosylated proteins (glycoconjugates) produced by epithelial tissues. Many epithelial cells produce mucin, but gel-forming mucins are produced primarily in the goblet or mucous cells of the tracheobronchial, gastrointestinal, and genitourinary tracts. In goblet cells, mucins are stored intracellularly in mucin granules from which they can be quickly secreted upon external stimuli.

Human salivary glands secrete 1000–1500 ml per day of saliva composed of water, proteins and low molecular mass substances (mainly electrolytes). Up to 26 % of the salivary proteins are mucins. The mucins of human saliva are extremely effective lubricants, which provide an effective barrier against desiccation and environmental insult. The functions of mucins include controlling permeability of mucosal membrane, limiting the penetration of potential irritants and toxins into mucous cells, protecting mucosal cell membranes against proteases generated by bacteria in the bacterial plaques around the teeth and regulating colonization of the oral cavity by bacteria and viruses.

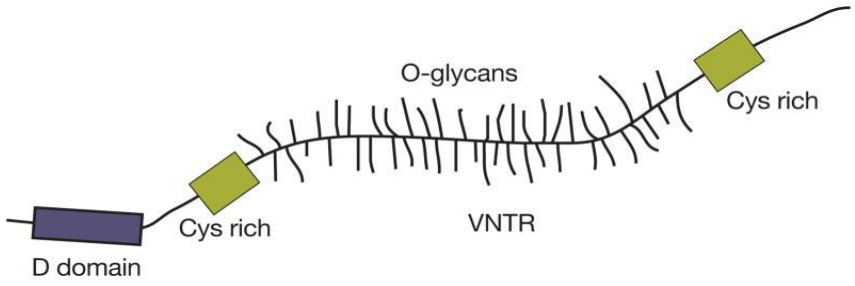

Figure 1.6: A simplified model of a large secreted mucin. Available at <http://www.ncbi.nlm.nih.gov/books/NBK1896/ > [Accessed; 08/08/2011].

Proline and serine/threonine constitute up to 20–55 % of total amino acids in mucin and are concentrated in one or several regions of the polypeptide. These serine/threonine residues are heavily glycosylated, and 40–80 % of the mass of such mucins consists of O-linked oligosaccharides. The cysteines at the N- and C-ends may link mucin monomers by disulphide bridges forming linear mucin oligomers. Two types of mucins are present in human saliva: oligomeric mucin glycoprotein (MG1) (Levine *et al.*, 1987) with molecular mass above 1 MDa, and monomeric mucin glycoprotein (MG2) with molecular mass of 200–250 kDa. The submandibulary glands containing mucous cells (producing MG1) and serous cells (producing MG2) secrete 30 % of the salivary mucins, while sublingual, labial and palatal glands (which contain mainly mucous cells) secrete 70 %. Concentration of mucin secreted by the sublingual glands is higher than that secreted by the submandibulary glands, while the secretion from the parotid glands is devoid of mucins (Zalewska *et al*., 2000).

The formation of electrostatic interactions between mucin and chitosan has been used to explain the mucoadhesivity with biological membranes (Silva *et al*., 2012). In addition, the formation of in-situ disulphide links between mucin and thiolated polymers such as chitosan, carbomers and alginates (Bernkop-Schnürch *et al*., 2001) has led to improved adhesion

performance (Smart, 2005). The use of mucin for mucoadhesion studies provides a relevant platform for predicting the performance of mucoadhesive delivery systems where prolonged attachment to the mucosal surface is required for overcoming drug absorption limitations via mucosal membranes.

1.4 Mucosal delivery routes

Bioadhesive systems engage in interfacial molecular attractive forces between the surfaces of the biological substrate and the constituent natural or synthetic polymers, thus allowing the delivery system to adhere to the biological surface for an extended period of time (Khutoryanskiy, 2007; Gu *et al*., 1998; Duchene *et al.*, 1998). The term "mucoadhesion" is used to describe the adhesion of polymers with the surface of a biological substrate when the immediate substrate is a mucosal layer (Robinson 1990). The two terms will be used interchangeably in this report. As noted earlier, the mucosal layer lines the GIT, the urogenital tract, the buccal, ocular and nasal cavities. These represent potential sites for the attachment of any bioadhesive system. Table 1.2 shows various mucosal delivery systems and routes for the delivery of insulin.

1.4.1 The oral route

The absence of specialized regulatory requirements such as sterility, pyrogenicity and particulate contamination for oral dosage forms make the gastrointestinal tract (GIT) the route of choice for the administration of most drugs, irrespective of molecular structure or weight. The successful oral delivery of proteins and peptides however, requires overcoming many barriers including enzymatic degradation, achieving epithelial permeability, and preserving the bioactivity of the drug during formulation processing.

A number of pharmaceutical strategies proposed to maximize protein bioavailability in oral delivery systems include the use of absorption enhancers, enzyme inhibitors, mucoadhesive polymeric systems, particulate carrier delivery systems and targeted delivery systems (Khafagy *et al.*, 2007). Table 1.3 shows current oral protein delivery technologies developed for marketing or clinical applications. Notwithstanding the advantages these strategies provide, they are limited by transport of undesirable molecules, high toxicity over long term use, low incorporation efficiency of hydrophilic drugs, the harsh hydrolytic environment of the GIT and the epithelial barriers to absorption.

1.4.2 The nasal route

Nasal protein delivery offers an alternative to subcutaneous injections due to the large surface area for drug absorption, highly vascularized sub-epithelial layer, high total blood perfusion, avoidance of first-pass metabolism, rapid onset of pharmacological activity, and a porous endothelial basement membrane which is readily accessible, delivering drug directly to the brain along the olfactory nerves (Kissel & Werner, 1998). A nasal delivery system of 2 % HPMC lyophilised insert formulation for INS achieved an extended nasal residence, demonstrating an optimum combination of rapid adhesion without over hydration (McInnes *et al*., 2007*)*. Intranasal absorption of high-molecular-weight and hydrophilic peptide drugs is however limited by mucociliary clearance, enzymatic activity, and the epithelial-mucus layer barriers. The use of absorption enhancers, enzyme inhibitors and mucoadhesive systems has been investigated to enhance drug bioavailability via the nasal mucosa (Khafagy *et al*., 2007).

Table 1.3 Marketed/under development protein oral delivery technology by companies. Adapted from Park *et al*., 2011.

Company	System	Product name	Outcomes for absorption	Marketed/under development products
Emisphere	Carrier molecules	Eligen®	Increase membrane permeability	Calcitonin, Insulin, Growth hormone, parathyroid hormone
Altus	Protein crystallization	CLEC®	Stable against proteolysis and self-aggregation	Calcitonin, other polypeptides, lipases, esterases and proteases
BioSante	Calcium phosphate nanoparticles	BioOral™	Protect proteins from acidic degradation and improve membrane permeability	Insulin and vaccines
NOBEX/Biocon	Amphiphilic oligomers	HIM2	Resist enzyme digestion and increase membrane permeation	Insulin, enkephalin, calcitonin, parathyroid hormone
Appolo Life Science	Nanoparticles	Oradel™	Protect proteins from enzyme digestion in the stomach and facilitates transport in the intestine	Insulin and TNF blocker
Eli-Lilly	Oral formulation	AI-401	Protect protein from enzyme digestion	Insulin
Provalis PLC	Lipid-based microemulsion	Macrulin™	Protect proteins from proteolysis and enhance protein absorption in GIT	Insulin, salmon calcitonin

Abbreviation: CLEC, Cross-Linked Enzyme Crystal; HIM", hexyl-insulin monoconjugate; TNF, tissue necrosis factor.

1.4.3 The pulmonary route

The lungs with a large surface area of approximately 140 m^2 and very thin alveolar epithelium (approximately 300 million) allows the passage of 5 L of blood per minute (Cázares-Delgadillo *et al.,* 2011) leading to rapid drug absorption in addition to avoiding first-pass metabolism. Furthermore, the metabolic enzymatic activities and pathways in the lungs differ from those observed in the GIT, making the pulmonary administration of various peptides and proteins very promising (Agu *et al.,* 2001). However, full optimization of pulmonary delivery systems requires addressing critical issues relating to particle size characteristics, obtaining good encapsulation efficiency, preventing protein degradation and predictable drug release. In addition, inhaled peptides may not be suitable for all patients with smokers or asthmatics requiring lower (Himmelmann *et al.,* 2003) or higher (Henry *et al.,* 2003) doses respectively. Furthermore, to achieve a similar glycaemic effect, patients receiving pulmonary INS may require a dose approximately 20 times that of subcutaneous injection (Gale, 2001) which might lead to breathing difficulties and variability in dosing regimen for different categories of patients (Lassmann-Vague & Raccah 2006).

1.4.4 The ocular route

Drug administration via the ocular route is much easier than injection with comparable systemic absorption rates. Drug absorption also by-passes the first-pass gastrointestinal and liver effects, resulting in increased bioavailability of peptides and other drugs. The eye tissues are much less likely to develop immunological responses compared with other tissues with prolonged safety (3 months) of use and no ocular side effects upon daily administration of INS eye drops (Chiou, 1994). Chitosan and chitosan derivatives have been developed as drug delivery systems for ocular delivery (Fuente *et al*., 2010, cited in Khutoryanskiy, 2011). The major drawback is the need for developing delivery systems that are compatible with the conjunctival, corneal and iris tissues with a prolonged residence time. These might raise issues with local tissue irritation, however the use of eye-drops which is rapidly eliminated seem better than an eye devices which must release the drug in a controlled manner.

1.4.5 Vaginal and rectal routes

The vaginal and rectal mucosal cavities offer potential alternative routes to attain systemic delivery. Although most of the products in the marketplace are designed for local mucosal administration, a few target systemic delivery. Valenta *et al*., (2001) used a thiolated

polyacrylic acid conjugate (NaC974P-Cys) composed of L-cysteine and polyacrylic acid (Carbopol 974P) to develop a mucoadhesive vaginal delivery system for progesterone. Recently, mucoadhesive HPMC and Carbopol tablets have been developed for vaginal delivery of benzydamine (Perioli *et al*., 2011). Patient compliance to these routes tends to be low due to socio-cultural acceptance. In addition, and from a delivery perspective, erratic local physiological activities such as rectal contents and menstrual-cycle, significantly impact drug dissolution and absorption at the site of delivery (Mathias & Hussain, 2009).

1.4.6 Buccal route

The buccal region is that part of the oral cavity bounded anteriorly and laterally by the lips and the cheeks, posteriorly and medially by the teeth and/or gums, and above and below by the reflections of the mucosa from the lips and cheeks to the gums (Figure 1.7 (a)). The oral mucosa consists of a non-keratinized area (sublingual and buccal mucosa) and the keratinized area (the gum or gingiva, the palatal mucosa, and the inner side of the lips). The non-keratinized regions are generally more permeable compared to the keratinized areas (Veuillez *et al*., 2001). The oral cavity offers a large surface area for absorption (100– 200 cm^2), is richly vascularized with little proteolytic activity. Blood reaches the buccal mucosa via the maxillary artery at a faster (and richer) flow rate (2.4 ml/min/cm^2) than that in the sublingual, gingival and palatal regions, thus facilitating passive diffusion of drug molecules across the mucosa. The estimated turnover time (cell regeneration) for the buccal epithelium is between 5 to 6 days (Harris & Robinson, 1992).

The buccal mucosa is composed of several layers of different cells as shown in Figure 1.7 (b). The epithelium is about 40–50 cell layers thick and is similar to stratified squamous epithelia found in the rest of the body. The epithelium lining of the buccal mucosa is made up of non-keratinized stratified squamous epithelium cells with a thickness of 500–800 μm and surface area of 50.2 cm^2. The rough textured buccal mucosa is thus suitable for retentive delivery systems (Rathbone *et al*., 1996). Basement membrane and lamina propria followed by the submucosa are found below the epithelial layer (Gandhi & Robinson, 1988). The lamina propria is rich with blood vessels and capillaries which open to the internal jugular vein. Lipids present in the buccal tissues include phospholipid (76.3 %), glucosphingolipid (23.0 %) and ceramide NS (0.72 %). The buccal epithelium is primarily designed to offer protection of the underlying tissue. In non-keratinized regions, lipid-based permeability barriers in the outer epithelial layers protect the underlying tissues against fluid loss and entry of potentially harmful environmental agents such as antigens, carcinogens, microbial toxins

and enzymes from foods and beverages (Squier & Finkelstein, 1989). This protective system also presents a barrier to drug absorption that needs to be overcome as previously mentioned.

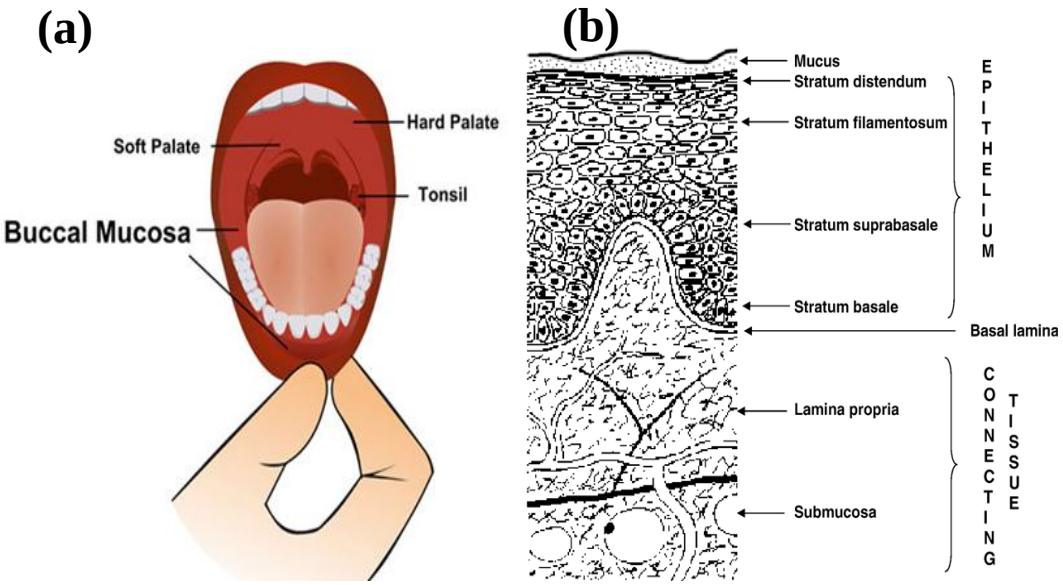

Figure 1.7: (a) Cartoon representation of the buccal mucosa (b) cross-section of the buccal mucosa structure. Available at < www.cedars sinai.edu/Patients/Programs and-Se..website.> [Accessed; 13/08/2010]

1.5 Buccal delivery of proteins

The buccal mucosa offers a potential portal for the administration of therapeutic agents for both systemic and local delivery. The buccal mucosa has fewer proteolytic enzymes than the oral (GIT), nasal, vaginal and rectal administration routes (Lee & Yamamoto, 1989). The predominant enzymes found in the buccal mucosa are aminopeptidases. The proteolytic enzymes such as trypsin, chymotrypsin and pepsin, which are present in the gastric and intestinal fluids, are principally absent (Veuillez *et al*., 2001; Stratford & Lee, 1986). This makes it ideal for the delivery of protein and peptide based drugs with relatively reduced risk of proteolytic degradation.

Generex (Toronto, Canada) has recently demonstrated the efficacy of a buccal INS delivery system based on an oral spray which delivers INS in the form of a high-velocity, fine particle aerosol directly into the subject's buccal cavity (Figure 1.8). The particles are composed of mixed micelles made from absorption enhancers that encapsulate INS (Guevara-Aguirre, 2004). The penetration of a thin membrane that guards the surface area in direct contact with the blood circulation is made possible by the fast moving fine particles. The penetrating particles combined with the effect of absorption enhancers, allow a rapid increase

in the uptake of insulin into the systemic circulation (Modi, 2002). The administered INS appears in the systemic circulation within 10 minutes of application. A maximum INS bioavailability of 7-8 % was reached in about 30 minutes after application compared to 60 minutes when a subcutaneous INS injection was administered in a proof-of concept study involving type 2 diabetic patients (Guevara-Aguirre, 2004). More clinical and toxicological data is required to establish the efficacy of this system, however, Generex Oral-lyn™, is available for sale in Ecuador for the treatment of patients with Type-1 and Type-2 diabetes and was approved for sale in India in October 2007. It is in various stages of clinical development around the world as the global Phase III clinical trial of Generex Oral-lyn™ has commenced in the USA, Canada, Russia, Ukraine, Romania, Bulgaria and Poland.

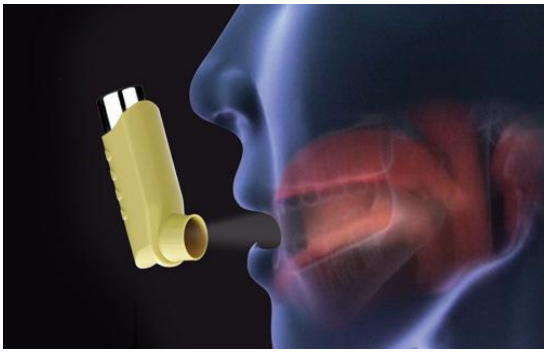

Figure 1.8: Buccal delivery of insulin from Generex Oral-lyn™. Available at <www.pharmapolis.net/news/drugs-and-therapy/32. > [Accessed; 26/05/2011]

1.5.1 Pros and cons of protein delivery via the buccal mucosa

Among the major mucosal routes, the buccal mucosa has received increased attention in recent years for the delivery of peptides as an alternative to currently used parenteral route for protein delivery. Its advantages include the avoidance of pain (Antosova *et al*., 2009), avoiding hepatic first-pass effect (Cornelius *et al*., 2005) and peptidase metabolism in the gastrointestinal tract (Sudhakar *et al*., 2006).

Protein (peptide) absorption via the buccal mucosa is however, limited by drug molecular size, hydrophobicity and low permeability of the mucosal membrane (Merkle & Wolany, 1992) due to the relatively thick multi-layered buccal barrier and the high rate of mucus turnover. An enzymatic barrier also exists at the mucosa which causes rapid degradation of peptides and proteins, limiting their transport across the buccal mucosa. The use of absorption enhancers, enzyme inhibitors and mucoadhesive systems which have been investigated as strategies to improve absorption of protein drugs across the buccal mucosa

(Veuillez *et al*., 2001; Nagai, 1986; Aungst and Rogers, 1988) have been discussed in section 1.3.

1.5.2 Mechanism of protein transport across buccal mucosa.

Epithelial and endothelial cell layers form selective permeable barriers. Transport of molecules and ions from the apical to the basolateral side and vice versa requires passage either through the cells (transcellular route) or between the cells and therefore through tight junctions (paracellular route) (Figure 1.9). Transport of ions and hydrophilic solutes occur by diffusion across the paracellular route along a concentration gradient. The tight junction serves as a regulated restricted semi-permeable diffusion barrier that is ion and size-selective (Steed *et al*., 2010). Materials delivered to the buccal mucosa may pass through the intracellular or the paracellular route. The aqueous paracellular pathway contains minimal peptidases which are located within the cells. It has been suggested that this is the pathway for high molecular weight peptides such as INS (Hoogstraate *et al*., 1996). Absorption and transport are affected by charge, conformation and lipophilicity.

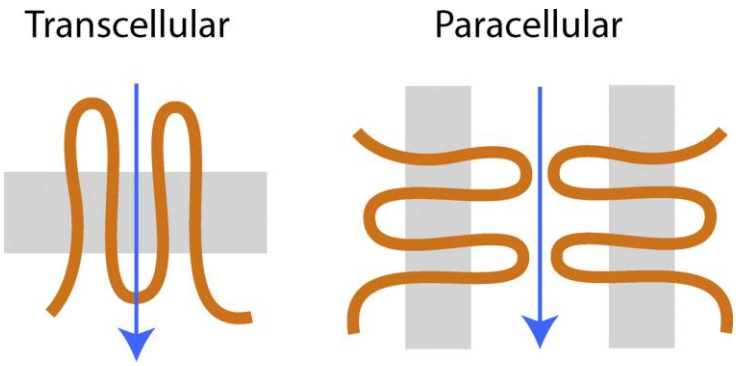

Figure 1.9: Mechanism of protein transport across epithelial cell layers. (Yu *et al.,* 2009)

1.6 Buccal adhesive polymers

The term buccal adhesive polymer encompasses a large and diverse group of molecules, including substances from natural polymers that are susceptible to enzymatic degradation, or synthetic polymers that possess hydrolyzable moieties, to biocompatible, biodegradable grafted copolymers and thiolated polymers. Bioadhesive formulations employ such polymers as the adhesive component. These formulations are often water soluble which readily attract water from the biological surface and this water transfer leads to a strong

interaction (Figure1.10). They also form viscous gels when hydrated with water which increases their retention time on mucosal surfaces and may lead to adhesive interactions.

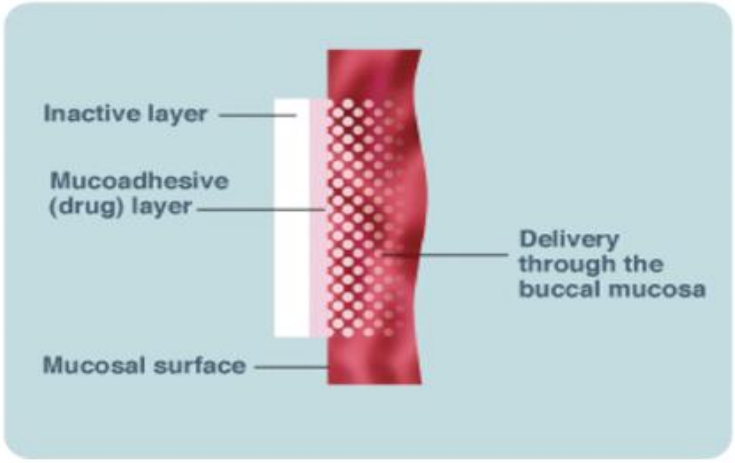

Figure 1.10: Mucoadhesive drug delivery system via the buccal mucosa. Available at <http://www.onsolishcp.com/About-Onsolis/About-Onsolis.php >[Accessed; 20/05/2011]

Certain physicochemical features such as hydrophilicity, hydrogen bond-forming groups, flexibility for interpenetration with mucus and epithelial tissue, and visco-elastic properties must be possessed by the bioadhesive polymers (Batchelor, 2004). In addition, the bioadhesive polymer should have these ideal characteristics:

- Polymer and its degradation products should be non-toxic, non-irritant and free from leachable impurities.
- Should have good spreadability, wetting, swelling and solubility and biodegradable properties.
- Should adhere quickly to buccal mucosa and should possess sufficient mechanical strength.
- Should possess peel, tensile and shear strengths within the bioadhesive range.
- Should show bioadhesive properties in both dry and liquid (gel) state.
- Should demonstrate local enzyme inhibition and penetration enhancement properties.
- Should have optimum molecular weight.
- Should be sufficiently cross-linked but not to the degree of suppression of bond forming groups and
- Should not aid in development of secondary infections such as dental caries. (Sudhakar *et al*., 2006).

1.6.1 Chitosan

Chitosan together with chitin is considered the second most abundant polysaccharide after cellulose. Chitosan has received a great deal of attention due to its well documented degradability by human enzymes, biocompatibility and low toxicity (Oungbho & Muller, 1997). However, unlike cellulose, the use of chitosan as an excipient in pharmaceutical formulations is a relatively new development. Chitosan (poly[-(1,4)-2-amino-2-deoxy-D-glucopiranose]) (Figure 1.11) differs from chitin in that a majority of the N-acetyl groups in chitosan have been hydrolysed.

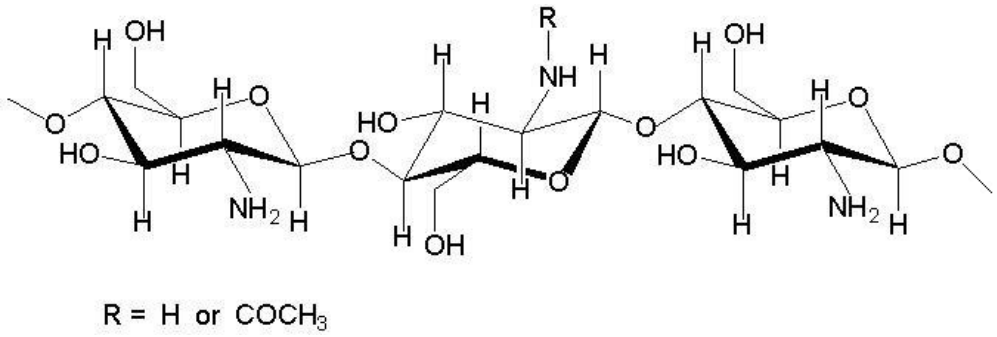

Figure 1.11: Chemical structure of chitosan. Available at <http://dietpilluniverse.com/uncategorized/chitosan/ > [Accessed; 20/05/2011]

The degree of deacetylation has significant effects on the solubility and rheological properties of the polymer. The amine group on the polymer has a pKa in the range of 5.5 to 6.5, depending on the source of the polymer (Payne *et al*., 1996). At low pH, the polymer is soluble, with the sol-gel transition occurring at approximately pH 7.0. The pH sensitivity, coupled with the reactivity of the primary amine groups, make chitosan a unique polymer for mucosal drug delivery applications. Furthermore, its gel and matrix-forming ability makes it useful for formulating solid dosage forms, such as granules, microparticles and xerogels. Microcrystalline chitosan as a gel-forming excipient for matrix-type drug granules has been studied by Sakkinen *et al*., (2003) who observed that crystallinity, molecular weight, and degree of deacetylation were major factors that affected the release rates from the chitosan-based granules. Combination of positively charged chitosan with negatively charged biomolecules, such as gelatin, alginic acid, and hyaluronic acid, were tested to yield novel matrices with unique characteristics for controlled release of drugs.

The excipient also has promise for site-specific delivery. Tozaki *et al.*, (2002) utilized chitosan capsules into which was encapsulated a 5-amino salicylic acid for colon-specific delivery to treat ulcerative colitis. It was observed that chitosan capsules delivered *in-vivo* to

male wistar rats after induction of colitis disintegrated specifically in the large intestines as compared to the control formulation (absence of chitosan) which demonstrated absorption of the drug in the small intestines.

Chitosan has mucoadhesive properties and is often exploited to enhance the residence time of a drug on the mucosal membrane thereby increasing the drug bioavailability. A comparison between chitosan and other commonly used polymeric excipients indicates that the cationic polymer has higher bioadhesivity compared to other natural polymers, such as cellulose, xanthan gum, and starch (Kotze *et al*., 1999).

1.6.2 Pharmaceutical and medicinal uses of chitosan

A number of clinical studies have reported the use of chitosan as cell scaffolds in tissue engineering, nerve regeneration tubes, and cartilage regeneration (Khor & Lim, 2003, Freier *et al*., 2005, Mwale *et al*., 2005). In addition, it has been used extensively as a biomaterial, owing to its immunostimulatory activities (Gorbach *et al*., 1994), anticoagulant properties, antimicrobial and antifungal action (Rabea *et al*., 2003) and for its action as a promoter of wound healing in the field of surgery (Khan *et al*., 2000). Because of its biocompatibility and biodegradation properties (Vandevord *et al*., 2002), chitosan has been used in a variety of pharmaceutical formulations, primarily for the purpose of controlled drug delivery (Agnihotri *et al*., 2004), such as mucosal (Illum *et al*., 2001, Van Der Lubben *et al*., 2001, Read *et al*., 2005), buccal (Giunchedi *et al*., 2002), and ocular (De Campos *et al*., 2004) delivery of drugs.

Due to its cationic nature, chitosan is capable of opening tight junctions in a cell membrane. This property has led to a number of studies to investigate the use of chitosan as a permeation enhancer for hydrophilic drugs such as peptides that may otherwise have poor oral bioavailability (Thanou *et al*., 2000). Because the absorption enhancement is caused by interactions between the cell membrane and positive charges on the polymer, the phenomenon is pH and concentration dependant. Furthermore, increasing the charge density on the polymer would lead to higher permeability. This has been studied by quaternizing the amine functionality on chitosan (Hamman *et al.*, 2003). The amine functionality is further explored in the proceeding section.

1.6.3 Chitosan derivatives

The excellent properties exhibited by chitosan have further been improved by derivatization via the primary amine functional group. A number of approaches, both chemical and enzymatic, have been attempted to exploit the reactivity of the amine functional group (Payne *et al*., 1996). A quaternary derivatized chitosan N-trimethylene chloride chitosan (TMC) has been shown to demonstrate higher intestinal permeability than unmodified chitosan. The TMC derivative was used as a permeation enhancer for large molecules, such as octreotide, a cyclic peptide. Hamman *et al.*, (2003) showed that the degree of quaternization of TMC influences its drug absorption-enhancing properties. Polymers with higher degrees of quaternization (> 22 %) were able to reduce the trans-epithelial electrical resistance and thereby increase epithelial transport *(in vitro)* in a neutral environment (pH 7.4). This degree of quaternization was also seen to be critical for *in-vitro* transport of model drugs across a Caco-2 monolayer. These and other useful characteristics (e.g. hydrophilicity, functional amino groups, and a net cationic charge) have made chitosan a suitable polymer for the intelligent delivery of macromolecular compounds, such as peptides, proteins, antigens, oligonucleotides, and genes.

Chitosan esters such as chitosan succinate and chitosan phthalate have been used successfully as potential matrices for the colon-specific oral delivery of sodium diclofenac. Aiedeh & Taha, (1999) converted the polymer from an amine to a succinate form, changing the solubility profile significantly. The modified polymers were insoluble under acidic conditions and provided sustained release of the encapsulated agent under basic conditions. They also reported the synthesis of an iron cross-linked derivative of hydroxamated chitosan succinate as a matrix for oral theophylline beads (Aiedeh & Taha, 1999). One of the most commonly used chitosan derivatives is thiolated chitosan which exhibits unique properties and is discussed further in the ensuing section.

1.6.3.1 Thiolated chitosans

A number of natural and synthetic polymers have generally been considered to be mucoadhesive. However, polymers with thiol groups exhibit better mucoadhesive properties. Figure 1.12 shows the formation of chitosan-thioglycolic acid (TG-chitosan). The formation of stronger covalent bonds between the thiolated polymer and the mucus layer forms the basis for the enhanced mucoadhesive property as opposed to weaker non-covalent bonds. Simple oxidative processes or disulphide exchange reactions are responsible for the interaction

between these thiolated ("thiomers") polymers (see Figure 1.13), with cysteine-rich subdomains of mucus glycoproteins (Snyder *et al*., 1983).

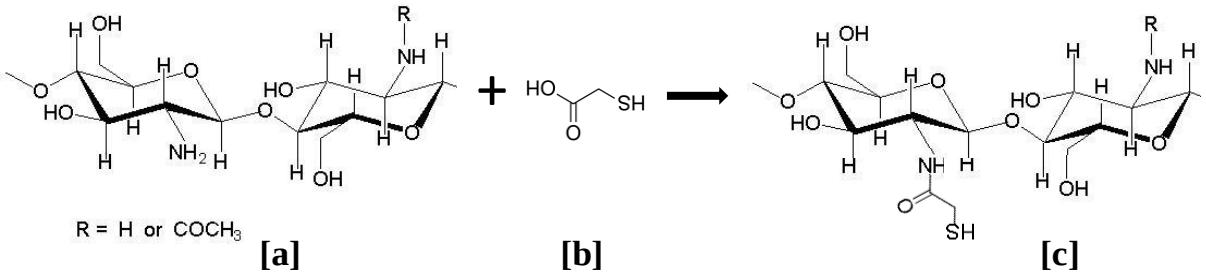

Figure 1.12: Synthesis of chitosan thioglycolic acid (TG-chitosan) (Ayensu *et al*., 2012a)

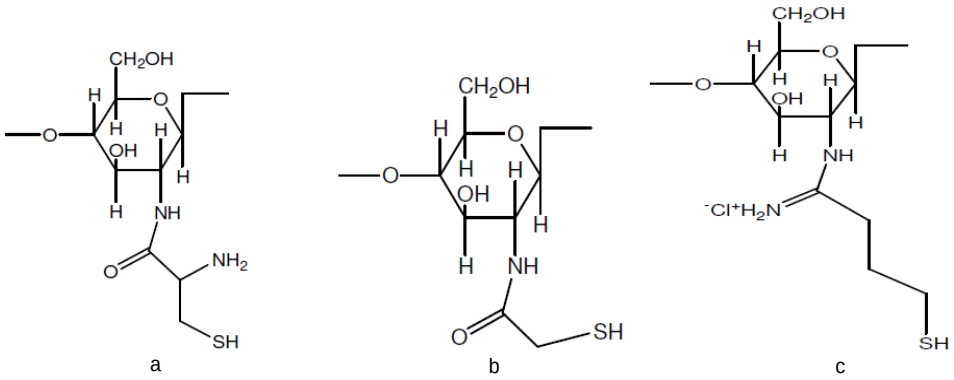

Figure 1.13: Thiolated chitosan moieties (a) chitosan cysteine (b) chitosan thioglycolic acid and (c) chitosan-4-thiobutylamidine (Roldo *et al*., 2004)

1.6.4 Functional properties of thiolated chitosan

1.6.4.1 Mucoadhesion

The stronger covalent bond between the thiol groups of the polymer and the cysteine rich subunits of glycoproteins in the mucus layer (Figure 1.14) have been used to explain the enhanced mucoadhesive properties of the thiolated chitosans (Leitner *et al*., 2003). These arise from the covalent interactions of the thiolated chitosan with anionic sub-structures of the mucus layer. The positive correlation between the degree of modification of thiol bearing moieties and the adhesive properties of thiolated chitosan tablets in a tensile study supported the theory (Kast & Bernkop-Schnürch 2001, Roldo *et al*., 2004). In another *in-vitro* mucoadhesive test system, the time of adhesion of thiolated chitosan tablets on intestinal mucosa was determined. The increase in contact time of the thiolated chitosan derivatives

with increasing amounts of immobilized thiol groups confirmed the findings (Kast & Bernkop-Schnürch & Walker, 2001, Bernkop-Schnürch *et al*., 2003a).

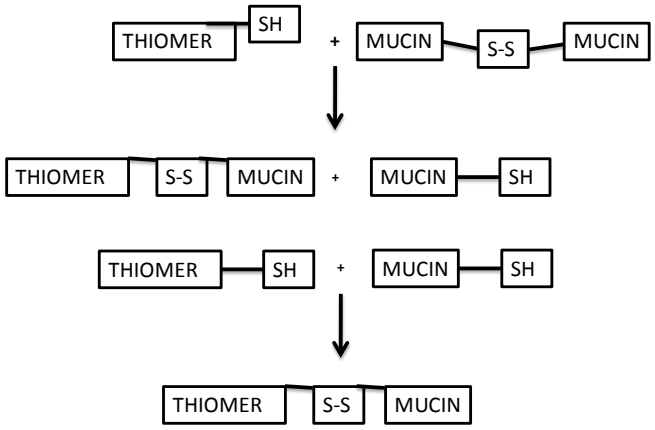

Figure 1.14: A schematic diagram showing the formation of disulphide linkages between thiomer and mucin. Adapted from Kast & Bernkop-Schnürch. 2001.

A 5–10-fold increase in mucoadhesion was achieved with chitosan-thioglycolic acid conjugates whiles chitosan-4-thio-butyl-amidine (chitosan-TBA) conjugate, displaying 264 mM thiol groups per gram of polymer, led to a more than 100-fold improvement in mucoadhesion compared to unmodified chitosan. This represents the most significant advancement made so far in the development of mucoadhesive polymers. This phenomenon can be explained by the fact that chitosan-TBA conjugates, achieved enhanced ionic interactions between its additional cationic amidine sub-structure and anionic sub-structures (siallic acids) within the mucus layer. Furthermore, tensile studies with chitosan-TBA conjugates of low, medium and high molecular weight (150, 400 and 600 kDa) indicated that medium molecular weight thiolated chitosans relatively displayed the highest mucoadhesiveness (Roldo *et al*., 2004).

1.6.4.2 Permeation enhancement

The permeation enhancing capabilities of chitosan was first shown by Illum and co-workers (Illum *et al.*, 1994). The use of chitosan in various studies carried out on Caco-2 cell monolayers demonstrated a significant decrease in the trans-epithelial electrical resistance, leading to enhanced membrane permeation (Artursson *et al*., 1994, Borchard *et al*., 1996, Dodane *et al*., 1999). Chitosan is able to improve the transport of hydrophilic compounds

such as therapeutic peptides and antisense oligonucleotides across the membrane via the paracellular route. Structural reorganization of tight junction-associated proteins, which stems from the interaction between the positive charges of the polymer and the cell membrane, results in the permeation enhancing effect (Schipper *et al*., 1997). However, in the presence of mucus layer, the permeation enhancing effect is comparatively lower, as chitosan cannot reach the epithelium due to size exclusion and/or competitive charge interactions with mucins (Schipper *et al*., 1999). On the other hand, the results obtained on Caco-2 cell monolayers were confirmed by *in-vivo* studies, showing an enhanced intestinal absorption of the peptide drug, buserelin, in rats owing to the co-administration of chitosan hydrochloride (Luessen *et al*., 1996**)**.

The permeation enhancing effect of chitosan has been significantly enhanced by the immobilization of thiol groups. Bernkop-Schnürch *et al*., (1999) employed freshly excised intestinal mucosa in Ussing-type chambers to demonstrate the permeation effect of thiolated chitosans. The use of 0.5 % chitosan-cysteine conjugate instead of unmodified chitosan led to a 1.6-fold improvement in the uptake of fluorescence-labelled bacitracin. Langoth *et al*., (2004) showed the permeation enhancing effect of chitosan-TBA in comparison to unmodified chitosan while the uptake of the cationic marker compound, rhodamine-123 was 3-fold higher in the presence of thiolated chitosan. The inhibition of the protein, tyrosine phosphatase (which mediates the opening and closing of the tight junctions) is the likely mechanism responsible for this improved permeation enhancement. Tyrosine phosphatase which is an essential trans-membrane protein of the tight junctions, functions by dephosphorylating the tyrosine subunits of the protein, occluden, resulting in the closure of the tight junctions. Phosphorylation of these tyrosine subunits, however, opens the tight junctions. Compounds such as phenylarsine oxide, pervanadate and reduced glutathione inhibit tyrosine phosphatase which leads to phosphorylation and opening of the tight junctions (Clausen *et al*., 2002, Barrett *et al*., 1999, Staddon *et al*., 1995).

The inhibitory activity of glutathione is however, lowered by rapid oxidation on the cell surface compared to the stable but toxic tyrosine phosphatase inhibitors, phenylarsine oxide and pervanadate (Grafstrom *et al*., 1980). However, the capability of thiomers to reduce oxidized glutathione can restrict the oxidation of the inhibitor on the membrane when reduced glutathione is used in combination with thiolated chitosans (Clausen *et al*., 2002). Data to support the use of chitosan and thiolated chitosans as permeation enhancers for buccal delivery of proteins is very scanty with respect to polymer interaction with tight junctions. The mechanism to explain the phenomenon can therefore be a subject of further research.

1.6.6.3 Thiolated chitosans as matrices for controlled drug release

The excellent mucoadhesive properties exhibited by chitosan make it a useful means for non-invasive drug delivery (Takeuchi *et al*., 2001). The improved bioavailability of incorporated drugs from mucoadhesive polymeric formulations is believed to result from the prolonged residence time at the site of absorption. However, such enhanced bioavailability is provided by formulations that permit controlled release of the active ingredient. Thiolated chitosans, in addition to forming disulphide bonds with mucus glycoproteins also forms inter- as well as intra-molecular disulphide bonds. Such cross-linking capability of the polymeric chains is responsible for the high stability of drug delivery systems based on thiolated chitosans (Roldo *et al*., 2004). Thiolated chitosans also display, excellent cohesive properties besides their strong mucoadhesive and permeation enhancing properties. The cohesion and stability of a drug delivery system over the intended duration of drug release is an important prerequisite for controlled release. Model drugs, such as clotrimazole have been used to demonstrate the effectiveness of thiolated chitosans as carrier matrices for controlled drug release (Bernkop-Schnürch *et al*., 2003a; Roldo *et al*., 2004; Langoth *et al*., 2004; Kast *et al*., 2002).

1.7 Formulation techniques

1.7.1 Lyophilisation

1.7.1.1 Lyophilisation principles

Lyophilisation is a dehydration technique which enables liquid or slurry products, which have previously been frozen to be dried under a vacuum. The basic idea of lyophilisation is to "lock in" the composition and structure of the material by drying it without applying the heat necessary for the evaporation process. Instead, the lyophilisation process converts solid water (ice) directly into water vapour (sublimation), skipping the liquid phase entirely (Kasper & Freiss, 2011; Wang, 2000). Sublimation occurs when a molecule gains enough energy to break free from the molecules around it. There are two major factors that determine what phase (solid, liquid or gas) a substance will adopt: temperature and atmospheric pressure. For a substance to assume any particular phase, the temperature and pressure must be within a certain range (Bindschaedler 1999, cited in Wang, 2000). Without these conditions, that phase of the substance cannot exist. The chart in Figure 1.15 shows the necessary pressure and temperature values of different phases of water.

Lyophilisation is often used to stabilize protein products with limited shelf lives in solution (Fox, 1995). It is therefore, not surprising that over 50% of the therapeutic protein products in the market are lyophiles (Constantino, 2004, cited in Kasper & Freiss, 2011). It is important to optimise the lyophilisation cycle because of the physical changes that occur for proteins in solution during the freezing and drying phases of the process. Due to the amorphous nature of proteins and stabilizer (most commonly sugars and polyols), lyophilized formulations often exhibit a glass–rubber transition that is an important parameter in the development of the optimum freeze–drying cycle (Nail *et al*., 2002, cited in Kasper & Freiss, 2011). Therefore it is imperative that the thermal events such as glass transition of a lyophilised product be studied and applied to improve processability, quality and stability of the final product (Chen & Oakley, 1995).

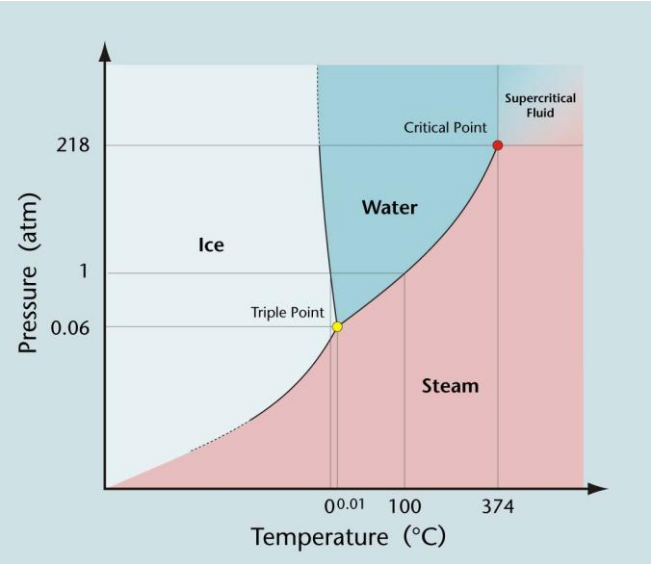

Figure 1.15: Phase diagram of water**.** Available at <http://langlopress.net/homeeducation/resources/science/content/support/illustrations/Chemistry/ > [Accessed; 25/05/2011]

1.7.1.2 Critical lyophilisation parameters

Historically, lyophilisation cycle development could involve 15 to 20 pilot runs before achieving an acceptable lyophilized product. The final product would then be assessed based on physical appearance, reconstitution time, the stability profile of the active constituents and residual moisture content. Without neglecting the preferred qualities mentioned above, time and cost implications and meeting market demand have however become major determining factors in modern lyophilisation cycle development and optimization. A strong foundation for novel cycle developed through to data review acquired from pre-formulation, formulation and

stability studies among others can assure an optimised cycle and a resultant stable product (Wang, 2000). In the selection of excipients and their respective concentrations, their effects on stability of bulk drug, existence of polymorphs, crystalline/amorphous/metastable characteristics, pH, oxidative and thermal stability profiles must be addressed in order to arrive at an optimised cycle (Franks, 1994). An understanding of the thermal characteristics and their determination are crucial in the cycle development (Schwegman, 2009).

Thermodynamic events such as glass transitions, eutectic temperatures and melting point which could occur with changing temperature need to be determined and their effects minimized on the stability of the final product. Glass transition temperature of polymeric amorphous materials has been determined by various methods (Utracki *et al*., 1989) such as dilatometry, differential scanning calorimetry (DSC) or differential thermal analysis (DTA), spectroscopy, diffraction, rheological and dielectric methods. Among them, the DSC method is one of the most convenient for determining the glass transition temperature of a polymer by measuring the difference in heat capacity (Crowe *et al*., 1998). Section 1.8.5 details the application of DSC in lyophilisation process

1.7.1.3 Lyophilisation cycle

Generally, the lyophilisation cycle consists of three different phases (Wang, 2000; Pikal, 2002): namely freezing stage, primary drying and secondary drying which are further discussed below.

1.7.1.4 Freezing

An initial freezing process is selected, with the intent that the product exhibits the desired crystalline structure and that the product is frozen below its eutectic temperature (lowest possible complete melting point). Upon completion of product freezing, the product will have acquired a frozen structure, which cannot be changed during lyophilisation (Pikal, 1990). Sublimation and the qualities of the finished product are greatly dependent on this crystal structure. In fact, it is considered the most crucial stage of the lyophilisation process (Willemer, 1992, cited in Wang, 2000). A typical initial shelf temperature of 5 °C is necessary for cycles that require pre-chilling before sample loading as this can impact on product stability. The samples must be arranged in a way as to help each vial reach temperature equilibration before freezing to the final set point. Strambini & Gabelleiri (1996) have indicated that stresses associated with freezing can damage some sensitive molecules such as proteins. It is therefore crucial that the selection of the rate of shelf cooling be informed by

preliminary investigation of the potential for freezing induced damage, super-cooling, product characteristics and the attainment of product stability. The final freezing set point must be selected below the glass transition (Tg') to avoid having fluid in the interstitial spaces of the product. The product must be completely frozen before the start of the primary drying stage.

1.7.1.5 Primary drying

The primary drying (sublimation) phase is the stage during which the partial pressure of the vapour surrounding the product must be lower than the pressure of the vapour from the ice at the same temperature (Willemer, 1992, cited in Wang, 2000). The energy supplied in the form of heat during primary drying must remain lower than the product's eutectic temperature (the highest allowable product temperature during the conditions of sublimation) (Wang, 2000). Once the product is properly frozen, it must be sublimated (evaporated) at a low temperature under reduced pressure. With the product maintained at a constant temperature, it will be necessary to supply the total energy required for sublimation, from a combination of the latent heat of fusion (which supplies the transformation of the liquid to the ice state) and the sublimation energy (about 700 calories per gram of ice evaporated). The temperature difference between the product and the condenser (a minimum of 20 °C below the product temperature) is the driving force for water sublimation (Franks, 1990).

1.7.1.6 Secondary drying

The secondary drying phase is aimed at eliminating the final traces of water which remain due to adsorption (Arakawa *et al*., 1993, cited in Wang, 2000), and where the partial pressure of the vapour rising from the product will be at its lowest levels. At the end of the sublimation phase (primary drying), all the ice will have disappeared. The product will begin to rise in temperature, and will tend to approach the control temperature of the shelf. This must be maintained at the most maximum permissible temperature to liberate the small amount of residual moisture embedded within the matrix. However, at this stage the product is not sufficiently dry for long term storage. For most products, the residual moisture is in the region of 5% to 7% (Ward *et al*., 2008). The lyophilisation cycle then enters the desorption phase during which the last traces of water vapour are removed, along with traces of the "bound" water within the product matrix (Bindschaedler, 1999, cited in Wang, 2000). The aim of this final phase is to reduce the product to the acceptable moisture levels needed for long term storage. The reasons for drying the product to these desired levels are to avoid product denaturation at higher water content and chemical or enzymatic changes at forced lower residual moisture content. The residual moisture content in the product is dependent on

the product matrix, the vacuum of the drying chamber, duration of the secondary phase and the maximum temperature allowed in the product during secondary drying.

At the completion of the freeze-drying process, the treated product will have retained its form, volume and original structure as well as all its physical, chemical and biological properties. It can then be stored for an almost indefinite period of time. As the product is porous, it can be re-dissolved by the simple addition of an appropriate solvent (Bunte *et al.*, 2010).

1.7.2 The Freeze-drier machine

A typical freeze drier machine [Figure 1.16(b)] consists of a freeze-drying chamber with several shelves attached to heating units, a freezing coil connected to a refrigerator compressor and a vacuum pump [Figure 1.16(a)]. The freeze dryer is also equipped with a condenser designed and constructed with the ability to condense all vapours from the product and to provide a route of minimum resistance to avoid hindering vapour flow. The ice condenser provides a vacuum effect via the pressure differential created between the surface temperature of the product and the condenser.

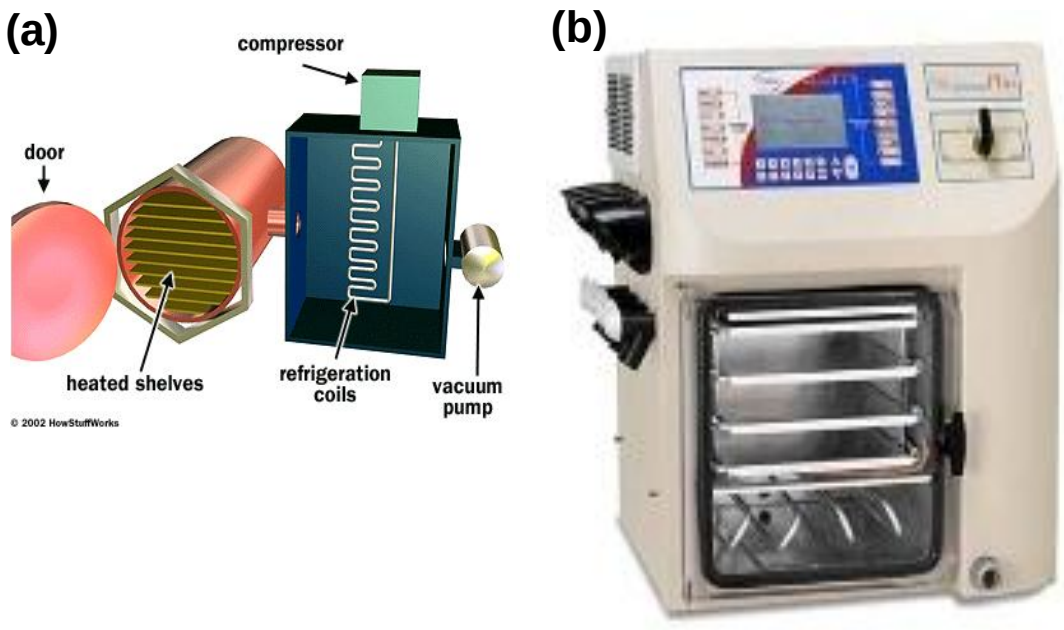

Figure 1.16: (a) Simplified freeze-dryer (b) Virtis AdVantage XL70 Freeze dryer. Available at <http://www.biopharma.co.uk/biopharma-process-systems > [Accessed; 2/04/2011].

1.7.3 Gel formation

A gel is a colloidal solution formed from a continuous solid phase within which molecules of a discontinuous liquid phase are dispersed. It is characterised by a network of polymeric chains connected by either chemical or physical bonds (Benguigui, 1999). Gels are mostly liquid; however, they behave like solids, because of the 3-D cross-linked arrangement within the liquid, trapping it through surface tension effects. The cross-linkages in gels impart hardness (structure) and tack (stickiness) as a result of physical or chemical bonds that are maintained within the extending fluid such as water (hydrogel), oil or air (aerogel). The fluidity of gels allows for the display of similar densities with those of their component liquids.

Natural or synthetic hydrogels formed from a network of polymer chains are hydrophilic, retaining large volumes of water in their swollen structures with a high degree of flexibility, resembling natural tissues (Vashist *et al*., 2011). They are therefore used as scaffolds in tissue engineering (El-Tahlawy *et al*., 2010, cited in Vashist *et al*., 2011), hydrogel coated wells for cell culture, intelligent drug delivery systems (DDS) (Cenci *et al*., 2012) and controlled drug release systems (Luo *et al*., 2008). Synthetic polymers used in hydrogel preparation include polyvinyl alcohol, acrylate polymers and sodium polyacrylate. Examples of natural hydrogel ingredients studied for tissue engineering and as DDS are chitosan and chitosan derivatives, agarose, methyl cellulose and hyaluronan.

1.7.4 Polymeric buccal drug delivery systems

1.7.4.1 Polymeric films for drug delivery

Polymeric films for drug delivery purposes are prepared from hydrogels using either solvent casting technique (Boateng *et al*., 2009, 2010) or hot melt extrusion technique (Morales & McConville 2011). Solvent cast is the most commonly used method because of ease of process and low cost. In the solvent cast method, a gel is prepared by mixing the polymer base with other excipients such as plasticizers and active pharmaceutical ingredient (API) in a suitable solvent that may be heated to aid dissolution. The rheological properties of the solution are of utmost concern during processing (Barnhart, 2008, cited in Morales & McConville 2011). The solution is kept under continuous mixing at a controlled temperature to ensure uniform drug distribution and viscosity. Entrapped air which affects film uniformity is then removed by dearation to obtain films with desired uniformity (Dixit & Puthli, 2009). The solution is then cast in moulds to the desired thickness and subjected to drying process in

an oven at an appropriate temperature to remove the solvent. The drying process may be controlled to achieve films with desired moisture content.

Due to convenience and patient compliance, polymeric films have gained significance as novel DDSs in the pharmaceutical arena. They have been studied for application as mucoadhesive buccal films for local (oral candidiasis) (Repka, 2003 cited in Morales & McConville, 2011) or systemic effect (INS delivery) (Giovino *et al*., 2012). Mucoadhesive hydrophilic polymers have the ability to swell, allowing interaction with mucin molecules in the mucosal membrane for prolonged attachment and subsequent drug release.

1.7.4.2 Lyophilised xerogels (wafers) as drug delivery systems

A xerogel is a solid formed from the drying of a gel that exhibits high porosity with an enhanced surface area. Solvent removal is mostly achieved by lyophilisation or under supercritical conditions that results in a solid with low-density and non-shrinking network.

Lyophilised xerogels (or wafers) are relatively novel formulations prepared by lyophilisation of polymeric solutions or gels to yield solid porous cakes that can easily be applied to mucosal surfaces (Mathews *et al*., 2003; Boateng *et al*., 2010). Xerogels provide a potential means of delivering pharmacological agents such as proteins to mucosal surfaces for both local and systemic applications. They offer advantages over other delivery systems such as semi solid polymer gels and solvent cast films. Unlike semi solid polymer gels which flow easily after application, xerogels, can maintain their swollen gel structure for a longer period and therefore longer residence time (Mathews *et al*., 2005) to allow for effective drug absorption. Due to their porous nature and larger surface area, xerogels have a higher drug loading capacity compared to the thin and continuous solvent cast equivalent (Boateng *et al*., 2010). Xerogels have been developed from sodium alginate and sodium carboxymethylcellulose for the delivery of hydrophilic drugs via mucosal surfaces (Boateng *et al*., 2010). Lyophilised xerogels produced from xanthan have been studied to provide an effective and stable storage medium for insoluble drugs intended for delivery at the site of action (Mathews *et al*., 2008).

1.8 Analytical techniques

1.8.1 Nuclear magnetic resonance (NMR) spectroscopy

Nuclear magnetic resonance (NMR) spectroscopy has been an important analytical technique for structural elucidation of organic compounds over the past five decades. It is the only spectroscopic technique that offers a complete analysis and interpretation of the entire spectrum. NMR is non-destructive requiring less than a milligram of samples to acquire good data though the sample size is usually more than that needed for mass spectroscopy (www2.chemistry.msu.edu) or circular dichroism. Proton NMR spectroscopy is a well-established novel application of NMR, where the NMR spectrometer is tuned to a proton (specific nucleus). The spectrum may be obtained by continuous wave (CW) (Figure 1.17) or the more preferred pulse Fourier transform technique.

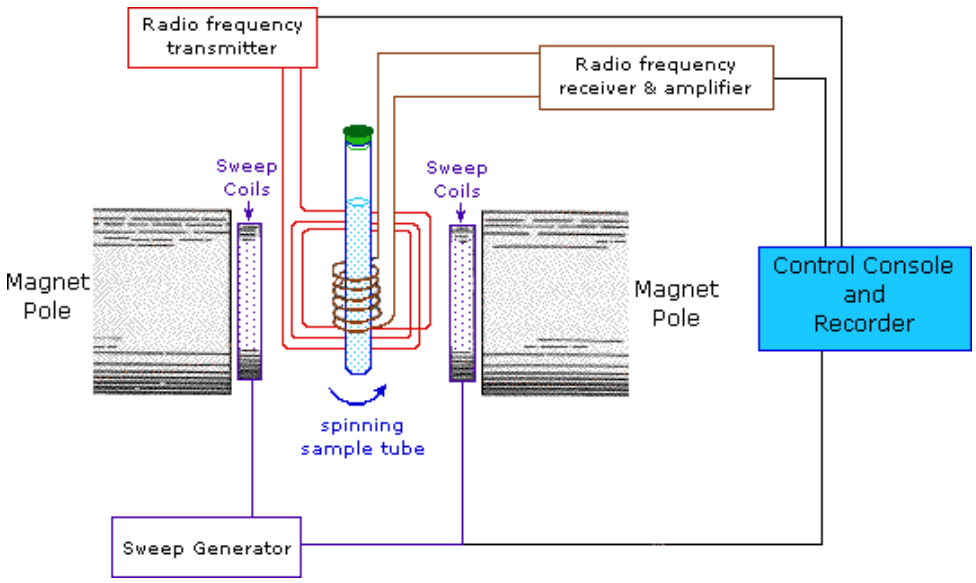

Figure 1.17: Typical Continuous wave spectrometer. Available at <http://www2.chemistry.msu.edu/faculty/reusch/VirtTxtJml/Spectrpy/nmr/nmr1.htm > [Assessed; 25/05/12]

Typically, a solution of the sample in a glass tube (5 mm) covered by a receiver coil is oriented between the poles of a strong magnet and spun to average out any magnetic field variation and tube imperfections. A radio frequency (rf) radiation is then sent from an antenna coil with appropriate energy and the absorbed rf energy emitted is monitored and recorded. Acquisition of NMR spectra occurs by magnetic field variation or sweeping, while monitoring the rf emission from the sample.

Several analytical procedures have been employed to characterise chitosan and thiolated chitosans. Techniques such as ^{1}H-NMR (Juntapram et al., 2012; Shigemasa *et al*., 1996, cited in Fernandez-Megia *et al*., 2005), solid state ^{13}C-NMR (Rinaudo, 2006), IR (Duarte *et al*., 2002 cited in Fernandez-Megia *et al*., 2005), and CD (Domard, 1987, cited in Fernandez-Megia *et al*., 2005) have been reported. However, standards requirements for IR and CD procedures and time consumption in the case of solid state ^{13}C-NMR makes ^{1}H-NMR an excellent technique for the characterisation of chitosan and its derivatives (Fernandez-Megia *et al*., 2005). In addition, ^{1}H-NMR is robust and allows the quick identification of impurities present in chitosan samples as well as serves as a calibration tool for other analytical procedures such as CD and mass spectrometry (Brugnerotto *et al*., 2001 cited in Fernandez-Megia *et al*., 2005).

1.8.2 Gel permeation chromatography (GPC)

Gel permeation chromatography (GPC) is an analytical technique that separates analytes based on size. The size exclusion chromatographic technique is often used to analyse and characterise polymers using polydispersity index (PDI) and the molecular weight. A variety of definitions for molecular weight are used when characterising polymers by GPC. These include number average molecular weight (M_n), the weight average molecular weight (M_w), the size average molecular weight (M_z) and the viscosity molecular weight (M_v). Information obtained from PDI and M_v are used with other data to determine the M_n, M_w and M_z. The intrinsic viscosity defines the shape function and the molecular volume which is actually measured by GPC. The use of comparable standards allows the use of this relative data to determine molecular weights within an accuracy of ± 5 %.

GPC works as a normal chromatographic procedure using carefully controlled gels as stationary phase which desirably lacks ionising groups with low affinity for the analyte in a given solvent. Gels such as cephalex, bio-gel, agarose gel and styragel are commercially available for different separation procedures. GPC gives well defined time separation as well as provides narrow bands. There is less likelihood for analyte loss as there is no physical or chemical interaction between the column and analyte (Skoog, 2006). GPC is convenient for determining the molecular weight of polymers as the method is less time consuming (Cowie *et al*., 2008).

1.8.3 Fourier transform infrared (FT-IR) spectroscopy

Infrared (IR) spectroscopy is a chemical analytical technique, which measures the infrared intensity versus wavenumber of light. Based upon the wavenumber, infrared light can be categorized as far infrared (4 ~ 400 cm^{-1}), mid infrared (400 ~ 4,000 cm^{-1}) and near infrared (4,000 ~ 14,000 cm^{-1}). An FT-IR spectrometer (Figure 1.18) acquires and digitizes the interferogram, performs the Fourier transform function, and outputs the spectrum. Infrared spectroscopic studies by Dong *et al*., (1995) concluded that the acute freezing and dehydration stresses of lyophilisation can induce protein unfolding. The enhanced FT-IR studied by Roy & Gupta (2004) in the case of basic fibroblast growth factor and γ-interferon showed large conformational changes and aggregation during freeze–drying. This could be prevented by using sucrose as a lyoprotectant. In the presence of moisture, freeze–dried proteins can undergo disulphide interchange and other reactions, which lead to inactivation. Such molecular changes during storage have been described for human INS, tetanus toxoid and interleukin-2. The underlying assumption is that IR spectral changes in the amides I and II regions upon protein dehydration are caused by protein structural changes (Tattini *et al*., 2005). This makes IR useful for providing information about protein conformation and stability during processing and storage.

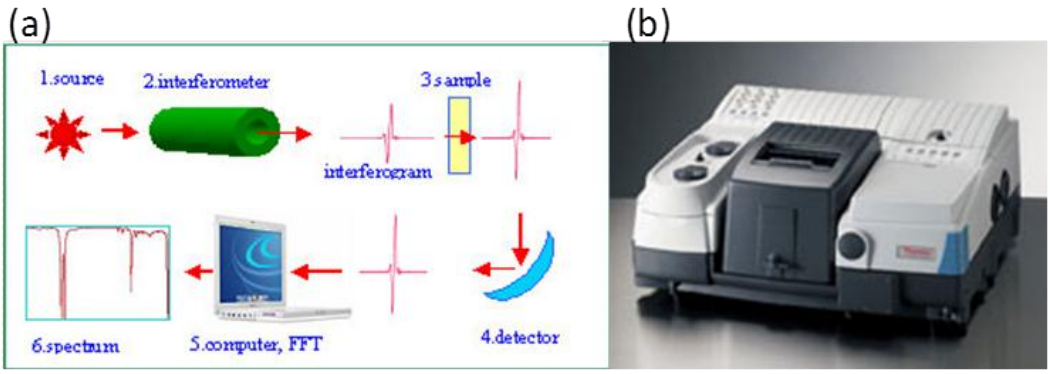

Figure 1.18: Schematic illustration (a) and (b) digital image of FT-IR system. Available at <http://thermoscientific.com > [Assessed; 20/07/2011]

1.8.3.1 Attenuated total reflection (ATR-FT-IR) spectroscopy

Attenuated total reflection (ATR) using FT-IR spectroscopy is considered one of the most simple, direct, flexible and sensitive *in situ* infrared technique for the analysis of the surface of materials. In ATR-FT-IR spectroscopy, the IR radiation is passed through an IR

transmitting crystal with a high refractive index, allowing the radiation to reflect within the ATR element several times.

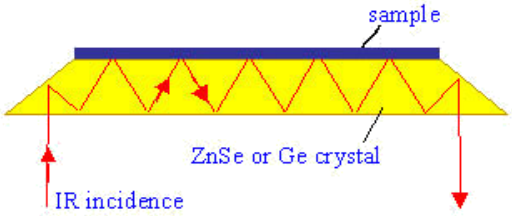

Figure 1.19: Schematic illustration of ATR-IR through a transmitting crystal. Available at <http://www.nuance.northwestern.edu/KeckII/Instruments/FT-IR/keck-ii%20pages1.html> [Assessed; 25/07/2011]

The sampling surface is pressed into intimate optical contact with the top surface of the crystal such as ZnSe or Ge. The IR radiation from the spectrometer enters the crystal, then reflects through the crystal and penetrating "into" the sample a finite amount with each reflection along the top surface via the so-called "evanescent" wave (Figure 1.19). To obtain internal reflectance, the angle of incidence must exceed the so-called 'critical' angle. This angle (equation 1.1) is a function of the real parts of the refractive indices of both the sample and the ATR crystal:

$$\Theta c = \sin^{-1}(n_2/n_1) \text{ .....equation 1.1}$$

Where n_2 is the refractive index of the sample and n_1 is the refractive index of the crystal. The depth of penetration of the evanescent wave d is defined as the distance from the crystal-sample interface where the intensity of the evanescent decays to $1/e$ (37 %) of its original value. It can be given by equation 1.2:

$$d = \lambda / \{2\pi n_1[\sin^2\Theta-(n_2/n_1)^2]^{1/2}\} \text{.....equation 1.2}$$

λ is the wavelength of the IR radiation. Different crystals have different refractive indices depending on the material used and are applied to different transmission ranges (ZnSe for 20,000~650 cm^{-1}, Ge for 5,500~800 cm^{-1}).

1.8.4 X-ray powder diffractometry (XRPD)

1.8.4.1 X-ray generation and properties

X-rays are electromagnetic radiation with typical photon energies in the range of 100 eV - 100 keV. For diffraction applications, only short wavelength X-rays (hard X-rays) in the range of a few angstroms to 0.1 angstrom (1 - 120 keV) are used. X-rays are generally produced by either X-ray tubes or synchrotron radiation. X-rays are generated when a focused electron beam accelerated across a high voltage field bombards a stationary or rotating solid target. As electrons collide with atoms in the target and slow down, a continuous spectrum of X-rays are emitted, which are termed Bremsstrahlung radiation. Common targets used in X-ray tubes include Cu and Mo, which emit 8 keV and 14 keV X-rays with corresponding wavelengths of 1.54 Å and 0.8 Å, respectively.

The peaks in an X-ray diffraction pattern are directly related to the atomic distances. For a given set of lattice planes with an inter-plane distance of "d" (Figure 1.20), the condition for a diffraction (peak) to occur can be simply written as equation 1.3 which is known as the Bragg's law, after W.L. Bragg, who first proposed it.

$$2\,d\sin\theta = n\lambda \quad \text{.....equation 1.3}$$

Where λ is the wavelength of the X-ray, θ the scattering angle, and n an integer representing the order of the diffraction peak.

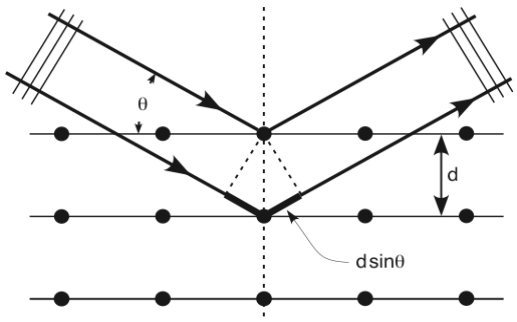

Figure 1.20: The relationship between atomic lattice planes and x-ray diffraction pattern Available at < http://web.pdx.edu/~pmoeck/phy381/Topic5a-XRD.pdf > [Assessed 25/07/2011].

1.8.4.2 Powder diffraction

Powder XRD (X-ray diffraction) is perhaps the most widely used X-ray diffraction technique for characterizing materials. Powder diffraction data can be collected using either transmission or reflection geometry, as shown in Figure 1.21. Because the particles in the powder sample are randomly oriented, these two methods will yield the same data.

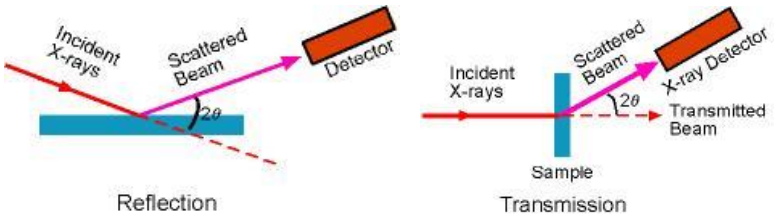

Figure 1.21: Reflection and transmission geometries

Figure 1.22 shows the Bruker D8 Advance X-ray equipment used in this project. It is a very easy to use X-ray diffractometer that measures powders and thin films in the two theta (2θ) configuration. The system is fitted with a Lynx Eye detector that is five times more sensitive than its predecessor. It is fast, high resolution, sensitive, and robust. The D8 can conveniently measure from 5 to 125 degrees 2θ. During measurements, the default power level is 40 kV and 40 mA. The X-ray source uses a copper target. By default there should be a 0.6 mm slit between the source and the sample.

Figure 1.22: Bruker D8 Advance XRD. Available at < http://www.bruker-axs.com/d8_advance.html > [Assessed; 27/07/2011].

1.8.5 Differential scanning calorimetry (DSC)

Materials that are exposed to changing temperatures will undergo physical or chemical changes to their structure. When a material goes through these physical or chemical changes as a function of temperature, they will either release a small amount of energy to the surrounding environment (exothermic), or absorb some heat from the surrounding environment (endothermic). This small amount of heat that is either given off or absorbed by the system is the basic principle behind DSC (Ford & Mann, 2012). The DSC instrument (Figure 1.23) is composed of a sample and reference chamber (furnaces). DSC incorporates a separate heating source for both the sample and reference cells. By having separate furnaces for the sample and the reference material, the DSC is capable of calculating the heat flow to the sample material. When the sample goes through a physical or chemical change in response to a change in temperature, it will give off or absorb a small amount of heat from the environment. The instrument senses this and applies or removes heat to keep the sample at the same temperature as the reference (Spink, 2008). Since the instrument is measuring heat flow instead of just the temperature difference between the sample and reference, it is possible to calculate some of the thermodynamic values for the transition.

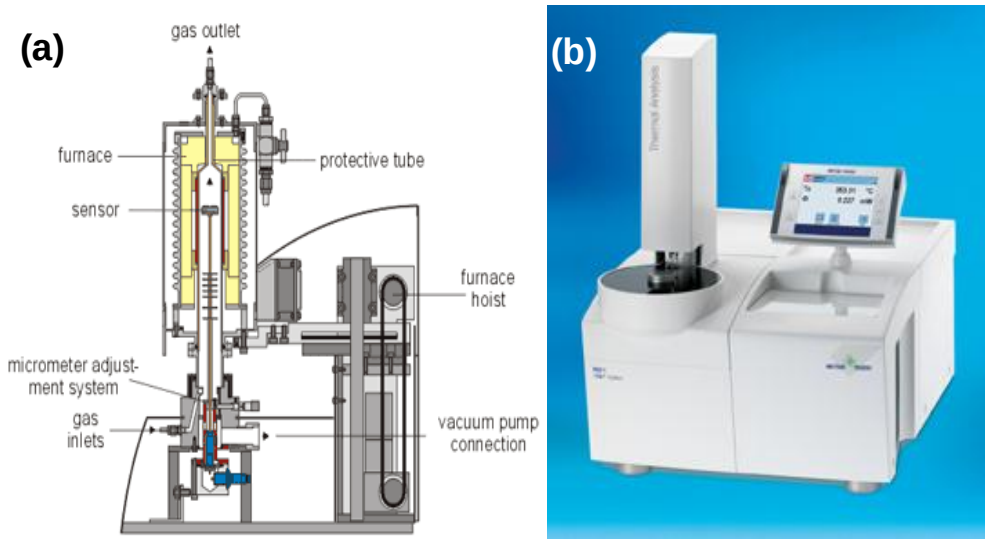

Figure 1.23: The DSC instrument (a) a schematic diagram showing the essential parts of a DSC (b) picture of thermal analysis DSC adapted from Mettler Toledo. Available at <us.mt.com/.../DSC_Module_DSC1.html > [Assessed; 28/5/2011].

1.8.5.1 Interpreting DSC thermogram in lyophilisation

The DSC technique has been used to provide qualitative and quantitative information about the physicochemical status of drug or excipient particles, which may be involved in either an endothermic or exothermic process (Mu & Feng, 2001). The DSC thermal analysis experiment gives two key pieces of information that were exploited for lyophilisation cycle development. The first information gained from these experiments is the physical form of the solids formed during freezing. Specifically, it helps in determining if the system is forming an amorphous glassy phase, a crystalline eutectic phase, a metastable glassy phase, or is a mixture of these different phases. The second information gained from these studies is the critical temperature associated with each of these phases. These critical temperatures are important, because they represent the maximum temperature that the product can withstand during primary drying without suffering from collapse or eutectic melting. The critical temperatures of interest determined through DSC thermal analysis are the glass transition temperature (Tg), the eutectic melting temperature (T*e*), and the collapse temperature (T*c*) of the product. Identification of the type of event that is occurring as the sample is warmed (eutectic melt, glass transition) is based upon the characteristic shape of the curve that is generated in the thermogram as the sample goes through that particular thermal event (Nail, & Gatlin, 1992). Generally, the Tg is read at the initial change in the slope of the heat capacity of the DSC thermogram, i.e. the temperature at the onset of a baseline step in the DSC curve (Sakurai *et al*., 1997). It represents the temperature at which a rubbery state is attained by an amorphous material from a glassy state (Bley, 2009, cited in Ford & Mann, 2012). T*e* refers to the point where crystallizing out of the least soluble component of an aqueous protein formulation and water occurs at the same time as a mixture, following a further reduction in temperature after the crystallization of the least soluble component (Wang, 2000). The T*c* is the temperature at which the interstitial water in the frozen matrix becomes significantly mobile (Jenning, 1999, cited in Wang, 2000).

Occasionally, sensitivity and or resolution enhancement of a thermogram will be needed. For example, some glass transitions occur with such low energy, they cannot be detected using a typical DSC heating protocol. Furthermore, transitions will sometimes overlap because their onset temperatures are so close. In these particular cases, resolution and sensitivity of the instrument can be improved by altering the heating rate through the different transitions (Nail *et al.,* 2000). Generally, increasing the heating rate (up to 60 °C/minute) through the transitions increases the sensitivity, and decreasing the heating rate (down to 0.1 °C/minute) through the transitions, increases the resolution. A standard protocol for a DSC thermal analysis study would involve cooling the sample from ambient to -60 °C at 5 to 10

°C/minute. Once the temperature stabilized, the sample would then be warmed back to ambient at approximately 20 °C/minute to remove previous thermal history (Boateng, 2005), followed by a second cycle of heating.

1.8.6 Circular dichroism (CD) spectroscopy

Circular dichroism (CD) refers to the differential absorption of left handed (L) and right handed (R) circular plane polarised light by a substance containing one or more chiral chromophores.

$$\text{Circular dichroism} = \Delta A(\lambda) = A(\lambda)_{LCPL} - A(\lambda)_{RCPL} \text{.....} \textit{equation 1.4}$$

where λ is the wavelength. The resultant radiation is said to possess elliptical polarisation which is the CD signal observed due to the chiral chromophoric groups measured as ellipticity (θ) in degrees. Figure 1.24 shows a typical CD spectrometer.

Figure 1.24: Chirascan™-plus Circular Dichroism Spectrometer. Available at <https://www.photophysics.com/chirascan_plus.php. > [Assessed; 28/05/2012]

CD spectroscopy finds its most important application in the study of large biological molecules. It is however used extensively in the study of chiral molecules of all types and sizes. CD has become a valuable spectroscopic technique for the study of protein structures in solution as well as folding thermodynamics (Greenfield, 2006, cited in Khrapunov, 2009). Conformational motifs such as α-helixes, β-pleated sheets, poly-β-proline II-like helices and turns of proteins exhibit characteristic far-UV CD spectra (absorption below 240 nm), the sum of which can be used to assess secondary structure. Disulphide bonds show weak broad absorption bands centred around 260 nm. Near-UV CD spectra may also serve as useful probes for protein tertiary structure due to chromophores of aromatic amino acid proteins

(absorption in the range 260 to 320 nm). Protein-ligand interactions and protein denaturation may also be followed quantitatively by CD technique (Greenfield, 1999). In addition, protein CD spectroscopy as a low resolution structural technique allows the description of the overall structural features unlike X-ray crystallography or NMR which are able to give structural information on proteins at atomic level of resolution but requires highly crystalline proteins and high protein concentration respectively. The technique is also rapid (less than 30 minutes), requires small amount of sample (0.1 -1 mg) and is also non-destructive (Kelly *et al*., 2005).

1.8.7 Thermogravimetry (TG)

Thermogravimetry (TG) measures the amount and rate of change in the weight of a material as a function of temperature or time in a controlled atmosphere. Measurements are used primarily to determine the composition of materials and to predict their thermal stability at temperatures up to 1000 °C. The technique can characterise materials that exhibit weight loss or gain due to decomposition, oxidation, or dehydration. The information that may be obtained from TG analysis include composition of multicomponent systems, thermal and oxidative stability of materials, estimating the shelf life of a product, decomposition kinetics of materials, the effect of reactive or corrosive atmospheres on materials, moisture and volatiles content of materials. The technique is also applied for the analysis of product deterioration following kinetic oxidation at high temperature (Rodrıguez-Spong *et al*., 2004).

The analyser (Figure 1.25) usually consists of a high-precision balance with a pan (generally platinum) loaded together with the sample. The sample is placed in a small electrically heated oven with a thermocouple to accurately measure the temperature. The atmosphere may be purged with an inert gas such as nitrogen to prevent oxidation or other undesired reactions. The instrument is linked with a computer for controls. A dynamic phase of heating is carried out by raising the temperature of the sample gradually and plotting weight (percentage) against temperature. Curve smoothing and other parameters may be input to determine the exact points of inflection after data acquisition. A current method known as hi-resolution TG is often employed to obtain greater accuracy in areas where the derivative curve peaks. In this method, temperature increase is isothermal as weight loss increases. This is to more accurately identify the exact temperature where a peak occurs. Several modern TG devices can vent burn-off to an infrared spectrophotometer to analyse composition.

Figure 1.25: Thermogravimetric analyser. Available at < http://www.tainstruments.com > [Assessed; 25/07/2011]

1.8.8 Scanning electron microscope (SEM)

The scanning electron microscope (SEM) is used for observation of specimen surfaces. When the specimen is irradiated with a fine electron beam (electron probe), secondary electrons are emitted from the specimen surface. Topography of the surface can be observed by two dimensional scanning of the eletron probe over the surface and acquisition of an image from the detected secondary electrons.

The SEM (Figure 1.26) requires an electron optical system, a specimen stage to place the sample, a secondary electron detector to collect secondary electrons, an image display unit, and an operation system to perform various operations. The electron optical system consists of an electron gun, a condenser lens, and an objective lens to produce an electron probe, a scanning coil to scan the electron probe, and other components. The electron optical system in the microscope column and the space surrounding the specimen are kept at vacuum to avoid collisions between electrons of the beam and stray molecule, to avoid damaging the filament and to prevent absorption of X-rays produced from the sample by air molecules (www4.nau.edu).

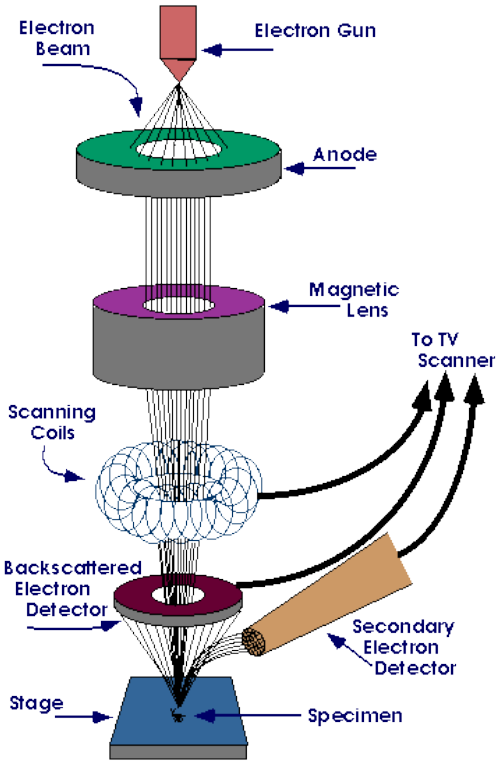

Figure 1.26: Representation of SEM. Available at < www.purdue.edu/rem/rs/sem.htm> [Assessed; 30/05/11]

In a typical SEM, an electron beam is thermionically emitted from an electron gun fitted with a tungsten filament cathode. Tungsten is normally used in thermionic electron guns because it has the highest melting point and lowest vapour pressure of all metals, thereby allowing it to be heated for electron emission, and because of its low cost. Other types of electron emitters include lanthanum hexaboride (LaB_6) cathodes. The electron beam, which typically has an energy ranging from 0.5 keV to 40 keV, is focused by one or two condenser lenses to a spot about 0.4 nm to 5 nm in diameter. The beam passes through pairs of scanning coils or pairs of deflector plates in the electron column, typically in the final lens, which deflect the beam in the *x* and *y* axes so that it scans in a raster fashion over a rectangular area of the sample surface. When the primary electron beam interacts with the sample, the electrons lose energy by repeated random scattering and absorption within a teardrop-shaped volume of the specimen known as the interaction volume, which extends from less than 100 nm to around 5 µm into the surface. The beam current absorbed by the specimen can also be detected and used to create images of the distribution of specimen current. Electronic amplifiers of various types are used to amplify the signals which are displayed as variations in brightness on a cathode ray tube (CRT). The raster scanning of the CRT display is

synchronised with that of the beam on the specimen in the microscope, and the resulting image is therefore a distribution map of the intensity of the signal being emitted from the scanned area of the specimen. The image is digitally captured and displayed on a computer monitor.

1.9 Aims and objectives

The main aim of this project was to develop, formulate, characterise and optimise novel lyophilised formulations (xerogels) that will deliver therapeutically relevant protein-based drugs via the buccal mucosa route. The development will be focused on obtaining formulations with optimized drug loading, drug release and permeation, long shelf-life and low toxicity.

The main objectives include:

1. Pre-formulation studies, to identify and characterise biocompatible and biodegradable polymeric systems, with potential for targeting particular organs/tissues and ability to deliver proteins via the buccal mucosa, will be carried out. Work will range from basic formulation (such as polymer gel preparation, film formation, lyophilisation of polymer gels including annealing studies to select the optimum freeze-drying parameters that will ensure product stability, *in vitro* and *ex vivo* evaluation and stability testing (including use of HPLC, DSC, ATR-FT-IR, and CD) of the novel formulations.
2. Lyophilisation cycle and formulation development using various polymeric systems in conjunction with the protein based drugs to obtain an optimised lyophilised buccal drug delivery system (xerogel).
3. Physico-chemical and bio-analytical methods (GPC, NMR, SEM, TA, TGA, DSC, ATR-FTIR, CD, UV, HPLC and XRD) will be used to characterise the physicochemical properties of the protein loaded lyophilised xerogels.
4. Toxicity (cell viability) studies during and after *ex vivo* drug permeation studies in Epi-Oral^{TM} buccal tissue constructs and sheep buccal tissue.
5. Accelerated and real time stability evaluation of the novel drug delivery systems using International Conference on Harmonisation (ICH) conditions will be determined.
6. Potential applications of these characterised systems in important areas such as buccal mucosal INS delivery will be explored.

CHAPTER TWO

FORMULATION DEVELOPMENT AND OPTIMISATION

2.1 Introduction

Parenteral injections have been the major route of systemic delivery of protein and peptide drugs for decades. The challenge of high injection frequency, pain, injection site reactions and consequent patient non-compliance still remains (Mathias & Hussain, 2010). Alternative non-invasive routes (e.g. buccal, nasal, ocular and GI tract) for the delivery of proteins and peptide drugs have been investigated (Khafagy *et al*., 2007; Hearnden *et al*., 2012). These potential routes may also be limited by factors such as enzymatic inhibition in the GIT and at mucosal sites, hepatic first pass metabolism and size exclusion at epithelial barriers (Morishita & Peppas, 2006). The buccal mucosa offers a potential portal for the administration of therapeutic proteins/peptides for both systemic and local delivery (Senel *et al*., 2000).

In developing alternative protein/peptide delivery systems with high bioavailability, the use of permeation enhancers (PE), enzyme inhibitors (EI) and the exploitation of bioadhesive delivery systems have been investigated as strategies to overcome protein permeation challenges and for the maintenance of the biological activity of the proteins (Bernkop-Schnürch & Dünnhaupt, 2012). Mucosal drug delivery systems promote less frequent dosing, site-specific targeting and maintains effective plasma concentration through prolonged attachment and subsequent drug release.

This chapter briefly discusses background to experimental techniques employed to develop chitosan and chitosan-thioglycolic acid (TG-chitosan) xerogels as novel drug delivery systems for potential protein drug delivery via the buccal mucosa. The chapter describes the various optimisation processes such as membrane dialysis, annealing, thiolation, addition of permeation enhancer and the use of enzyme inhibitors. The formulation process involved developing xerogels from chitosan based matrices which aim to achieve a drug delivery system with optimum functional characteristics including higher drug loading, improved hydration and subsequent drug dissolution and mucoadhesion compared to related mucosal delivery systems such as films (Boateng *et al*., 2009). The addition of appropriate concentrations of glycerol (GLY) and D-mannitol (D-MANN) with the application of membrane dialysis and annealed lyophilisation during processing are expected to impart critical characteristics to the xerogel such as flexibility, toughness, reduced crystallinity and enhanced microscopic architecture.

The advantages of lyophilisation as a drying technique for protein containing xerogels have been discussed in chapter one. Model protein drug BSA and the antidiabetic hormone, INS, will be incorporated in the xerogels that are expected to combine permeation enhancement, protease enzyme inhibition and improved mucoadhesion. These would be achieved by the addition of a permeation enhancer, an enzyme inhibitor and thiolation of chitosan. These strategies are designed to combat drug hydrophilicity, molecular size and proteolytic degradation which limit the permeation of proteins across the buccal membrane. In addition, the xerogels will be laminated on one surface by an impervious EC backing membrane film to ensure release of the protein drug in one direction after application to the buccal membrane.

2.1.1 Annealing

Ice crystallization occurs during the freezing step of lyophilisation with the solute phase becoming highly concentrated. Vitrification of the solute phase to a viscous glass occurs as the temperature of the maximally freeze concentrated solute is reduced below the Tg' (Pikal, 2002). During freezing, primary drying or even storage, however, a number of drugs and excipients tend to undergo incomplete or delayed crystallization resulting in formation of mixtures of different polymorphic forms or vial breakage as in the case of mannitol (Kim *et al*., 1998; Liao *et al*., 2007). These may cause characterisation and reproducibility problems for the product. The purpose of annealing is to remove stresses, soften the material, toughen and reduce brittleness and to obtain a desired structure. It involves heating a material to, and holding at a suitable temperature, followed by relatively slow cooling. In the design of a lyophilisation cycle for a formulation which incorporates a crystallisable compound, this thermal treatment or annealing must be incorporated into the initial freezing step before the primary drying phase is initiated (Searles *et al*., 2001a). The process of annealing allows the product to attain a temperature at or above the glass transition and is therefore employed to facilitate quantitative crystallization of the solutes.

Elevation of product temperature above the $Tg^{'}$ of the crystallizing component results in a significant reduction in viscosity with increased solute mobility. Crystalline and single polymorphic forms are then formed under these conditions. It should however, be noted that the product temperature must be kept below the eutectic point to avoid ice melting. An added advantage of the annealing process is the formation of ice and solute crystals, resulting in 'Ostwald ripening' which is characterised by reduced product resistance, faster water vapour transport and reduction in primary drying times (Searles *et al*., 2001b). Searles *et al*., (2001a)

have recommended annealing time of between two and six hours as additional holding hours do not offer any further advantage. After holding the product at the annealing temperature for the required period of time, it must then be cooled back to the original freezing temperature, allowing adequate time to achieve equilibrium. X-ray powder diffraction (XRPD) and Raman spectroscopy have been used to evaluate the effectiveness of annealing through the characterisation of physical properties of pharmaceutical formulations (Liu, 2006). Luthra *et al*., (2008) demonstrated that annealing decreases the degradation rate of lyophilized aspartame/sucrose and aspartame/trehalose formulations. Their results support the hypothesis that thermal history affects the molecular mobility required for structural relaxation and such an effect is critical for chemical stability.

2.1.2 Effect of cryoprotectants

A cryoprotectant is a substance that is used to protect biological tissue from freeze damage (due to solute concentration). Conventional cryoprotectants include glycols such as ethylene glycol, propylene glycol, glycerol (GLY) and mannitol (D-MANN) (Warne, 2011). Dimethyl sulfoxide (DMSO) is also regarded as a conventional cryoprotectant. Mixtures of cryoprotectants at reduced concentrations have less toxicity and are more effective than single-agent cryoprotectants at higher concentration (Ayensu *et al*., 2011). Cryoprotectant mixtures have been used for vitrification (glass formation), i.e. solidification without any crystal ice formation. Some cryoprotectants function by lowering a solution's or a material's glass transition temperature. In this way, the cryprotectants prevent actual freezing of the material, and the solution maintains some flexibility in a glassy phase. Many cryoprotectants also function by forming hydrogen bonds with biological molecules as water molecules are displaced. Hydrogen bonding in aqueous solutions is important for proper protein and DNA function. Cryoprotectants have also been used to preserve foods. These polyhydroxy compounds are typically inexpensive and do not pose any toxicity concerns (Wang, 2000).

Cryoprotectants have been found to reduce or eliminate the perturbation caused by freezing. Slow freezing (3 °C/h) results in markedly less turbidity after freezing compared to dipping vials in liquid nitrogen (quench freezing), presumably because the relative area of the ice-liquid interface is smaller after slow freezing. Jiang & Nail (1998) measured recovery of enzymatic activity of lactate dehydrogenase and β-galactosidase as a function of freezing rate and found that the rapid freezing of solutions of these proteins using liquid nitrogen consistently resulted in decreased recovery of activity relative to slower freezing methods.

Lee *et al.,* (2009) observed that freezing rate and concentration affect the effectiveness of cryoprotectants used (sucrose, lactose, mannitol, and polyethylene glycol) for a naproxen nano-suspension. Fast freezing rate and high cryoprotectant concentration were generally favoured, when they used an apparatus with a freezing gradient to systematically investigate the effect of cryoprotectants on the re-dispersibility of nanoparticles as a function of freezing rate. In a few cases however, a slower freezing rate resulted in better re-dispersibility under certain conditions such as temperature dependence of solubility or crystallization behavior of the cryoprotectant. This is probably because slow freezing can produce a more cryo-concentrated liquid phase, and the concentrated cryoprotectant in the liquid phase can more effectively protect the nano-particles.

There is a significant body of literature supporting the idea that loss of protein integrity during freezing and freeze-drying is, at least in part, an interfacial phenomenon involving partial denaturation of protein at the ice/freeze-concentrate interface (Strambini & Gabellieri, 1996; Kendrick *et al*., 1995b cited in Wang, 2000). Liu *et al*., (2005) observed the recovery of activity of the model proteins lactate dehydrogenase and glucose 6-phosphate dehydrogenase in a sucrose-glycine-based excipient system after freeze drying by adding 0.01 % polysorbate 80 (a surface active agent) to the formulation. Their data was consistent with an interfacial model for lyophilisation-associated loss of protein activity involving denaturation at a solid/freeze-concentrate interface. Trehalose, glucose, mannitol, and sucrose were chosen as the cryoprotectants in investigating the diameter and the entrapment efficiency of ibuprofen-loaded solid lipid microparticles (SLM) during the freeze-drying process. Trehalose and glucose at concentrations of 15 % and 5 % (w/w) respectively were adjudged to be the most effective in preventing particle aggregation and in inhibiting leakage from drug-loaded particles during the SLM freeze-drying process (Zhang *et al*., 2008). Although the literature is replete with protein physical stabilization during lyophilisation by the use of sucrose, trehalose, D-MANN (Figure 2.3) and polyethylene glycol as cryoprotectants (Lee *et al*., 2009; Wang *et al*., 2009; Zhang *et al*., 2008), these studies did not employ the process of annealing in addition to a cryoprotectant in preventing premature crystallisation of the crystallisable cryoprotectants.

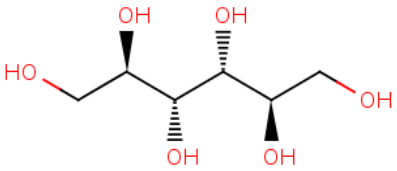

Figure 2.1: Chemical structure of cryoprotectant, D-MANN. Available at <http://www.bmrb.wisc.edu/metabolomics/mol_summary/?molName=D_mannitol> [Accessed; 25/07/2011]

2.1.3 Effect of plasticisers

Low molecular weight, non-volatile and non-separating substances capable of modifying the physical and mechanical properties of polymers are often termed as plasticizers. Their addition to polymeric dosage forms impart flexibility, reduce brittleness, increase toughness and improve flow. Common examples include water, GLY (Figure 2.2), glycol, propylene glycol and ethylene glycol (Boateng *et al*., 2009). A plasticizer acts by interposing itself between the polymer chain, interacting with the functional group which results in reduced interaction and therefore the intermolecular cohesive forces between the polymer chains. Greater freedom of mobility occurs within the chain segments due to an enlarged space created between the polymer chains by the plasticizer. The enhanced mobility and flexibility lowers the glass transition, converting the rigid glassy polymer to the rubbery state. Molecular aggregates are therefore formed from the intermolecular secondary valence forces which hold the plasticizer and polymer together.

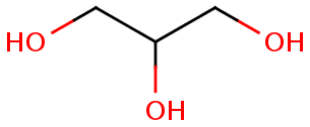

Figure 2.2: Chemical structure of plasticiser GLY. Available at <http://www.bmrb.wisc.edu/metabolomics/mol_summary/?molName=GLY > [Accessed; 25/07/2011].

2.1.4 Permeation enhancers

A large number of permeation enhancers have been studied to enhance the absorption of proteins across the buccal mucosa. These include synthetic surfactants such as sodium

lauryl sulphate, alkyl glycosides (Veuillez *et al*., 2001), non-ionic surfactants such as polysorbate 80 and Brij 35 (Rai *et al*., 2011).

2.1.4.1 Brij L23 (Brij 35)

Brij® L23 (Brij 35) also called tricosaethylene glycol dodecyl ether is a synthetic non-ionic polyoxyethylene ether (surfactant) with molecular formula $CH_3(CH_2)_{10}CH_2(OCH_2CH_2)_nOH$ (www.sigmaaldrich.com). It is used for selective and rapid solubilisation of microbial membrane aldehyde dehydrogenase (Hommel & Kleber, 1990). In general, non-ionic compounds are less irritant than ionic compounds (Volkering *et al*., 1995 cited in Rai *et al*., 2011) due to volume of hydrophilic heads that limits greater membrane penetration by the former (Vives *et al*., 1997). With respect to membrane permeation, the critical micelle concentration (CMC) and the hydrophilic-lipophilic balance (HLB) parameters of surfactant enhancers have been shown to be the key factors that determine their ability to disrupt biological membranes and subsequently increase permeation (Egan, 1976, cited in Rai *et al*., 2011).

Based on these parameters, Brij 35 (MW = 1225; CMC = 0.05-0.1 mM; HLB = 16.9) (www.mbio.com) was selected for this study. The choice of Brij 35 as the permeation enhancer for this work stemmed from its high HLB coupled with the low CMC, above which the surfactant is effective. The permeation enhancing effect of Brij 35 in combination with thiolated chitosan and GSH in the delivery of PACAP formulation via the buccal mucosa has been demonstrated by Langoth *et al*., (2006).

2.1.5 Enzyme inhibitors (EI)

Though the buccal membrane seems deficient in GIT proteinases such as chymotrypsin, pepsin and trypsin, a major challenge in buccal protein delivery is the rapid degradation by proteolytic enzymes such as aminopeptidases (Stradford & Lee, 1986), endopeptidases, carboxypeptidases and deaminases which are found in various buccal epithelia (human, porcine, rat rabbit and cultured hamster buccal cells) (Ho *et al*., 1992, cited in Veuillez *et al.*, 2001). The enzymatic activities in the buccal epithelium may cause protein drug degradation before they are absorbed. However, the use of enzyme inhibitors has been studied to overcome this challenge (Hearnden *et al*., 2012). This work focuses on the use of glutathione and aprotinin as enzyme inhibitors for xerogels containing BSA and INS as the

model proteins for buccal delivery. Development studies were conducted to determine the optimum concentration of EI for subsequent *in vitro* permeation studies.

2.1.5.1 Glutathione (GSH, γ-L-Glutamyl-L-cysteinyl-glycine)

Glutathione (GSH) is a tripeptide which is attached by a peptide linkage between the amine group of glycine and the carboxyl group of cysteine. The amine group of cysteine is however attached by an unusual peptide linkage with the carboxyl group of the glutamate side-chain (Figure 2.3). As an antioxidant, it prevents damage of important cellular components by reactive oxidative species such as peroxides and free radicals (Pompella *et al*., 2003)

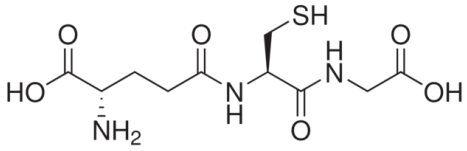

Figure 2.3: γ-L-Glutamyl-L-cysteinyl-glycine (GSH). Available at <http://www.sigmaaldrich.com/catalog/product/sial/g4251?lang=en&region=GB >[Assesses 24/05/2012]

Disulphide bonds formed within cytosolic proteins to cysteines are reduced by glutathione via electron donation, converting it to oxidised glutathione (GSSG). Glutathione reductase reduces GSSG back to reduced glutathione using NADPH as the electron donor (Pastore *et al*., 2003). Recently, GSH has been used as an inhibitor of melanin in the cosmetic industry through competitive interference of L-DOPA (L-3,4-dihydroxyphenylalanine) to bind to tyrosinase during the synthesis of melanin (Matsuki *et al.*, 2008).

It has been suggested by Langoth *et al*., (2005) that oxidised glutathione located on the surface of the buccal mucosa in the presence of free thiol groups such as thiolated chitosan are reduced. Protein-tyrosine-phosphatase is therefore inhibited by reduced glutathione with subsequent phosphorylation of occludin. The phosphorylation leads to the opening of tight junctions and hence the transport of proteins and peptides across the membrane (Barrett *et al*., 1999, cited in Langoth *et al*., 2005).

2.1.5.2 Aprotinin (APR)

Aprotinin is a naturally occurring monomeric globular polypeptide (Figure 2.4) derived from bovine lung tissue. Aprotinin, also termed basic pancreatic trypsin inhibitor (BPTI) has a molecular formula of $C_{284}H_{432}N_{84}O_{79}S_7$, an approximate molecular weight of 65112 and consists of 16 different amino acids containing 3 disulphides, a twisted β-hairpin and C-terminal α-helix (www4.mpbio.com).

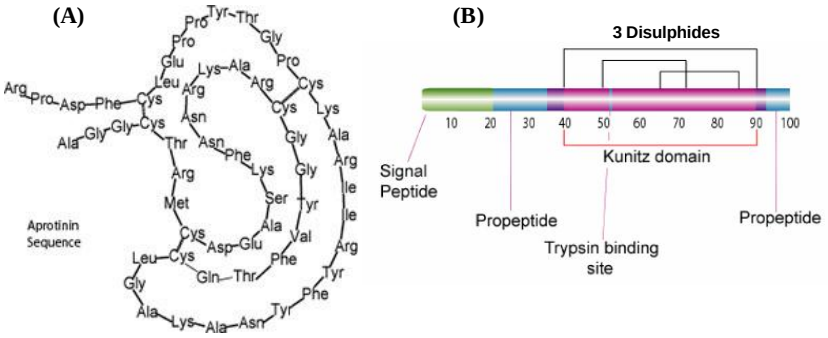

Figure 2.4: Showing (A) the amino acid sequence of aprotinin and (B) cartoon representation of the polypeptide showing sites of disulphide bonds and trypsin binding. Available at <http://www.sigmaaldrich.com/life-science/metabolomics/enzyme-explorer/aprotinin-monograph.html > [Accessed; 24/05/2012].

Aprotinin has a concentration dependent effect as a serine protease inhibitor (Engles, 2005) and has many beneficial clinical activities as well as complex effects on functions such as coagulation and inflammation. It exhibits a complex interaction with drugs such as angiotensin converting enzyme (Waxler & Rabito, 2003). The competitive inhibitor forms stable complexes with enzymes and blocks their active sites. The reversible aprotinin-protease complexes dissociates at pH < 3.2 or >10. One trypsin inhibitor unit (TIU) decreases the activity of 2 trypsin units by 50 %, where 1 trypsin unit will hydrolyse 1.0 µmole of N-α-benzoyl-DL-arginine p-nitroaniline (BAPNA) per minute at pH 7.8 and 25°C (www.sigmaaldrich.com). It is reactive against trypsin, chymotrypsin, plasmin, kallkrein, urokinase, clotting factor XIIa, protein C, proteinases of the complement system and leucocytes and tissue proteinases (www4.mpbio.com)**.**

Aprotinin is relatively stable against denaturation at high temperature, acids, alkalis, proteolytic degradation and organic solvents due to its compact tertiary structure. The serine protease inhibitor has been used as an enzyme inhibitor to increase the bioavailability in a

microemulsion formulation containing recombinant human INS (Çilek *et al*., 2005). The protective effect of aprotinin and other protease inhibitors against digestive enzymes pepsin, trypsin and α-chymotrypsin has also been studied by Morishita *et al*., (1997) using Eudragit L100 INS microspheres. Their results indicated that protease inhibitors are capable of protecting INS from proteolytic degradation. Aprotinin has also been used to minimise the degradation of proteins in the rabbit buccal mucosa (Yamamoto *et al*., 1990, cited in Walker *et al*., 2002).

2.2 Materials and methods

2.2.1 Materials

Table 2.1: Details of materials used in the formulation development and optimisation

Material	Description	Supplier
Chitosan (medium molecular weight) 75-85 % deacetylated	448877-250 G	Sigma-Aldrich, Gillingham, UK.
Thioglycolic acid	T 3758-100 ML	Sigma-Aldrich, Gillingham, UK.
N-(3-Dimethylaminopropyl) - N- ethyl carbodiimide hydrochloride (EDAC)	E 6383-5 G Assay ≥ 98%	Sigma-Aldrich, Gillingham, UK.
Glycerol (GLY) (anhydrous)	Assay ≥ 98 %	Sigma-Aldrich, Gillingham, UK.
D-mannitol (D-MANN)	M9546-250 G	Sigma-Aldrich, Gillingham, UK.
BSA (mol wt. ~66 kDa)	A7906-100 G	Sigma-Aldrich, Gillingham, UK.
Acetic Acid	A /0360/PB17	Fisher Scientific, (Leicester UK)
Hydrochloric acid	H /1150/PB 17	Fisher Scientific, (Leicester UK)
Sodium chloride	S /3120/60	Fisher Scientific, (Leicester UK)
Sodium hydroxide	S 240697	Sigma-Aldrich, Gillingham, UK
Potassium dihydrogen phosphate	P /4760/53	Fisher Scientific,(Leicester UK)
PBS tablets	pH 7.4	Sigma-Aldrich, Gillingham, UK
Ethylcellulose powder	200646-250G	Sigma-Aldrich, Gillingham, UK
Ethanol (absolute)	02865-2.5L	Sigma-Aldrich, Gillingham, UK
Recombinant human insulin	12643-50MG	Sigma-Aldrich, Gillingham, UK
Brij 35	16005-250G-F	Sigma-Aldrich, Gillingham, UK
L-Glutathione reduced	G4251-25G	Sigma-Aldrich, Gillingham, UK
Aprotinin (bovine lung)	A1153-25MG	Sigma-Aldrich, Gillingham, UK

Table 2.2: Details of consumables used in the formulation development and optimisation

Consumable	Supplier
75 µL Aluminium crucibles	Setaram, UK
Magnetic stirrer	Fisher Scientific,(Leicester UK)
40 µL Aluminium crucibles	Mettler Toledo, UK
Aluminium lids	Mettler Toledo, UK
1 mL Eppendorf tubes	Fisher Scientific,(Leicester UK)
Blue, white and yellow micropipette tips	Fisher Scientific,(Leicester UK)
100 Ml, 250 mL, 500 mL, 1 L, 5 L beakers	Fisher Scientific,(Leicester UK)

2.2.2 Preliminary investigations: solution preparation and membrane dialysis

500 mg of chitosan (CS) was dissolved in 50 mL of acetic acid (1 % v/v) and the pH adjusted to 6 ± 0.1 with 5M NaOH added dropwise. The resulting polymer gel was dialysed against 5 L of 5 mM HCl five (5) times, replacing the dialysate medium every 8 hours using Spectra/Por® Float-A-Lyzer® G2 dialysis device (8-10 kDa molecular weight cut-off; cellulose ester membrane, Sigma, Gillingham, UK) (Bernkop-Schnürch *et al*., 2003b). The process was repeated but omitting the exhaustive dialysis phase in order to assess the effect of excess acetic acid and the newly formed sodium acetate on formulation characteristics.

Formulation studies were carried out as summarised in Tables 2.3 and 2.4. Varying amounts (0-20 % relative to polymer weight) of GLY and D-MANN as plasticizer and cryoprotectant respectively were added to the undialysed or recovered dialysed gel. The optimised formulation was then loaded with BSA at two different concentrations as a model protein drug (see Table 2.3).

Table 2.3: Matrix chitosan formulations prepared in preliminary stages

Component	**Content of formulations (mg)**								
	Non drug loaded							**Drug loaded**	
	Control	A	B	C	D	E	F	G1	G2
Chitosan	100	100	100	100	100	100	100	100	100
GLY (plasticizer)	-	-	10	20	20	10	10	10	10
MANN (cryoprotectant)	-	10	10	10	20	-	20	10	10
BSA (model drug)	-	-	-	-	-	-	-	50	100

Table 2.4: Optimised drug loaded chitosan/TG-chitosan formulations with permeation enhancer and various amounts of different enzyme inhibitors (cf Table 2.3)

Component	Formulations (mg)			
	G1a	**G1b**	**G1c**	**G1d**
Chitosan/ TG-chitosan	100	100	100	100
MANN	10	10	10	10
GLY	10	10	10	10
Brij 35	10	10	10	10
APR	0	5	0	0
GSH	0	0	5	10
BSA	50	50	50	50

The effects of varying amounts of different enzyme inhibitors (EI) and permeation enhancer (PE) on formulation characteristics was studied by incorporating 0-10 % (relative to polymer weight) of reduced glutathione (EI), 0-5% aprotinin (EI) and 10% Brij 35 (PE) (Langoth *et al.,* 2006) (Table 2.4). The final chitosan gel was stirred continuously for 15 minutes to obtain a uniform gel at room temperature and kept for 30 minutes to remove all air bubbles.

2.2.3 Synthesis of chitosan-4-thioglycolic acid (TG-chitosan)

TG-chitosan was synthesised as previously described (Saboktakin *et al.,* 2011). 500 mg of chitosan was dissolved in 50 mL of 0.1 M HCl. An equivalent of 500 mg of thioglycolic acid (TGA) was added, followed by 50 mM EDAC in order to activate the carboxylic moieties of TGA and the pH adjusted to 5 with 1M NaOH. After an incubation period of 4 hours at room temperature under continuous stirring at 150 rpm in the dark, the resulting thiolated polymer was dialysed to eliminate unconjugated TGA against different aqueous media: (i) 8 hours against 5 L of 5 mmol/L HCl, (ii) 8 hours against 5 mmol/L HCl containing 1% NaCl (twice) to curtail ionic interactions between the cationic CS and the anionic sulfhydryl ligand and finally (iii) 8 hours against 5 L of 5 mmol/L HCl (twice) in the dark using the dialysis device previously described. The dialysed products were either used directly for formulation or first lyophilised (section 2.2.5) and stored at 4 °C pending further analysis. The process is summarised in Figure 2.5.

Gel formulations were prepared as previously described in section 2.2.2 (formulation G1, Table 2.3 with TG-chitosan replacing chitosan) and the final gel containing 1 % w/v TG-

chitosan was stirred continuously for 15 minutes to obtain a uniform gel at room temperature and kept for 30 minutes to remove all air bubbles. Unmodified chitosan served as the control.

2.2.4 Preparation and permeability studies of ethyl cellulose (EC) backing membrane

To ensure unidirectional release of BSA in the buccal mucosa, an impervious backing film (laminate) made of 1 g ethyl cellulose dissolved in 20 mL of ethanol and plasticized with 2 g of GLY (Cui *et al.*, 2008) was prepared. 250 mg of the resultant gel was poured into 24 well polystyrene moulds (diameter 12 mm) (Thermo Fisher Scientific, Leicester, UK) and dried over silica beads in a desiccator for 24 hours and subsequently at room temperature for 24 hours. The dried films were covered with parafilm and kept in the refrigerator till required.

To assess the permeability of the EC laminates, the final weights of the films after immersion in phosphate buffered saline (PBS) pH 6.8 was statistically compared with their initial weights. In addition, the EC laminate was used as a membrane between the donor and receiver compartments of a Franz-type diffusion cell and sealed with parafilm. 1.50 mL 10 % w/v solution of BSA in 0.1 M PBS (pH 6.8) was placed in the donor compartment and the receiver compartment filled with 8.00 mL 0.1 M PBS with magnetic stirring. The permeability of the EC laminate was determined by evaluating the amount of BSA in both compartments after 1 hour using Bradford's assay.

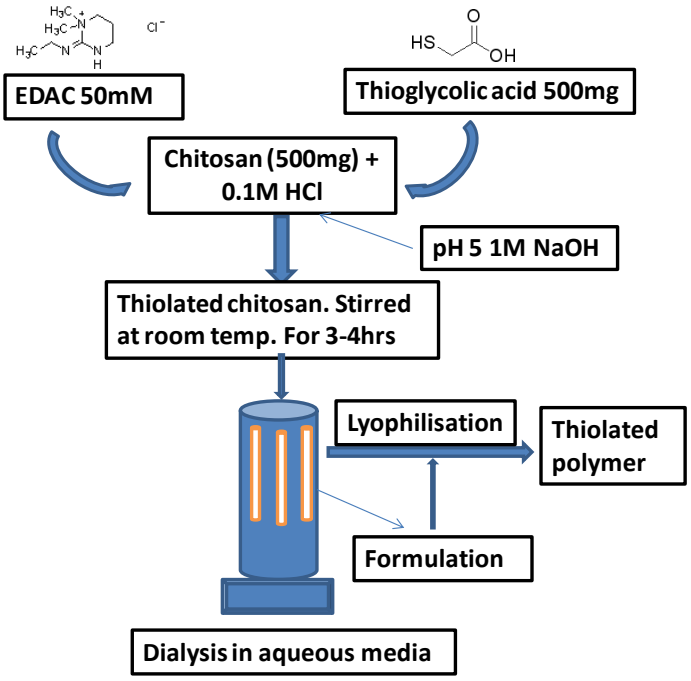

Figure 2.5: A schematic diagram for the synthesis of thiolated chitosan.

2.2.5 Annealing studies

A DSC-1 Thermal Analyser (Mettler Toledo Ltd, Leicester, UK), calibrated with indium was used to analyse the thermal events in the formulated gels to determine a suitable lyophilisation cycle. The chitosan gels (undialysed, unmodified dialysed and thiolated) were initially cooled in 40 µL aluminium pans with pierced lids on the DSC from 25 to - 55 °C at a rate of 10 °C/min. They were then heated to 25 °C at a rate of 20 °C /min to improve sensitivity and the cycle repeated twice. Based on thermal events observed during the heating cycles, an annealing temperature of -25 °C was deemed optimum. The samples were then warmed to -25 °C after initial cooling to - 55 °C and held at this temperature for 10 minutes. They were cooled back to the original freezing temperature and then warmed through to 25 °C at 20 °C /min (Ayensu *et al*., 2011).

2.2.6 Lyophilisation

1 g each of the homogeneous (formulated chitosan and TG-chitosan) gels were added unto the dried hydrophobic EC films in the moulds and lyophilised using the automated novel lyophilisation cycle shown in Table 2.5 on a Virtis AdVantage XL 70 freeze dryer (Biopharma Process Systems, Winchester, UK). The freeze-drying cycle was developed based on the preliminary thermal characterization (annealing) by DSC as described in section 2.2.5 above. The end of the primary drying (ice sublimation) stage was determined by probes signalling equal product and shelf temperatures. The effect of annealing on the drug loaded formulations was determined by carrying out the lyophilisation cycle with and without the process of annealing. The resulting lyophilised xerogels were stored over silica gel in desiccators to maintain low water content ideal for maintaining protein stability, till ready for characterisation. In addition, xerogels obtained directly from lyophilised dialysed TG-chitosan gel were assessed against those formulated from freeze-dried TG-chitosan powder. The characteristics of the optimised formulation were further explored by loading with recombinant human INS powder (Table 2.6) which had previously been dissolved in a minimal amount of 0.01 M HCl (200 µL HCl/mg insulin) (Portero *et al.,* 2007). The effects of the EI on INS containing xerogel properties were studied.

Table 2.5: Lyophilisation cycles with and without an annealing process

Step	Thermal treatment				Primary drying process		
	Temperature (°C)		Time (min)	Ramp/Hold R/H	Temperature (°C)	Time (min)	Vacuum (mTorr)
	Annealed	Non-annealed					
1	+05	+05	30	H	-30	420	50
2	-05	-05	30	H	-30	420	20
3	-55	-55	120	H	Secondary drying process		
4	-25	-55	180	H	+20	360	10
5	-55	-55	180	H			

Table 2.6: Optimised chitosan/TG-chitosan formulations loaded with INS.

Component	**Formulations (mg)**		
	INS[1]	**INS[2]**	**INS[3]**
TG-chitosan	100	100	100
MANN	10	10	10
GLY	10	10	10
Brij 35	10	10	10
APR	0	5	0
GSH	0	0	10
INS	20	20	20

INS[1], TG-chitosan-INS; **INS[2]**, TG-chitosan-APR-INS; **INS[3]**, TG-chitosan-GSH-INS.

2.3 Results and discussion

2.3.1 Preliminary investigations:

2.3.1.1 Gel preparation

In the present study, medium molecular weight chitosan of concentration 1% w/v was used as the base matrix in order to guarantee high mucoadhesive properties (Roldo *et al*., 2004). Various formulations containing different combinations of a plasticiser and a cryoprotectant were screened for acceptable lyophilisation behaviour and visual elegance of the resulting product. Physical examination of the unplasticised formulation (A), revealed strong but brittle xerogels that were easily broken along fractured surfaces. There was

increased flexibility with increasing GLY content as it lowered the stresses generated during lyophilisation, allowing the xerogels to accommodate the stress. The plasticizer acts by interposing itself between the polymer chains and interacting with the functional groups which resulted in reduced interaction and therefore the intermolecular cohesive forces between the polymer chains. In the case of highly plasticized formulations 'D' and 'C' (Table 2.3), the xerogels were sticky, making removal from the mould and handling difficult. 10 % (per polymer weight) of GLY in formulations 'B' (Figure 2.6 image a) and 'E' (Table 2.3), however, produced adequately flexible, tough and non-brittle xerogels.

During the formulation optimization studies, 10 % (per polymer weight) of D-MANN was found effective, as xerogels with no cryoprotection could not be expected to maintain stability of the protein in the lyophilised product. Although loading up to 20 % (per polymer weight) of D-MANN formed tough, flexible, porous and structurally stable xerogels, combinations with varying concentrations of GLY produced xerogels with rough and cracked surfaces with the sides caving inwards as was observed in formulations 'D' (Figure 2.6 image b) and 'F' (Table 2.4). Such formulations were difficult to remove from the mould without damaging the xerogels. D-MANN as a cryoprotectant for the model protein drug (BSA) is important in preventing actual freezing of the drug and causing the solution to maintain some flexibility in a glassy state. During the freezing stages, hydrogen bonds form between the cryoprotectant and the protein molecules as water molecules are displaced. As the cryoprotectant replaces the water molecules, the protein material retains its native physiological structure (and function), although they are no longer immersed in an aqueous environment.

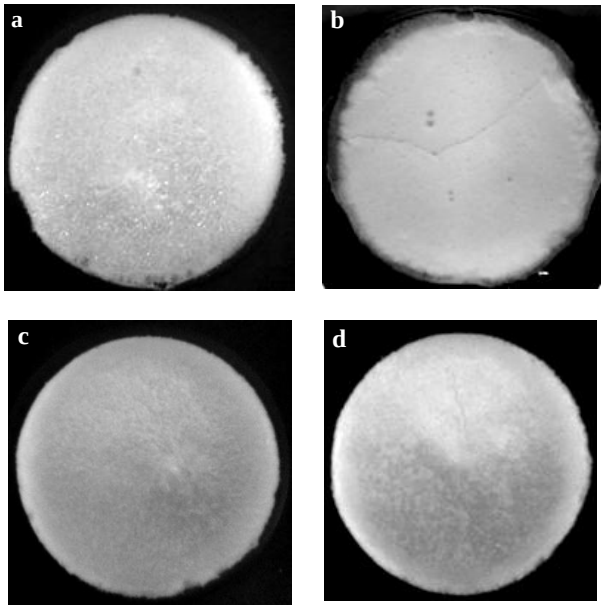

Figure 2.6: Photographs of non-drug loaded chitosan xerogels prepared from formulation 'B' (image a) showing a flexible, tough and non-brittle xerogel and formulation 'D' (image b) showing a rough and cracked surface. Images labelled (c) and (d) are annealed and non-annealed BSA loaded chitosan xerogels respectively.

Functionally, both GLY and D-MANN could act as plasticizers as well as cryoprotectants (Dashnau *et al.,* 2006, Karbowiak *et al.,* 2006, Tommaso *et al.,* 2010). When used on their own however, the formulations obtained were not deemed ideal whilst a combination of the two in a single formulation creates a synergistic effect. Additionally, using a combination of the two compounds, each at a lower concentration, produced better formulations as undesirable effects of a single agent at a higher concentration were minimized.

On the basis of structural integrity of xerogels and prevention from structural collapse after lyophilisation, the formulation 'B' containing equal proportions of both GLY and D-MANN (10% each respectively) was the formulation of choice for drug loading (Table 2.3). These xerogels were white, flexible and tough, porous, of uniform mass, texture and thickness. Furthermore, they were elegant in appearance with no visible cracks, easily regained their original configuration upon gentle compression and did not break when bent. Such optimised characteristics make formulation 'B' suitable for easy application and potentially ensuring patient compliance.

Optimised BSA amount of 50 % per polymer weight in the optimised formulation was adequate to prevent problems encountered with high-dose products during the lyophilisation

process. These include the inability to form xerogels of the same thickness as the original gel but instead resulted in a powdery product similar to freeze-dried powder injections for reconstitution. This made it difficult to test for hydration, mucoadhesion and drug dissolution characteristics. Formulations with high drug loading do not leave much room for lyophilisation agents. A CS: BSA ratio of 2:1 gave a better lyophilised xerogel compared to the powdery product that was obtained when a 1:1 ratio of CS: BSA was used.

2.3.1.2 Membrane dialysis

The process of dialysis was employed to remove excess acetic acid and sodium acetate (NaAc) that crystallizes during lyophilisation and interfere with the physico-mechanical properties and characterisation of the lyophilised chitosan cakes. Physical examination of dialysed xerogels (17.1 ± 2 mg), with theoretical composition by weight of chitosan (10.0 mg), BSA (5.0 mg), GLY (1.0 mg) and D-MANN (1.0 mg) per xerogel, revealed tough and flexible (non-brittle) xerogels. Although the undialysed xerogel (33.9 ± 3 mg) which had a similar theoretical composition by weight of chitosan, BSA, GLY and D-MANN as in the dialysed xerogel above, seemed elegant in appearance, a closer physical examination showed much brittleness and hardness even with the presence of plasticiser. It showed approximately double, the average weight per xerogel and the difference in weight (16.8 mg) is attributable to the formation of NaAc during the gel preparation stage (Ayensu *et al*., 2012b)

2.3.2 Synthesis of chitosan-4-thioglycolic acid (TG-chitosan)

In the thiolation study, TGA was bound to chitosan via amidation between the carboxylic group of TGA and primary amino groups of the polymer. The reactivity of the primary amino group at the 2-position (Figure 1.11, chapter 1) of the glucosamine subunit of chitosan was exploited for the immobilization of thiol groups. The primary amino group was covalently attached to the sulfhydryl bearing agents via an amide linkage. For ligands such as cysteine and thioglycolic acid, the amide bond formation between the carboxylic acid group and the primary amino group is mediated by a water soluble coupling agent, N-(3-Dimethylaminopropyl)-N-ethyl carbodiimide hydrochloride (EDAC), (Kast & Bernkop-Schnürch, 2001). The process was performed at a pH ≤ 5 to prevent the accidental formation of disulphide bonds by air oxidation during synthesis. The reactive thiolate anion concentration for the oxidation of thiol groups is low at this pH, excluding the formation of disulphide bonds. Inert conditions may alternatively be employed for the coupling reaction. A

simple one step coupling reaction involving the use of 2-iminothiolane as a coupling reagent offers an advantage in the case of amidine bond formation (Bernkop-Schnürch *et al*., 2003a). The chemical structure of the reagent protects the thiol group of the reagent against oxidation. This reaction is however, limited by cost and time.

2.3.3 Preparation of ethylcellulose (EC) backing membrane

The thin opaque films of thickness range 230 ± 15 nm obtained were flexible and tough. The controlled drying in the desiccator followed by drying at room temperature prevented rapid evaporation of alcohol that results in the formation of patched brittle films. The use of GLY as plasticizer helped to increase flexibility in addition to improving the adhesion process for the attachment of chitosan/TG-chitosan gel to the hydrophobic EC laminate (Cui *et al*., 2008). The films were deemed impervious as no statistically significant differences were observed between the initial and final weights after submersion in PBS for 4 hours. The impermeability of the EC laminate was further confirmed with the complete absence of BSA in the receiver compartment of the Franz-type diffusion cell. In addition, there was no change in the concentration of BSA in the donor compartment of the Franz-type diffusion cell.

Figure 2.7 summarises the processes involved in the gel formulation and drying of the EC backing membrane, on which the chitosan/TG-chitosan polymeric gel formulations were added and subsequently lyophilised to obtain the EC laminated chitosan/TG-chitosan xerogels which were stored over silica gel in desiccators until ready for characterisation.

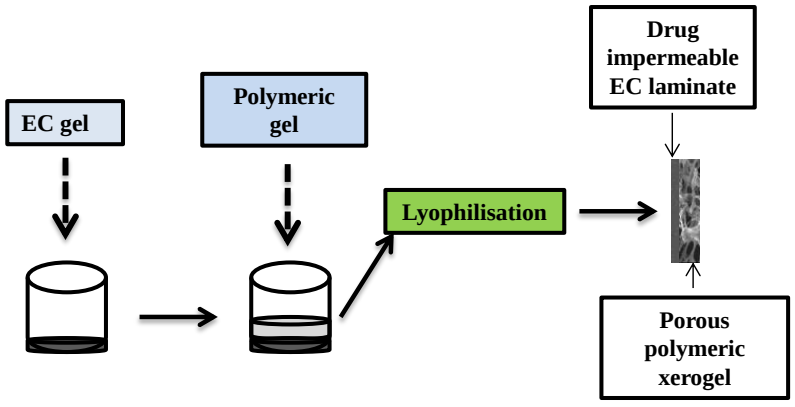

Figure 2.7: A schematic diagram for the preparation of EC laminated chitosan/TG-chitosan xerogels.

2.3.4 Annealing studies

Representative DSC thermograms of chitosan-BSA gel (undialysed and dialysed) are shown in Figure 2.8. Glass-transition (Tg') temperature of -44.5 °C (Figure 2.8 [b]) was observed for the undialysed non-annealed Chitosan-BSA gel. The eutectic and ice melts were observed between an onset of -5 °C and midpoint of 13.0 °C. To avoid the formation of a

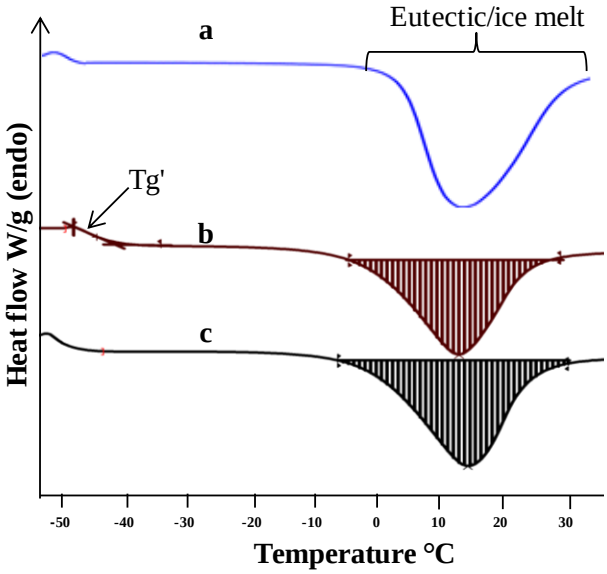

Figure 2.8: DSC thermograms of different CS-BSA gels which were (a) dialysed annealed (b) undialysed non-annealed and (c) undialysed annealed.

metastable glass which will eventually crystallize and affect the stability of the protein, samples were heated to -25 °C above the measured glass transition temperature (but below the eutectic and/or ice melting temperature) of the mixture, allowing the glass to relax and crystallize during the freezing stage. Figure 2.8 (c) shows the thermogram of the heating stage of the undialysed annealed Chitosan-BSA gel, where no glass transition but rather the eutectic/ice melt, was observed between onset -4 °C and midpoint 14.5 °C. The effectiveness of the annealing process was evidenced by the disappearance of the glass transition in the heating cycle. Based on the thermal events observed during the heating cycle, an annealing temperature of -25°C was chosen and incorporated into the thermal treatment step for the freezing stage of the lyophilisation cycle. For the dialysed Chitosan-BSA gel in Figure 2.8 (a), no glass-transition was detected by the DSC in the frozen concentrate implying no phase separation during the freezing stage of the lyophilisation process.

2.3.5 Lyophilisation

The primary drying phase of the lyophilisation cycle was deemed complete when the product temperature measured by means of probes equalled the shelf temperature of -30 °C after 14 hours (Figure 2.9). The incorporation of an annealing process helped to achieve faster water vapour transport, shorter primary drying time and elegant porous xerogels.

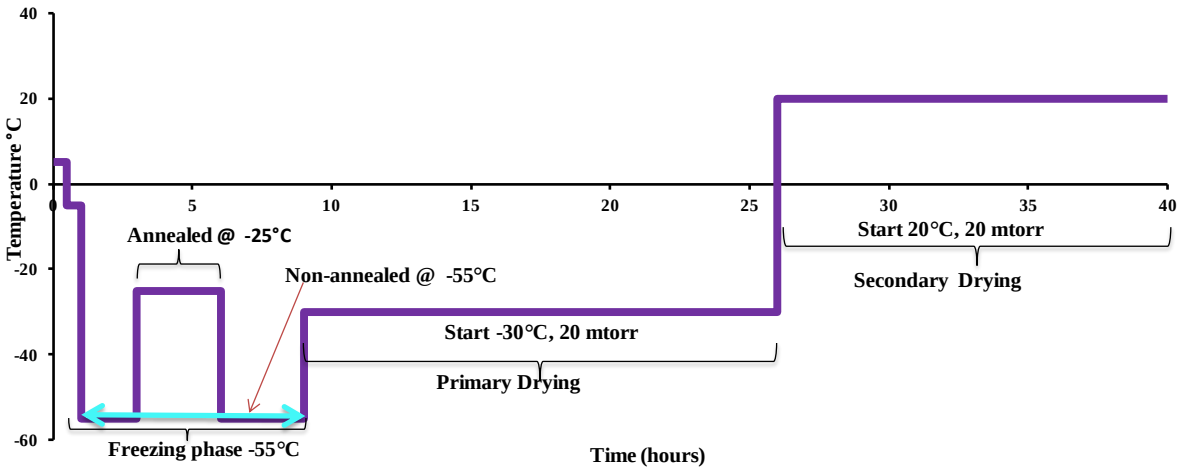

Figure 2.9: Schematic diagram of the annealed and non-annealed lyophilisation cycles

Annealing as a process step maintained the samples at a specified temperature below the equilibrium freezing point but above the glass transition temperature (-25 °C) for 3 hours. This allowed for the formation of larger ice crystals resulting in increased sublimation rate during the primary drying stage, creating larger pores in the process (chapter 3, Figures 3.30 A and C). In addition, the process of annealing facilitated quantitative crystallisation of the active ingredients and led to improved pore size distribution of ice crystals as in Ostwalt ripening, a process that allows smaller ice crystals to fuse together, forming large crystals that leaves in its wake, large pores following ice sublimation [Searles *et al*., 2001(b)].

Flexible, tough, non-brittle and porous lyophilised TG-chitosan xerogels were also produced. The presence of GLY in the TG-chitosan xerogel led to enhanced flexibility as freeze induced stress generated during lyophilisation is lowered, allowing the xerogels to accommodate the stress as was observed with the chitosan xerogels. A combination of two different cryoprotectants (or plasticizers), each at reduced concentration, has a better outcome since undesirable effects such as brittleness (D-MANN) or stickiness (GLY) produced by higher concentrations of a single agent was reduced. Furthermore, elegant porous TG-chitosan xerogels were achieved by incorporating an annealing process during the freezing stage. Annealing also promotes ice crystal growth and complete crystallisation of MANN (maximise the degree of crystallinity in materials), thus preventing premature crystallisation of mannitol

(Searles *et al*., 2001a). The reason for annealing MANN is to allow crystal formation from the amorphous phase so that metastable MANN does not re-crystallize on storage, which will affect product stability.

Xerogels obtained directly from dialysed TG-chitosan gel were evaluated against those formulated from lyophilised TG-chitosan powder. The dialysed gel produced elegant xerogels and prevented double lyophilisation, saving time and cost. Since no significant differences were observed between the characteristics of the xerogels from the two processes, industrial applicability of direct formulation would be of more benefit than manufacture via lyophilised TG-chitosan powder

Different xerogels were obtained from the optimised formulations containing different EI (GSH and APR) at varying concentration and a PE (Brij 35). The presence of EIs and PEs in formulations intended for protein delivery via the buccal mucosa is critical to allow improved absorption of the protein drug through the buccal membrane which exhibits limited absorption for protein drugs due to peptidase activities and low epithelial permeability. The effect of the EIs on xerogel characteristics such as drug dissolution, mucoadhesion and permeation are reported elsewhere in this report. The characteristics of optimised xerogels containing INS were also determined and have been described elsewhere.

2.4 Conclusions

Mucoadhesive systems for potential protein delivery via the buccal mucosa using lyophilised chitosan based xerogels have been developed. The removal of NaAc by membrane dialysis was essential for obtaining optimised xerogels with excellent characteristics for application to the buccal mucosa surface. On the basis of characteristic performance and structural integrity after lyophilisation, the non drug-loaded xerogel formulation ‘B’ containing 10 % (per polymer weight) each of plasticizer and cryoprotectant was the formulation of choice for drug loading and further development. Stable TG-chitosan based system has also been developed. Annealing, plasticisation and cryoprotection procedures were critical in obtaining porous and flexible dialysed xerogels. The annealing step in the lyophilisation cycle helped to remove stresses, softened the components, toughened and reduced brittleness to obtain the desired porous structure for the final optimised formulations. The final lyophilised products backed with an impervious EC laminate film were elegant, mechanically strong cakes and are expected to exhibit long-term storage stability. In addition EI and PE have been incorporated in the xerogels to offer improved permeability of the buccal mucosa.

The foremost implication of these findings is the potential application of the novel lyophilised system for the delivery of proteins via the buccal mucosa. These will be characterised by a number of analytical techniques and further be investigated using *in vitro* and *ex vivo* mucosal environments, drug dissolution, permeation and long-term stability evaluation.

CHAPTER THREE

ANALYTICAL, PHYSICO-CHEMICAL CHARACTERISATION OF XEROGELS AND STABILITY EVALUATION OF MODEL PROTEIN DRUGS (BSA, INSULIN) IN OPTIMISED TG-CHITOSAN XEROGELS

3.1 Introduction

The development and characterisation of chitosan based xerogels for the delivery of proteins via the buccal mucosa has been the major goal for this report. It is however essential to have an optimised system that ensures that the model protein drug incorporated in the xerogels be found conformationally stable during and after lyophilisation and over a long storage period. Further, proteins by nature have a narrow stability window when exposed to conditions that lead to aggregation, hydrolysis and denaturation caused by heat, moisture and other organic solvent (Estey *et al*., 2006). It is therefore critical that appropriate conditions of storage be established for the novel protein delivery systems developed. Bradford's assay and HPLC procedures were employed to estimate the protein content of the xerogels. The Bradford assay for protein quantification is a rapid and accurate method with less interference by non-protein components (Kruger, 2008).

Although drug content is a crucial stability indicating parameter, the method of determination must also be able to identify and quantify possible degradation products in order to assure safety and efficacy. Accordingly, the International Committee for Harmonisation (ICH) (2003) recommends that stability studies must include testing of those attributes of the drug substance that are liable to change during storage and are likely to affect quality, safety and/or efficacy. These may include physical, chemical, biological and microbiological attributes, using validated stability indicating analytical procedures.

The current chapter discusses the analytical characterisation of chitosan and TG-chitosan xerogels as polymeric matrices for the delivery of protein via the buccal mucosa using various analytical techniques. The principles underlying the techniques used and their application in the bioanalytical characterisation of pharmaceutical and biopharmaceutical materials have been reviewed (chapter 1, section1.8). The characterisation of the model hydrophilic protein drugs; BSA and INS, both in the pure form and incorporated in the chitosan based xerogels using the various analytical techniques is reported. The chapter also details accelerated stability studies of BSA and INS incorporated in the optimised TG-chitosan xerogels using ICH (2003) conditions. Results covering the first six months of 12 months study are presented.

3.2 Materials and methods

3.2.1 Materials

Table 3.1: Materials

Material	Description/Batch	Supplier
L-cysteine hydrochloride	C1276-10G	Sigma, (Gillingham, UK)
5,5′-Dithiobis (2-nitrobenzoic acid) (Ellman's reagent)	D8130-5G	Sigma-Aldrich, (Gillingham, UK)
Pullulan 200,000 standard	01615-25MG	Sigma-Aldrich, (Gillingham, UK)
Sodium acetate	W302406-1KG-K	Sigma-Aldrich, (Gillingham, UK)
Bradford's reagent	B6916-500ML	Sigma-Aldrich, (Gillingham, UK)
BSA powder	A7906-100 G	Sigma-Aldrich, (Gillingham, UK)
Acetic acid	A /0360/PB17	Fisher Scientific (Leicester, UK)
PBS tablets	pH 7.4	Sigma-Aldrich, (Gillingham, UK)
Human INS	12643-50MG	Sigma-Aldrich, (Gillingham, UK)
Acetonitrile	34967-2.5L (Fluka)	Sigma-Aldrich, (Gillingham, UK)
Copper(II) chloride	451665-5G	Sigma-Aldrich, (Gillingham, UK)
Trifluoroacetic acid (TFA)	302031-100ML	Sigma-Aldrich, (Gillingham, UK)
Potassium dihydrogen phosphate	P /4760/53	Fisher Scientific(Leicester UK)

3.2.2 Structural elucidation of chitosan and TG-chitosan-^{1}H-NMR

Proton nuclear magnetic resonance (^{1}H-NMR) spectra were acquired using a Jeol ECA, 500 MHz FT NMR spectrometer, incorporating a NM-50TH5AT/FG2 probe (Tokyo, Japan). Chitosan powder and TG-chitosan were dissolved in 2 % deuterium chloride (DCl) solution in D_2O and placed in a 5 mm borosilicate glass NMR tube and spun at 15 Hz. ^{1}H spectra were acquired using a single pulse experiment and the ^{1}H –NMR parameters are summarised in Table 3.2. The degree of acetylation (DA) was determined from equation 3.1

$$DA = (I_{CH3}/3)/(I_{H2\text{-}H6}/6) \times 100\ \%\ \text{equation 3.1}$$

Where I_{CH3} is the integral intensity of N-acetyl protons and $I_{H2\text{-}H6}$ is the sum of the integral intensities of H-2. -3, -4, -5 and H-6 of the acetylated rings (Sogia *et al*., 2008).

Table 3.2: ^{1}H parameters for Jeol ECA, 500 MHz FT NMR

Parameter	^{1}H-NMR
Frequency	500 [MHz]
Scans	64
Pulse angle	45°
Points	32768
Offset	6.0 [ppm]
Sweep	8.75 [kHz]
Relaxation delay	6 [s]
Pulse width	8 [μs]
Acquisition delay	3.74[s]
Temperature	27 °C

3.2.3 Quantification of immobilised thiol group

The amount of thiol group immobilised was determined by Ellman's reaction (Bernkop-Schnürch *et al*., 2004). 2 mg/mL solution of thiolated polymer was prepared in deionised water. 250 μL aliquots were added to 250 μL of 0.5 M phosphate buffer pH 8.0 and to 500 μL of Ellman's reagent (0.3 mg/mL of DTNB in 0.5 M phosphate buffer pH 8.0) to obtain a final thiolated polymer concentration of 0.5 mg/mL. The reaction was allowed to proceed for 2 hours at room temperature and the absorbance was measured at a wavelength of 405 nm with a Multiskan EX microplate photometer equipped with Ascent software (Thermo Scientific, Hampshire UK). The amount of thiol moieties immobilised was estimated from the corresponding standard curve of L-cysteine HCl *(0.25-1.50 μmol/mL, $r^2 > 0$ .99)* (Figure 3.12). Unmodified chitosan was used as control.

3.2.4 Molecular weight monitoring of chitosan and TG-chitosan by gel permeation chromatography (GPC)

The weight average molecular weights (Mw) of chitosan and TG-chitosan were monitored with Agilent 1100 series gel permeation chromatography (GPC) analysis system equipped with an isocratic pump and a refractive index detector. Samples were dissolved in buffer 0.2M CH_3COOH/0.1M CH_3COONa (Yu *et al*., 2010) and eluted through a Tosoh TSK-GEL PW column (7.8 x 300mm, 10 μm) at a flow rate of 1mL/min at 30 °C using the same buffer as mobile phase and pullulan 200,000 as reference standard. Collected GPC data

were analysed with Agilent Chemstation software. The Mw of chitosan and TG-chitosan were estimated from equation 3.2:

$$Log\ Mw\ (S) = Log\ Mw\ (R) \times \frac{Vo/Ve\ (S)}{Vo/Ve\ (R)} \quad \text{.....equation 3.2}$$

where *Mw (S)* is the molecular weight of the sample polymer, *Mw (R)* is the molecular weight of the reference polymer, *Vo/Ve (S)* is the ratio of the free volume elution time to analyte volume elution time of the sample and *Vo/Ve (R)* is the ratio of the free volume elution time to analyte volume elution time of the reference polymer.

3.2.5 ATR-FT-IR analysis

ATR-FT-IR spectra of the xerogel samples as well as other materials listed in Table 3.3 were acquired on an Excalibur series FTS 3500 ARX Fourier transform infrared spectrophotometer (FT-IR), equipped with Specac Golden gate (Varian, Oxford UK). A WIN-IR PRO software of wavenumber range 600 – 4000 cm^{-1} was used for the analysis. The spectra were collected at a resolution of 1.5 cm^{-1} with 16 scans per spectrum. A background spectrum of CO_2 was acquired and assigned for use on subsequent spectral acquisitions.

Table 3.3: Xerogels and materials characterised by ATR-FT-IR

Xerogels	Other materials
Chitosan-BSA (dialysed)	Chitosan powder
Chitosan-BSA (undialysed)	TG-Chitosan powder
TG-Chitosan-BSA	BSA powder
TG-chitosan-INS	INS powder
	Sodium acetate powder (anhydrous)

3.2.6 X-ray powder diffraction (XRPD)

The physical form (crystalline or amorphous) of the formulations was determined on a D8 ADVANTAGE X-ray diffractometer (Bruker AXS GmbH, Karlsure, Germany) equipped with a Goebel mirror with exit slits of 0.6 mm and a Lynx eye detector. The 5 mm width lyophilised xerogels were compressed to a width size of 0.5 mm using a clean pair of compression glasses and inserted in the sample holder. The transmission diffractograms were acquired using DIFFRAC plus XRD Commander over a start to end diffraction angle of 2θ = 5°– 45°, step size of 0.02 and a scan speed of 0.4 s. The operating conditions during the

experiment were 40 kV and 40 mA with Cu Kα radiation. Data was processed with EVA software for native BSA powder, chitosan powder, Chitosan-BSA (dialysed and undialysed) and TG-chitosan-BSA xerogels. INS loaded TG-chitosan xerogels were also analysed.

3.2.7 Differential Scanning Calorimetry (DSC)

The lyophilised protein loaded xerogels were studied for possible phase separation by observing the thermal events that occurred in the samples after lyophilisation on a DSC-1 Thermal Analyser (Mettler Toledo Ltd, Leicester, UK), calibrated with indium (based on heating range). This involved the initial cooling on the DSC at 10 °C/min from 25 to - 50 °C. It was then heated at 20 °C /min to 200 °C and the cycle repeated. An empty aluminium pan was used as reference. Mettler STARe software was used to analyse and evaluate the DSC thermograms.

3.2.8 Physical stability of model drugs by far-UV CD spectroscopy

The conformational structure of BSA was examined by far-UV CD. Spectra of a 1 mg/mL solution of native BSA in 0.01M PBS (pH 6.8) as the negative control or BSA released from the xerogels were recorded at 25 °C from wavelength range $240 \geq \lambda \geq 190$ with bandwidth 1 nm, time-per-point 0.5 s, and cell path-length of 0.1 mm using CD spectroscopy (Chirascan, Applied Photophysis). The same conditions were applied to native and released INS in 0.01M HCl (pH = 2.3) and 0.01 M PBS (pH = 6.8) using cell path-length of 0.05mm. The mean residue ellipticity $[\theta]_{mrw,\,k}$ was determined using equation 3.3 below:

$$[\theta]_{mrw,\,k} = \text{MRW} \times \theta_{\kappa} / 10 \times d \times c \qquad \text{..... } \textit{equation 3.3}$$

where MRW is the mean residue weight, θ_k is the observed ellipticity (degrees) at wavelength k, *d* is the pathlength (cm), and *c* is the concentration (g/mL) (Kelly *et al*., 2005).

3.2.9 Thermogravimetric analysis for moisture content

The percentage residual moisture of the lyophilised xerogels was estimated using a Thermal Advantage TGA 2950 (TA Instruments, Crawley UK) (Wang, 2000). A dynamic phase of heating at 15 °C/min from ambient temperature to a maximum of 150 °C was applied with a constant stream of dry nitrogen to the xerogels weighing between 3 – 6 mg in a

previously tarred 70 µl aluminium crucible. The TA Universal Analysis 2000 programme was used to determine the percentage weight loss from a second derivative plot.

3.2.10 Calibration curves for BSA and INS

Standard concentrations of BSA (25 µg/mL - 400 µg/mL) were prepared in 1 % $^{v}/_{v}$ acetic acid and 0.01M PBS (pH 6.8). 50 µL of each standard was placed in a 1 mL eppendorf tube and 1ml of Bradford's reagent was added, generating a characteristic blue colour. The absorbances of the standard solutions were measured at 595 nm. The measurements were repeated at 450 nm and the ratio of the absorbances 595/450 nm was plotted against the concentration to obtain linearised calibration curves as shown in Figures 3.27 and 3.28 for BSA in 1% acetic acid and 0.01 M PBS respectively. Similarly, standard INS concentrations (25 µg/mL - 400 µg/mL) were prepared in 0.01 M HCl and treated with Bradford's reagent as above and absorbances measured at 450 and 595 nm. The linearised calibration curve for INS from the plot of absorbance ratio 595/450 against INS concentration is shown in Figure 3.19.

3.2.11 Drug loading capacity

The drug loading capacity was determined from the ratio of actual and theoretical BSA loading x 100 %. 35 mg of drug loaded xerogel was dissolved in 25 ml of 1 % v/v acetic acid. The solution was magnetically stirred at 50 rpm to avoid bubble formation for 10 minutes at room temperature. 50 µL of the solution was withdrawn and treated with 1ml Bradford's reagent and the absorbance measured at 595 nm and 450 nm for linearisation of absorbance (Zor & Selinger, 1996; Ernst & Zor, 2010) using a Multiskan EX microplate photometer equipped with Ascent software (Thermo Scientific, Hampshire UK). The amount of BSA was determined by interpolation from the linearized calibration curve ($r^2 > 0.99$) (Figure 3.18). To estimate the recovery of this method, the same procedure was carried out using a known amount of non-drug loaded xerogel (25 mg) seeded with BSA powder (10 mg). The amount of BSA was evaluated using the Bradford's method as described in section 3.2.10.

3.2.12 Scanning electron microscopy (SEM)

The lyophilised xerogels were prepared for morphological studies on SEM by placing double-sided adhesive carbon tape on labelled stainless steel stubs. The samples were placed on the exposed side of the carbon adhesive being careful not to dent the surface topography of

the xerogels. These were sputter coated with gold for 120 seconds at 1 kV and 30 mA (Edwards Sputter Coater S150B) and placed in the chamber of a Cambridge Stereoscan S-360 SEM (Class one equipment, London UK). Images were acquired at an accelerating voltage of 20 kV, a working distance of 15 mm and processed with i-scan2000 software.

The laminated xerogels were carefully cut from the upper surface all through the laminate. The cut xerogels were placed on double sided adhesive carbon tape previously stuck onto labelled stainless steel stubs with the cross-sectional surface on the exposed side of the adhesive, sputter coated for 2 minutes at 25 mA and 1 kV with chromium (EmiTECH K575X Sputter Coater) and placed in the chamber of a Hitachi SU8030 Scanning electron microscope (Hitachi, Krefeld Germany). Images acquired at an accelerating voltage of 20 kV and working distance of 15 mm were processed with i-scan2000 software. Similarly, images of undialysed chitosan xerogels and the impervious EC backing film were acquired for characterisation.

3.2.13 Stability evaluation

3.2.13.1 Preparation and storage of BSA/INS xerogels for stability studies

BSA loaded xerogels (prepared in chapter 2 section 2.2.2 and section 2.2.6) were either stored in a refrigerator (long-term study) or kept under ICH conditions (for drug products intended for storage in a refrigerator) in a humidity chamber with 60 % relative humidity (RH) ± 5 % RH maintained with $CuCl_2$ (solubility 0.76 g/mL) (www.mitegen.com) at 25 °C (ICH, 2003) for accelerated stability studies (Table 3.4). Similarly, INS containing xerogels for stability studies prepared using method described in chapter 2, (Table 2.6 section 2.2.6) were stored according to ICH conditions (ICH, 2003) in Table 3.4 until ready for analysis at selected time points.

Table 3.4: ICH conditions for drug products intended for storage in a refrigerator

Study	Storage condition	Minimum time period covered by data at submission
Long-term	5 °C ± 3 °C	12 months
Accelerated	25 °C ± 2 °C/ 60 % RH ± 5% RH	6 months

3.2.13.2 Assay of BSA and INS content by Bradford's assay

The BSA and INS contents in xerogels at the various time points (0, 3 and 6 months) were determined using the Bradford's assay (chapter 3, section 3.2.11). The xerogels were analysed for protein content immediately after freeze-drying to represent the zero time point determination.

3.2.13.3 HPLC assay of BSA and INS content.

The amount of BSA at the zero time point was determined with an Agilent 1100 series size-exclusive high performance liquid chromatography (SE-HPLC) analysis system equipped with an isocratic pump and a UV detector. Samples were dissolved in 0.01 M PBS pH 7 (Estey *et al*., 2006) filtered (0.45 µm membrane, Minisart biotech.) and eluted through a Tosoh TSK-GEL PW column (7.8 x 300mm, 10 µm) with a flow rate of 1 mL/min at ambient temperature and detected at a wavelength of 215 nm using the same PBS as mobile phase and pure BSA powder as reference standard. Collected SE-HPLC data were analysed with Agilent Chemstation software and content of BSA was estimated from a calibration curve with linearity verified over concentration range of 0.1–1.00 mg/mL ($r^2 > 0.99$). The procedure was repeated for the time points of three (3) and six (6) months for the various storage conditions (Table 3.4) as specified in the ICH protocol.

The amount of INS loaded in the xerogels was determined by reversed-phase High-Performance Liquid Chromatography (RP-HPLC) (Agilent Technologies, Santa Clara, CA, USA) with a Jupiter 5-µm C18 column (250 mm × 4.6 mm, 300A˚) (Phenomenex, USA) with the following conditions: mobile phase—water: acetonitrile (67: 33, v/v) containing 0.1% (v/v) of TFA; flow rate—1 mL/min; detection wavelength—220 nm and injection volume - 20 µL (Giovino *et al*., 2012). All samples were analysed in duplicate and the protein concentration was determined based on interpolation from a calibration curve with linearity verified over concentration range of 50–250 µg/mL ($r^2 > 0.99$). The procedure was carried out for the time points of zero (0), three (3) and six (6) months for the various storage conditions (Table 3.4).

3.3 Results and Discussion

3.3.1 Structural elucidation of chitosan and TG-chitosan-^{1}H-NMR

The ^{1}H-NMR spectra of chitosan and TG-chitosan determined in 2 % DCl are shown in Figure 3.1. The proton signal assignments for the various residues summarised in Table 3.5 were based on previous works by Fernandez-Megia *et al.,* (2005) and Rinaudo, (2006). The calculated degree of acetylation of chitosan and TG-chitosan were consistent with the degree of deacetylation of 75 - 85 % provided by the supplier. The ^{1}H-NMR also confirmed the purity of the chitosan as well as the derivatised TG-chitosan.

The aqueous acidic media, 2 % DCl is usually considered the optimum solvent for ^{1}HNMR of chitosan (Fernandez-Megia *et al.,* 2005), which naturally causes hydrolysis of some of the N-acetyl groups and production of free acetic acid (AcOH) with a proton peak at 1.82 ppm in both chitosan and TG-chitosan. The multiplet peak at 3.52- 3.68 was assigned to the proton peaks of glucosamine unit, H-3, H-4, H-5 and H-6 (Li *et al*., 2010).

No new peaks corresponding to protons of thiol group from the covalent attachment between thioglycolic acid and chitosan to form TG-chitosan were identified. Nuclear magnetic resonance (NMR) was therefore not suitable for evaluating the level of free thiol groups and disulphide bonds since two equivalent carbons and two equivalent protons of thioglycolic acid appeared overlapped with those of chitosan in the NMR spectrum as reported by Juntapram *et al*., (2012) and Lee *et al*., (2007).

Table 3.5: ^{1}H-NMR signal assignments for chitosan and TG-chitosan

Proton residue	Chemical shifts (ppm)	
	Chitosan	TG-chitosan
NAc	1.81	1.81
AcOH	1.82	1.82
H-2 ($GluNH_2$)	2.95	2.95
H-2 (GluNAc) /H-3-H-6	3.52-3.68	3.52-3.68
H-1 (GluNAc)	4.38	4.38
H-1 ($GluNH_2$)	4.74	4.74

Abbreviations: NAc; (N-acetyl group), AcOH; (Acetic acid) D-glucosamine; ($GluNH_2$), N-acetyl-D-glucosamine; (GluNAc).

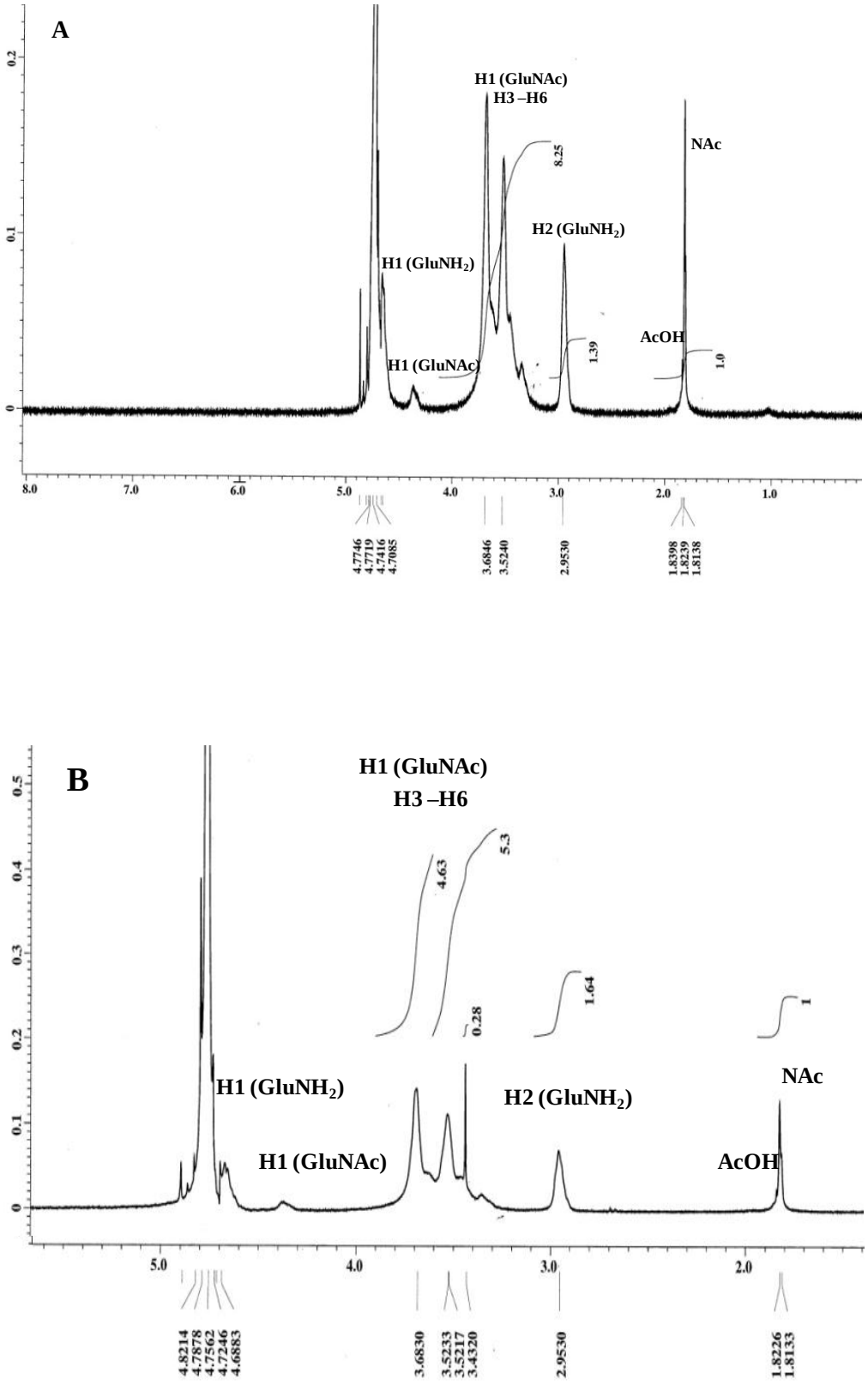

Figure 3.1: ^{1}H-NMR spectra of (A) chitosan and (B) TG-chitosan in 2 % DCl.

3.3.2 Quantification of immobilised thiol group

The calibration curve for standard cysteine HCl is shown in Figure 3.2. Spectrophotometric assay using Ellman's reagent was employed in the determination of the amount of reduced and oxidized thiol groups immobilized (Hornof *et al*., 2003) without previous quantitative reduction of disulphide bonds using borohydride.

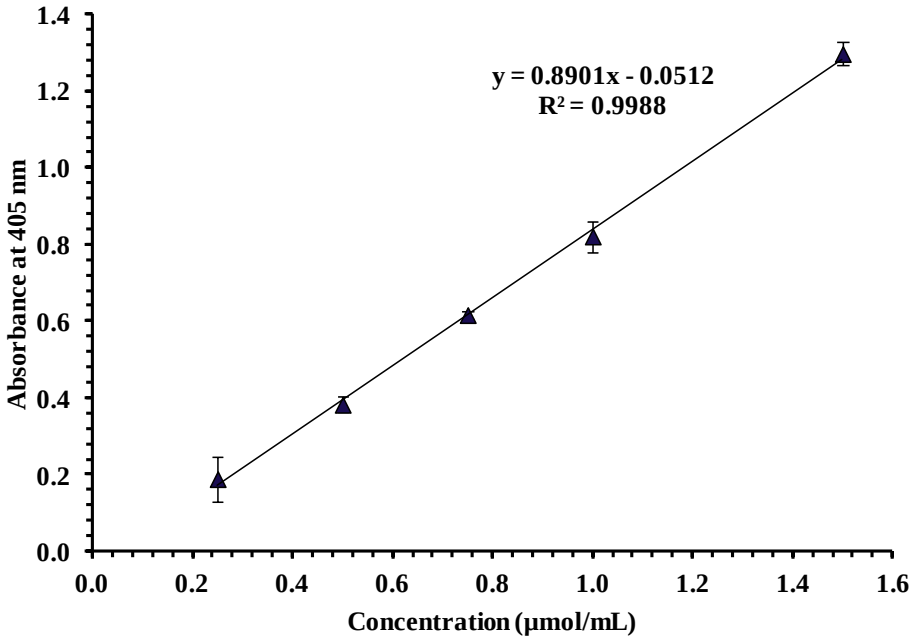

Figure 3.2: Calibration curve of L-cysteine HCl

The TG-chitosan conjugate had 236 ± 26 µmol thiol groups per gram of polymer. Unmodified chitosan showed no thiol groups after addition of thioglycolic acid in the absence of water soluble coupling agent N-(3-Dimethylaminopropyl)-N-ethyl carbodiimide hydrochloride (EDAC). According to Sreenivas & Pai (2009), a degree of modification of 25–250 µmol thiol groups per gram of chitosan results in the highest improvement in the mucoadhesive and permeation enhancing properties of these TG-chitosans. This range fits in with the results obtained for the current study which is interesting and is expected to impact on the mucoadhesive (chapter 4) and permeation (chapter 6) characteristics of the TG-chitosan xerogels.

3.3.3 Molecular weight monitoring of chitosan and TG-chitosan - GPC

Figure 3.3 shows a representative GPC chromatogram of chitosan. GPC analysis for monitoring the polymer Mw before and after derivatization showed no statistically significant difference ($p = 0.2709$, $n = 4$) between the calculated mean molecular weights.

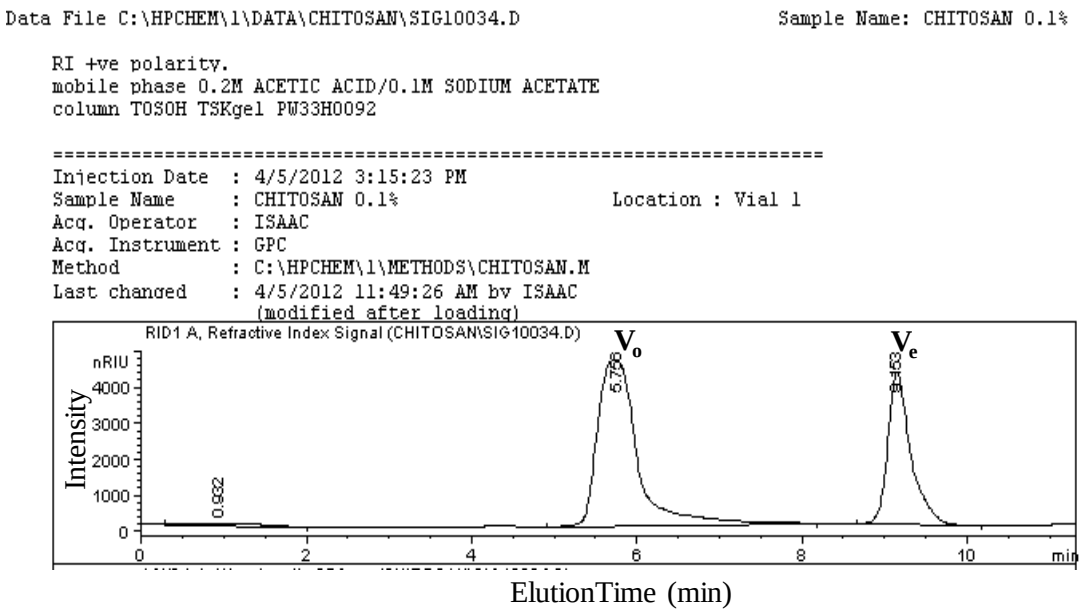

Figure 3.3: Representative chromatogram of chitosan from GPC analysis. V_o is the free volume elution time and V_e is the analyte volume elution time.

However the slight difference in the calculated Mw of chitosan (196.7 ± 5.1 kDa) and TG-chitosan (200.7 ± 2.1 kDa) after the conjugation reaction could be attributed to the addition of thioglycolic acid molecules unto the chitosan chains. This suggests that polymeric chains may not have been degraded during the synthesis process.

3.3.4 ATR-FT-IR analysis

Structural information was obtained for the protein loaded lyophilised xerogels through the analysis of the conformationally sensitive amide I band, which is located between 1600 and 1700 cm^{-1} (Figure 3.4). This band is due to the in-plane C=O stretching vibration, weakly coupled with C-N stretching and in-plane N-H bending. Each type of secondary structure (i.e. α-helix, β-turn and disordered) gives rise to a different C=O stretching frequency and hence, has a characteristic band position. The secondary structural types present in a protein are determined by band positions.

The ATR-FT-IR spectra (Figure 3.4) show the respective absorption peaks of chitosan and TG-chitosan at 1666.35 and 1618.27 cm^{-1} which corresponds to the characteristic amide I band (Qin *et al*., 2006). The peaks at 1556.55 cm^{-1} and 1522.67 cm^{-1} were assigned to amide II band (CN stretching and NH bend) present in both chitosan and TG-chitosan respectively. The absorption bands at 3271.26 cm^{-1} and 3255.48 cm^{-1} are for NH stretch and the weak peak at 2525.68 cm^{-1} corresponds to SH (Saboktakin *et al*., 2011), confirming the conjugation

between thioglycolic acid and primary amine of chitosan in TG-chitosan. The absorption bands at 3342.63 cm^{-1} and 3332.98 cm^{-1} were for chitosan-OH and TG-chitosan-OH respectively, the band at 997.19 -1060.85 cm^{-1} was due to CO and the 2850-2900 cm^{-1} band resulted from aliphatic CH stretch.

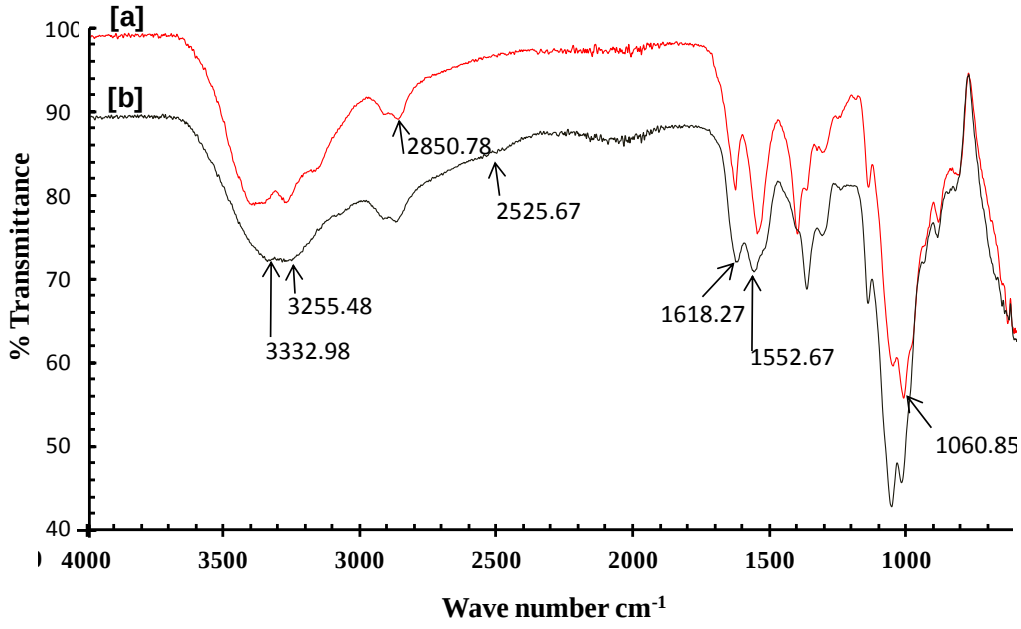

Figure 3.4: ATR-FT-IR spectra of [a] chitosan and [b] TG-chitosan

The AT-FT-IR spectra in Figure 3.5 show the absorption peaks of [d] dialysed and [e] undialysed xerogel at 1653 and 1568 cm−1 which corresponds to the characteristic amide I and II bands (CN stretching and NH bend), respectively, present in both chitosan and BSA. Analysis of the amide I band showed that the conditions employed in the formulation process prevented perturbation of the protein secondary structure, maintaining the conformation of the model drug. Spectral assignments for the undialysed xerogel, consistent with the results of Kakihana *et al.*, (1982) for solid NaAc were however, obtained with similar peaks at 623, 646, 922 and 1556 cm−1 corresponding to out-of-plane O–C–O rock, O–C–O bend, C–C stretch and asymmetric C–O stretch. These peaks were conspicuously missing in the spectral assignments for the dialysed chitosan-BSA xerogel (Figure 3.5 [d]). This confirmed the importance of the dialysis step which helped remove the formed NaAc.

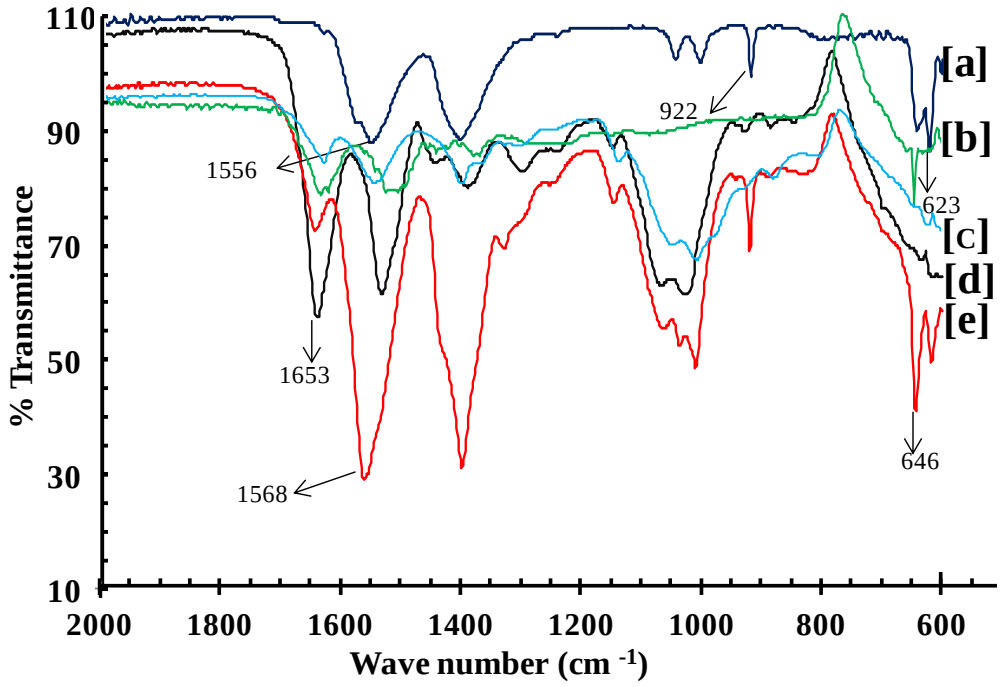

Figure 3.5: AT-FT-IR spectra of [a] NaAc powder, [b] BSA powder, [c] chitosan powder, [d] dialysed xerogel and [e] undialysed xerogel.

To investigate the secondary structure of INS loaded TG-chitosan xerogels containing different EIs, the vibrations were monitored *via* ATR-FT-IR spectroscopy (Figures 3.6 and 3.7). A typical INS FT-IR pattern is characterized by a very marked band in the range 1648-1660 cm^{-1}, that represents the predominant content of α-helix, and other two bands at a range of 1690-1625 cm^{-1} and 1681-1678 cm^{-1} attributed to the β-sheet and β-turn, respectively (Nielsen *et al*., 2000). Usually, the intensity of these two latter bands is lower than that observed at 1648-1660 cm^{-1}, indicating that the α-helix is the main contributor to the secondary structure of INS. As illustrated in Figure 3.16 ATR-FT-IR spectra of pure INS is dominated by bands around 1254, 1646, 3190 and 3300 cm^{-1} assigned to the amide III, I, B and A, respectively. Specifically, the main strong bands were detected at 1646 cm^{-1} which reflects the stretching C=O of the amide I, while the band around 1550 cm^{-1}, usually attributed to the amide II reflects CN stretching and NH bend. Figures 3.6 and 3.7 also show the ATR-FT-IR spectra of TG-chitosan-INS, TG-chitosan-APR-INS and TG-chitosan-GSH-INS. In comparison with the pure INS spectra, it could be observed that the characteristic absorption peak of the amide I occurs around 1650 cm^{-1} for all formulated xerogels. However,

though the position of this band is not significantly different from that of pure INS, it is evident that the shapes and intensities decreased.

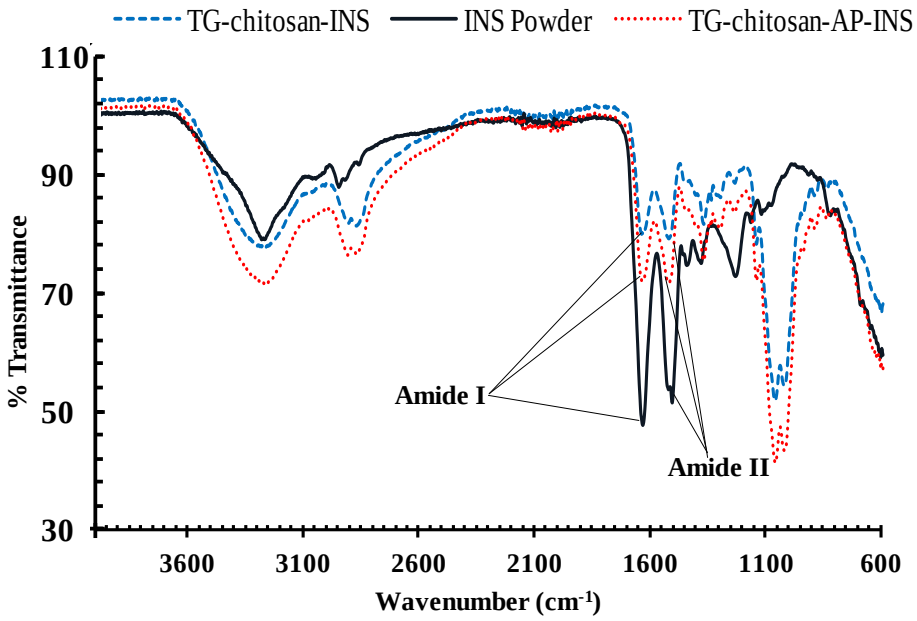

Figure 3.6: ATR-FT-IR spectra of TG-chitosan-INS, INS powder and TG-chitosan-APR-INS.

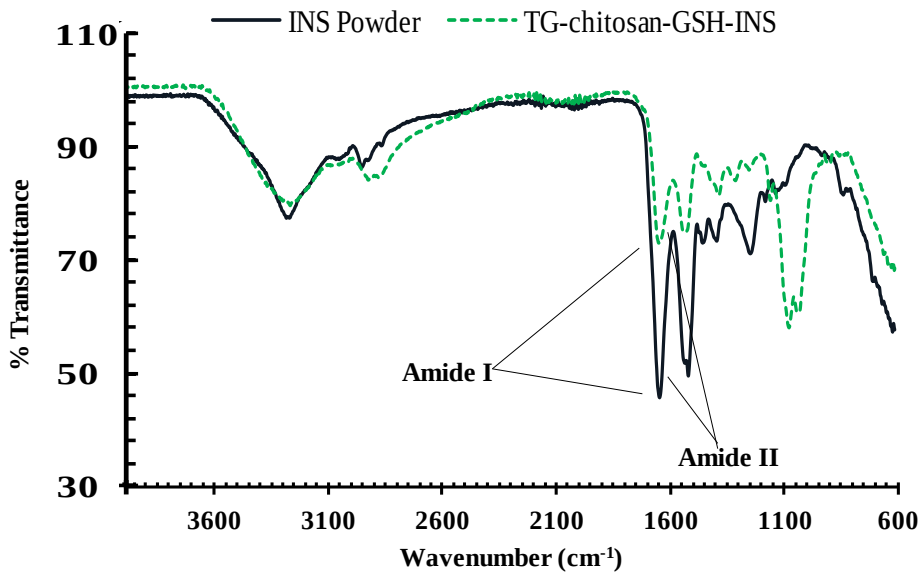

Figure 3.7: ATR-FT-IR spectra of INS powder and TG-chitosan-GSH-INS

This effect could be linked to the presence of absorption peak around 1550 cm^{-1} attributed to the secondary amide (C-N stretching and N-H bend) present in both INS and chitosan. In all the ATR-FT-IR spectra, the main peaks corresponding to α-helical chain remained unchanged, suggesting that the protein structure was not unfolded, degraded or hydrolysed

during the xerogel preparation process. Similar results were reported by Zhang *et al*., (2008), demonstrating that the protein secondary structure was not significantly altered in terms of α-helix and β-sheet during the production of chitosan based xerogels.

3.3.5 X-ray powder diffraction (XRPD)

XRPD analysis was used to study the physical form (crystalline or amorphous) of chitosan and chitosan derivatives since these properties are known to affect water uptake and biodegradability characteristics of polymers (Prabaharan & Gong, 2008). Figure 3.8 shows representative XRPD transmission diffractograms of pure chitosan powder, TG-chitosan, chitosan-BSA xerogel, TG-chitosan-BSA xerogel and native BSA. Crystalline chitosan showed its characteristic intense peak at 2θ = 20° (Nagahama *et al*., 2009). The synthesised TG-chitosan and the formulated xerogels however, had the intensity of this peak minimized, leaving the peak at 2θ between 22° to 24° which was a shoulder to the right of the main chitosan peak.

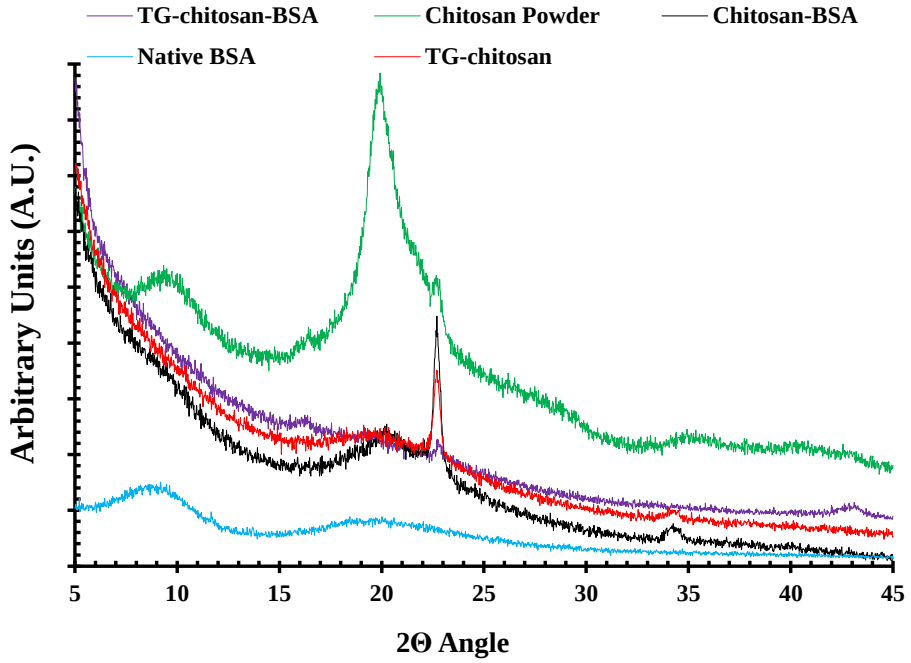

Figure 3.8: XRD-transmission diffractogram of chitosan powder, TG-chitosan, chitosan-BSA xerogel, TG-chitosan-BSA xerogel and native BSA powder.

These results revealed the existence of amorphous structures in the xerogels that resulted from chemical modification of chitosan following formulation with amorphous BSA, and other excipients (GLY and D-MANN), leading to the alteration of the original crystalline

structure. The interposing of plasticizer and cryoprotectant between the polymer chains and their interaction with functional groups of chitosan resulted in reduced intermolecular cohesive forces of attraction between the polymer chains. They also show that the freeze-drying procedure did not alter the amorphous structures formed during gel formulation prior to the freezing step when ice crystal formation occurs. The final amorphous xerogel could help in maintaining the stability of the model protein drug which was originally added as an amorphous powder and also enhance the mucoadhesive properties of the formulated polymer (Prabaharan & Gong, 2008) as a result of improved hydration and reduced rigidity (Kasper & Freiss, 2011).

Figure 3.9 shows the XRPD patterns of undialysed xerogel, dialysed xerogel and chitosan powder. The undialysed xerogel demonstrated a crystallinity of 96% whereas that of the dialysed xerogel was 32%. The three-fold increase in crystallinity showed by the undialysed xerogel was a result of the presence of NaAc produced as a process impurity.

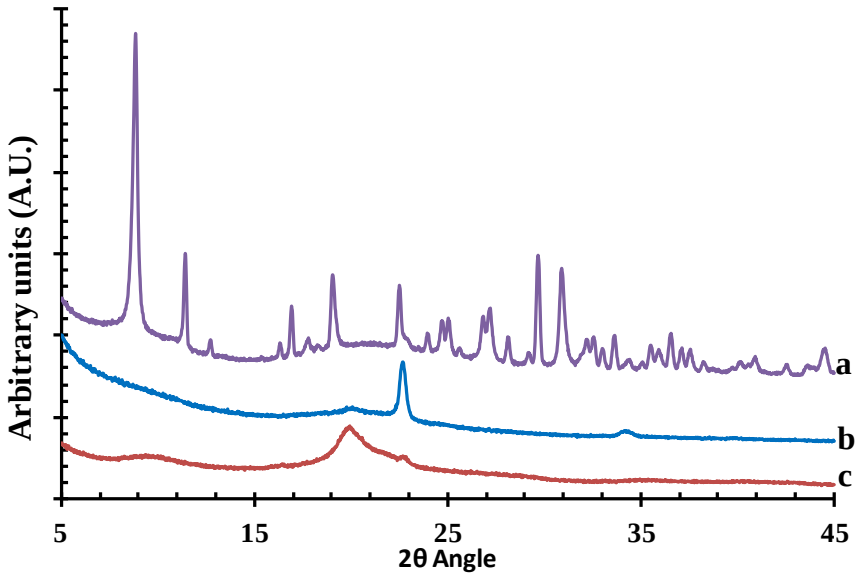

Figure 3.9: X-ray-transmission diffractogram of (a) Undialysed xerogel (depicting NaAc peaks), (b) dialysed xerogel and (c) chitosan powder.

The brittleness observed in the undialysed xerogel could be attributed to the newly formed crystalline NaAc from the use of NaOH to neutralise acetic acid, which was used to protonate the chitosan in order to improve its solubility for gel formation. The data highlights the importance of the dialysis step during processing.

The effect of EIs (10 % GSH and 5 % APR) on the physical form of TG-chitosan xerogel containing either BSA or INS were also evaluated. Figure 3.10 and 3.11 show representative X-ray diffractograms of TG-chitosan-BSA and TG-chitosan-INS xerogels with

and without APR respectively. The reduced peak of chitosan at 2θ around 22° to 24° was observed in all the formulations irrespective of whether there was EI present or not. Moreover loading the polymer matrix with a different protein (INS) did not affect the amorphous nature of the lyophilised xerogels.

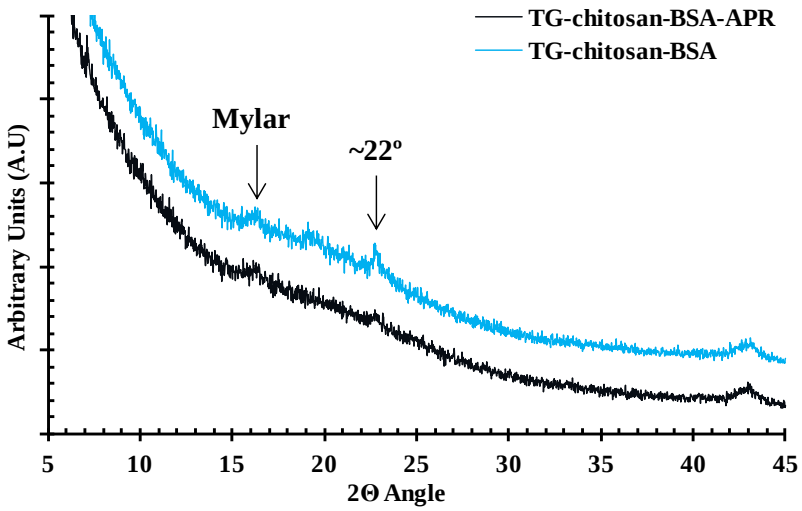

Figure 3.10: XRD-transmission diffractogram of TG-chitosan-BSA xerogels with and without the EI, aprotinin.

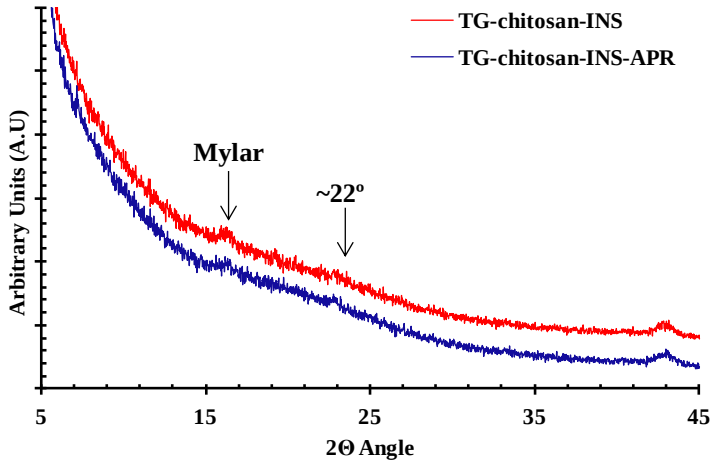

Figure 3.11: XRD-transmission diffractogram of TG-chitosan-INS xerogels with and without the EI, aprotinin.

3.3.6 Differential scanning calorimetry (DSC)

For phase separation studies after lyophilisation, multiple glass-transition (Tg) temperatures were detected at 40.3 °C and 130.1 °C in the undialysed xerogels (Figure 3.12 c) due to possible formation of metastable glass and subsequent crystallisation of the formed NaAC which might result in product instability during storage. However, for the dialysed chitosan-BSA and TG-chitosan-BSA xerogels in Figures 3.12 (a) and (b) respectively, no glass-transition temperatures were detected after lyophilisation, an indication of potential product stability during storage (Seales *et al*., 2001b)

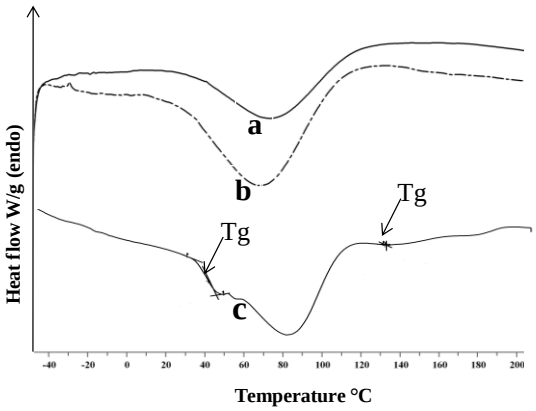

Figure 3.12: DSC thermograms of (a) chitosan-BSA (b) TG-chitosan-BSA and (c) undialysed chitosan-BSA xerogels.

The endothermic events observed from the representative thermograms in Figure 3.12 during the first heating cycles are the result of changes in heat capacity due to water loss from the xerogels. The application of the annealing process prevented the formation of metastable glass which would have eventually crystallized and affect the stability of the protein in the xerogels. It is however, important to note that it is difficult to detect the Tg´ of a freeze-concentrated chitosan (an aminopolysaccharide) as it is extremely weak (Ford & Mann, 2012) and this challenge could be exacerbated by a period of annealing the freeze-concentrate. The effectiveness of the annealing process led to no glass-transition detection by the DSC in the frozen concentrate as well as the lyophilised xerogel, implying no phase separation of the amorphous protein drug. Furthermore, the process of dialysis was critical in averting interferences from the effect of the excess acetic acid and the sodium acetate formed during the preliminary gel formation stages.

3.3.7 Physical stability of BSA and INS by far-UV CD spectroscopy

CD spectroscopy was applied to determine the conformational stability of the protein loaded lyophilised xerogels. An absolute requirement for a successful biotherapeutic is a correctly folded protein whose desired conformational stability is maintained by a suitable formulation. The knowledge of the secondary structure before and after gel formulation and lyophilisation was an essential step in determining possible conformational changes in the model protein drugs in the chitosan based xerogels.

Figure 3.13 shows the far-UV CD spectra of BSA released from dialysed and undialysed xerogels and native BSA in PBS. The two minima bands observed at 209 and 222 nm were respectively assigned to the α and β-helical structures of BSA as reported by Quiming *et al.*, (2005). BSA released from the chitosan xerogels and native BSA demonstrated similar mean residue ellipticity ratios at 209 and 222 nm ($[\theta]_{209}/[\theta]_{222}$) of 1.10.

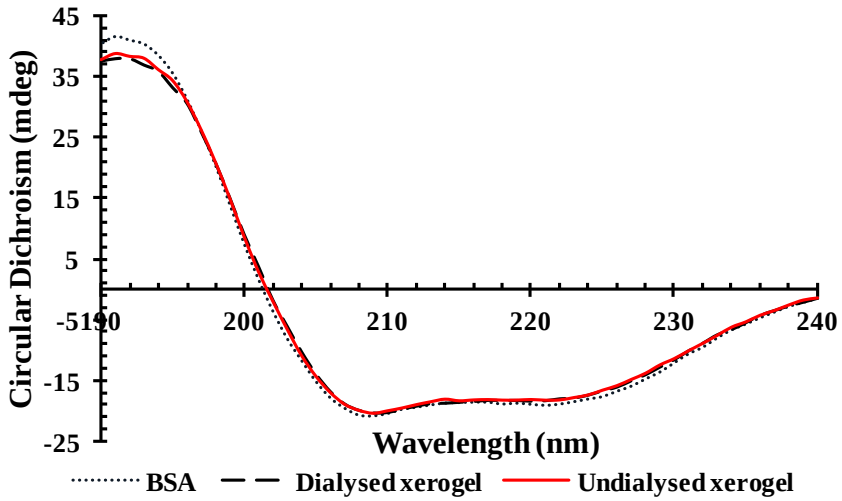

Figure 3.13: CD spectra of native BSA, dialysed and undialysed xerogels loaded with BSA

The similarity of the far-UV CD spectra and the mean residue ellipticity ratios obtained confirmed the conformational stability of BSA in the lyophilised xerogels. The presence of salts such as NaAc in the undialysed xerogel has been reported to induce protein unfolding (McNay *et al.*, 2001). However, in all the CD spectra, the main bands corresponding to α-helical structure remained unchanged, suggesting that the protein structure maintained its folded conformation, and was neither degraded nor hydrolysed during the production of lyophilised chitosan xerogels irrespective of whether there was a dialysis step involved or not.

Figure 3.14 shows the CD profiles of native BSA and BSA released from the chitosan-BSA, TG-chitosan –BSA and TG-chitosan –GSH-BSA xerogels in PBS at pH 6.8 in far-UV range. The ratios between the mean residue ellipticity at 209 and 222 nm ($[\theta]_{209}/[\theta]_{222}$) were 1.10, 1.10, 1.10 and 1.14 for native BSA, BSA released from the chitosan-BSA, TG-chitosan-BSA and TG-chitosan-GSH-BSA respectively. The similarity of the far-UV CD spectra and the mean residue ellipticity obtained confirmed the conformational stability of BSA in the lyophilised xerogels except for the GSH containing xerogel where possible adsorption of BSA by GSH at pH 6.8 caused a slight increase in the α-helical structure of BSA released.

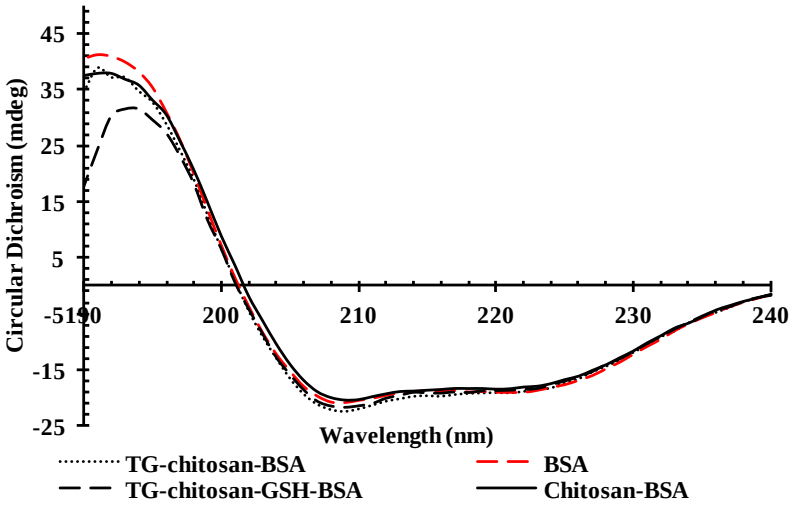

Figure 3.14: CD spectra of native BSA, chitosan-BSA, TG-chitosan–BSA and TG-chitosan –GSH-BSA xerogels.

The conformational stability of native INS, *in vitro* released INS from TG-chitosan-INS and TG-chitosan-INS-APR were also assessed by CD. The CD profiles in 0.01 M HCl at pH 2.3 and 0.01 M PBS at pH 6.8 in the far UV range are shown in Figures 3.15 and 3.16 respectively. As is evident from these figures, the native INS had two minima around 209 and 222 nm. The first band was assigned to the α-helical structure, while the second band was assigned to the β-structure. These results are consistent with the crystal structure of the hexamer determined by Wood & Blundell (1975) and the structure of native INS by Cui *et al*., (2008). These were similar to INS released from the TG-chitosan xerogels with or without the EI, 5 % APR in 0.01 M HCl.

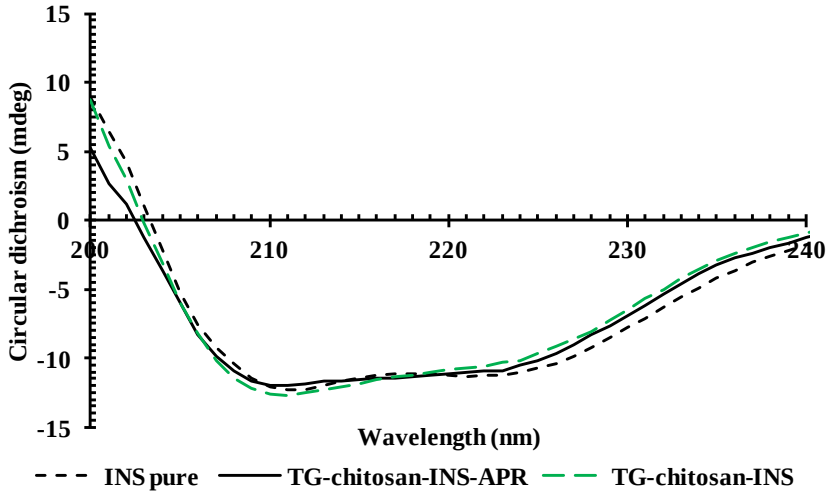

Figure 3.15: CD spectra of insulin released from TG-chitosan xerogels in 0.01M HCl (pH 2.3)

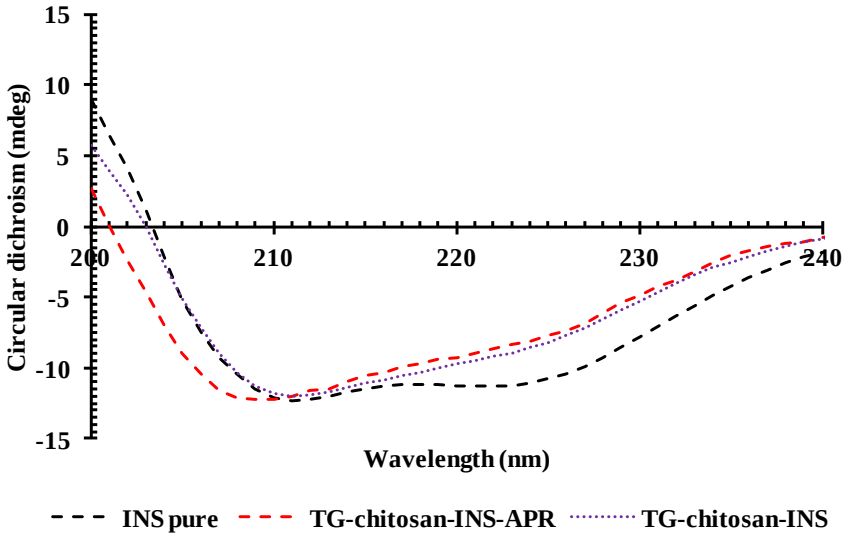

Figure 3.16: CD spectra of insulin released from TG-chitosan xerogels in 0.01 M PBS (pH 6.8)

The CD spectrum of INS released from the xerogels in PBS however, showed marked negative peaks at 209 nm with weak peaks at 222 nm. The ratios between the mean residue ellipticity at 209 and 222 nm ($[\theta]_{211}/[\theta]_{222}$) were also calculated and have been presented in Table 3.6. It is well known that the addition of chitosan to a system intended for protein delivery affects the circular dichroism band (Zhang *et al*., 2003). It was observed that the release of INS in PBS resulted in a higher mean residue ellipticity ratio due mainly to the

Table 3.6: Mean residue ellipticity ratios at 209 and 222 nm for INS loaded Xerogels

Formulation	0.01 M HCl (pH 2.3) $([\theta]_{211}/[\theta]_{222})$	0.01 M PBS (pH 6.8) $([\theta]_{211}/[\theta]_{222})$
Pure INS	1.09	1.09
TG-chitosan-INS	1.20	1.26
TG-chitosan-INS-APR	1.09	1.34

intermolecular interaction between the positively charged chitosan derivative and INS (isoelectric point 5.4) which would carry a negative charge at the environmental pH of 6.8. The enhanced value for the xerogel with APR may be due to further interaction between this EI and the released INS. The formulation process however preserves the protein conformational structure and physical stability. In addition, because the presence of INS in the monomeric form is higher than the native form, it is expected that it will result in better *in vivo* adsorption when applied to the buccal mucosal area (Blundell *et al*., 1972).

3.3.8 Thermogravimetric analysis - Moisture content

The residual moisture contents of the lyophilised xerogels are shown in Table 3.7. The range of residual moisture content from 1.8 ± 0.7 % to 2.7 ± 0.3 % falls within the recommended residual moisture content range of ≤ 1 % - ≤ 3 % for protein lyophiles (Ward *et al*., 2008). The loss in weight observed for all the samples during the dynamic heating stage occurred between 60 °C and 120 °C, is an indication of the fact that weight loss was due to bound water.

Table 3.7: Percentage drug loading capacity and moisture content of xerogels

Sample	% Drug loading (*n=4,mean ±SD)*	% Moisture content (*n=4,mean ± SD)*
Undialysed Chitosan-BSA	54.0 ± 5.4	2.7 ± 0.3
Annealed Chitosan-BSA	91.6 ± 4.0	1.8 ± 0.7
Non-annealed Chitosan-BSA	90.5 ± 4.0	2.2 ± 0.2
Annealed TG-chitosan-BSA	94 ± 1.6	1.8 ± 0.1
Non-annealed TG-chitosan-BSA	88.8 ± 4.0	1.8 ± 0.4

Since no product melt-back was observed after the freeze drying process, the robustness of the freeze drying cycle is depicted, with the primary drying stage removing all the loose water. The formation of a dry state by lyophilisation is essential to prevent premature release of the active protein drug. Attaining adequate residual moisture content for the xerogels was also vital as lower water content reduces molecular mobility and increases shelf-life by avoiding premature hydration of the active protein drug. The annealed xerogels had a slightly lower residual moisture content compared to the non-annealed products, as ice crystals were large enough for easy sublimation, allowing the drying phase to reach the bottom of the mould. The presence of GLY in the formulations could account for the levels of residual moisture observed. This was expected as GLY could slow down the drying process due to its humectant property. Again the combination of water, GLY and MANN results in synergistic plasticizing effect that can affect the thermal properties of the formulations.

3.3.9 Calibration curves for BSA and INS in 1% acetic acid, 0.01 PBS and 0.01 M HCl.

The calibration curves for BSA in 1% acetic acid and 0.01M PBS are shown in Figures 3.17 and 3.18 respectively with Figure 3.19 showing that of INS in 0.01 M HCl. The Bradford method relies on the binding of Coomasie blue G250 dye (Bradford reagent) to proteins. Although different ionic forms of the dye exist, the more anionic blue form of the dye binds to protein with a characteristic absorption maximum at 590 nm.

In this project, the assay was based on the improved Bradford protein assay protocol by Ernst & Zor (2010) that measures the ratio of the absorbance at 590 nm and 450 nm and provides significant advantages over the original Bradford protocol involving single measurement of absorbance at 590 nm. They further recommended the measurement of absorbance at 590-600 nm, to achieve maximal sensitivity to protein concentration change, and at 450-485 nm, to ensure linearization. This simple procedure increases the accuracy and improves the sensitivity of the assay about 10-fold, permitting quantification down to 50 ng of BSA. With the original Bradford protocol, diminished response to protein would result due to the interference by detergents. The improvement of sensitivity by one order of magnitude enables dilution of the samples up to a point where the interference by detergents is eliminated.

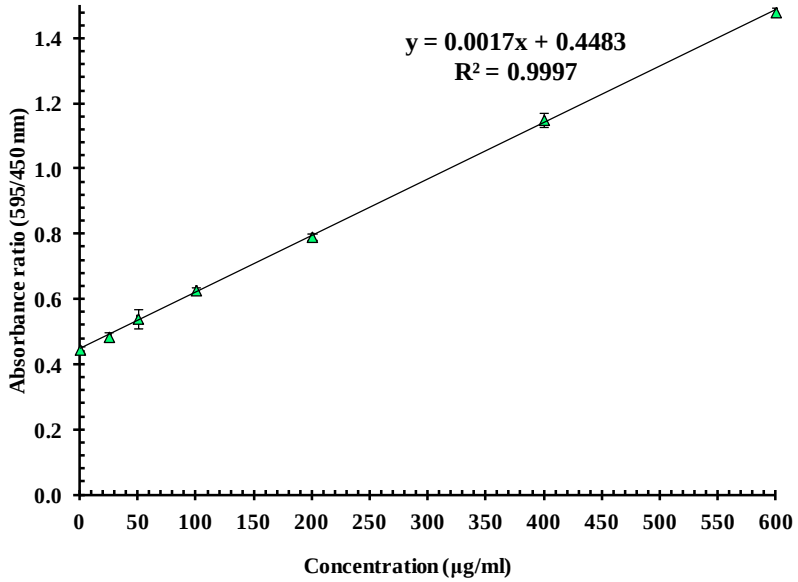

Figure 3.17: Calibration curve of BSA in 1% acetic acid.

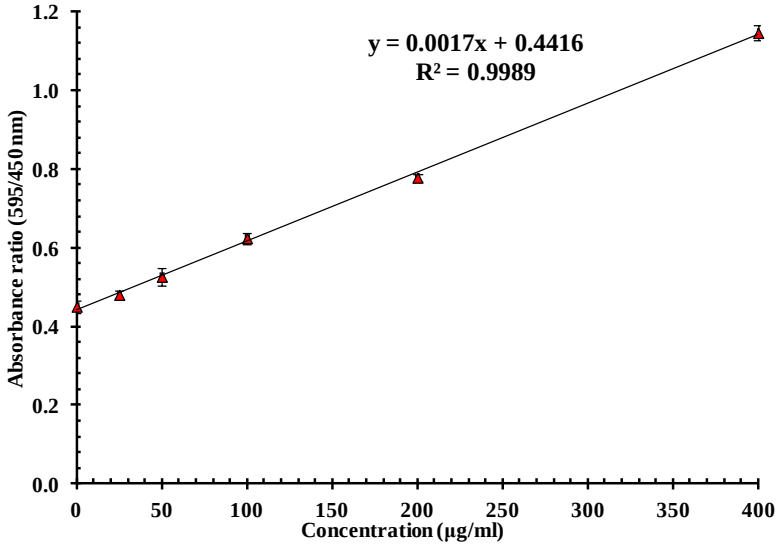

Figure 3.18: Calibration curve of BSA in 0.01 M PBS

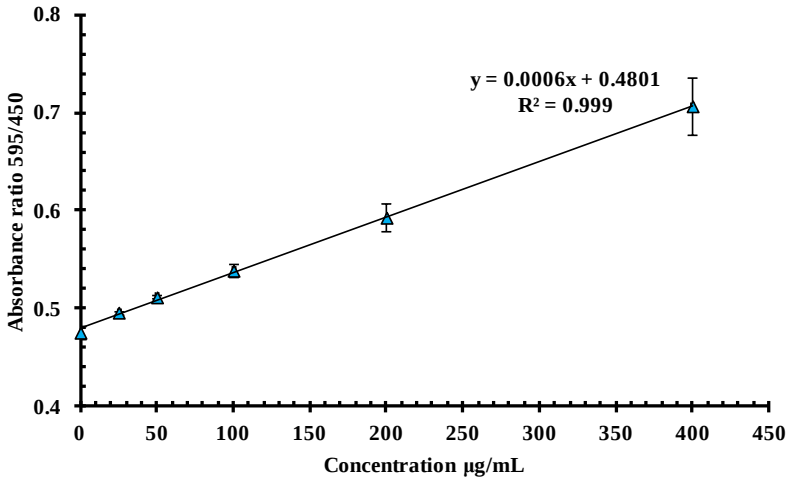

Figure 3.19: Calibration curve of INS in 0.01 M HCl

3.3.10 Drug loading capacity

A high drug loading capacity above 90 % (Table 3.7) explains the high total percentage cumulative release profiles observed for the annealed Chitosan-BSA and TG-chitosan-BSA xerogels (see chapter 5). The porous and fibrous networks of the lyophilised cakes allowed for higher drug loading capacity compared to related formulations such as solvent cast films. This is due to the fact that lyophilised xerogels maintain their original volume during the freezing stage while solvent cast films collapse during drying to yield a dense product with precipitation of excess drug on the surface (Boateng *et al*., 2010). There was no impedance from formulation excipients during analysis by the direct dissolution method. The drug loading capacities above 90 % also gave an indication of the efficiency of the drug incorporation into the gels and the recovery efficiency through formulation and freeze-drying (lyophilisation) steps to obtain the xerogels. The annealing and thiolation processes did not seem to have had much effect on the loading capacity as non-annealed Chitosan-BSA and TG-chitosan-BSA had similar values. The undialysed xerogels however, showed a low drug loading capacity of 54.0 ± 5.4 % due to interferences from sodium acetate and excess acetic acid present within the xerogel.

3.3.11 Scanning electron microscopy (SEM)

Representative scanning electron micrographs of the lyophilised xerogels are shown in Figure 3.20 [A-F]. The porous structure shows the effect of dialysis on the pore thickness and configuration. Dialysed chitosan-BSA xerogel (Figure 3.20 A) formed a porous polymeric network which had thinner walls as well as many smaller sub-pores. The undialysed xerogel

(Figure 3.20 B) on the other hand had similar pore sizes (150–200µm) and distribution but with thicker walls and fewer sub-pores within the network structure. Gel dehydration induced by the lyophilisation process resulted in the formation of NaAc crystals in the undialysed xerogel (Figure 3.21). Crystallisation and subsequent deposition of NaAc on the outer and inner walls of the interconnecting pores of the xerogels explains the rather thick walls observed in the undialysed xerogel (Ayensu *et al*., 2012b).

The micrographs also show the effect of annealing on the pore size. The optimally plasticized annealed chitosan-BSA xerogels formed a porous interconnecting polymeric network of sponge-like circular pores, with closer pore distribution and larger pore sizes with an average pore diameter of 200 µm (Figure 3.20 A and C). Non-annealed xerogels (Figure 3.20 D) also formed an interconnecting network, but with relatively smaller sized pores with an average pore diameter of 133µm. The sublimation of larger ice crystals formed from the merging of smaller ice crystals due to annealing, resulted in xerogels with large pores. The variation in the performance of the different formulations with respect to hydration capacity, *in vitro* mucoadhesion properties and release characteristics, could be attributed to differences in pore size of the annealed and non-annealed xerogels. The micrographs also show the effect of thiolation on xerogel pore size (Figure 3.20 E-F).

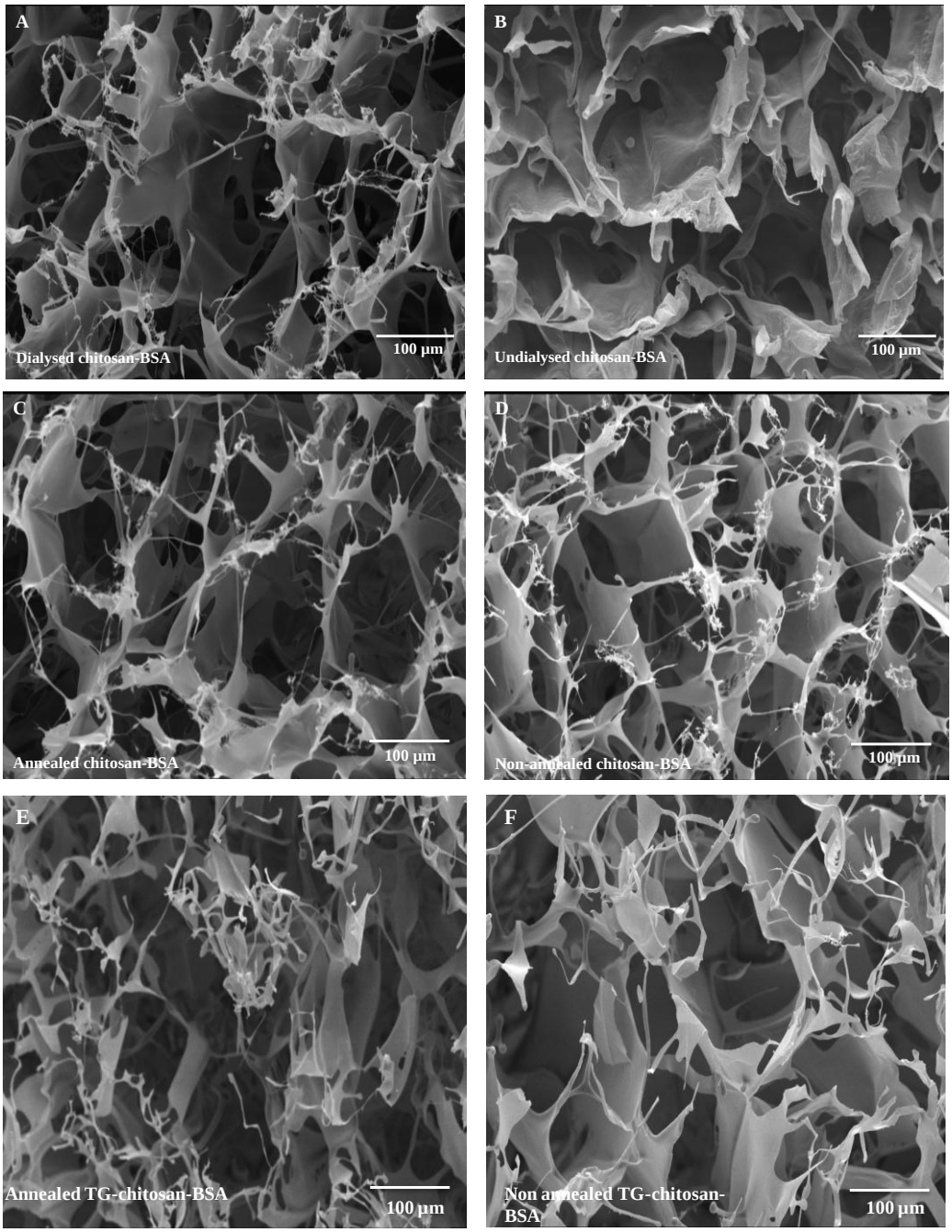

Figure 3.20: Representative SEM micrographs of lyophilised xerogels (magnification x 200).

Whereas unmodified chitosan-BSA xerogels were more regularly distributed, the TG-chitosan-BSA xerogels formed a fibrous, sponge-like, porous interconnecting polymer network but with smaller pore sizes and a more irregular pore distribution. The presence of low molecular weight compounds such as GLY, D-MANN and thiol ligand with high affinity for water is likely to have an effect on ice crystal ripening during the slow freezing process, which affects ice crystal size and subsequently pore size, hence the differences observed in the morphologies of the chitosan-BSA and TG-chitosan-BSA xerogels. Such differences in morphology (such as in pore size) can affect functional properties including rate of hydration,

swelling, mucoadhesion and subsequent drug release rates. This arises primarily from the differences in rate of water ingress, swelling and subsequent diffusion of drug from the swollen matrix (Boateng *et al*., 2010). Wu *et al*., (2009) have observed that pore size qualitatively correlated with the degree of swelling of hydrogels. In addition, the possible formation of disulphide bonds in the thiolated xerogels could affect pore size as distances between polymer chains are decreased by the degree of cross-linkages (Wu *et al*., 2009).

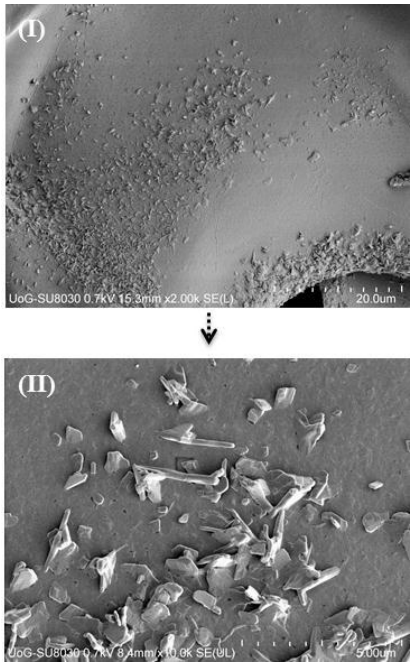

Figure 3.21: High magnifications of undialysed chitosan-BSA xerogel showing crystals of NaAc (Magnification: (I) x2000), (II) x10000).

The optimised thiolated chitosan xerogel was loaded with INS and the representative SEM micrograph as shown in Figure 3.32 also displayed smaller circular pores with thin sheet-like walls.

Figure 3.22: SEM micrographs of xerogel loaded with insulin (magnification x200)**.**

High magnification SEM micrograph of the EC laminate used as a backing membrane to ensure uni-direction release of protein loaded in the chitosan based xerogels is shown in Figure 3.33. The non-porous EC laminate formed a dense continuous sheet with no fractures.

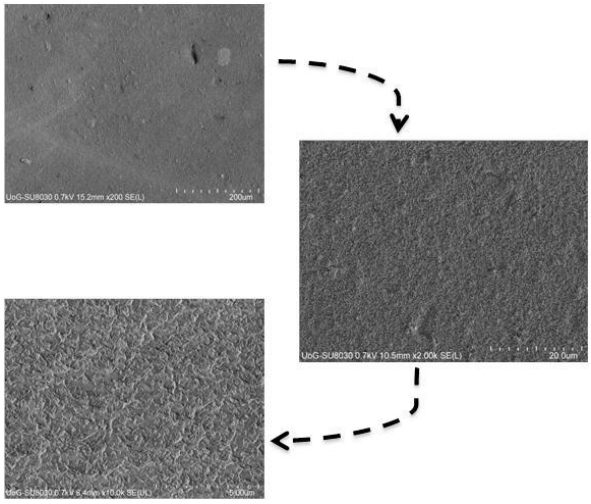

Figure 3.23: High magnification SEM micrographs of impervious EC laminate to be used as a backing membrane for xerogels (magnification x200 – x10000).

Figure 3.24 'A' shows a representative cross-sectional micrograph of a porous chitosan based xerogel overlaid on dried EC laminate prepared by solvent casting. The presence of GLY in the EC laminate as a plasticizer aids in the attachment of the xerogel to the laminate film as seen from the SEM micrograph. An enhanced stereo-paired image of the laminated xerogel (Figure 3.24 B) is shown to the right which is better viewed using a red/green filter.

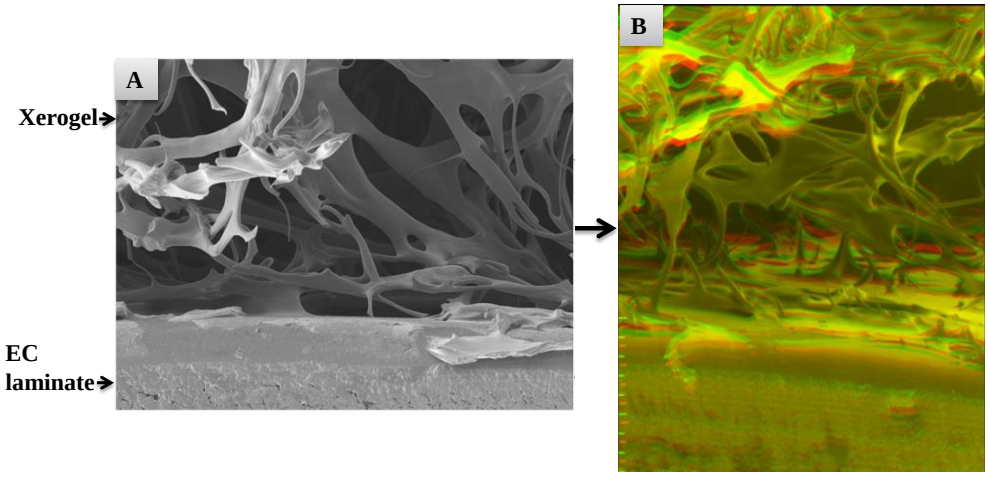

Figure 3.24: SEM micrographs of 'A' porous xerogel with an impervious EC laminate as a backing membrane and 'B' Stereo-paired image of laminated xerogel viewed with red/green filters (magnification x200).

3.3.12 Stability evaluation

The BSA and INS contents of the optimised TG-chitosan xerogels were initially estimated by Bradford's assay and HPLC methods. Xerogels were kept in 24 well plates sealed with parafilm and lids to limit moisture absorption, stored in the refrigerator (RF) at 5 °C ± 3 °C and analysed for BSA and INS content at a frequency of 3 months intervals. The accelerated stability studies of BSA and INS incorporated in the chitosan based xerogels was by the International Committee for Harmonisation (ICH)'s conditions for drug products intended for storage in a refrigerator. The exposure of the xerogels to varying conditions of temperature and moisture (relative humidity) had a profound effect on the chemical stability of the model protein drugs. Generally, INS xerogels stored in the refrigerator showed no signs of protein degradation/fragmentation throughout the entire period of evaluation with the assayed protein content within the range of 95 – 105 % as specified by the British Pharmacopoeia (BP 2012) for INS. This was however, not the case with xerogels stored at ambient temperature at a relative humidity of 60 % in a humidity chamber.

3.3.12.1 BSA and INS content by Bradford's assay

Figure 3.25 shows the stability curves for TG-chitosan xerogels containing BSA and INS determined using Bradford's assay. No significant differences were observed between the mean protein content of all xerogels irrespective of storage conditions ($p < 0.05$). In addition, all time points of analysis showed that the protein content of all xerogels were intact indicating product stability after storage under ICH conditions. However, since the Bradford method of protein estimation depends on binding with proteins, the possibility of binding all degraded/fragmented protein products may exist, thus giving a determination of total protein present. This constitutes a limitation of the method if all fragmented products contain arginyl and lysyl residues of proteins which bind readily with the Coomasie blue dye (Congdon *et al*., 1993 cited in Kruger, 2008). Such a method cannot be used to detect the presence of degraded proteins and thus will not be suitable to differentiate between the protein products in the xerogels after storage under the ICH conditions.

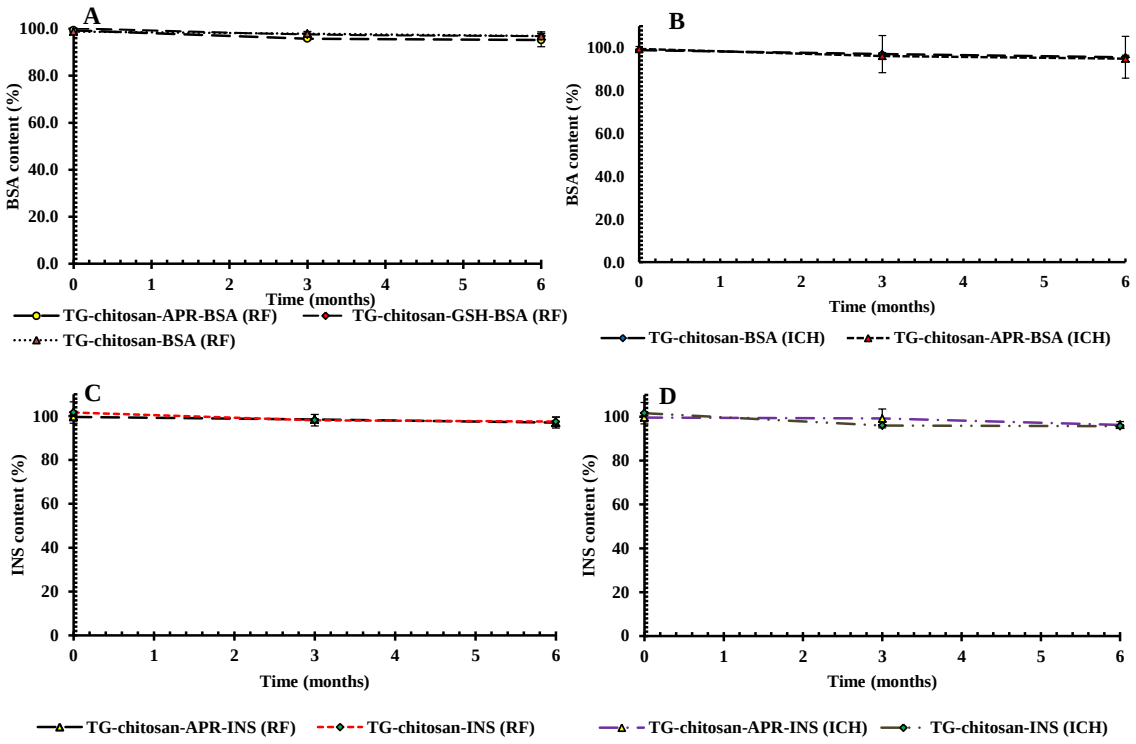

Figure 3.25: Stability curves obtained by Bradford's assay. (A) and (B) show the content for BSA while (C) and (D) show the content of INS in TG-chitosan xerogels after six months storage in the refrigerator (RF) and under ICH conditions.

3.3.12.2 HPLC determination of BSA and INS content.

Figure 3.26 shows the calibration curves for BSA 'A' and INS 'B' using SE-HPLC and RP-HPLC respectively. The respective SE-HPLC and RP-HPLC estimation of BSA and INS contents provided evidence for the existence of fragmented proteins from xerogels stored under ICH conditions. Storage of xerogels in the refrigerator resulted in the maintenance of their initial content after six months storage. No significant loss in protein was detected when stored in the refrigerator (Figure 3.27 'A' and 'C'). However, storage at 25°C and relative humidity of 60 % showed significant reduction in protein content down to 40 % and 20 % for BSA and INS respectively (Figure 3.27 'B' and 'D') after six months of storage.

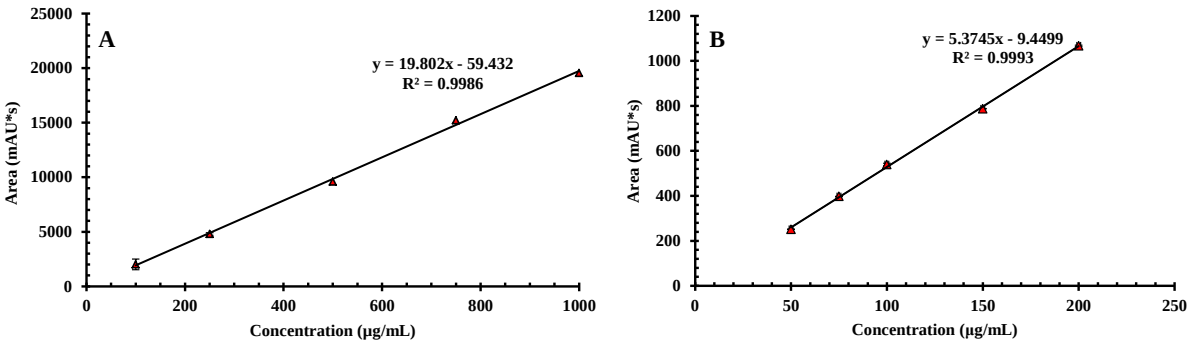

Figure 3.26: BSA ‘A’ and INS ‘B’ calibration curves using SE-HPLC and RP-HPLC respectively.

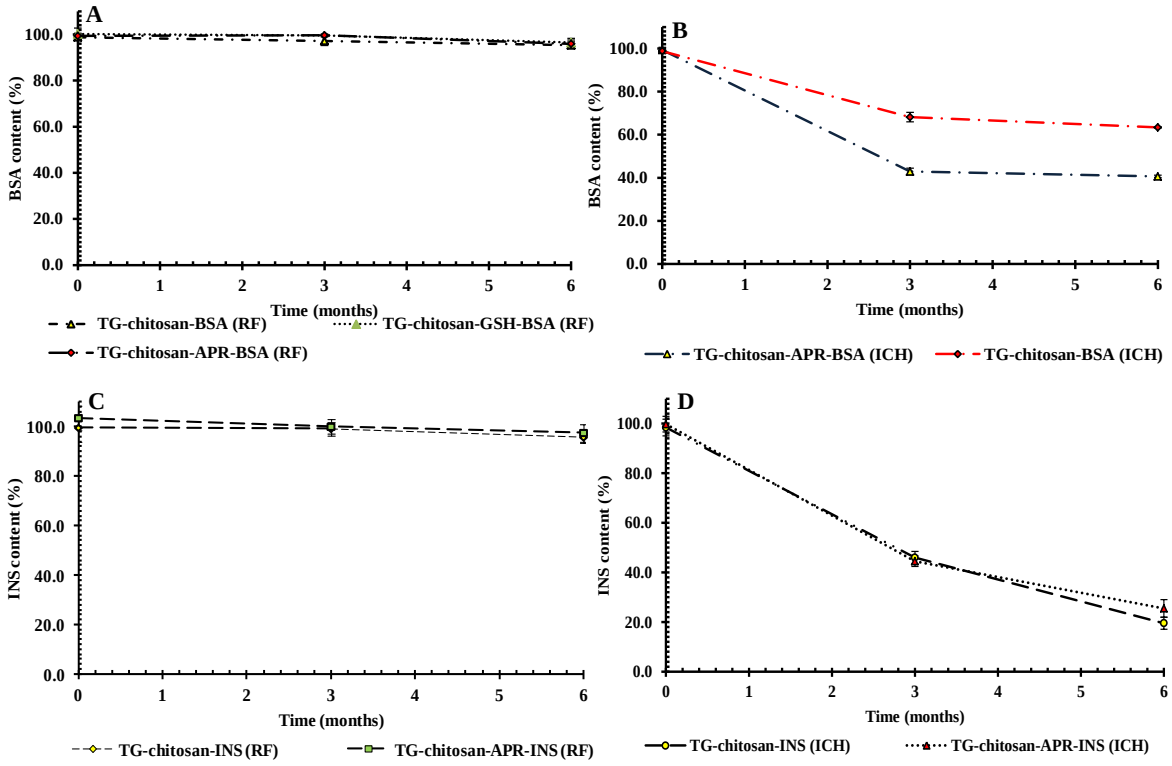

Figure 3.27: Stability curves obtained by SE-HPLC and RP-HPLC for BSA and INS respectively. (A) and (B) show the content for BSA while (C) and (D) show the content of INS in TG-chitosan xerogels after six months storage in the refrigerator (RF) and under ICH conditions.

The representative HPLC chromatograms in Figure 3.28 also show the peaks of chemically degraded BSA and INS along with the remaining BSA and INS originally present in the xerogels (Figure 3.28 ‘C’ and ‘F’). The exposure of the xerogels to extreme moisture

conditions leads to protein hydrolysis. The fragmented protein species from the BSA containing TG-chitosan xerogels stored under ICH conditions are most likely the result of hydrolysis of peptide bonds (Manning *et al*., 1989, cited in Estey *et al*., 2006). They appeared as unresolved species eluting before the minimised BSA peak as a result of progressive BSA loss. The reduced content of BSA detected at the end of the incubation suggests that the hydrolysis process was continuous throughout the incubation period and was incomplete at the last time point of six months.

The stability of INS in the xerogels stored in a refrigerator could stem from formulation TG-chitosan, which as a hydrophilic polymer would deposit on the substrate surface, preventing moisture from reaching the proteins and thus limiting continuous INS degradation (Maroni *et al*., 2009). However the poor stability of most therapeutic proteins under room conditions is well documented (Strickley & Bradley, 1997 cited in Maroni *et al*., 2009). Non- enzymatic degradation reactions occur with both solid and aqueous state INS leading to the formation of degradation products. Several INS degradation products including A21-desamido insulin, Other Insulin Related Compounds (OIRCs) and High Molecular Weight Proteins (HMWPs) have been described in the literature (Brange, 1992, cited in Maroni *et al*., 2009). The degradation of INS from the TG-chitosan xerogel at 25 °C/60 % RH could stem from hydration and hydrolysis of the polymer matrix allowing moisture to reach the exposed large surface area of INS.

The primary packaging of parafilm sealing on the 24 well plates does not seem to have limited moisture absorption as originally suggested. In addition the instability of the model protein drugs could be due to poor air and moisture tightness of the sealing material

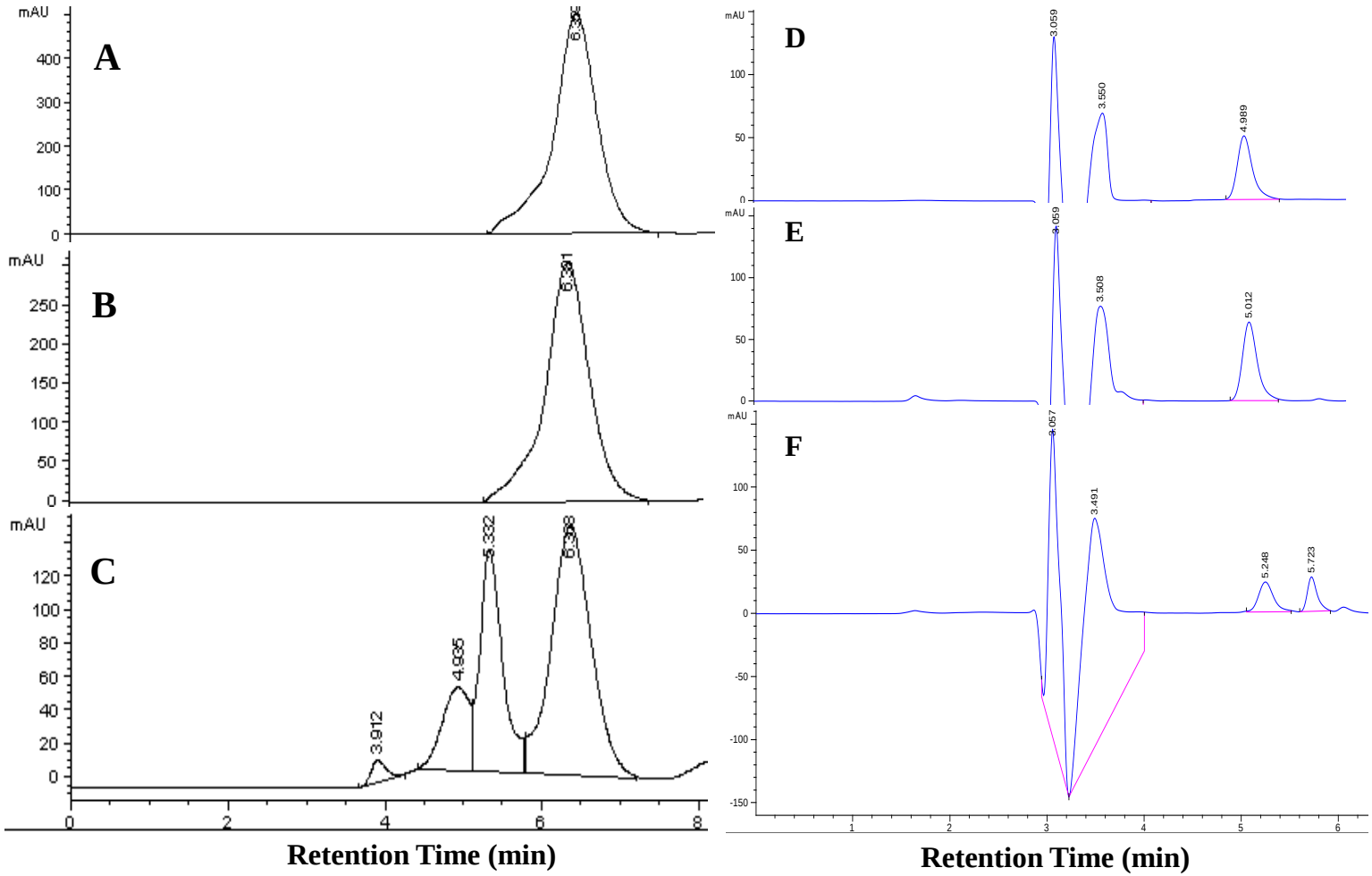

Figure 3.28: SE-HPLC chromatograms ‘A’ shows BSA powder peak (retention time around 6.3 minutes), ‘B’ BSA released from TG-chitosan xerogels stored at 5 ℃ and ‘C’ BSA and degraded BSA products released from TG-chitosan xerogel stored under ICH accelerated stability conditions for six months. The RP-HPLC chromatogram ‘D’ shows the peak of pure INS powder (retention time around 5 minutes), ‘E’ the peak of INS from TG-chitosan stored in a refrigerator and ‘F’ INS and degraded INS products from xerogels stored under ICH conditions.

3.4 Conclusions

Analytical characterisation of the chitosan based xerogels has been carried out using various analytical techniques. Structural information obtained from the ^{1}HNMR and ATR-FT-IR spectra have been used to confirm the chemical functional groups present in chitosan and TG-chitosan. ^{1}HNMR was however not suitable for the determination of free thiol groups or disulphide bonds. Therefore UV spectroscopy using Ellman's reaction was employed to quantify the amount of thiol groups immobilised covalently on the primary amine groups of chitosan to obtain TG-chitosan. The difference in polymer molecular weight between chitosan and TG-chitosan monitored by GPC confirmed the covalent attachment.

ATR-FT-IR analysis of the conformational sensitive amide I and amide II bands indicated the conformational stability of the secondary structures of the loaded model protein drugs BSA and INS which were confirmed by CD spectroscopy. With respect to protein physical stability, no multiple glass-transition temperatures were detected by DSC after lyophilisation for all formulations except for the undialysed chitosan xerogel. The XRPD analysis of crystalline chitosan powder displayed its characteristic peak which was minimised in the formulated xerogels resulting in amorphous structures. However the presence of NaAc crystals identified by ATR-FT-IR spectra and XRPD diffractogram and confirmed with SEM microscopy resulted in thick walled xerogels for the undialysed chitosan samples. Furthermore, the SEM micrographs showed highly porous xerogels due to annealing which allowed for high drug loading capacities of the dialysed and annealed xerogels which also exhibited optimal moisture content for maintaining protein stability. The EC laminate however formed a continuous non porous sheet which effectively attached to the chitosan based xerogel, to serve as a backing membrane to assure uni-directional release of protein drug.

The chemical stabilities of BSA and INS incorporated in chitosan based xerogels have been critically examined in this study. The results showed that storage of xerogels using accelerated stability conditions at 25 °C/ 60 % RH for six months resulted in substantial loss of native protein. Such reduction in protein content observed may have resulted from increased peptide bond hydrolysis due to enhanced moisture ingress during storage. Storage of xerogels at 5 °C in a refrigerator maintained protein nature up to six month however, further studies to establish the full extent of stability after storage in the refrigerator for up to 12 months is required. The use of SE-HPLC and RP-HPLC methods respectively for BSA and INS estimation yielded chromatograms that suggested the presence of degraded protein products for xerogels under accelerated stability studies. The employment of Bradford's assay

for protein quantification, however, could not be used to determine the presence of protein degraded products from all xerogels.

It is essential that the development of chitosan based delivery systems for controlled release of therapeutic proteins takes into consideration the stability of the protein drug. In addition, to improve stability of proteins within chitosan based systems, formulations must be protected from potentially extreme hydrolysing conditions to ensure maintenance of the native structure.

CHAPTER FOUR

HYDRATION CAPACITY AND *IN VITRO* MUCOADHESION STUDIES

4.1 Introduction

Mucoadhesive polymeric drug carriers can have intimate contact with mucosal surfaces without absorption to induce systemic toxic side effects. In addition, they provide prolonged residence time of drugs on the mucosal surface, creating higher drug concentration and consequent controlled release of drugs (Grabovac *et al*., 2008). Other advantages of buccal mucoadhesive polymeric delivery systems include overcoming environmental factors such as salivary flow and shearing forces generated from tongue movements, chewing and swallowing, which can displace an adhered system (Eouani *et al*., 2001). For this reason, mucoadhesive polymeric systems have been used as an established alternative strategy for the delivery of proteins and peptides to combat low membrane permeability. Furthermore, thiolated polymers have also been studied and applied to impart improved mucoadhesion as well as permeation enhancing properties (Bernkop-Schnürch, 2005).

Several approaches including the use of mucoadhesive polymeric gels (Patel *et al*., 2011), films and wafers (Boateng *et al*., 2009) have been explored as putative mucoadhesive dosage forms for controlled drug delivery. Physical entanglement and secondary bonding such as hydrogen bonding and Van der Waals forces have been proposed as the major interaction between the mucoadhesive polymers and mucin (Eouani *et al*., 2001). Recently, thiomers with sulphydryl ligands have also been suggested to form disulphide covalent bonds with cysteine-rich mucin glycoproteins (Albrecht *et al*., 2006). These forces of interaction which contribute to this type of adhesion are related to the surface functional groups of the mucoadhesive polymers such as amines, amides, carboxyls, hydroxyls and sulphydryl groups. The mucoadhesivity and consequent duration of retention of the polymeric matrices are significantly impacted by physical properties such as rate of hydration and rheological properties (Smart, 1999, cited in Eouani *et al*., 2001). Hydration study of mucoadhesive polymeric systems is essential as it gives information on polymer chain structural behaviour and allows complete analysis of the rigidity as well as deformability of the polymeric system (Eouani *et al*., 2001). In addition, the determination of the hydration capacity informs functional characteristics such as swelling and rate of drug diffusion from the polymer matrix.

In this chapter, the hydration capacities of various chitosan based xerogels containing BSA or INS as model protein drugs are evaluated and the effect of formulation processes such as membrane dialysis, annealing and thiolation determined. In addition, the driving mechanism for hydration in the thiolated xerogels was examined by carrying out the procedure with or without the presence of a reducing agent dithiotreitol (DTT). The

mucoadhesive performance of the xerogels was assessed in an *in vitro* environment using a texture analyser to measure the peak adhesive force (PAF), total work of adhesion (TWA) and cohesiveness. The effect of mucin concentration, membrane dialysis, annealing, thiolation and enzyme inhibitors (EI) on mucoadhesion properties were determined.

4.2 Materials and methods

4.2.1 Materials

Table 4.1: Details of materials used in hydration and mucoadhesion studies.

Material	Description	Supplier
Sodium hydroxide	S 240697	Sigma-Aldrich, Gillingham, UK
Potassium dihydrogen phosphate	P /4760/53	Fisher Scientific (Leicester UK)
Mucin from bovine submaxillary gland, Type I-S	M 3895-1 G	Sigma-Aldrich, Gillingham, UK
Gelatine (pulverised)	G /0150/53	Fischer Scientific (Leicester UK)
DL Dithiotreitol (DTT)	D0632-1G	Sigma-Aldrich, Gillingham, UK
PBS tablets (pH 7.4)	4P4417-50TAB	Sigma-Aldrich, Gillingham, UK

4.2.2 Hydration capacity

The hydration capacities of the formulated lyophilised xerogels containing BSA (see Tables 4.3) were determined by incubating the samples in 25 mL of 0.01M PBS solution (pH 6.8 ± 0.1 simulating salivary pH) at 37 ± 0.1°C. The solution was prepared by dissolving a tablet of PBS (pH 7.4) in 200 mL of deionised water and adjusting the pH to 6.8 using potassium dihydrogen phosphate and sodium hydroxide. The xerogels were initially weighed and the hydration and swelling behaviour observed at predetermined time intervals (Wu *et al*., 2009). The samples were removed and blotted off carefully between tissue papers to remove the surface-adhered liquid droplets and reweighed on an electronic balance to constant weight. These studies were performed in quadruplicate (n = 4) for each set of formulated samples and average values were calculated for data analyses. The percentage water uptake (hydration capacity) was calculated using equation 4.1:

$$\textit{Water uptake (\%)} = 100 \times (W_s - W) / W \quad \text{..... equation 4.1}$$

where W_s is the weight of the hydrated xerogel, and W is the initial weight of xerogel.

4.2.2.1 Effect of formulation processes on xerogel hydration capacity

Xerogel hydration characteristics with respect to annealing, dialysis, thiolation and in the presence of EI were investigated. In addition, the effect of a reducing agent on hydration capacity of thiolated xerogels (Table 4.3) was studied with or without the addition of 10 mM Dithiotreitol (DTT) (Verheul *et al*., 2011) to the PBS solution. The neutrality or otherwise of the xerogels was also established by immersing the samples in de-ionised water (pH 7.0) for 4 hours and determining the subsequent pH.

4.2.3 In-vitro mucoadhesion studies

The *in vitro* mucoadhesion (peak adhesive force-PAF; total work of adhesion-TWA and cohesiveness) properties of the lyophilised xerogels were studied utilizing a texture analyser. The samples (n = 4) were attached to a 75 mm diameter adhesive rig probe with a double sided adhesive tape on a TA.HD.*plus* Texture Analyser (Stable Micro Systems, Surrey, UK) fitted with a 5 kg load cell in tension mode [Fig 4.1 (a)]. A 6.67 % gelatine solution allowed to set as a gel in a Petri-dish (diameter 88 mm), was equilibrated with 1 mL of 1-5 % mucin solution (pH of 6.8 ± 0.1) for 60 seconds to represent the buccal mucosal surface was placed on the instrument platform. The optimum mucin concentration was selected to equilibrate the mucosal substrate in subsequent determinations (see section 4.2.3.1). The probe, lined with xerogel was set to approach the model buccal mucosal surface with the set parameters for adhesivity as shown in Table 4.2 (Thirawong *et al*., 2007), allowing 60s for complete contact and hydration before being detached.

Texture Exponent 32 software was employed to record and process the data. The maximum force required to detach the xerogel from the mucosal surface, (PAF) was determined. The area under the curve (AUC) representing total work of adhesion (TWA) was estimated from the force-distance plot whiles the cohesiveness of the samples was determined by the distance of travel [Fig.4.1 (b)].

Table 4.2: Texture analyser settings for determining the peak adhesive force (PAF), total work of adhesion (TWA) and cohesiveness of formulations.

Parameters	TA settings
Pre-test speed	0.5 mm/sec
Test speed	0.5 mm/sec
Post-test speed	1.0 mm/sec
Applied force	100.0 g
Return distance	10.0 mm
Contact time	60.0 sec
Trigger type	Auto
Trigger force	5.0 g

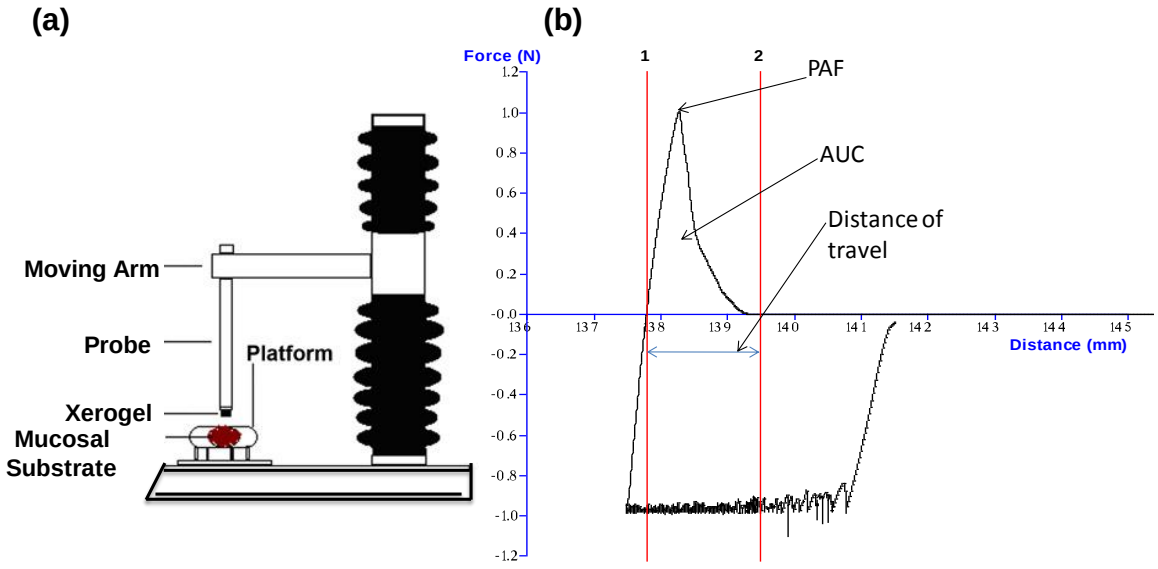

Figure 4.1: (a) Schematic diagram of texture analyser with xerogel attached to the probe and the mucosal substrate on the platform (b) Typical texture analysis force-distance plot.

4.2.3.1 Investigation of factors affecting mucoadhesion properties of xerogels.

The influence of various parameters on adhesive properties of the lyophilised xerogels was investigated as follow:

(a) ***Mucin concentration***; varying concentrations of mucin solution (1-5 %) prepared with 0.01 M PBS (pH 6.8) were used in equilibrating the gelatine

substrate in order to select the optimum concentration for further mucoadhesion characterisation of the xerogels.

(b) ***Effect of membrane dialysis***; the mucoadhesive properties of chitosan xerogels obtained from gels formulated by incorporating membrane dialysis were evaluated against xerogels obtained from gels formulated without the membrane dialysis stage.

(c) ***Annealing***; mucoadhesive properties of annealed and non-annealed xerogels were evaluated.

(d) ***Thiolation***; the effect of thiolation on mucoadhesive properties was studied using unmodified and thiolated chitosan xerogels.

(e) ***Enzyme inhibitors (EI)***; using thiolated xerogels loaded with BSA/INS with or without an EI, the effect of varying concentrations of reduced GSH (0 – 10 %) and APR (5 %) on mucoadhesive characteristics were measured. Optimised GSH concentration was selected for further development and characterisation.

4.2.4 Statistical data analysis.

Statistical data evaluation was performed using two tailed student t-test with 95 % confidence interval (p-value < 0.05) as the minimal level of significance. The pairs of data evaluated included the following; 'dialysed *vs* undialysed xerogels', 'annealed *vs* non-annealed xerogels', 'thiolated *vs* unmodified chitosan xerogels' and 'EI xerogels *vs* non-EI xerogels'.

4.3 Results and Discussion

4.3.1 Hydration capacity

Adequate hydration capacity of a buccal adhesive system is an essential property for uniform and prolonged release of the protein drug and effective mucoadhesion (Peppas & Bury, 1985). During the preliminary hydration studies, the hydration capacity was observed to increase with increasing concentration of GLY and D-MANN. However, physical examination of these xerogels with higher GLY and D-MANN content revealed the 'inward-caving' of the xerogels after lyophilisation. An enlarged space may have been created

between the polymer chains by the plasticizer resulting in a loose and unstable micro-porous structure, which allowed a higher rate of water ingress and hence the enhanced water absorption capacity.

The difference in the hydration capacity of the optimised annealed xerogel (1110.3 ± 23.3 %) and the non-annealed xerogel (800.0 ± 21.4 %) was statistically significant ($p < 0.05$). The water uptake of the samples reached the maximum value within 30 minutes of incubation, due to increased hydrophilicity of the chitosan xerogels with the presence of GLY and D-MANN. In addition, the annealing process enhanced ice crystal pore size during the freezing stage to increase xerogel porosity as shown in the previous chapter. Furthermore, the difference in the hydration capacities of annealed and the non-annealed TG-chitosan-BSA xerogels (Table 4.3) was statistically significant ($p < 0.05$). It is interesting to note that all the annealed xerogels maintained structural integrity after 4 hours of incubation due possibly to the mechanically stronger formulations obtained by annealing. The non-annealed xerogels however, formed a loose jelly-like and unstable swollen structure that consequently disintegrated after two (2) hours of incubation in PBS at 37 °C.

The difference in the mean hydration capacities between dialysed and undialysed (both annealed) xerogels was not statistically significant ($p > 0.05$). The large pore sizes of both dialysed and undialysed xerogels were responsible for the high rate of water access with hydration capacities of 1110.3 ± 23.3 and 1090.0 ± 10.8, respectively. The presence of hygroscopic GLY in the xerogels could have enhanced the swelling capacities by increasing the intermolecular spaces between the polymer chains. In spite of the high capacities recorded, the dialysed xerogel was structurally stable under the excessive hydrated weight, resisting collapse for up to 4 h. The undialysed xerogels however, formed slippery gelatinous masses after 2 h of incubation, making handling difficult and was therefore discontinued. In addition, there was a reduction in the pH of the PBS solution containing the undialysed xerogels from 6.8 to 6.6 during the hydration studies due to the possible presence of excess acetic acid.

However, upon the addition of xerogels to 10 mL of deionised water (pH 7), the pH of water was observed to have decreased to 6.0 for the dialysed xerogels and 6.5 for the undialysed xerogels. It is essential that xerogel's pH does not significantly alter the environmental pH of the buccal mucosa to induce irritation when applied. This explains the rational for neutralising the excess acetic acid used in dissolving chitosan with NaOH during the gel formulation stage. The dissociation of NaAC (present as a by-product during gel formation) in the undialysed xerogels, to form NaOH and acetic acid in solution could explain the difference in pH observed when the xerogels were added to the deionised water.

Table 4.3 Hydration capacity of xerogels

Sample	Treatment	Hydration capacity (%) (n=4, mean ± SD)
Chitosan-BSA	Non-annealed	800.0 ± 21.4
Chitosan- BSA	Annealed/dialysed	1110.3 ± 23.3
Chitosan- BSA	Annealed/undialysed	1090.0 ± 10.8
TG-chitosan-BSA	Non-annealed	433.6 ± 3.1
TG-chitosan-BSA	Annealed	480.0 ±18.2

The evaluation of the hydration capacities of dialysed chitosan-BSA and TG-chitosan-BSA xerogels (annealed) revealed the effect of thiolation on xerogel hydration characteristics. The difference in the hydration capacities of the chitosan-BSA xerogel (1110.3 ± 23.3 %) and TG-chitosan-BSA xerogel (480.0 ± 18.2%) (Table 4.3) was statistically significant ($p < 0.05$) in the absence of a disulphide reducing agent (DTT). The swelling capacity of the chitosan-BSA xerogel reached the maximum value within 30 minutes of incubation, which was due to the increased hydrophilicity of chitosan in the presence of GLY and D-MANN as discussed above. In addition, the enhanced pore size allowed for a higher rate of water ingress with a swelling capacity greater than 2-fold that of the TG-chitosan. It was observed that the rate of water ingress and swelling was slower for the TG-chitosan-BSA xerogel which prevented the formation of an excessively hydrated structure. This could be attributed to the oxidation of free thiol groups to form inter- and intra-molecular disulphide bonds in PBS at a higher pH of 6.8 which subsequently limited the hydration process during the incubation period. It has been shown by Plunkett *et al*., (2003 cited in Wu *et al*., 2009) that osmotic pressure changes may occur with the formation of disulphide bonds and that the extent of hydration is decreased with increased cross-linking density (Shu *et al*., 2002, cited in Wu *et al*., 2009). However, in the presence of a disulphide reducing agent (DTT), a dramatic increase in hydration capacity was observed for the TG-chitosan xerogel (Table 4.4) due to the breaking of the disulphide bonds with subsequent decrease in cross-linking density. This gives evidence that the swelling characteristic was driven by the formation of internal disulphide cross-linkages in the TG-chitosan xerogels (Ayensu *et al*., 2012b). Mucoadhesive xerogels are expected to be hydrated on the underlying mucosal tissue by water absorption, swelling and capillary action resulting in stronger adhesion (Eouani *et al*., 2001).

Table 4.4 Effect of reducing agent 10 mM DTT on hydration capacity of thiolated chitosan xerogels

Sample	Treatment	% Hydration capacity (n=4, mean + SD)
TG-chitosan-BSA	Annealed without DTT	480.0 ±18.2
TG-chitosan-BSA	Annealed with DTT	1086.8 ± 5.1
TG-chitosan-GSH-BSA	Annealed without DTT	912.5 ± 25.1
TG-chitosan-GHS-BSA	Annealed with DTT	910.2 ± 24.7

The hydration capacities of annealed thiolated xerogels with 10 % GSH as EI were evaluated with or without the presence of the reducing agent DTT. No statistical significant difference ($p > 0.05$) was found between the mean hydration capacities of the xerogels with or without DTT (Table 4.4). The presence of GSH in the xerogel could have prevented disulphide bond formation in the thiolated chitosan xerogels at the pH of 6.8 resulting in the improved hydration capacity observed. Thiolated chitosans have shown the capacity to reduce oxidised glutathione by restricting oxidation of GSH on membranes when the two are used in combination as permeation enhancers (Clausen *et al*., 2002). Therefore, the interaction between the thiomer and GSH in the xerogels does not result in the formation of disulphide cross-linkages that have the ability to reduce hydration capacity. It was however, observed that the GSH containing xerogels formed loose gels after 2 hours of incubation, affecting their structural integrity over a prolonged period.

4.3.2 Mucoadhesion

Gelatine as a representative mucosal substrate was chosen over non-protein based gel sources as the presence of methionine (a sulphur-containing proteinogenic amino acid), and the equilibration of the surface with cysteine-rich mucin glycoprotein augmented the adhesion process. The hydration of xerogels contributes to their mucoadhesion properties. Sufficient hydration of the xerogels facilitates the establishment of hydrogen bonding, allowing the polymeric chains to spread easily while diffusing along the xerogel/mucosal substrate interface. Initial hydration of the xerogels results in a hydrated gel layer which exposes the adhesive sites via relaxed molecules and allows easy interpenetration of the substrate molecules which subsequently creates the adhesive bonds (Tamburic *et al*., 1997).

4.3.2.1 Factors affecting mucoadhesive properties of xerogels

(a) ***Effect of mucin concentration***; mucoadhesive characteristics were exhibited by the chitosan xerogels as a result of hydrogen bonding, electrostatic forces and hydrophobic interactions between the functional groups of chitosan and the sialic acid residues found in mucin (Sogia *et al*., 2008) [Figure 4.2 (a)]. Enhanced mucoadhesion properties were however observed for the thiolated chitosan xerogels as a result of stronger covalent bonding between the thiol ligands and the cysteine rich residues on the glycoproteins of mucin [Figure 4.2 (b)]. The differences

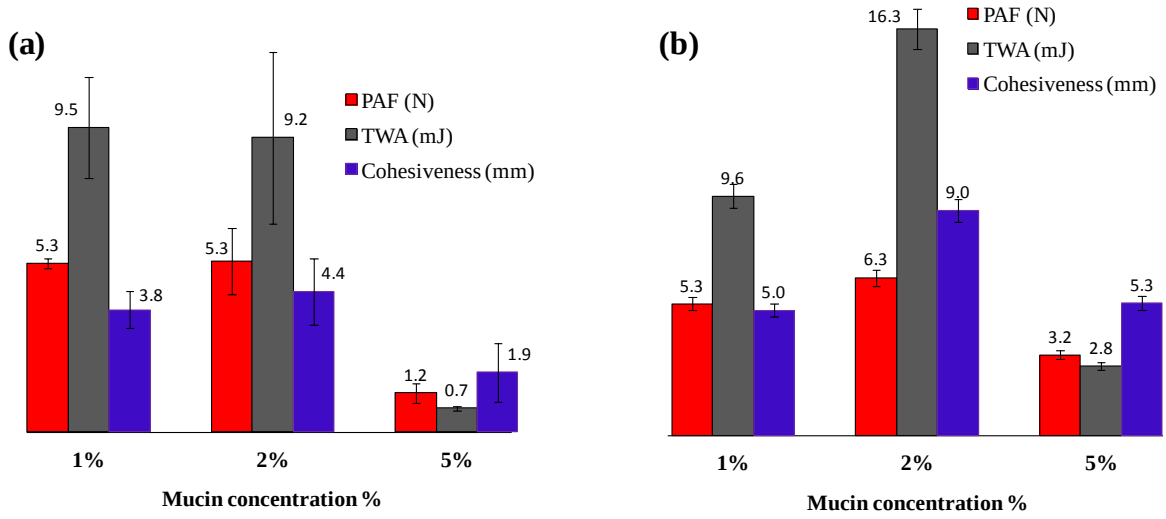

Figure 4.2: *In-vitro* mucoadhesion measurements of (a) chitosan and (b) TG-chitosan xerogels showing the effect of mucin concentration on PAF, TWA and cohesiveness *(n=4 mean ± SD).*

observed between the varying concentrations of mucin were the result of reduced intermolecular ionic bond and enhanced hydration in the dilute 1 % mucin solution and the increased intra-molecular attraction of the concentrated 5 % mucin solution. The increased likelihood of the formation of internal disulphide cross-linkages within the 5 % mucin solution prepared with PBS of pH 6.8 could lead to an entangled structure that might limit solvent diffusion into the polymeric matrix. However, at the optimum mucin concentration (2 %), the interpenetration between polymer and mucin was not restrained due to adequate rate of ingress of mucin solution with subsequent improvement in mucoadhesion properties. 2 % mucin solution exhibited mucoadhesive characteristics that were similar to that of 1 % mucin solution for chitosan xerogel and with more than 2-fold increase in the adhesion properties for the TG-chitosan xerogels when compared with 5 % mucin solution. Since excessive hydration in the case of 1 % mucin solution could affect structural integrity during mucoadhesion

measurements, as well as limited hydration, coupled with reduced interpenetration in the case of 5 % mucin solution, both of which adversely affect mucoadhesion characteristics, 2 % mucin solution was selected for further mucoadhesion measurements.

(b) ***Effect of membrane dialysis***; statistically significant differences were observed between the PAF, TWA and the cohesiveness of the dialysed and undialysed xerogels (Figure 4.3).

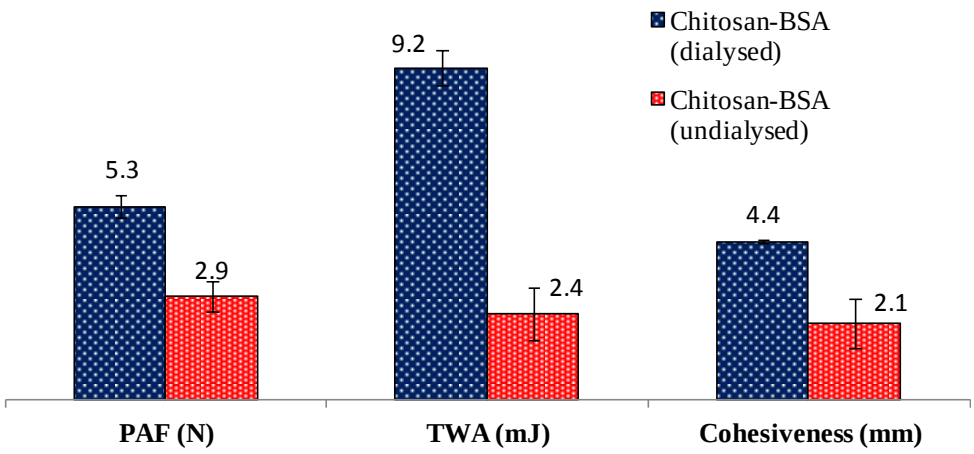

Figure 4.3: *In-vitro* mucoadhesion measurements of chitosan-BSA xerogels showing the effect of membrane dialysis on PAF, TWA and cohesiveness *(n=4 mean ± SD).*

The dialysed xerogel showed a higher PAF of 5.3 ± 0.7 N compared to 2.9 ± 0.4 N of the undialysed xerogel ($p < 0.05$). TWA values of 9.2 ± 1.0 and 2.4 ± 0.7 mJ were recorded for the dialysed and undialysed xerogels respectively ($p < 0.05$). In addition, the dialysed xerogel showed a cohesiveness of 4.4 ± 0.2 mm against 2.1 ± 0.7 mm of undialysed xerogels ($p < 0.05$). The enhanced mucoadhesive properties exhibited by the dialysed xerogels may be attributed to the ease of wetting by the mucosal substrate, formation of strong intermolecular hydrogen bonding with the mucosal substrate and improved penetration of the mucosal substrate crevices (Sudhakar *et al*., 2006). In the case of the undialysed xerogels, the presence of NaAc may have interfered with the physical properties of the delivery matrix and reduced the extent of adhesion to the mucosal substrate (Sudhakar *et al*., 2006). In addition, the resultant change in the pH of PBS during the hydration of the undialysed xerogel may have influenced the mucoadhesive properties.

Chitosan exhibits excellent mucoadhesive properties in alkaline or neutral environment (Park *et al*., 1989), however, this slight reduction in the pH of the environment

impacted on the mucoadhesive properties of undialysed xerogel by increasing the dissolution of the polymer matrix to form the slippery gel previously described. Consequently, the contact and consolidation stage of the adhesion process were affected by the reduced physico-chemical interaction between the slippery chitosan gel and the mucosal substrate (Smart, 2005; Andrew *et al*., 2009).

(c) ***Effect of annealing***; The PAF was used as a measure of the *in-vitro* mucoadhesive performance (Figure 4.4). The annealed xerogels with larger pore size distribution [see Figure 3.22(A), chapter 3] and better hydration capacity, had higher PAF (5.3 ± 0.7 N) compared to the non-annealed xerogels (4.1 ± 0.1 N) which was statistically significant ($p < 0.05$). Again the absorbent properties of GLY in combination with D-MANN could have aided in the stronger initial attachment of the formulations to the model mucoadhesive surface.

The TWA represented by the AUC gave dissimilar profiles for the formulations, with the annealed and non-annealed xerogels showing values of 9.2 ± 1.0 and 6.4 ± 1.2 Nmm respectively. The difference observed in the TWA of the xerogels which was statistically significant ($p < 0.05$) could be attributed to differences in pore size distribution and stability of the mechanically strong structure. Furthermore, the cohesiveness of the xerogels showed a statistically significant ($p < 0.05$) difference between the annealed (4.4 ± 0.6 mm) and non-annealed xerogels (3.1 ± 0.2 mm). The reduced cohesiveness of the non-annealed xerogels may have given rise to the collapse of the mechanically weak structure of the xerogels two (2) hours into the hydration test.

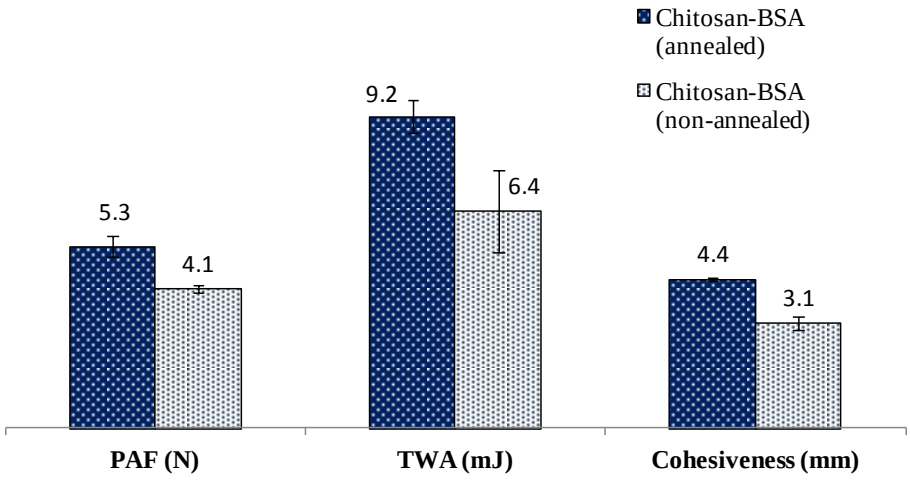

Figure 4.4: *In-vitro* mucoadhesion measurements of chitosan-BSA xerogels showing the effect of annealing on PAF, TWA and cohesiveness *(n=4 mean ± SD).*

The process of annealing also led to significant differences in the mucoadhesive properties of the TG-chitosan xerogels. The annealed TG-chitosan-BSA xerogels showed a significant improvement in mucoadhesive properties (Figure 4.5) compared to the non-annealed TG-chitosan-BSA xerogels. The annealed TG-chitosan-BSA xerogels with enhanced swelling capacity had higher PAF and cohesiveness compared to the non-annealed TG-chitosan-BSA xerogels. The total work of adhesion (TWA) further showed a statistically significant difference ($p < 0.05$) between the annealed and non-annealed TG-chitosan-BSA xerogels, with an approximate 3-fold increase in mucoadhesive strength. The major differences observed in the PAF, TWA and cohesiveness of the xerogels were largely due to the increased mucoadhesive strength influenced by the mechanically strong and fibrous porous structure of the annealed xerogels.

Mucoadhesive performance is important as it determines the residence time of formulations at the absorption site to allow for sustained drug release and ultimately bioavailability.

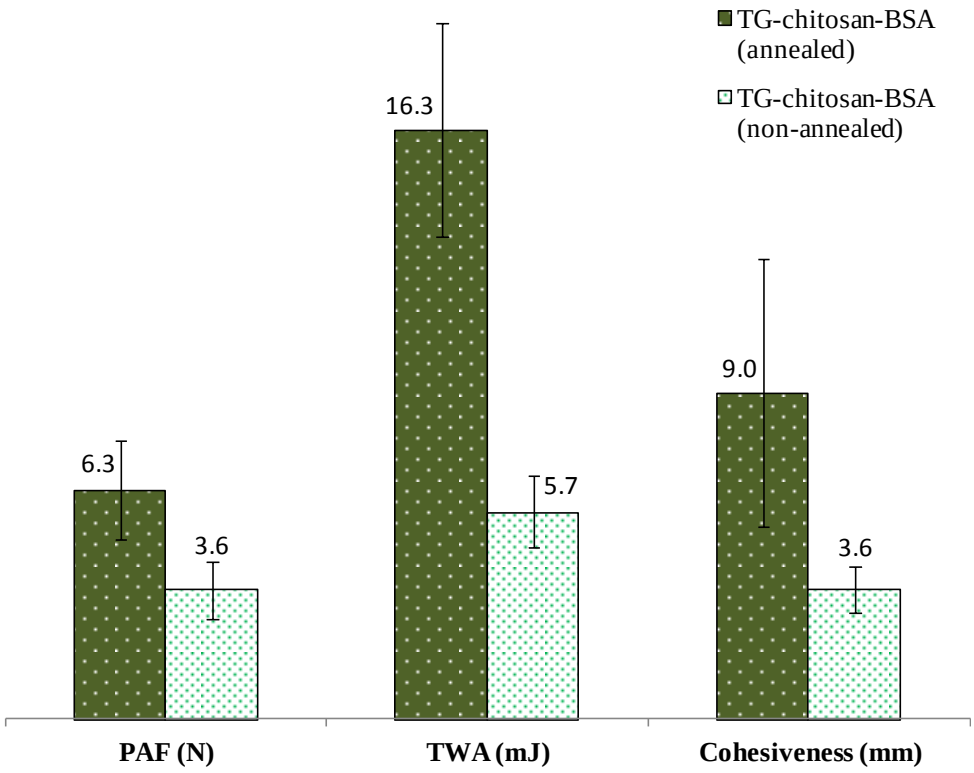

Figure 4.5: *In-vitro* mucoadhesion measurements of TG-chitosan-BSA xerogels showing the effect of annealing on PAF, TWA and cohesiveness *(n=4 mean ± SD).*

(d) ***Effect of thiolation;*** the effect of thiolation on *in vitro* mucoadhesive performance was measured by evaluating the PAF, the TWA and the cohesiveness of the annealed chitosan

and TG-chitosan xerogels. The chitosan-BSA xerogels had lower PAF compared to the TG-chitosan-BSA xerogels (Figure 4.6) with mean difference that was statistically significant ($P < 0.05$). This difference was expected to be much higher, however, the combined effect of the absorbent properties of GLY and D-MANN and the enhanced inter molecular hydrogen bonding with the gelatine substrate employed could have aided in the strong initial attachment of both chitosan-BSA and TG-chitosan -BSA xerogels to the model mucoadhesive substrate.

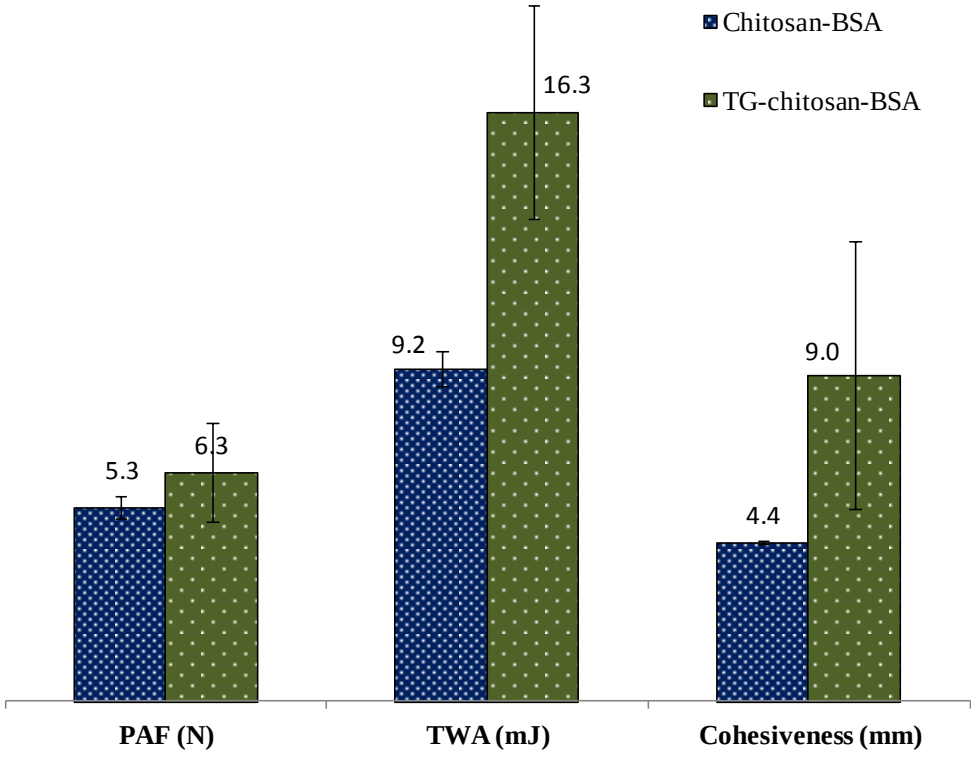

Figure 4.6: *In-vitro* mucoadhesion measurements of xerogels showing the effect of thiolation on PAF, TWA and cohesiveness *(n=4, mean ± SD).*

The total work of adhesion (TWA) represented by the area under the curve also showed a statistically significant difference ($p < 0.05$) between the chitosan-BSA and TG-chitosan -BSA xerogels, with about two-fold increase in mucoadhesive strength of the latter. Furthermore, the cohesiveness of the xerogels also displayed a two-fold increase in the TG-chitosan based xerogels which was statistically significant ($p < 0.05$).

The major differences observed in the PAF, TWA and cohesiveness of the xerogels were attributed largely to the increased mucoadhesive strength arising from the thiolation process via the formation of stronger covalent interactions between the cysteine-rich mucin glycoproteins and the sulphydryl ligands of TG-chitosan. In addition, the formation of inter and intra molecular disulphide linkages within the TG-chitosan xerogels and the stability of

the fibrous structure may have augmented the mucoadhesive strength (Ayensu & Boateng, 2012). The relatively low mucoadhesive strength of the unmodified chitosan xerogels may have arisen from the excessive hydration of the porous structure leading to the formation of a slippery gel that lost its mucoadhesive strength. The excessive hydration of the chitosan xerogels leading to the significant reduction in adhesive strength was due to disentanglement at the xerogel/mucosal substrate interface resulting in separation of the xerogel and mucosal substrate due to slippage of the macromolecular chains of the formulation (Eouani *et al*., 2001).

Mucoadhesive strength is a key property for the determination of the functional characteristic of residence time of xerogels at the absorption site to allow for sustained drug release and eventually bioavailability. Though significant differences were observed in the mucoadhesive performance between the chitosan and TG-chitosan xerogels, the differences were much lower compared to those reported by Roldo *et al*., (2004) where different formulation systems and bioadhesion membranes were used. It must however be emphasised that the process of thiolation greatly influenced the mucoadhesive performance.

(e) ***Effect of EIs;*** the effect of GSH concentration (EI) on the mucoadhesive properties of thiolated xerogels containing BSA was evaluated. The formulation containing 5 % GSH showed significant reduction in mucoadhesion characteristics compared to thiolated xerogel without an EI (Figure 4.7). Statistically significant differences were observed between the mean PAF ($p < 0.05$) and TWA ($p < 0.05$) of the xerogels with no GSH and with 5 % GSH. The difference between the cohesiveness values was not statistically significant ($p > 0.05$).

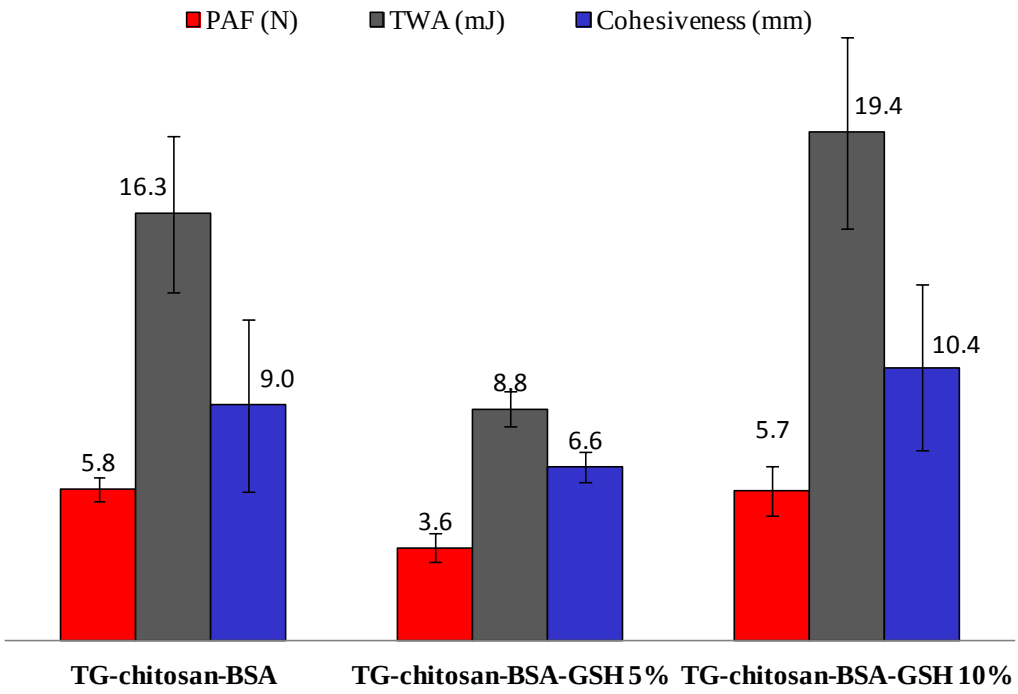

Figure 4.7: *In-vitro* mucoadhesion measurements of xerogels showing the effect of varying GSH concentration on PAF, TWA and cohesiveness *(n=4, mean ± SD).*

However, the formulation containing 10 % GSH demonstrated enhanced mucoadhesion properties though there was no statistically significant difference between its mean TWA and that of the control formulation with 0 % GSH ($p = 0.241$). Similar trends were observed for the PAF and the cohesiveness. The hydration studies in the presence of a reducing agent DTT (see Table 4.4), has shown that the presence of GSH limits the formation of disulphide bonds from free thiol groups in the thiolated xerogels. However, the reduced mucoadhesion observed with the presence of 5% GSH indicates that the ability of GSH to inhibit disulphide formation is concentration dependent. Furthermore, the adsorption of BSA by GSH (Vallee *et al*., 2008) at the physiological pH (6.8) must have depleted the 5 % GSH such that not much was available to prevent disulphide bond formation in the thiolated xerogel. A concentration of 10 % GSH was optimum to allow for the availability of free thiol groups and for interaction with BSA, with the resultant enhanced mucoadhesion observed. The free thiol groups present in xerogels with 10 % GSH may have formed stronger covalent bonds with cysteine-rich residues in mucin glycoproteins on the surface of the mucosa substrate as discussed earlier. Thiolated xerogel with 10 % GSH was deemed optimum for further development and characterisation.

The thiolated chitosan formulation was loaded with INS and the mucoadhesive properties measured from xerogels with or without EIs. Xerogels containing 10 % GSH or 5 % APR were evaluated against xerogels containing 0 % of EI. A statistically significant difference ($p < 0.05$) was observed between the PAF of formulations B and C (Figure 4.8). There was however, no statistically significant differences ($p > 0.05$), between the TWA and the cohesiveness of all the formulations. Formulation B showed improved mucoadhesion properties compared to formulations A and C which had similar characteristics. The results confirm the ability of GSH to limit disulphide bond formation in the thiolated xerogel which allowed more free thiol groups to interact covalently with cysteine-rich mucin glycoproteins to enhance mucoadhesion characteristics. It also demonstrates the importance of EI specificity.

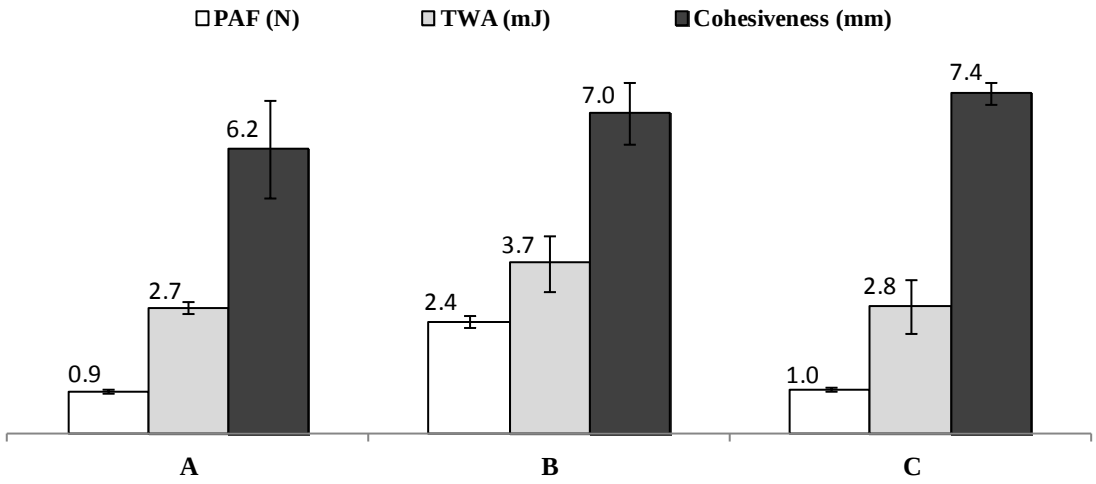

Figure 4.8: *In-vitro* mucoadhesion measurements (PAF, TWA and cohesiveness) of TG-chitosan-INS xerogels containing (A) 5% aprotinin, (B) 10% GSH and (C) no EI. (*n=4*, *mean* ± *SD*).

4.4 Conclusions

Significantly higher hydration capacity was recorded for annealed chitosan xerogel compared to non-annealed xerogel. The formulation process of annealing in addition to plasticization (GLY) and cryoprotection (D-MANN) may have created enlarged pore spaces within the polymer chains which allowed for easy water ingress and enhanced the hydration capacity. Membrane dialysis did not have any significant effect on the hydration capacity, however, the presence of process impurity NaAc resulted in xerogels with poor structural stability as was observed for non-annealed chitosan xerogels which gelled and subsequently collapsed within two hours of hydration.

Annealed TG-chitosan xerogel similarly showed higher hydration capacity compared to non-annealed TG-chitosan xerogel which was mechanically weak, forming a loose gel. However, disulphide bond formation in the thiolated xerogel limited the hydration capacity hence the significant difference observed between hydration capacities of the thiolated and unmodified chitosan xerogels. The hydration capacity of the thiolated xerogel increased significantly in the presence of a reducing agent DTT which confirms that the hydration characteristics is driven by the cross-linked disulphide bond formation. The introduction of GSH as an EI to the thiolated xerogel may have prevented the formation of disulphide bonds leading to a higher hydration capacity with or without DTT.

The hydration capacity of the xerogels directly impacted their mucoadhesion properties determined in the presence of 2 % optimal mucin concentration. The annealed chitosan xerogels showed better mucoadhesion properties compared to non-annealed chitosan xerogels. However, undialysed chitosan xerogel demonstrated reduced mucoadhesion characteristics due to the presence of NaAc. Improved mucoadhesion properties were obtained for the annealed thiolated xerogels compared to non-annealed thiolated and unmodified chitosan xerogels. Covalent interactions between the free thiol moieties on the thiolated xerogels and cysteine-rich mucin glycoproteins have been used to explain the improved mucoadhesion.

The effect of EI on mucoadhesion was concentration dependent as 10 % GSH led to increased mucoadhesion compared to 5 % GSH. The effect was also inhibitor specific as significant differences were observed between the mucoadhesion properties of the thiolated xerogel loaded with INS and containing either 10 % GSH or 5 % APR.

CHAPTER FIVE

IN VITRO DRUG DISSOLUTION CHARACTERISTICS AND RELEASE MECHANISMS OF CHITOSAN AND TG-CHITOSAN XEROGELS LOADED WITH BSA AND INS.

5.1 Introduction

The increased understanding of the human body anatomy and physiology, the elucidation of disease pathophysiology and the continuous advancement experienced in the pharmaceutical world have provided the impetus for research into novel delivery systems with 'smart' characteristics over the last decade (Sood & Panchagnula, 2003; Friend, 2005). The overall objective for the development of novel drug delivery systems is to enhance the efficacy of the active pharmaceutical ingredient, reduce side effects and to improve patient compliance. Polymeric hydrogel matrices and controlled drug delivery systems offer a great potential for achieving better control of administered drugs (Jain *et al*., 2009). The flexibility offered by hydrogels in obtaining desirable drug release profiles, biocompatibility, biodegradability and cost effectiveness have rendered them useful in a wide range of controlled drug delivery systems (Morales & McConville, 2011). A complex interaction between diffusion, dissolution and erosion mechanisms has been used to explain drug release from hydrophilic matrices. A number of polymeric hydrogels including hydroxypropyl methylcellulose (HPMC), chitosan and its derivatives have been employed in formulations due to their advantage of offering robust mechanisms and reproducibility of drug release profiles, cost effectiveness and choice of viscosity grades (Shoaib *et al*., 2006). The hydration capacity of the polymeric matrix which results in a gel barrier through which the drug diffuses controls water ingress, polymer swelling, drug dissolution, drug diffusion and matrix erosion (Sung *et al*., 1996 cited in Shoaib *et al*., 2006).

A number of mathematical kinetic models have been proposed to elucidate water and drug transport through polymeric matrices and to predict the consequent drug release kinetics (Korsmeyer *et al*., 1986; Ju *et al*., 1995; Gao *et al*., 1995; Siepmann *et al*., 1999, cited in Shoaib *et al*., 2006). In using these mathematical models to describe the entire drug release process, a number of physical characteristics such as rate of water diffusion into polymer matrix, polymer swelling, drug diffusion out of the delivery system, axial and radial movement in a 3-dimensional system, porosity and composition must be taken into consideration. The above parameters make the description a complex process which requires

that each model makes assumptions that are applicable to certain drug-polymer systems (Siepmann *et al*. 2000, cited in Shoaib *et al*., 2006).

Different kinetic models have been employed to describe the release kinetics of drugs from polymeric matrices based on drug dissolution or release data. A zero order rate equation [5.1] is used to describe a system where the drug release rate is concentration independent (Hadjiioannou *et al*., 1993, cited in Shoaib *et al*., 2006) whereas a first order rate equation [5.2] describes a concentration dependent drug release rate (Bourne 2002, cited in Shoaib *et al*., 2006). The Fickian diffusion equation [5.3] proposed by Higuchi (1963, cited in Shoaib *et al*., 2006) describes the release of drugs from insoluble matrices as being dependent on the square root of time. The Hixson-Crowell cube root law equation [5.4] on the other hand describes drug release systems which involve a change in surface area and diameter of particles or tablets (Hixson and Crowell, 1931 cited in Shoaib *et al*., 2006)

$$M = k_0 t \qquad \text{equation [5.1]}$$

where, k_0 is rate constant for the zero-order drug release and t is the time.

$$\text{Log } M = \text{Log } M_0 - kt / 2.303 \qquad \text{equation [5.2]}$$

where, M_0 is the drug initial concentration and K is first order rate constant.

$$M = Kt^{1/2} \qquad \text{equation [5.3]}$$

where, M is the drug concentration and K is the constant that relates to the design variables of the system.

$$M_0^{1/3} - Mt^{1/3} = K_{HC}\, t \qquad \text{equation [5.4]}$$

where, Mt is the amount of drug released in time t, M_0 is the initial amount of drug in tablet/formulation and K_{HC} is the rate constant for Hixson-Crowell rate equation.

For a polymeric system, Korsmeyer *et al*., (1983, cited in Shoaib *et al*., 2006) proposed a relationship that may be used to determine the drug release mechanism by fitting the first 60% drug release data in the Korsmeyer-Peppas model; equation [5.5].

$$Mt / M\infty = Kt^{n} \qquad \text{equation [5.5]}$$

where Mt / M∞ is the fraction of drug released at time t, k is the rate constant and n is the release exponent. The value of n is used to describe different release mechanisms shown in Table 5.1 for polymeric matrices of cylindrical shape.

Table 5.1: Diffusion exponent and drug diffusion mechanism for cylindrical shaped matrices

Diffusion exponent (n)	Drug diffusion mechanism
0.45	Fickian diffusion
$0.45 < n < 0.8$	Anomalous (non-Fickian) diffusion
0.89	Case-II transport
$n > 0.89$	Super case-II transport

The Moore and Flanner (1996) equations [5.6 - 5.7] which are model independent, are employed to estimate the difference (f_1) and the similarity (f_2) factors which compare the dissolution profiles of different formulations under evaluation. The f_1 value determines the percent error between two curves over all time points and the f_2 value is a logarithmic transformation of the sum-squared error of differences between the test (T_j) and reference (R_j) formulations over all time points. *N* is the number of samples.

$$f_1 = \frac{\sum_{j=1}^{n} |Rj - Tj|}{\sum_{j=1}^{n} Rj} \times 100 \qquad \text{equation [5.6]}$$

$$f_2 = 50 \times \log \{ [\frac{1}{N}\sum_{j=1}^{n} |Rj - Tj|^2]^{-0.5} \times 100\} \qquad \text{equation [5.7]}$$

Test and reference formulations may be considered similar if f_1 value is less than 15 % (0.15). F_2 value higher than 50 (50-100) which shows similarity of the dissolution profiles is used when f_1 is more than its limit of 15 % (Dash *et al*., 2010). The Food and Drug Administration (FDA) advice that two dissolution profiles be declared similar for f_2 values between 50 and 100 (www.fda.gov).

The present chapter aims to determine the release profiles of BSA and INS from lyophilised chitosan and TG-chitosan xerogels. These xerogels have been formulated by incorporating appropriate concentrations of GLY and D-MANN as plasticizer and cryoprotectant respectively (see chapter two). In addition, formulation processes such as membrane dialysis, annealing during lyophilisation and thiolation have been applied and their effects on drug release characteristics investigated. Furthermore, the effects of the EI (presence or absence) on protein drug release were investigated. The mechanisms of drug release were evaluated by fitting the drug release data to different kinetic models including, zero order, first order, Higuchi, Hixson-Crowell and Korsmeyer-Peppas equations. Model

independent difference and similarity factors were used to evaluate the release profiles of the xerogels.

5.2 Materials and methods

5.2.1 Materials

Table 5.2: Materials for drug release studies

Material	Description	Supplier
BSA (mol wt. ~67 kDa)	A7906-100 G	Sigma-Aldrich Gillingham, UK.
Acetic Acid	A /0360/PB17	Fisher Scientific (Leicester UK)
Hydrochloric acid	H /1150/PB 17	Fisher Scientific (Leicester UK)
Potassium dihydrogen phosphate	P /4760/53	Fisher Scientific (Leicester UK)
Sodium hydroxide	S 240697	Sigma-Aldrich, Gillingham, UK
PBS tablets (pH 7.4)	4P4417-50TAB	Sigma-Aldrich, Gillingham, UK
Recombinant human INS	12643-50MG	Sigma-Aldrich, Gillingham, UK
Bradford's reagent	B6916-500ML	Sigma-Aldrich, Gillingham, UK

5.2.2 *In vitro* BSA release profiles using beakers

The BSA loaded lyophilised xerogels from the preliminary formulation investigations were immersed in beakers containing 50 ml of 0.01M PBS (pH 6.8 ± 0.1) solution as dissolution medium at 37 ± 0.1 °C and covered (Nochos *et al*., 2008). The dissolution medium was pepared by dissolving a tablet of PBS (pH 7.4) in 200mL of deionised water and adjusting the pH to 6.8 with potassium dihydrogen phosphate and sodium hydroxide. The dissolution medium was stirred at 150 rpm with a magnetic stirrer. For each sample, 50 µL of the dissolution medium was sampled at predetermined time intervals and replaced with the same amount of the PBS solution to maintain a constant volume for 7 hours. The sampled dissolution medium was treated with 1 mL Bradford's reagent and the absorbance measured as previously described in chapter 3 section 3.2.10. The concentration of BSA released from the xerogels was determined by interpolation from the linearized calibration curve ($r^2 > 0.99$) (Chapter 3, Figure 3.18). Corresponding cumulative percentage drug release profiles of BSA were then plotted for the different formulations: (i) dialysed and undialysed chitosan xerogels; (ii) annealed and non-annealed chitosan xerogels and (iii) annealed and non-annealed TG-chitosan xerogels. The BSA release profiles from the chitosan and TG-chitosan xerogels were

evaluated in order to obtain optimised formulations for further development and characterisation.

5.2.3 *In vitro* release of BSA and INS using Franz-type diffusion cell

20 mg of drug loaded optimised laminated xerogels were placed in the donor compartment (chamber) on stainless steel wire mesh (0.5 mm x 0.5 mm) which separated the donor and receiver compartments, with the mucoadhesive surface in contact with the wire mesh and facing the receiver compartment of the modified Franz diffusion cell (Cui *et al*., 2009). The receiver chamber was filled with 8 mL of 0.01M PBS pH 6.8 at 37 °C with magnetic stirring at a speed of 150 rev/min. The chambers were held together by a cell clamp and sealed with parafilm to limit evaporation (Figure 5.1).

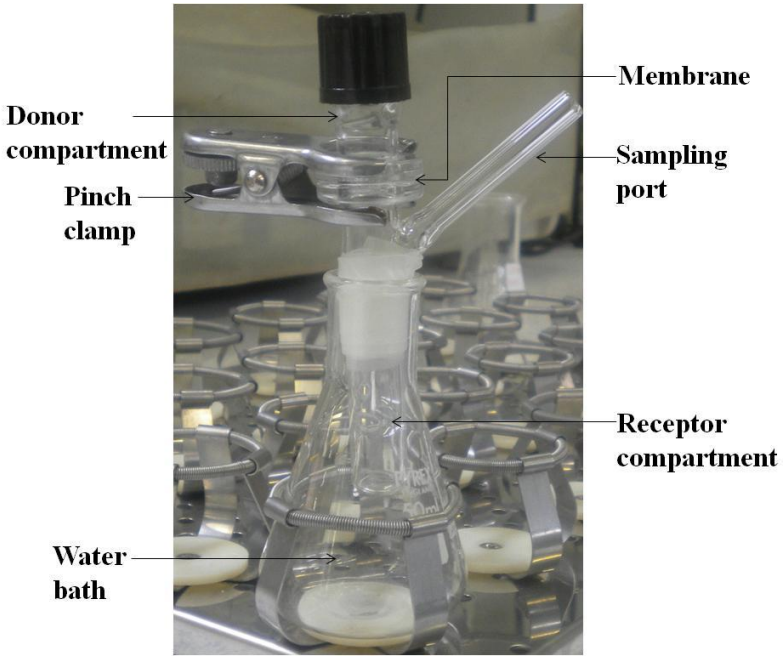

Figure 5.1: Photograph of modified Franz-type diffusion cell as set up for drug release experiment.

50 µL of the dissolution medium was sampled at predetermined time intervals and replaced with the same amount of fresh medium to maintain a constant volume for 4 or 7 hours. The sampled dissolution medium was treated with 1ml Bradford's reagent and the absorbance measured at 595 nm and 450 nm for linearisation of absorbance using a Multiskan EX microplate photometer equipped with Ascent software (Thermo Scientific, Hampshire UK). The concentration of the BSA and INS released from the xerogels was determined by interpolation from the linearized calibration curve ($r^2 > 0.99$) and cumulative percentage drug

release profiles plotted. Blank control was determined with non-drug loaded laminated xerogel. The release profiles of BSA from xerogels containing different EIs at varying concentrations (TG-chitosan-BSA, TG-chitosan-GSH-BSA 5 % and TG-chitosan-GSH-BSA 10%) were determined. INS released from xerogels with or without EI (TG-chitosan-INS, TG-chitosan-APR-BSA and TG-chitosan-GSH-INS) using 0.01 M PBS as dissolution medium were also analysed.

5.2.4 Evaluation of drug release mechanisms

Model dependent release mechanisms:

Based on the drug dissolution results, the following plots with their corresponding kinetic/mechanism models in Table 5.3 were constructed by fitting the drug release data to equations [5.1 – 5.5] (section 5.1 above).

Table 5.3 Various plots with corresponding kinetic /mechanism model

Plot	Kinetic/mechanism model
Cumulative % drug release against time	Zero order kinetic model
Log cumulative of % drug remaining against time	First order kinetic model
Cumulative % drug release against square root of time	Higuchi model
Log cumulative % drug release against log time	Korsmeyer model
Cube root of % drug remaining in matrix against time	Hixson-Crowell cube root law

Model independent release mechanism:

The difference (f_1) and similarity (f_2) factors were estimated using equations 5.6 – 5.7 (section 5.1.1.2). The values were used to compare the release profiles of the different formulations.

5.3 Results and Discussion

5.3.1 *In vitro* BSA release profiles

The drug release profile determined for the dialysed chitosan-BSA xerogel showed a three-fold increase in total cumulative BSA release, compared to the undialysed chitosan-BSA xerogel (Figure 5.2). The ideal characteristics of a mucoadhesive polymer matrix

include minimum interference to the release of the active agent (Sudhakar *et al*., 2006). This was exhibited by the dialysed xerogels where typical controlled release of active ingredient was obtained, reaching a total cumulative per cent release of 91.8 ± 4.0 after 7 hours of incubation. The release of the model protein from the undialysed xerogel was however, inhibited to a greater extent by the presence of the crystalline NaAc as only 30.1 ± 2.6 % BSA was released within 7 hours.

Although the undialysed xerogel showed a porous structure due to annealing (Chapter 3, Figure 3.22 [B]), the release profile was not characteristic of chitosan. The presence of crystals in the undialysed xerogel affected the initial hydration, thus slowing down the rate of water ingress into the polymeric network. In addition, the differences observed in the thickness of the xerogel walls consequently affected the release of drug by differences in the thickness of swollen gel formed during the release studies.

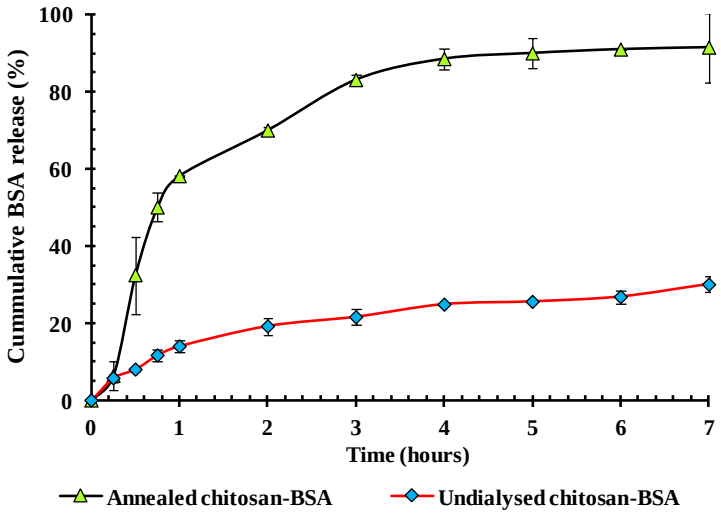

Figure 5.2: Cumulative percent BSA release from dialysed and undialysed chitosan-BSA xerogels. *(n=4 mean ± SD).*

Interferences with the release of BSA could also have resulted from the altered environmental pH originating from a solution of NaAc (conjugate base of a weak acid) and acetic acid acting as a new buffer maintaining a relatively constant pH of 6.6, different from the original PBS pH of 6.8. Furthermore, the presence of the crystalline NaAc may have caused a decrease in surface area of the dispersed drug in the porous cake, decreasing dissolution rate considerably with consequent suppression of drug release (Bunte *et al*., 2010).

A stronger charge to charge interaction between BSA and chitosan could lead to decreased cumulative per cent BSA release from both xerogels (Ma *et al*., 2002) observed in

the second phase of the release process after 1 hour. However, Boeris *et al*., (2010) have shown that the non-covalent chitosan-BSA complex gradually dissolves in the presence of NaCl, supporting the higher % release of BSA from the dialysed xerogel. A common ion effect however, results from the sodium ions in PBS and NaAc, limiting the solubility of the crystalline NaAc which subsequently affects the rate of release of BSA from the BSA-chitosan complex in the undialysed xerogel.

Figure 5.3 shows the dissolution profiles of BSA from annealed and non-annealed chitosan xerogels. The total cumulative percent BSA release in 7 hours from the annealed and non-annealed chitosan xerogels were 91.5 ± 3.7 % and 80.1 ± 4.9 % respectively which was statistically significant ($p < 0.05$), though both formulations exhibited a sustained (controlled) release typical of chitosan based formulations. In addition, the rate of release (indicated by the slope of the initial linear portion of the curve) was faster from the non-annealed than the annealed xerogels within the first hour of release due to its lower cohesiveness and mechanically weak structure which formed a gel that easily disintegrated in the dissolution medium during the initial stages of the drug dissolution study. Bunte *et al*., (2010) observed that drug release is facilitated by the porous network of lyophilised xerogels. An increased surface of the dispersed drug in the porous cake occurs, accelerating dissolution significantly. Annealed xerogels showed a loose but stable structure, with many micropores (Chapter 3, Figure 3.22 [A]), which allowed for easy hydration and therefore faster drug release rate. The amine and hydroxyl groups of chitosan can both couple with proteins under mild conditions (Yang *et al*., 2001). Hydrophobic interactions between chitosan and BSA within the network might also be favoured. Strong charge to charge interactions have also been demonstrated between proteins and chitosan with a reduced cumulative release in the amount of protein even after dissolution of the chitosan matrix (Ma *et al*., 2002).

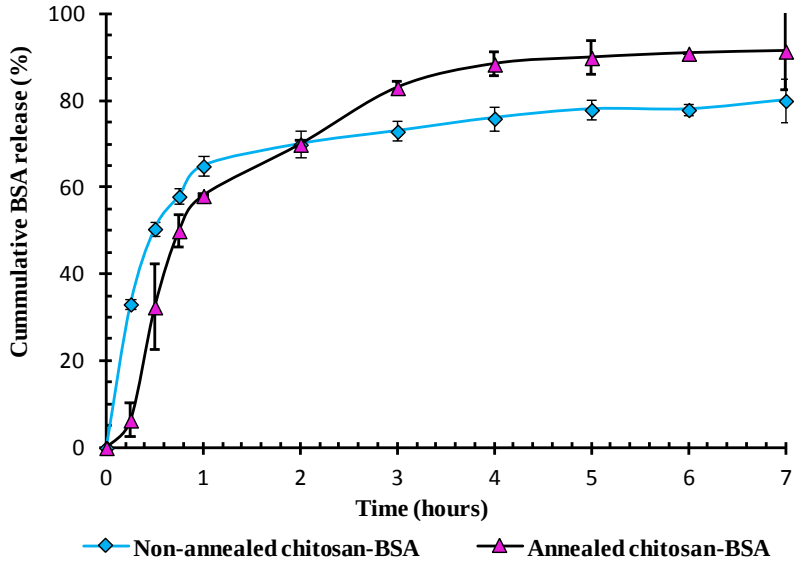

Figure 5.3: Cumulative percent BSA release from annealed and non-annealed lyophilised chitosan-BSA xerogels. *(n=4 mean ± SD).*

BSA release rate from the xerogels could have been influenced concurrently by these factors to different extents. The dissolution profiles of BSA from the lyophilised annealed and non-annealed TG-chitosan xerogels in 0.01M PBS is shown in Figure 5.4. The total cumulative percent BSA release from the annealed and non-annealed TG-chitosan -BSA were 95.2 ± 7.3 % and 84.0 ± 4.7 % respectively. This difference was statistically significant ($p < 0.05$) with both formulations exhibiting sustained release profiles, typical of chitosan based formulations. The drug release may have been facilitated by the porous polymeric network of the freeze-dried xerogels as a result of increased surface of the dispersed drug in the porous cake which accelerates dissolution significantly (Bunte *et al*., 2010).

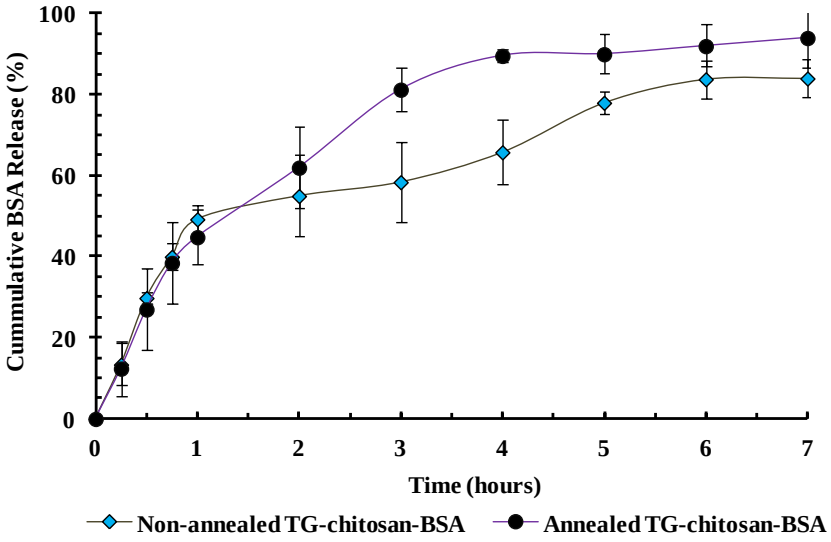

Figure 5.4: Cumulative percent BSA release from annealed and non-annealed TG-chitosan-BSA xerogels *(n=4 mean ± SD).*

The total cumulative percent release was higher from the annealed TG-chitosan than the non-annealed TG-chitosan xerogels due to its higher rate of hydration and enhanced cohesiveness. The cohesion and stability of a drug delivery system over the intended duration of drug release is often a requirement for controlled release (Peppas & Bury, 1985).

The dissolution profile of BSA from annealed chitosan-BSA and TG-chitosan-BSA xerogels in 0.01M PBS is shown in Figure 5.5. The total cumulative percent BSA release from the chitosan-BSA and TG-chitosan-BSA were 91.5 ± 3.7 % and 94.4 ± 7.3 % respectively. This difference was not statistically significant ($p > 0.05$) with both formulations exhibiting classical sustained release profiles characteristic of chitosan based formulations. The similar release profiles from the xerogels exhibited a burst release of about 57% and 45% for chitosan and TG-chitosan respectively in the first 1 hour, followed by a constant controlled release. This could be attributed to two different release mechanisms; (a) diffusion of protein molecules based on concentration and (b) degradation of polymer matrix. The initial BSA burst release was due to drug molecules adsorbed to the xerogel surface or loosely associated with the surface which easily diffused out in the initial incubation period of 1 hour (Xu & Du, 2003).

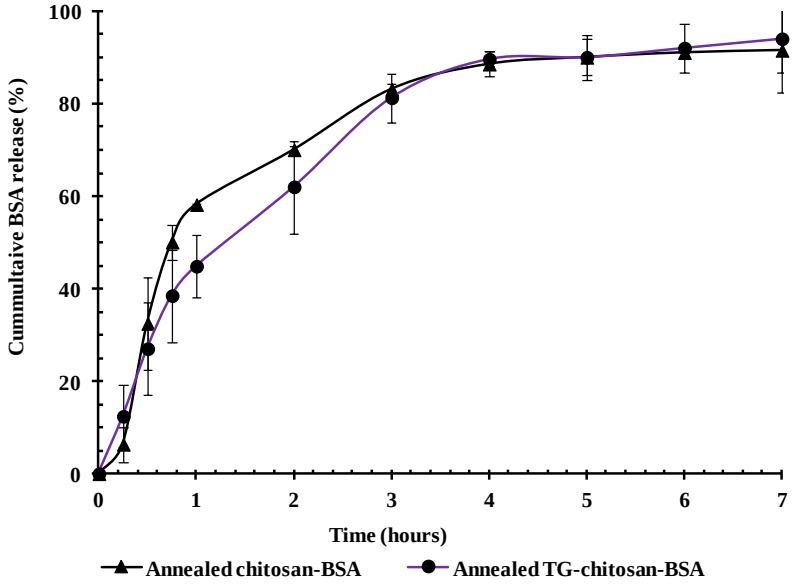

Figure 5.5: Cumulative percent BSA release from annealed chitosan and TG-chitosan xerogels from 0.01M PBS at 37 ± 0.1 °C *(n=4 mean ± SD).*

The movement of water molecules containing dissolved hydrophilic proteins is not restricted between the release medium and the polymer matrix (Kang & Song, 2008). The high loading concentration of BSA enhanced its release from the xerogels as the large concentration gradient between the release medium and the polymer surface resulted in a high diffusion rate. In addition, proteins dispersed within the polymer matrix may have escaped through cracked pores formed during processing, therefore increasing the initial release.

A prolonged release period however, ensued after the initial burst release due to BSA-chitosan complexation. At pH 6.8, BSA (isoelectric point around 5) carries a net negative charge and complexes with positively charged chitosan. As a result, a slower diffusion of entrapped protein from hydrated chitosan and TG-chitosan xerogels occurred (Wang *et al.*, 2009). Disulphide formation in TG-chitosan could have limited TG-chitosan-BSA complexation as fewer chitosan amino groups were available for interaction. Subsequently, the TG-chitosan xerogel released more BSA than the chitosan xerogel though the difference was not statistically significant ($p > 0.05$). The disulphide bond results in a stronger and stable swollen gel (maintained physical integrity) that displayed excellent cohesive properties. The cohesion and stability of a drug delivery system over the intended duration of drug dissolution helps in controlling drug release. The non-covalent complex however, gradually dissolves in the presence of NaCl (Boeris *et al*. 2010) present in PBS to support the higher % release of BSA observed in both xerogels. The usefulness of TG-chitosan as a carrier matrix for

controlled drug release has been demonstrated with model drugs such as metronidazole and clotrimazole (Saboktakin *et al*., 2011; Kast *et al*., 2002).

5.3.3 *In vitro* release of BSA and INS using Franz-type diffusion cell

The use of the Franz-type diffusion cell to investigate the *in vitro* release of the model protein drugs stems from the fact that it offers an opportunity to simulate the buccal epithelium by the presence of a barrier system between the donor and the receiver compartments. Although the barrier used in this work seems extremely porous compared with the buccal epithelium, it represents an efficient system to estimate the release profile of the model protein drugs and to predict the release mechanisms as well as the kinetics using various kinetic models.

Figure 5.6 shows the release profiles of BSA from TG-chitosan xerogels with varying concentrations of GSH as EI. The optimum concentration of GSH for the formulation was determined by the mucoadhesive performance and the release profiles. The presence of GSH

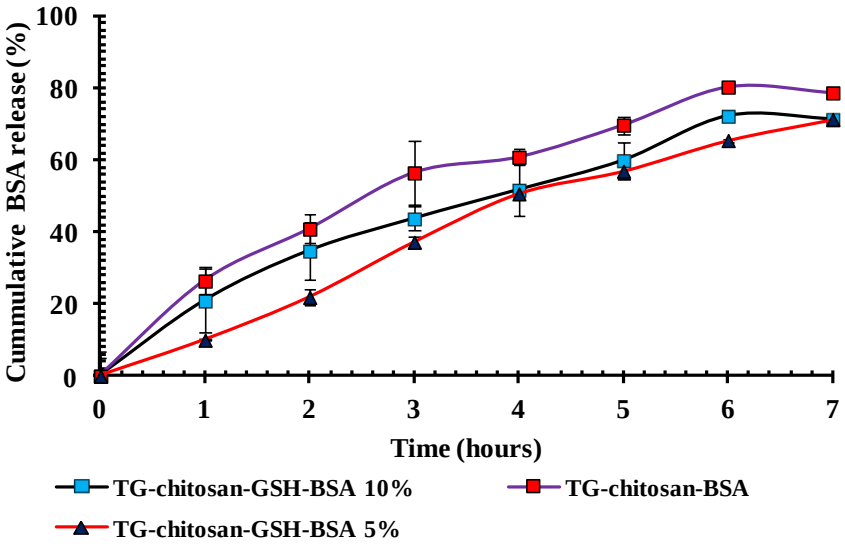

Figure 5.6: Cumulative percent BSA release from TG-chitosan xerogels containing varying amounts of GSH as EI from 0.01M PBS at 37 ± 0.1 °C using Franz-type diffusion cell *(n=4 mean ± SD).*

had a considerable effect on the release of BSA with statistically significant differences in the mean cumulative percent release after 7 hours observed between the control formulation with no EI and the formulations containing 5 % and 10 % GSH as EIs ($p < 0.05$). The slow controlled diffusion of entrapped BSA from the hydrated xerogels was the result of the complex interactions between BSA, TG-chitosan matrix and the GSH added. BSA adsorption

at pH 6.8 (Vallee *et al*., 2008) and limitation of disulphide bond formation from free thiol groups in thiolated xerogels by GSH may have been responsible for the lower BSA percent cumulative release from the xerogels containing EI.

However, the effect of EI on BSA release was not concentration dependent throughout the experimental period as was observed in the mucoadhesion studies (see chapter 4). The difference in mean cumulative percent after 7 hours between the xerogels with 5 % and 10 % GSH was not statistically significant ($p > 0.5$) though some differences were observed between the release profiles up to the fourth hour. Based on mucoadhesive performance and release profiles, the xerogel with 10 % GSH was considered for further development and characterisation.

The release of another model protein drug from the TG-chitosan xerogel was also studied by loading with recombinant human INS and different EIs (5 % APR and 10 % GSH). Figure 5.7 shows the biphasic cumulative percent release profiles of INS from the various formulations with initial burst release resulting from drug adsorbed on the polymer surface. INS with an isoelectric point of 5.4 and a net negative charge around pH 6.8 (Brange *et al*., 1990; Gursky *et al*., 1992; cited in Thomsen *et al*., 2008) exhibited slow release in the second phase due to INS-TG-chitosan complexation. Furthermore, possible interaction between GSH and INS led to statistically significant difference ($p < 0.05$) between the total cumulative release from formulations with 10 % GSH and the control formulation with no EI. The percent release of INS from the formulation containing APR was also found to be statistically different from that of the control formulation ($p < 0.05$). However, the release of INS was affected to different extents by the two different EIs employed. The release from APR containing xerogels showed a higher release than that from the GSH loaded xerogels, which was statistically significant ($p < 0.05$). This suggests that the EIs may have different interactive mechanisms with the thiolated polymer as well as the model protein drug, and may explain the differences observed in the effect of the EIs on the INS release from the xerogels.

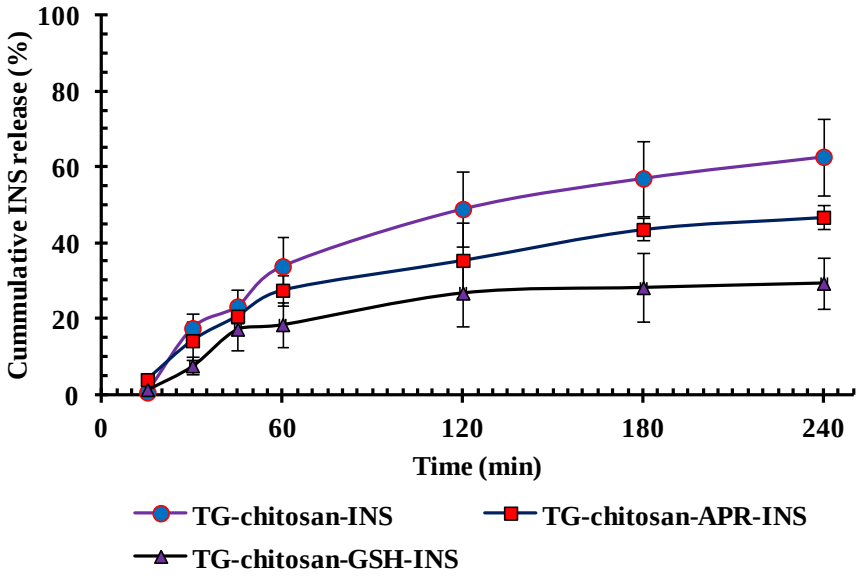

Figure 5.7: Cummulative percent INS release from TG-chitosan xerogels showing the effect of different EIs on release profiles in 0.01M PBS at 37 ± 0.1 °C *(n=4 mean ± SD)* using Franz-type diffusion cell.

5.3.4 Evaluation of drug release kinetics from chitosan and TG-chitosan xerogels

Model dependent methods based on mathematical functions were used to describe the dissolution profiles of BSA and INS released from the chitosan and TG-chitosan xerogels. These included zero order, first order, Higuchi, Hixson-Crowell and Korsmeyer-Peppas models which have been represented by the plots in Figure 5.8 (a-e) based on the initial linear portions of the release profiles and for the Korsmeyer – Peppas model, initial 60 % of cumulative drug release. Release parameters obtained from fitting experimental dissolution release data to the different kinetic equations have been summarised in Tables 5.4-5.6.

The *in-vitro* release profiles of BSA from the chitosan/TG-chitosan xerogels could best be described by first order kinetic model as the plots showed highest linearity (R^2 = 0.9791 – 0.9957) (Table 5.4). This indicates that the amount of drug released is dependent on the matrix drug loading irrespective of formulation process. First order kinetics has been proposed as the most appropriate model for dosage forms containing water-soluble drugs in porous matrices (Narashimhan *et al*., 1999; Silvina *et al*., 2002, cited in Dash *et al*., 2010). The release of BSA from all formulations also displayed close fitting with Hixson-Crowell cube root model (R^2 = 0.9743 – 0.9919) (Table 5.4) which suggests that the drug release mechanism was by dissolution and changes in the surface area and

dimensions of the xerogel (Rahman *et al*., 2011). The Higuchi plots however showed less linearity (R^2 = 0.7050 – 0.9751) compared with the other models an indication that diffusion was not the major driving force for the release of BSA from the xerogels.

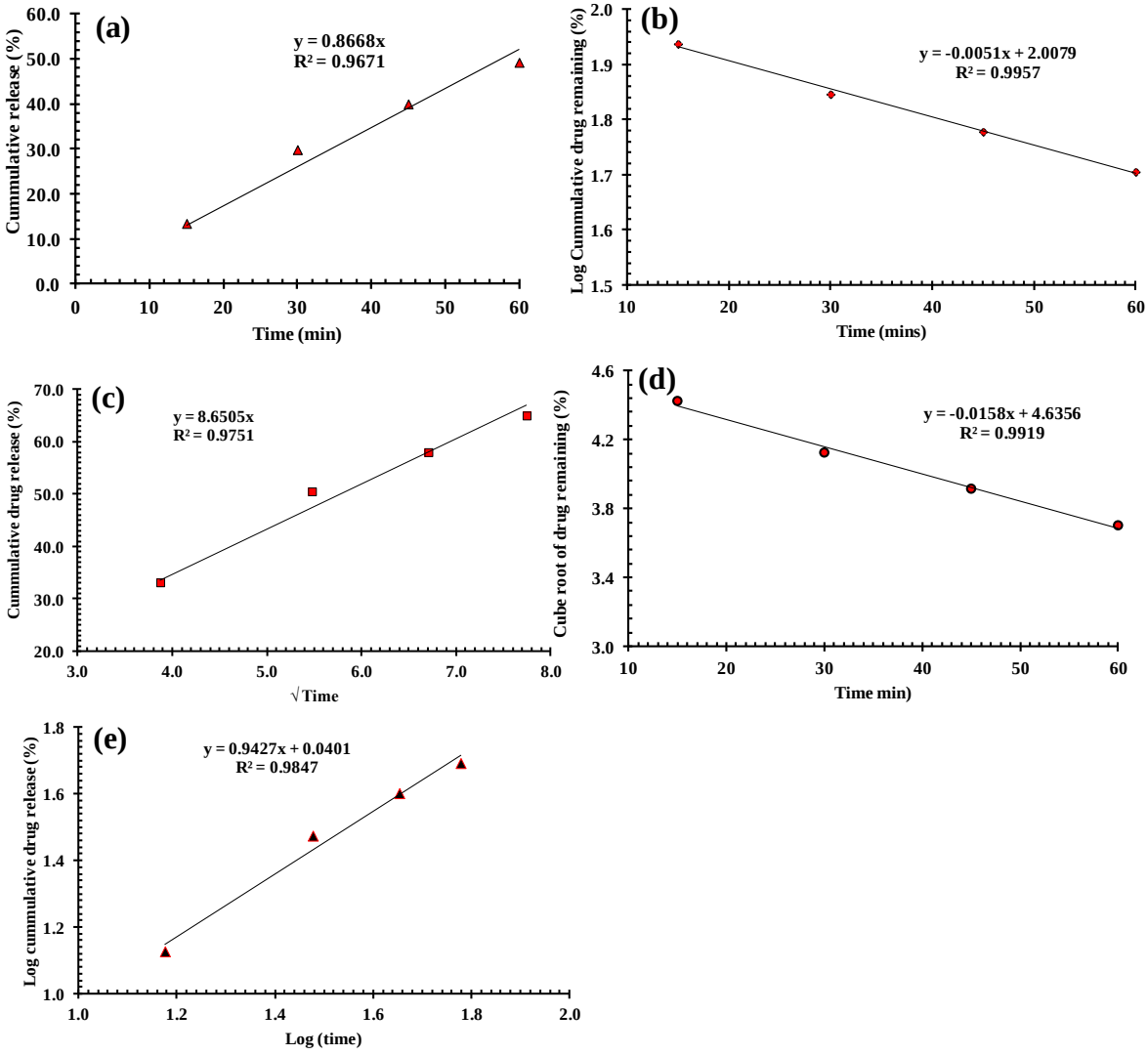

Figure 5.8: Representative plots of experimental release data of protein drug loaded chitosan/TG-chitosan xerogels fitted into different kinetic models, showing (a) Zero order (b) First order (c) Higuchi (d) Hixson-Crowell cube root law and (e) Korsmeyer-Peppas.

To confirm the release mechanism, the release data were fitted into Korsmeyer-Peppas equation. Good linearity (R^2 = 0.9796 – 0.9847) (Table 5.4) was observed for all formulations except chitosan-BSA (dialysed/annealed) (R^2 = 0.9369) (Table 5.4). The slope (n) values which characterises the release mechanism of drugs from cylindrical matrices as described in Table 5.2, ranged from 0.4855 – 1.6348. The undialysed chitosan-BSA xerogel showed an anomalous or non-Fickian diffusion (0.45 < n <0.89) release mechanism which was similar to

that of non-annealed dialysed chitosan-BSA xerogel. This is consistent with the results obtained by Chavda and Patel (2010) for a chitosan superporous composite hydrogel-based floating drug delivery system. Furthermore, the thiolated (annealed/non-annealed) as well as the dialysed annealed chitosan xerogels displayed $n > 0.89$ values, an indication of a super case-II transport mechanism where drug release rate is controlled by more than one process (erosion and diffusion) (Shoaib *et al.*, 2010). None of the formulations could fit a zero order model ($R^2 = 0.8750 – 0.9705$) as the release mechanism is concentration dependent and the drug under investigation is not a poorly soluble drug (Narashimhan *et al*., 1999, cited in Dash *et al.*, 2010).

Formulations containing GSH as EI in TG-chitosan xerogels displayed release mechanisms closely related to first order, Hixson-Crowell and Korsmeyer-Peppas kinetic models (Table 5.5) as described above. The mechanisms observed were concentration and dissolution controlled for all the formulations. TG-chitosan-BSA and TG-chitosan-GSH-BSA 10 % showed diffusional exponent values $0.45 < n < 0.89$ which confirms the non-Fickian diffusion or anomalous release mechanism. The mechanism for the TG-chitosan-GSH-BSA 5 % was a super case-II transport. Again Higuchi linearity was low for all formulations ($R^2 = 0.7283 – 0.9611$) (Table 5.5), indicating that release was not predominantly by diffusion. The addition of GSH did not considerably affect the mechanism of release of BSA from the TG-chitosan xerogels.

The release parameters of INS loaded TG-chitosan xerogels with different EIs are shown in Table 5.6. Higher linearity was observed with first order and Hixson-Crowell models for the control TG-chitosan-INS and the TG-chitosan-INS-APR (5 %) formulations, which is consistent with data obtained from other TG-chitosan xerogels loaded with BSA. The introduction of 10 % GSH to the INS loaded TG-chitosan xerogel however, gave release parameters that showed higher linearity with Korsmeyer-Peppas model ($R^2 = 0.9565$) (Table 5.6) followed by first order ($R^2 = 0.9340$) and Hixson-Crowell ($R^2 = 0.0.9336$). In addition to evaluating the INS loaded xerogels with different EIs, TG-chitosan loaded with BSA was further examined with APR as an EI. The release parameters similarly showed better linearity with first order, Hixson-Crowell and Korsmeyer-Peppas models (Table 5.6). These further support the suggestion that more than one mechanism was responsible for the release which could include concentration, xerogel morphology and diffusion. The diffusional coefficients ($n > 0.89$) for all formulations indicated a super case II transport which confirms the involvement of more than one mechanism of drug release.

Table 5.4: Release parameters obtained from fitting experimental drug dissolution (release) data to different kinetic equations for chitosan and TG-chitosan xerogels loaded with BSA.

Xerogel	Zero order		First order		Higuchi		Hixson-Crowell		Korsmeyer-Peppas		
	K_O (% min^{-1})	R^2	K_1 (min^{-1})	R^2	K_H (% $min^{-1/2}$)	R^2	K_{HC} (% $min^{-1/3}$)	R^2	K_P (% min^{-n})	n	R^2
Chitosan (dialysed/annealed)	1.009	0.9308	0.0182	0.9838	6.5917	0.7050	-0.0250	0.9743	0.0907	1.6348	0.9369
Chitosan (undialysed)	0.2505	0.8687	0.0020	0.9906	1.6851	0.9225	-0.0031	0.9907	0.9380	0.6551	0.9796
Chitosan (Non-annealed)	1.2626	0.1503	0.0140	0.9791	8.6505	0.9751	-0.0171	0.9692	9.1517	0.4855	0.9815
TG-chitosan (annealed)	0.8028	0.9584	0.0104	0.9880	5.3437	0.8478	-0.0142	0.9834	1.0032	0.9461	0.9844
TG-chitosan (non-annealed)	0.8668	0.9671	0.0117	0.9957	5.7670	0.8505	-0.0158	0.9919	1.0967	0.9427	0.9847

K_0, K_1, K_H, K_{HC} and K_P are the release rate constants for zero order, first order, Higuchi, Hixson-Crowell and Korsmeyer-Peppas models respectively, R^2 is the correlation coefficient and n is the release exponent.

Table 5.5: Release parameters obtained from fitting experimental drug dissolution (release) data to different kinetic equations for TG-chitosan xerogels loaded with BSA containing GSH using Franz-type diffusion cell.

Xerogel	Zero order		First order		Higuchi		Hixson-Crowell		Korsmeyer-Peppas		
	K_O (% h^{-1})	R^2	K_1 (h^{-1})	R^2	K_H (% $h^{-1/2}$)	R^2	K_{HC} (% $h^{-1/3}$)	R^2	K_P (% h^{-n})	n	R^2
TG-chitosan-BSA	17.356	0.7109	0.2195	0.9703	30.3570	0.9528	-0.2758	0.9663	26.6563	0.6271	0.9863
TG-chitosan-BSA-GSH 5 %	12.262	0.9843	0.2019	9873	20.6610	0.7283	-0.2739	0.9924	9.9129	1.1809	0.9990
TG-chitosan-BSA-GSH 10 %	14.264	0.7864	0.1626	0.9961	24.8900	0.9611	-0.2145	0.9926	21.2520	0.6547	0.9955

K_0, K_1, K_H, K_{HC} and K_P are the release rate constants for zero order, first order, Higuchi, Hixson-Crowell and Korsmeyer-Peppas models respectively, R^2 is the correlation coefficient and n is the release exponent.

Table 5.6: Release parameters obtained from fitting experimental drug dissolution (release) data to different kinetic equations for TG-chitosan xerogels loaded with INS and BSA containing different EIs.

Xerogel	Zero order		First order		Higuchi		Hixson-Crowell		Korsmeyer-Peppas		
	K_O (% min^{-1})	R^2	K_1 (min^{-1})	R^2	K_H (% $min^{-1/2}$)	R^2	K_{HC} (% $min^{-1/3}$)	R^2	K_P (% min^{-n})	n	R^2
TG-chitosan-INS	0.5336	0.8932	0.0087	0.9751	3.4312	0.6254	-0.0125	0.9715	0.0002	3.0443	0.8786
TG-chitosan-INS-APR (5 %)	0.4536	0.9705	0.0062	0.9942	2.9606	0.7260	-0.0090	0.9923	0.0946	1.4121	0.9702
TG-chitosan-INS-GSH (10 %)	0.3144	0.8750	0.0046	0.9340	2.0268	0.6183	-0.0068	0.9336	0.0066	2.0069	0.9565
TG-chitosan-BSA-APR (5 %)	0.6387	0.8925	0.0106	0.9397	4.1171	0.6190	-0.0149	0.9397	0.1606	1.3461	0.9325

K_0, K_1, K_H, K_{HC} and K_P are the release rate constants for zero order, first order, Higuchi, Hixson-Crowell and Korsmeyer-Peppas models respectively, R^2 is the correlation coefficient and n is the release exponent.

The effect of formulation processes such as annealing, dialysis and thiolation on drug release were further evaluated by comparing the dissolution profiles using the model independent difference (f_1) and similarity (f_2) factors. Chitosan-BSA (annealed/dialysed) was chosen as the reference for the dissolution profile comparisons between the various formulations as it is the pre-change formulation and the others are the post-change formulations (Test formulations). Table 5.7 shows the calculated (f_1) and (f_2) values for all formulations. Similarity was observed only in the annealed TG-chitosan-BSA xerogels and the reference annealed/dialysed chitosan-BSA xerogels (f_2 = 53.4, f_1 = 2.7). This is consistent with the statistical student t-test discussed earlier in this section.

Table 5.7: Model independent difference (f_1) and similarity (f_2) factors for release profiles of BSA (determining the effect of membrane dialysis, annealing and thiolation on formulations) with annealed/dialysed chitosan-BSA and annealed TG-Chitosan-BSA xerogels as reference (R_j) formulations.

Formulations (T_j)	Reference (R_j): Chitosan-BSA (annealed/dialysed)	
	Difference factor (f_1)	Similarity factor (f_2)
Chitosan-BSA (non-annealed)	12.5	39.4
Chitosan-BSA (undialysed)	67.2	40.4
TG-Chitosan-BSA (annealed)	2.7	53.4
	Reference (R_j): TG-Chitosan-BSA (annealed)	
TG-chitosan-BSA (non-annealed)	10.6	46.4

The dissolution profiles of the non-annealed and undialysed chitosan-BSA xerogels were found not to be similar to that of the reference formulation with (f_2) values less than 50 (Table 5.7). The difference factors for the undialysed xerogel (f_1 = 67.2) and the non-annealed xerogels (f_1 = 12.5) were far from zero signifying the difference between the release profiles. Using annealed TG-chitosan-BSA as the reference formulation, the difference (f_1 = 10.6) and similarity factors (f_2 = 46.4) for non-annealed TG-chitosan-BSA (test) was also determined (Table 5.7). Based on the FDA guidelines, the dissolution profiles were found to be different with $f_2 < 50$. Annealing and dialysis therefore led to changes in dissolution profile while thiolation did not affect the dissolution profile of the chitosan based lyophilised xerogels.

The effect of an EI concentration on dissolution profile of the thiolated xerogel was determined using TG-chitosan-BSA as the reference against TG-chitosan-BSA containing 5 % and 10 % GSH as the EI. Whereas the dissolution profile of the xerogel with 10 % GSH was found to be similar (f_2 = 65.4) to the reference, the xerogel with 5 % was not similar (f_2 = 49.8) though the f_1 values were similar (Table 5.8). With the 5 % GSH xerogel as the reference and the 10 % GSH as the test formulation, the two were found to be similar, having f_1 and f_2 values of 1.3 and 55.2 respectively.

Table 5.8: Model independent difference (f_1) and similarity (f_2) factors for release profiles of BSA (determining the effect of EI concentration on release) with TG-Chitosan-BSA and TG-Chitosan-GSH-BSA (5 %) xerogels as reference (R_j) formulations.

Formulations (T_j)	Reference (R_j) : TG-Chitosan-BSA	
	Difference factor (F1)	Similarity factor (F2)
TG-Chitosan-GSH-BSA (5 %)	11.2	49.8
TG-Chitosan-GSH-BSA- (10 %)	10.1	65.4
	Reference (R_j): TG-Chitosan-GSH-BSA (5 %)	
TG-Chitosan-GSH-BSA (10 %)	1.3	55.2

The dissolution profiles of thiolated chitosan loaded with INS and incorporated with different EIs (5 % APR and 10 % GSH) were also evaluated with the model independent approach and the difference and similar factors are as shown in Table 5.9. The difference factors (f_1) were far above 15 for both formulations using TG-chitosan-INS as the reference formulation which indicates a highly significant difference. However, the similarity factors (f_2) were above 50 for both formulations indicating that all the INS containing formulations have similar dissolution profiles. Shah *et al*., (1998) have however argued that f_2 comparison has been the focus in Agency guidance since it assures similarity in product performance and it gives a measure as to which is more sensitive to large differences at any particular time point. The comparison between TG-chitosan-APR-INS and TG-chitosan-APR-BSA were also found to be similar with an f_2 value of 54.1. The different EIs in the INS loaded xerogels did not affect the dissolution profile as all formulations were found to be similar.

Table 5.9: Model independent difference (f_1) and similarity (f_2) factors for release profiles of INS and BSA (determining the effect of different EIs on release) with TG-Chitosan-INS xerogels and TG-Chitosan-APR-INS (5 %) as reference (R_j) formulations.

Formulations (T_j)	Reference (R_j): TG-Chitosan-INS	
	Difference factor (F1)	Similarity factor (F2)
TG-Chitosan-APR-INS	25.5	62.0
TG-Chitosan-GSH-INS	53.2	52.0
	Reference (R_j): TG-Chitosan-APR-INS	
TG-chitosan-APR-BSA	28.3	54.1

5.4 Conclusions

The effects of formulation processes including membrane dialysis, annealing and thiolation on *in vitro* drug release profiles from chitosan based lyophilised xerogels have been studied. Dialysed and annealed chitosan-BSA xerogels exhibited an initial burst release of BSA due to high drug loading and a subsequent controlled release phase from chitosan-BSA complex. The presence of crystalline NaAc in the undialysed chitosan-BSA xerogel, however, resulted in a three-fold reduction in BSA release due to decreased surface area of dispersed drug and changes in pH of release media. The 7 hr total cumulative percentage drug release of 91.5% and 80.1% observed for the annealed and non-annealed chitosan-BSA xerogels respectively was due to the annealing process, enabling a porous network which led to ease of hydration and consequent improved drug release. Furthermore, annealed TG-chitosan-BSA demonstrated higher BSA release compared to non-annealed TG-chitosan-BSA xerogels. The reduced total percent release of BSA could be attributed to the reduced cohesiveness of the non-annealed xerogels. Although the process of thiolation has been associated with enhanced mucoadhesion characteristics, its effect on drug release was not significant as unmodified chitosan-BSA and TG-chitosan-BSA xerogels showed no difference in drug release profiles.

Adsorption of BSA by GSH, as EI in the TG-chitosan-BSA xerogel caused a significant reduction in BSA release and this was not concentration dependent. Similarly, the presence of different EIs (5 % APR and 10 % GSH) in INS loaded TG-chitosan xerogels led to reduced INS release. However, the influence of GSH with respect to reduction in INS

release was much pronounced, indicating the involvement of different mechanisms of inhibition by the different enzyme inhibitors.

The model dependent mathematical functions used in describing the release profiles of BSA from the xerogels showed that first order, Hixson-Crowell and Korsmeyer-Peppas equations fitted the dissolution data best, suggesting the complex nature of release based on drug concentration, dissolution and polymer characteristics from all the chitosan based formulations. The presence of EI did not alter the release mechanism in the TG-chitosan xerogel loaded with either BSA or INS which involved more than one process. This was confirmed by the release exponents displaying non-Fickian diffusion and super case-II transport release mechanisms for all the formulations under investigation.

Based on the model independent difference (f_1) and similarity (f_2) factors, the release profiles of annealed and dialysed chitosan-BSA and annealed TG-chitosan-BSA xerogels were found to be similar compared to non-annealed chitosan-BSA and non-annealed TG-chitosan-BSA xerogels. The release profiles of TG-chitosan-BSA and TG-chitosan-GSH-BSA 10 % were similar against that of TG-chitosan-GSH-BSA 5 %. However, with TG-chitosan-GSH-BSA 5 % as the reference, the release profile was similar to that of TG-chitosan-GSH-BSA 10 %. The different EIs in the INS loaded xerogels did not affect the release profile of INS from all formulation. Release profiles of BSA and INS xerogels containing APR were also similar.

The principal implication of these findings is the potential application of the novel lyophilised system for the delivery of proteins via the buccal mucosa. These *in vitro* characterisations can help to predict the *in vivo* performance of the various formulations which would be expected to impact on the drug release rate and duration based on the varied physical properties of the xerogels.

CHAPTER SIX

PERMEATION STUDIES USING EPIORAL™ BUCCAL TISSUE AND SHEEP BUCCAL TISSUE

6.1 Introduction

Buccal drug delivery involves the direct exposure and subsequent permeation of drugs through the mucosal tissues for systemic or local effect. The advantages and limitations of buccal drug delivery have been reviewed in chapter 1 section 1.5.1. The diffusion of drugs across the buccal mucosa has been studied in controlled environments such as temperature, pH and osmolarity using drug permeability models to determine the barrier properties of different biological tissues (Nicolazzo & Finnin, 2008, cited in Patel *et al*., 2012). Generally, animal tissues are employed but are however limited compared to human buccal tissue because the oral mucosa of animals such as rats and hamsters are keratinised as opposed to the non-keratinised human buccal mucosa (Tsutsumi *et al*., 1999, cited in Patel *et al*., 2012). Results obtained from rabbit buccal mucosa which is partly non-keratinised can be unreliable due to identification and isolation of limited tissue (Squier, & Wertz, 1996). Animal species such as dogs and monkeys with non-keratinised buccal tissues but thinner mucosal epithelium exhibit greater permeability compared to human buccal tissue (Mehta *et al*., 1991, cited in Patel *et al*., 2012). Researchers have therefore frequently used pig buccal tissue as it demonstrates greater correlation to that of humans (Squier, & Wertz, 1996). Recently, permeability studies for venlafaxine have also been carried out using sheep buccal mucosa (Kumar *et al*., 2011). Maintaining buccal tissue integrity and viability during isolation and storage before experimental testing is crucial to obtaining reliable permeation results (Patel *et al*., 2012). For example, the storage of porcine buccal mucosa in Krebs bicarbonate Ringer solution helped to retain its integrity whiles storage in other solutions such as PBS at 4 °C for 24 h led to loss of epithelial integrity (Kulkarni *et al*., 2010).

Buccal epithelial cell culture models grown from hamster cheek pouch did not completely differentiate to form a keratinised surface and therefore displayed greater permeability to drugs compared to the original tissue. The hamster cell culture model therefore mimics the human buccal mucosa and has been deemed suitable for predicting human buccal mucosa permeability (Tavakoli-Saberi & Audus, 1989 cited in Patel *et al*., 2012). The TR146 cell line, originally from human buccal carcinoma, has also been used as a human buccal mucosa model since it shows differentiation patterns closely resembling the

human non-keratinised epithelium. It however displays greater permeability compared to native human or porcine buccal tissue (Nielsen, & Rassing, 2000).

The recent development and commercialisation of EpiOral™ buccal construct (MatTek, Ashland, MA, USA) has paved the way for better permeation experimental controls. In addition, advantages such as cell homogeneity, reasonable cost, availability and ease of use have been reported (Sohi *et al*., 2010). The multilayered buccal tissue model (Figure 6.1) is cultured in serum-free medium on the surface of collagen-coated inserts to form three-dimensional differentiated tissues consisting of an organised basal layer and multiple non-cornified layers which are histologically and morphologically similar to native human buccal tissue (www.mattek.com).

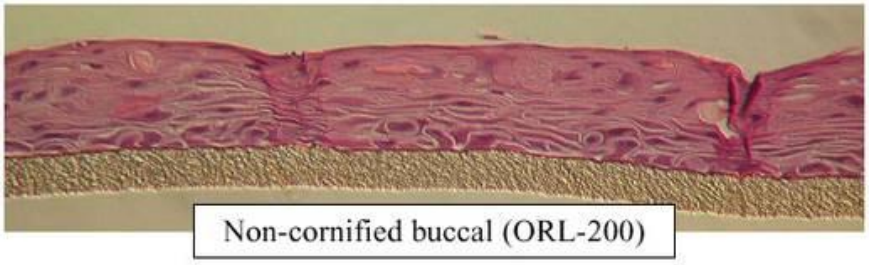

Figure 6.1: Histology of EpiOral™ (buccal phenotype) Formalin fixed, Paraffin embedded, Haematoxylin and Eosin (H&E) stained. Available at< http://www.mattek.com/pages/ > Accessed [08/07/2012]

The 8 – 11 cell layered *in vitro* tissue model has the characteristics of native buccal tissue differentiated from human primary oral keratinocytes (Koschier et al, 2011). The naturally occurring antimicrobial peptides human beta defensins (HBD-1 and HDB-3) are constitutively expressed by the tissue (www.mattek.com).

The current chapter investigates the permeation of the protein model drugs; BSA and INS released from optimised chitosan based xerogels using human equivalent EpiOral™ buccal tissue construct. Further, the effect of EIs on the permeation of INS released from TG-chitosan xerogels was examined with sheep buccal tissues and the cumulative amounts of INS permeating correlated with data from the EpiOral™ experiment.

6.2 Materials and Methods

6.2.1 Materials

Table 6.1: Details of materials used in permeation studies

Material	Description	Supplier
EpiOral™ Buccal Tissue Kit	ORL-200	MatTek, Ashland MA, USA
PBS tablets	pH 7.4	Sigma-Aldrich, (Gillingham, UK)
Bradford's reagent	B6916-500ML	Sigma-Aldrich, (Gillingham, UK)
BSA powder	A7906-100 G	Sigma-Aldrich, (Gillingham, UK)
Human INS	12643-50MG	Sigma-Aldrich, (Gillingham, UK)
3-[4,5-dimethylthiazol-2-yl] 2,5-diphenyltetrazolium bromide (MTT)	M5655-500MG	Sigma-Aldrich, (Gillingham, UK)
Isopropanol	I9030-500ML	Sigma-Aldrich, (Gillingham, UK)
Krebs-Ringer Bicarbonate Buffer	K4002-10X1L	Sigma-Aldrich, (Gillingham, UK)

6.2.2 EpiOral™ permeation studies

0.3 mL of EpiOral™ assay media (MatTek, Ashland, MA) warmed to 37 °C, was pipetted into 4 wells of 24 well plates and labelled 1 hr equilibration. The remaining wells were filled with sterilised 0.01M PBS (pH 7.4) as the receiver fluid and labelled as 0.5, 1.0, 2.0, 3.0 and 4.0 hrs. The EpiOral™ constructs cultured on the surface of tissue inserts with diffusional surface area of 0.6 cm^2 were transferred aseptically into the EpiOral™ assay media filled 24 well plates. The tissues were then placed in a 37 ± 1 °C, 5 ± 1% CO_2 incubator for 1 hr to equilibrate. The EpiOral™ tissue inserts were then transferred into the 0.5 hr labelled receiver fluid, treated with 0.5 mL of donor solution (0.01M PBS, pH 6.8, simulating salivary fluid) into which was added 15 mg of drug loaded laminated xerogels (test materials) with the mucoadhesion layer in contact with the apical surface of the EpiOral™ tissue and returned to the incubator. The tissues were moved to the 1 hr wells after 0.5 hrs of elapsed permeation time. Similarly the tissues were moved after 2.0, 3.0 and 4.0 hrs of total elapsed time. 50 µL of the receiver fluid was sampled at the predetermined time intervals, treated with 1 mL Bradford's reagent and the absorbance measured at 595 nm and 450 nm for linearisation of absorbance using a Multiskan EX microplate photometer equipped with Ascent software (Thermo Scientific, Hampshire UK). A graphical representation of the full procedure is

shown in Figure 6.2. The concentration of the BSA released from the xerogels was determined by interpolation from the linearized calibration curve ($r^2 > 0.99$) (chapter 3, Figure 3.28) and permeation parameters such as the flux (J), apparent permeability coefficient (P_{app}) and enhancement factor (EF) were determined using equations 6.1, 6.2 and 6.3 respectively.

$$J = dQ/d_t \, .1/A \qquad \textit{equation 6.1}$$

$$P_{app} = dQ/d_t.1/A \, .1/C \qquad \textit{equation 6.2}$$

$$EF = P_{app}\,(formulation)/\, P_{app}\,(pure\ drug) \qquad \textit{equation 6.3}$$

where J is the steady state flux, dQ/d_t is the amount of drug permeated, A is the effective diffusion area, C is the initial drug concentration and P_{app} is the apparent permeability coefficient (Fetih *et al.*, 2011).

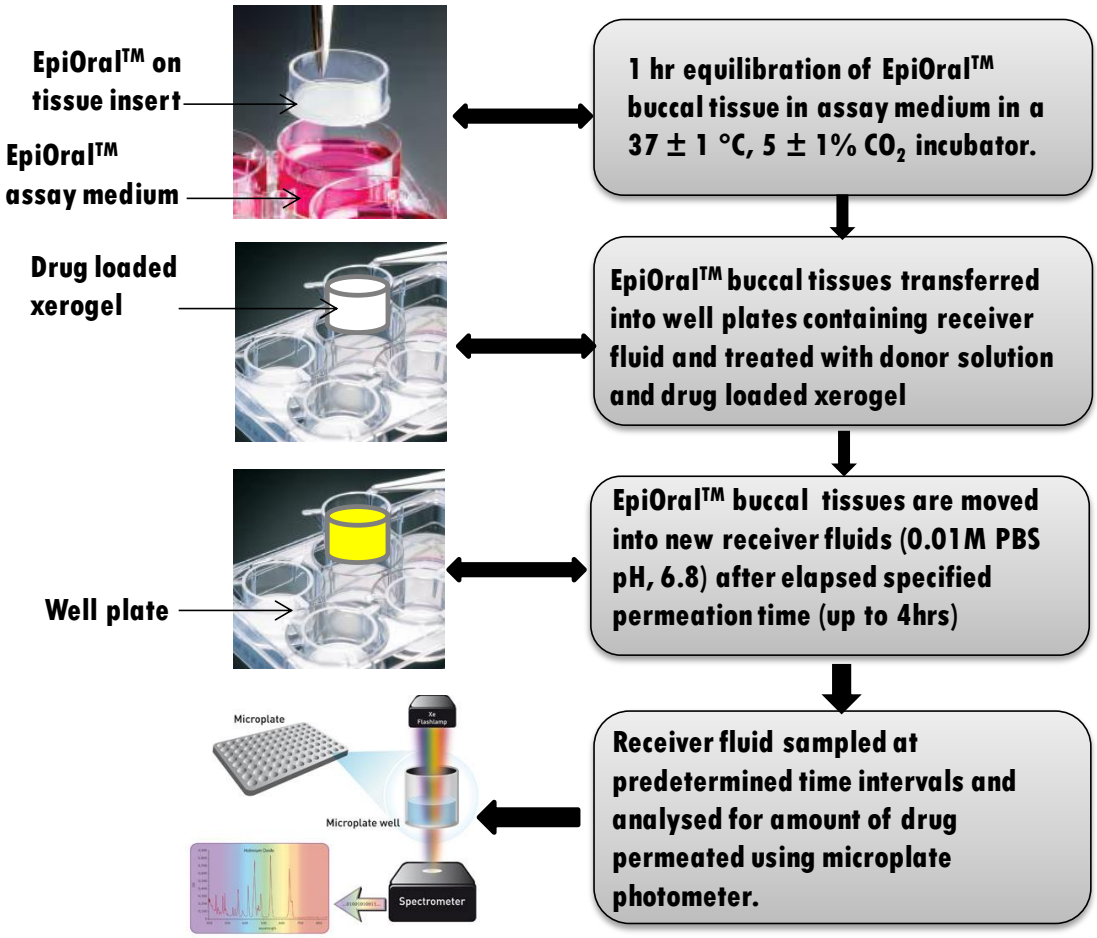

Figure 6.2: Graphical representation of the EpiOral™ experimental procedure

Permeation studies were conducted for the following optimised xerogels in Table 6.2. Non-treated EpiOral™ tissue was used as the negative control while 10 mg/mL and 4 mg/mL solutions of BSA and INS respectively were used as positive controls for BSA and INS containing xerogels.

Table 6.2 Optimised drug loaded xerogels used for permeability studies

BSA loaded xerogels	INS loaded xerogels
Chitosan-BSA	TG-chitosan-INS
TG-chitosan-BSA	TG-chitosan-GSH-INS
TG-chitosan-GSH-BSA	TG-chitosan-APR-INS

6.2.3 Tissue integrity (MTT assay)

After 4 hrs of permeation experiment, the EpiOral™ tissue inserts were transferred into 24 well plates pre-filled with MTT solution (0.3 mL) dissolved in PBS (5 mg/mL), incubated for 3 hrs and the MTT medium was gently aspirated from all wells. After the incubation, the cultures were extracted in 2 mL of acidified isopropanol for 2 hrs with gentle shaking (120 rpm). Two, 200 µL aliquots of extract were placed into 96 well plates and the absorbance of the extracted (purple coloured) formazan was determined using a Multiskan EX microplate photometer equipped with Ascent software (Thermo Scientific, Hampshire UK) at 570 nm. Viable cells had the greatest amount of MTT reduction and hence the highest absorbance values. Relative cell viability was calculated for each tissue as % of the mean of the negative control tissues. Data was processed from three replicates for the mean percentage viability.

6.2.4 *In vitro* buccal permeation studies (sheep buccal tissue)

In vitro INS permeation through sheep buccal mucosa was carried out using Franz-type diffusion cell with diffusional surface area 0.6 cm^2. Fresh sheep buccal mucosa obtained from a local slaughterhouse was immediately kept in Krebs-Ringer bicarbonate buffer (modified with sodium carbonate) and used within 2 hrs of slaughter (Patel *et al.,* 2007). The underlying fat and loose tissues were removed and the mucosal membrane was washed with physiological PBS (pH 6.8) at 37 °C. The obtained buccal mucosa membrane was mounted between the donor and receiver compartments of the Franz-type diffusion cell, with the epithelial side facing the donor compartment (Attia *et al.,* 2004). The receiver chamber was filled with 8 mL of 0.01 M PBS (pH 7.4) at 37 °C and uniform mixing was provided by

magnetic stirring at 150 rev/min. After an equilibration period of 30 minutes, 0.5 mL of 0.01 M PBS (pH 6.8) was placed in the donor compartment and 15 mg of the INS loaded laminated xerogels were placed in the donor chamber with the mucoadhesion layer in contact with the epithelial surface. The chambers were held together by cell clamp and sealed with parafilm to limit evaporation. At predetermined time intervals, samples (1 mL) were withdrawn from the sampling port of the receiver compartment and replaced with the same amount of PBS to maintain a constant volume for 4 hrs. 50 μL of the sampled medium was treated with 1 mL of Bradford's reagent and permeation parameters determined as described in section 6.2.2.

6.2.5 Permeation correlation between EpiOral^{TM} and sheep buccal tissues.

The effect of the EI aprotinin (APR) on the permeation of INS via the tissue engineered buccal epithelium and the sheep buccal tissue was further investigated by constructing a correlation curve for EpiOral^{TM} cumulative permeation against cumulative permeation of TG-chitosan-INS through sheep buccal tissue. The linear regression (R^2) coefficient obtained from the curve was compared with that obtained from TG-chitosan – APR-INS curve.

6.3 Results and discussion

6.3.1 EpiOral^{TM} permeation studies

The generally low flux across the buccal mucosa poses a significant challenge for buccal drug delivery (Langoth *et al*., 2005). The intercellular links in the buccal tissue is characterised by desmosomes and tight junctions, however the permeation of peptide drugs across the buccal epithelium is believed to be mediated via the paracellular route by passive diffusion (Rathbone *et al*., 1994, cited in Langoth *et al*., 2005). The cumulative permeation curves of BSA released from the chitosan based xerogels is shown in Figure 6.3. Table 6.3 shows the permeation parameters of BSA and INS for all the chitosan based xerogels used in this study. A lag-time of 30 minutes was generally observed for the BSA and INS permeation for all the xerogels examined using the EpiOral^{TM} buccal tissue construct. For BSA permeation studies, the highest permeation enhancement was observed for the TG-chitosan followed by TG-chitosan-GSH and then unmodified chitosan xerogels. Ranaldi *et al*., (2002, cited in Langoth *et al*., 2005) have demonstrated the ability of unmodified chitosan to enhance paracellular absorption across the buccal membrane. The enhancement factor showed a 12.3-

fold increase in transport of BSA from the unmodified chitosan xerogels across the EpiOral™ buccal tissue construct compared to the BSA control. This increase seems to be dependent on the ability of the cationic polymer to interact with the negatively charged membrane, resulting in structural reorganisation of the tight junction associated proteins (Schipper *et al*, 1997; Senel, & Hıncal, 2001). This is consistent with the results obtained by Schipper *et al*., (1999) in which chitosan produced a 10- to 15-fold permeation enhancement of atenolol through mucus-free Caco-2 layers.

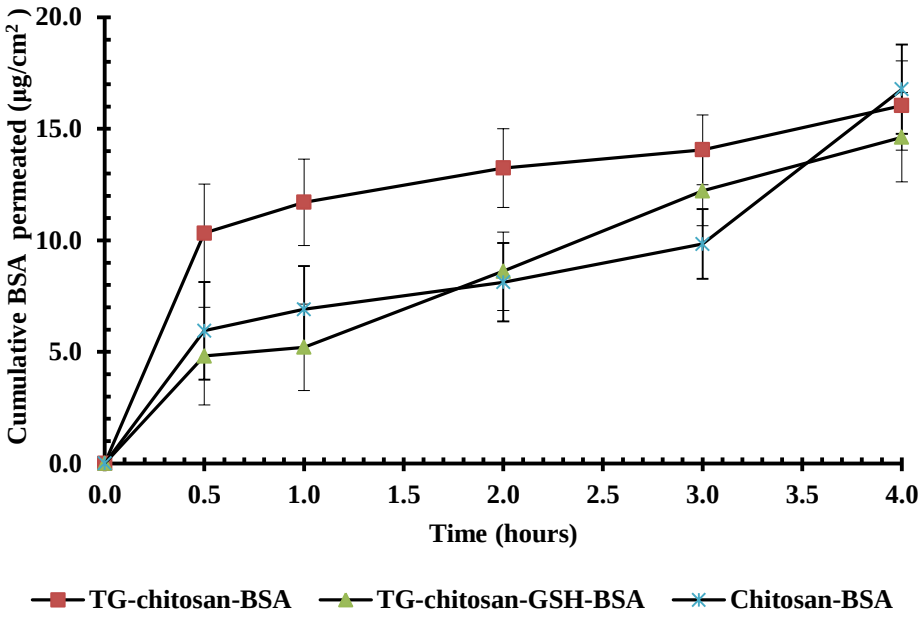

Figure 6.3: Cumulative permeation curves of BSA released from chitosan based xerogels

Table 6.3: Permeation parameters of xerogels from EpiOral™ buccal construct

Formulation	Flux (µg/cm^2 /hr) (n=3, mean ± SD)	Apparent permeability coefficient (x 10^{-2} cm^2 /hr) (n=3, mean ± SD)	Enhancement factor
Chitosan-BSA	4.2 ± 1.0	4.2 ± 0.9	12.3
TG-chitosan –BSA	4.0 ± 0.8	4.6 ± 0.6	13.7
TG-chitosan-GSH-BSA	3.7 ± 0.7	4.2 ± 1.1	12.6
TG-chitosan-INS	1.3 ± 0.2	3.1 ± 0.7	1.8
TG-chitosan-GSH-INS	0.3 ± 0.1	1.3 ± 0.2	0.6
TG-chitosan-APR-INS	1.2 ± 0.3	3.8 ± 0.5	1.8

The slight improvement in permeation for the thiolated chitosans over that of unmodified chitosan (13.7-fold) could have stemmed from their enhanced bioadhesive properties (see chapter 3) that allowed the polymer to act as a penetration enhancer due to the covalent attachment of thioglycolic acid. Free thiol groups have been shown to reduce oxidised glutathione found on the surface of buccal mucosa. The reduced glutathione inhibits the enzyme protein-tyrosine-phosphatase which subsequently leads to the phosphorylation of occludin resulting in the opening of tight junctions, therefore, allowing the transport of macromolecules across the membrane (Barrett *et al*., 1999). It must however, be added that the presence of tight junctions in the human equivalent buccal tissue (EpiOral™) could not be confirmed in this study and this requires further investigation. That notwithstanding, the evidence of tight junctions in a similar human equivalent tissue EpiAirway™ by the same manufacturer (MatTek Corporation, www.mattek.com) has been confirmed. Drug permeability may also have been increased by the improved drug availability (Figueiras *et al*., 2009) at the apical surface of the EpiOral™ due to high drug release from the chitosan based xerogels which allows a higher concentration diffusion gradient in the direction of absorption across the membrane.

The addition of reduced GSH which has a dual action as a permeation enhancer as well as enzyme inhibitor to TG-chitosan ostensively increases the amount of reduced GSH on the membrane. A synergistic effect to further improve the permeation enhancing effect of TG-chitosan –GSH xerogel was therefore expected. Furthermore, GSH in combination with thiolated polycarbophil was observed to have increased the permeation of sodium fluorescein across guinea pig small intestinal mucosa by 2.9-fold (Clausen *et al*., 2002, cited in Langoth *et al*., 2005). However, this expected improvement in permeation was not achieved in the current study as the observed permeation parameters for TG-chitosan-GSH shown in Table 6.3 were slightly lower than those of TG-chitosan. This could be attributed to the interaction between GSH and BSA (Vallee *et al*., 2008) which may have limited the permeation of BSA through the Epi-oral™ buccal tissue construct as was observed in the drug release studies (see chapter 5). In addition, the large size of BSA (67 kDa) could have limited its permeability through the EpiOral™ buccal tissue however, this will require further investigation.

The cumulative permeation curve of INS loaded TG-chitosan xerogels with different EIs is shown in Figure 6.4. Similar permeation curves were observed for TG-chitosan and TG-chitosan-APR xerogels which showed no significant differences ($p > 0.05$) in the flux and enhancement factor (Table 6.3).

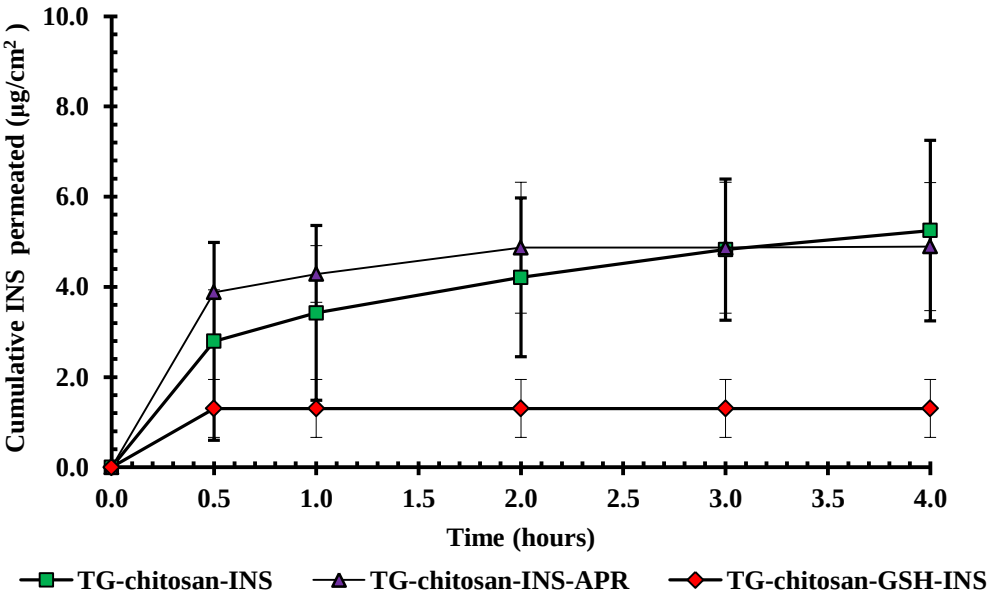

Figure 6.4: Cumulative permeation curves of INS released from TG-chitosan xerogels showing the effect different EI on permeation through EpiOral^{TM} buccal tissue.

The apparent permeability was slightly higher for the TG-chitosan-APR xerogel but the difference was not statistically significant ($p > 0.05$). APR therefore had no significant effect on the permeability of INS from the TG-chitosan-APR xerogel through Epi-oral^{TM}. No report on expression of enzymatic activities in Epi-oral^{TM} was found in the literature and that might possibly explain the insignificant effect of the EI on the permeation of INS through Epi-oral^{TM}. A significant reduction in the permeation of INS, approximately half that of pure INS solution (control), was however, obtained for the TG-chitosan-GSH xerogel. The significant effect of GSH on INS permeation, confirms the apparent chemical interaction of the two resulting in the reduced release of INS from the TG-chitosan-GSH xerogel in the release studies (see chapter 5). GSH may have had a greater affinity for INS thus its effect on inhibiting disulphide bond formation in the thiomer was absent (see chapter 4). The formation of disulphide bonds has a limiting effect on xerogel hydration which resulted in poor INS release and subsequent reduced permeation through the EpiOral^{TM} buccal tissue construct. The permeation enhancing effect of the thiolated chitosan was therefore diminished by the presence of GSH-INS interaction. The choice of an EI for a particular protein formulation intended for buccal deliver plays a significant role in the permeability of the protein. Based on these results, APR appears to be a better EI for the delivery of INS via the buccal mucosa and was therefore considered for further evaluation using sheep buccal membrane.

6.3.2 Tissue integrity (MTT assay)

Tissue viability was assessed using the 3-[4,5-dimethylthiazol-2-yl] 2,5-diphenyltetrazolium bromide (MTT) reduction assay where yellow MTT is reduced to purple formazan primarily by enzymes located in the mitochondria of viable cells (Koschier *et al*., 2011). Figure 6.5 'A' and 'B' shows the respective cell viability data for BSA and INS containing xerogels exposed to the EpiOral^{TM} buccal tissue construct as measured by the MTT assay.

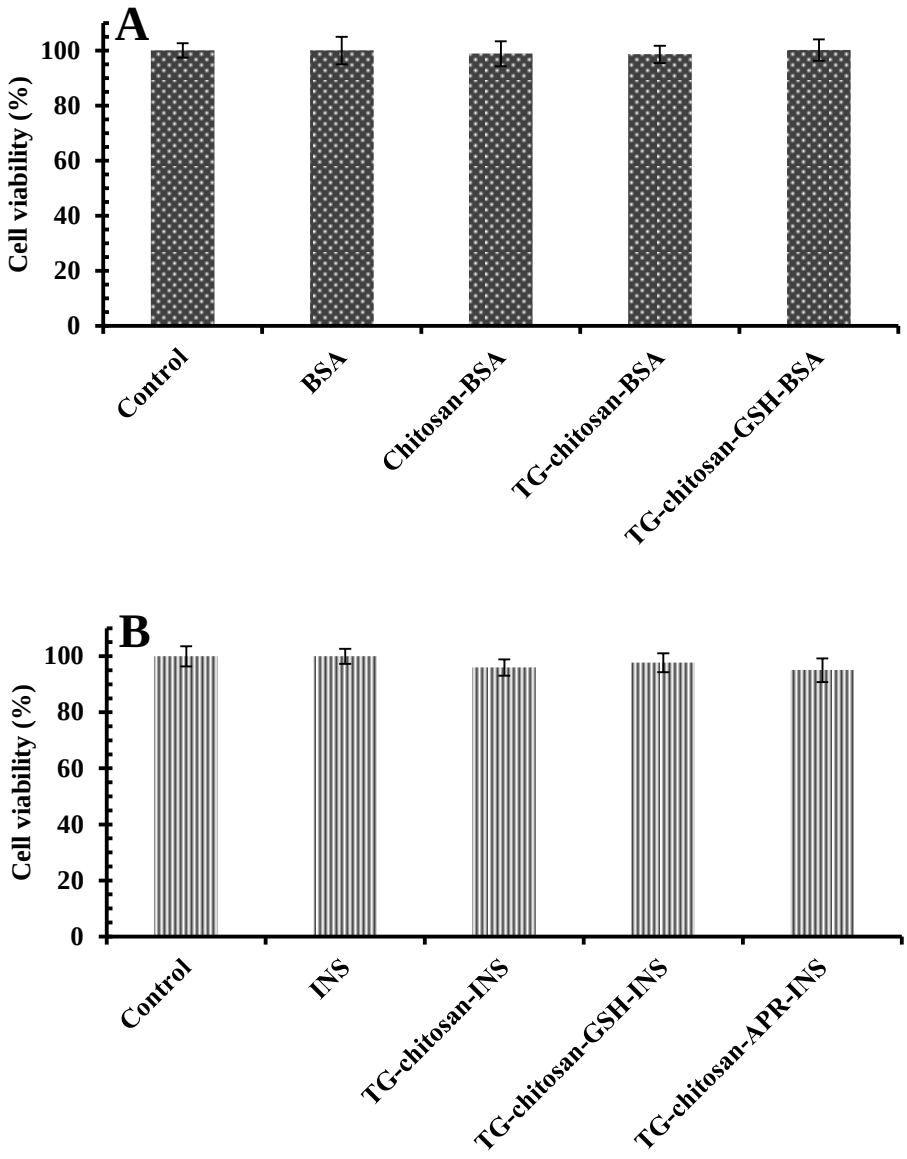

Figure 6.5: EpiOral^{TM} tissue viability showing 'A' BSA containing chitosan based xerogels with negative (non-treated) and positive (BSA solution) controls. 'B' shows the tissue viability of INS containing xerogels along with negative (non-treated) and positive (INS solution) controls.

Average percentage viability was plotted for the different test conditions using non-treated control as the 100% viable tissue. The cell viability was measured after 4 hrs exposure, to measure the toxicity of the chitosan based xerogels. All test conditions maintained > 95 % viability as measured by the MTT reduction assay, indicating that the excipient as well as model protein drugs had no toxic effect on the cells of the EpiOral™ buccal tissue construct.

6.3.3 *In vitro* buccal permeation studies (sheep buccal tissue)

The effect of EI on INS permeation was further investigated using sheep buccal membrane (Figure 6.6). The amount of INS permeating was approximately 450-fold higher (1700 - 2900 µg/cm^2) than was observed from the EpiOral™ studies (4.9 – 5.2 µg/ cm^2). This suggests that the sheep buccal membrane is more permeable than the human equivalent buccal tissue (EpiOral™). Linearity was observed for both samples up to 2 hours of permeation (R^2 > 0.98) and followed a first order kinetic release which is concentration dependent but the curves levelled off due to a possible change in release kinetics. 30 minutes lag-time was observed for INS permeation via the sheep buccal tissue. The permeation parameters (Table 6.5) indicated that TG-chitosan-APR-INS xerogel had an effect on the biological membrane, leading to a 1.7-fold increase in INS permeation compared to TG-chitosan-INS and control INS solution. Higher flux and apparent permeability coefficients were obtained for the xerogel containing APR. The protease inhibitor (APR) may have minimized the degradation of the INS on the sheep buccal mucosa and with a resultant increase in INS permeation.

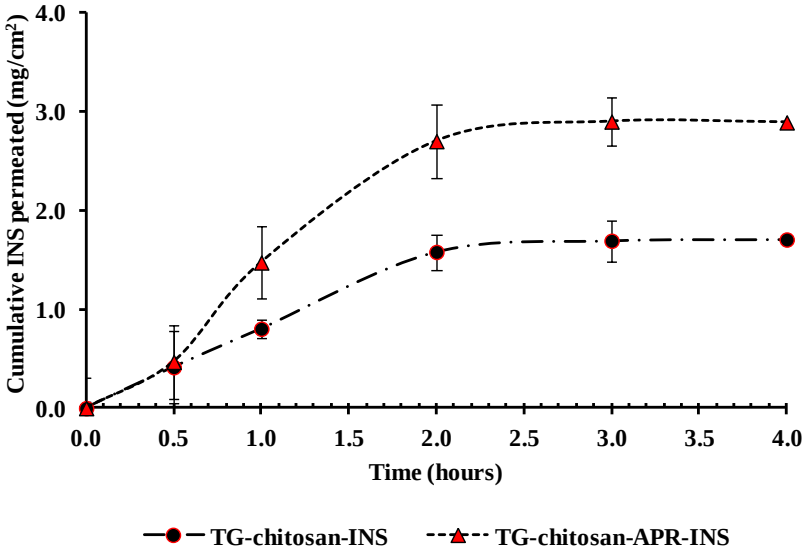

Figure 6.6: Cumulative permeation curves of INS released from TG-chitosan xerogels showing the effect different EI on permeation through sheep buccal tissue.

The enhancement factor (*EF* = 1) observed for the TG-chitosan-INS xerogel suggests that the TG-chitosan had no permeation enhancing effect on the biological membrane compared to the control. The results also indicate that TG-chitosan did not limit the release of INS from the xerogel. However, due to poor physical contact with the sheep buccal epithelial surface or possibly absence (or very little) of mucosal fluid (mucin) on the membrane, no significant covalent or electrostatic bond (mucoadhesion) could be established. This is plausible as the membrane was initially washed in a physiological fluid during preparation before mounting on the donor compartment of the Franz-type diffusion cell, which was later filled with 0.01 M PBS without mucin, before data acquisition. Further investigation with different physiological fluids will be an interesting to compare with the results obtained.

Table 6.4: Permeation parameters of xerogels from sheep buccal tissue

Formulation	Flux (mg/cm^2 /hr) (n=4, mean ± SD)	Apparent permeability coefficient (cm^2 /hr) (n=4, mean ± SD)	Enhancement factor
TG-chitosan-INS	0.43 ± 0.07	0.19 ± 0.01	1.00
TG-chitosan-APR-INS	0.72 ± 0.05	0.33 ± 0.03	1.70

6.3.4 Permeation correlation between EpiOral™ and sheep buccal tissues.

The study has shown that there is good correlation during the *in vitro* permeation of INS between the human equivalent buccal tissue (EpiOral™) and *ex vivo* sheep buccal membrane (Figures 6.7). It was however, interesting to observe that xerogels with EI demonstrated better linear correlation (R^2 = 0.9953) than xerogels without EI (R^2 = 0.9124). This could be due to the lack of interaction between the TG-chitosan and the sheep buccal membrane discussed in section 6.3.3 above. In the EpiOral™ study, there were no significant differences between the permeability parameters (Table 6.4) however, the experiments with sheep buccal membrane showed statistically significant differences between the mean flux ($p < 0.05$) and apparent permeability ($p < 0.05$) data of the TG-chitosan-INS and the TG-chitosan-APR-INS xerogels. It is quite clear that the presence of the EI was important in enhancing INS permeation through the sheep buccal mucosa but this effect was not significant in the EpiOral™ study.

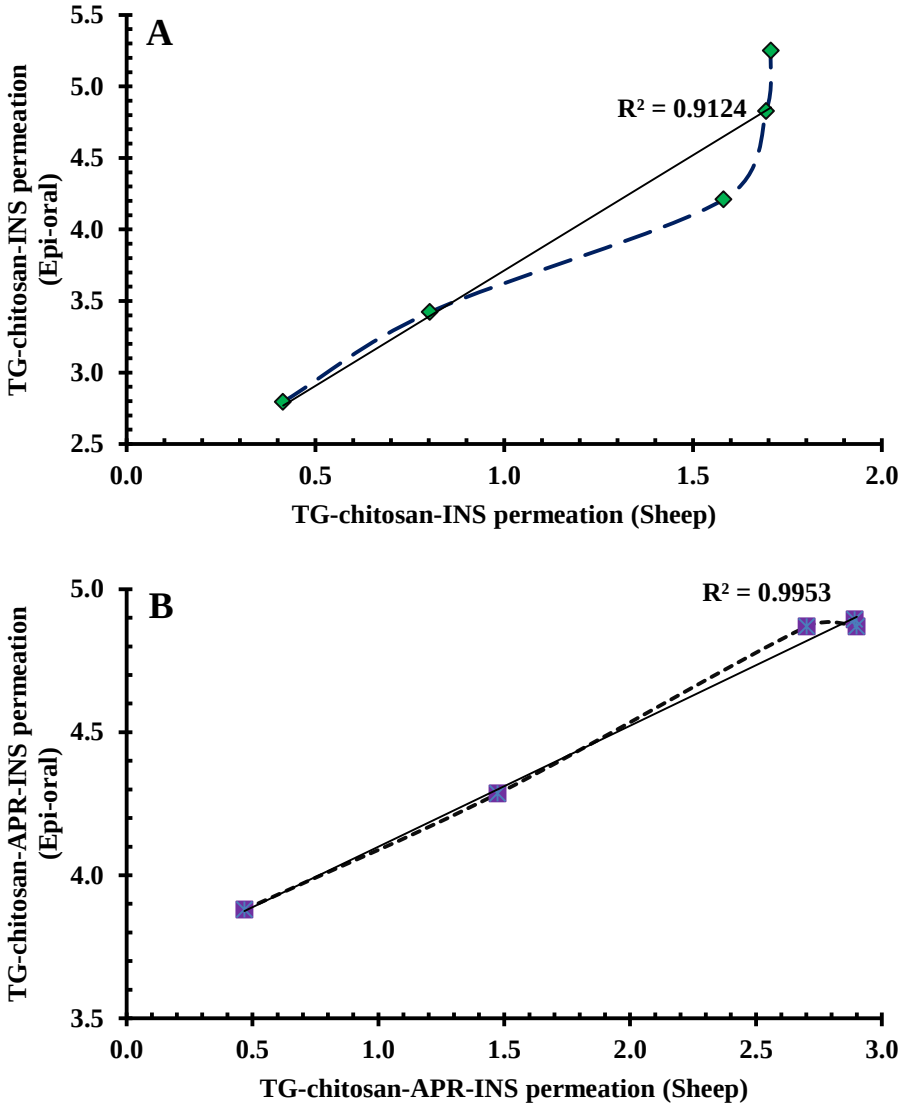

Figure 6.7: Correlation curves of 'A' TG-chitosan-INS and 'B' TG-chitosan-APR-INS xerogels using data from EpiOral™ and sheep buccal tissue permeation experiments.

6.3 Conclusions

This study has investigated the permeation of BSA and INS released from chitosan based xerogels using a commercially available model human equivalent buccal tissue (EpiOral™) and sheep buccal membrane. Permeation parameters obtained for the BSA containing xerogels showed significant improvement of 12- to 14-fold increase in permeation enhancement compared to control. TG-chitosan xerogels demonstrated slightly higher apparent permeability coefficient and enhancement factor over unmodified chitosan. However, the addition of GSH as an EI to the TG-chitosan xerogel led to reduced permeation parameters due to possible adsorption of BSA by GSH. The presence of GSH in INS

containing xerogels further confirmed the effect of the EI on drug permeation through EpiOral™ by causing a reduction in the flux, apparent permeability coefficient and enhancement factor of TG-chitosan-GSH-INS xerogel compared to those of TG-chitosan-INS and TG-chitosan-APR-INS. This study has established that GSH containing xerogels actually caused inhibition rather than enhancement of INS permeation. Cells in the tissue engineered buccal membrane were however found viable by MTT reduction assay after 4 hrs in contact with all the test and control samples.

INS permeation via the sheep buccal membrane was significantly improved by employing APR as an EI in the TG-chitosan xerogel. Thiolated chitosan showed no increase in INS permeation relative to control INS permeation due possibly to the reduced mucosal fluid as a result of the initial wash-off or absence of mucin on the epithelial surface of the sheep buccal membrane for covalent attachment. Good linear correlations were obtained for the permeation curves of INS in both the EpiOral™ and sheep buccal membrane experiments with the APR containing xerogels showing higher correlation coefficient.

The need for the presence of an EI in formulations intended for buccal delivery of therapeutic proteins has been underscored by this study. The foregoing discussion suggests the possibility of predicting experimental *in vivo* trends for INS permeation through sheep buccal membrane with EI containing chitosan based xerogels since a good linear correlation between *in vitro* and *ex vivo* experiments has been achieved.

CHAPTER SEVEN

SUMMARY CONCLUSIONS AND FUTURE WORK

7.1 Summary conclusions

The aim of this project was to develop, formulate, characterise and optimise novel lyophilised formulations (xerogels) that will deliver therapeutically relevant protein-based drugs via the buccal mucosa route. In this section, a summary of the conclusions on the formulation design, optimisation, analytical characterisation and determination of physico-chemical properties including hydration, mucoadhesion, release profile and kinetics and permeation characteristics of lyophilised chitosan and thiolated chitosan xerogels as potential protein drug delivery systems to the buccal mucosa membrane is presented.

Mucoadhesive lyophilised systems from chitosan and TG-chitosan were developed as potential protein drug delivery systems via the buccal mucosa, by lyophilising aqueous gels of the polymers. Annealing, plasticisation and cryoprotection procedures were critical in obtaining porous and flexible dialysed xerogels. DSC was used to determine an appropriate lyophilisation cycle by evaluating thermal events before lyophilisation to select a suitable annealing temperature. The annealing step in the lyophilisation cycle helped to obtain the desired porous structure for the final optimised formulations. The non drug-loaded xerogel formulation containing 10 % (per polymer weight) each of plasticizer (GLY) and cryoprotectant (D-MANN) was deemed optimum for drug loading and further development. Improved flexibility was obtained by incorporating GLY while the presence of D-MANN in the xerogels was critical in preventing protein instability due to perturbation by freezing. The removal of NaAc formed as a result of neutralisation of excess acetic by sodium hydroxide in the preliminary formulation development stage by membrane dialysis, was essential for obtaining optimised xerogels with excellent characteristics for application to the buccal mucosa surface. Stable TG-chitosan xerogels were also developed by covalently attaching thioglycolic acid to chitosan via amidation using water soluble carbodiimide (EDAC) as coupling agent. The optimised xerogels were drug loaded with 50 % and 20 % (per polymer weight) of BSA and INS respectively. The final lyophilised xerogel was backed with an impervious EC laminate which is expected to ensure uni-directional drug release at the mucosal surface. In addition, enzyme inhibitors (reduced GSH and APR) and permeation enhancer (Brij 35) were incorporated in the xerogels to offer improved permeability of the buccal mucosa.

Analytical characterisation of the chitosan based xerogels was carried out using various analytical techniques. Structural information on chitosan and TG-chitosan were confirmed from ^{1}HNMR and ATR-FT-IR spectra. UV spectroscopy using Ellman's reaction was employed to quantify the amount of thiol groups immobilised covalently on chitosan to obtain TG-chitosan. The difference in polymer molecular weight between chitosan and TG-chitosan was monitored by GPC, which confirmed the covalent attachment. ATR-FT-IR and CD spectroscopic analyses of the secondary structures of the loaded model protein drugs BSA and INS indicated the conformational stability of the proteins. With respect to protein physical stability, no multiple glass-transition temperatures were detected by DSC after lyophilisation for all formulations except for the undialysed chitosan xerogel. The XRPD analysis of the formulated xerogels indicated amorphous structures, however the presence of NaAc crystals identified by ATR-FT-IR spectra and XRPD diffractogram and confirmed with SEM microscopy resulted in thick walled xerogels for the undialysed chitosan samples. Furthermore, the SEM micrographs displayed highly porous xerogels due to annealing which allowed for high drug loading capacities of the dialysed and annealed xerogels which also exhibited optimal moisture content for maintaining protein stability. Storage of xerogels at 25 °C/ 60 % RH for six months resulted in protein chemical instability while storage at 5 °C maintained protein stability up to six month as per HPLC determination.

Annealed chitosan xerogel showed significantly higher hydration capacity compared to non-annealed xerogel. Membrane dialysis did not have any significant effect on the hydration capacity however the presence of process impurity NaAc resulted in xerogels with poor structural stability. Annealed TG-chitosan xerogel similarly showed higher hydration capacity compared to non-annealed TG-chitosan xerogel however, disulphide bond formation in the thiolated xerogel limited the hydration capacity. DTT was used to confirm that the hydration capacity is driven by the cross-linked disulphide bond formation. The hydration capacity of the xerogels had a direct impact on xerogel mucoadhesion properties. The annealed chitosan xerogels showed better mucoadhesion properties compared to non-annealed chitosan xerogels. However, undialysed chitosan xerogel demonstrated reduced mucoadhesion characteristics due to the presence of NaAc. Improved mucoadhesion properties were obtained for the annealed thiolated xerogels compared to non-annealed thiolated and unmodified chitosan xerogels. The results also indicated that the effect of EI on mucoadhesion was concentration dependent as well as inhibitor specific.

Formulation processes such as membrane dialysis, annealing and thiolation had significantly varying effects on the *in vitro* drug release profiles from the chitosan based lyophilised xerogels using 0.01 M PBS as dissolution medium. An initial burst release of BSA

was observed for dialysed and annealed chitosan-BSA xerogels followed by a controlled release phase due to chitosan-BSA complexation. Enhanced porosity led to ease of hydration and consequent improved drug release in annealed xerogels. A three-fold reduction in BSA release was however obtained for the undialysed chitosan-BSA xerogel. Thiolation effect on drug release was not significant as unmodified chitosan-BSA and TG-chitosan-BSA xerogels showed no difference in drug release profiles. A significant reduction in protein release was caused by the presence of EIs in both the BSA and INS containing xerogels to different extents. The release kinetics described by model dependent mathematical functions indicated a complex nature of drug release based on drug concentration, dissolution and polymer characteristics since the dissolution data from all xerogels best fitted First order, Hixson-Crowell and Korsmeyer-Peppas equations. The release exponents also displayed non-Fickian diffusion and super case-II transport release mechanisms for all the formulations. The presence of EI did not alter the release mechanism in the TG-chitosan xerogel loaded with either BSA or INS. Similarities in BSA release profiles were found between annealed xerogels based on analysis from model independent difference (f_1) and similarity (f_2) factors. The release profiles of TG-chitosan-BSA and TG-chitosan-GSH-BSA 10 % were also similar. The different EIs in the INS loaded xerogels did not show any difference in the release profile of INS from all formulations.

The permeation parameters obtained using a commercially available model human equivalent buccal tissue (EpiOral^{TM}) for BSA containing xerogels showed significant improvement of 12- to 14-fold increase in permeation enhancement compared to control. Slightly higher apparent permeability coefficient and enhancement factor were demonstrated by TG-chitosan xerogels over unmodified chitosan. However, the addition of GSH as an EI to the TG-chitosan xerogels led to reduced permeation parameters. Similarly, GSH in INS xerogels caused a reduction in the permeation parameters of TG-chitosan-GSH-INS xerogel compared to those of TG-chitosan-INS and TG-chitosan-APR-INS. This study has established that GSH containing xerogels actually caused inhibition rather than enhancement of INS permeation. On the other hand, APR in the TG-chitosan xerogel significantly improved INS permeation via sheep buccal membrane while showing a better linear correlation with permeation curve of INS from the EpiOral^{TM} experiment compared to TG-chitosan xerogel without APR.

7.2 Key research findings

- Novel chitosan based lyophilised xerogels with excellent mucoadhesion, penetration enhancing, enzyme inhibitor and drug release properties have been developed. Membrane dialysis was determined to be essential for obtaining xerogels with excellent physical characteristics.
- The research has established that it is essential that the development of chitosan based delivery systems for controlled release of therapeutic proteins takes into consideration the stability of the protein drug upon storage. In addition, to improving stability of proteins within chitosan based systems, formulations must be protected from potentially extreme hydrolysing conditions to ensure maintenance of protein native structure.
- The hydration capacity of the developed thiolated xerogels is controlled by the presence of disulphide linkages. Thiolation was confirmed to be responsible for enhanced mucoadhesion characteristics however the type and concentration of EI employed significantly affects the mucoadhesion properties. These *in vitro* characterisations can help to predict the *in vivo* performance of the various formulations which would be expected to impact on the drug release rate and duration, based on the varied physical properties of the xerogels.
- The need for the presence of an EI in formulations intended for buccal delivery of therapeutic proteins has been underscored by this study. The foregoing results indicate the possibility of predicting experimental *in vivo* trends for INS permeation through sheep buccal membrane with EI containing chitosan based xerogels since a good linear correlation between *in vitro* and *ex vivo* experiments has been achieved.
- The foremost implication of these findings is the potential application of the novel lyophilised system for the delivery of proteins via the buccal mucosa

7.3 Future work

1. Mucoadhesion properties of the xerogels could be studied by using animal buccal tissue model and the results compared with that obtained in this project. However, recent research using hydrogels as substitutes for animal studies is gaining attention (Khutoryanskiy, 2011). An investigation of the mucoadhesive characteristics of the chitosan based xerogels using hydrogel substitutes will be a useful evaluation tool.

2. The long-term stability evaluation for xerogels stored at 5 ± 3 °C would require continuity to obtain data to fully establish the stability of xerogels stored at that temperature.
3. Analytical evaluation of protein conformational stability using CD, DSC and FT-IR techniques to determine the extent of secondary structural changes after storage of the xerogels at ICH conditions of 25 °C/60 % RH is suggested. Possible studies to determine the mechanism of degradation will be an interesting research. The molecular weight of the chemically degraded proteins could be determined by the use of sodium dodecyl sulphate polyacrylamide gel electrophoresis (SDS-PAGE) and mass spectrometry.
4. Final product packaging material needs to be investigated and the stability re-evaluated based on the ICH conditions.
5. Characterisation of the chitosan based xerogels after loading with other model biotechnologically produced protein drugs to compare with INS.

CHAPTER EIGHT

REFERENCES

1. Agnihotri, S.A., Mallikarjuna, N.N., Aminabhavi, T.M. 2004. Recent advances on chitosan-based micro- and nano-particles in drug delivery. *Journal of Controlled Release.* 100, 5–28.

2. Aiedeh, K., Taha, M.O. 1999. Synthesis of chitosan succinate and chitosan phthalate and their evaluation as suggested matrices in orally administered, colon-specific drug delivery systems. *Arch Pharm* (Weinheim). 332, 103-107.
3. Albrecht, K., Greindl, M., Kremser, C., Wolf, C., Debbage, P., Bernkop-Schnürch, A. 2006. Comparative in vivo mucoadhesion studies of thiomer formulations using magnetic resonance imaging and fluorescence detection. *Journal of Controlled Release*. 115, 78-84.
4. Andrew, G.P., Laverty, T. P., Jones, D. S. 2009. Mucoadhesive polymeric platforms for controlled drug delivery. *European Journal of Pharmaceutics and Biopharmaceutics.* 71, 505-518.

5. Agu, R.U., Ugwoke, M.I., Armand, M., Kinget, R., Verbeke, N. 2001. The lung as a route for systemic delivery of therapeutic proteins and peptides, *Respiratory Research*. 2, 198–209.

6. Antosova, Z., Mackova, M., Kral, V., Macek, T. 2009. Therapeutic application of peptides and proteins: parenteral forever? *Trends in Biotechnology*. 27, 628-635.

7. Artursson, P., Lindmark, T., Davis, S., Illum, L. 1994. Effect of chitosan on the permeability of monolayers of intestinal epithelial cells (Caco-2). *Pharmaceutical Research.* 11, 1358–1361.
8. Attia, M.A., El-Gibaly, I., Shaltout, S.E., Fetih, G.N. 2004. Transbuccal permeation, anti-inflammatory activity and clinical efficacy of piroxicam formulated in different gels. *International Journal of Pharmaceutics.* 276, 11–28.

9. Aungst, B. J., Rogers, N. J. 1988. Site dependence of absorption promoting actions of laureth-9, Na salicylate, Na_2EDTA, and aprotinin on rectal, nasal, and buccal insulin delivery. *Pharmaceutical Research*. 5, 305-308.

10. Ayensu, I., Mitchell, J.C., Boateng, J.S. 2011. Development and physico-mechanical characterisation of lyophilised chitosan wafers as potential protein

drug delivery systems via the buccal mucosa. *Colloids and Surfaces B: Biointerfaces*. 91, 258– 265.

11. Ayensu, I., Mitchell, J.C., Boateng, J.S. 2012a. In vitro characterisation of chitosan based xerogels for potential buccal delivery of proteins. *Carbohydrate Polymers*. 89, 935– 941.
12. Ayensu, I., Mitchell, J.C., Boateng, J.S. 2012b. Effect of membrane dialysis on characteristics of lyophilised chitosan wafers for potential buccal delivery of proteins. *International Journal of Biological Macromolecules*. 50, 905– 909.
13. Ayensu, I., Boateng, J.S. 2012. Development and evaluation of lyophilized thiolated-chitosan wafers for buccal delivery of protein. *Journal of Science and Technology*. 32 (2), 11-17.
14. Bai, J. P., Chang, L. L., Guo, J. H. 1996. Effects of polyacrylic polymers on the degradation of insulin and peptide drugs by chymotrypsin and trypsin. *Journal of Pharmaceutics and Pharmacology*. 48, 17-21.
15. Barrett, W.C., Gnore, J.P.D., Konig, S., Fales, H.M., Keng, Y.F., Zhang, Z.Y., 1999. Regulation of PTP1B via glutathionylation of the active site cysteine 215. *Biochemistry*. 38, 6699–6705.
16. Batchelor, H. 2004. Novel bioadhesive formulations in drug delivery, The Drug Delivery Companies Report Autumn/Winter, Pharma Ventures Ltd.
17. Baudry, B., Fasano, A., Ketley, J. And Kaper, J. B. 1992. Cloning of a gene (zot) encoding a new toxin produced by *Vibrio cholerae*. *Infection and Immunology*. 60, 428-434.
18. Benguigui, L. 1999. Fracture of polymer gels. *Physica A*. 270, 1-7.
19. Bernkop-Schnürch, A. 1998. The use of inhibitory agents to overcome the enzymatic barrier to perorally administered therapeutic peptides and proteins. *Journal of Controlled Release*. 52, 1-16.
20. Bernkop-Schnürch, A. 2005. Thiomers; a new generation of mucoadhesive polymers. *Advanced drug delivery reviews*. 57, 1569-1582.
21. Bernkop-Schnürch, A., Brandt, U.M., Clausen A.E. 1999. Synthesis and *in vitro* evaluation of chitosan-cysteine conjugates. *Scientia Pharmaceutica*. 67, 196–208.
22. Bernkop- Schnürch, A., Dünnhaupt, S. 2012. Chitosan-based delivery systems. *European Journal of Pharmaceutics and Biopharmaceutics*. http://dx.doi.org/10.1016/j.ejpb.2012.04.007.

23. Bernkop-Schnürch, A., Guggi, D., Pinter Y. 2003. Thiolated chitosans: development and in vitro evaluation of a mucoadhesive, permeation enhancing oral drug delivery system. *Journal of Controlled Release*. 94, 177– 186.

24. Bernkop-Schnürch, A., Hornof, M., Zoidl, T. 2003. Thiolated polymers – thiomers: modification of chitosan with 2- iminothiolane. *International Journal of Pharmaceutics*. 260, 229–237.

25. Bernkop-Schnürch, A., Walker, G. 2001. Multifunctional matrices for oral peptide delivery. *Critical Reviews in Therapeutic Drug Carrier Systems.* 18, 459– 501.

26. Blundell T., Dodson G., Hodgkin D., Mercola D. Insulin: The Structure in the Crystal and its Reflection in Chemistry and Biology. 1972. *Advances in Protein Chemistry*. 26, 279-402.

27. Boateng, J.S. 2005. Development of formulations for delivery of drugs to wounds, *PhD Thesis*, Department of Pharmaceutical Sciences, Strathclyde Institute of Pharmaceutical and Biomedical Sciences, University of Strathclyde in Glasgow.

28. Boateng, J.S., Auffret, A.D., Matthews, K.H., Humphrey, M.J., Stevens, H.N.E., Eccleston, G.M. 2010. Characterisation of lyophilised wafers and solvent evaporated films as potential drug delivery systems to mucosal surfaces. *International Journal of Pharmaceutics*. 389, 24–31.

29. Boateng, J.S., Stevens, H.N., Eccleston, G.M., Auffret, A.D., Humphrey, M.J., Matthews, K.H. 2009. Development and mechanical characterization of solvent-cast polymeric films as potential drug delivery systems to mucosal surfaces. *Drug Development and Industrial Pharmacy*. 35, 986–996.

30. Boeris, V., Farruggia, B., Picó, G. 2010. Chitosan-bovine serum albumin complex formation: A model to design an enzyme isolation method by polyelectrolyte precipitation. *Journal of Chromatography. B*. 878, 1543-1548.

31. Borchard, G., Luessen, H.L., Boer A.G.D., Verhoef, J.C., Lehr, C.M., Junginger, H.E. 1996. The potential of mucoadhesive polymers in enhancing intestinal peptide drug absorption. III: Effects of chitosan glutamate and carbomer on epithelial tight junctions in vitro. *Journal of Controlled Release*. 39, 131–138.

32. British Pharmacopoeia. 2012. The Stationery office, London.

33. Bunte, H., Drooge, D.J., Ottjes, G., Roukema, R., Verrijk, R., Yessine, M. 2010. Key considerations when developing freeze-dried formulation and current trends. *Pharmaceutical Technology Europe Digital*. 22, 2-4.
34. Carvalho, F.C., Bruschi, M.L., Evangelista R.C., Gremião, M.P.D. 2010. Mucoadhesive drug delivery systems. *Brazilian Journal of Pharmaceutical Sciences.* 46, 1-17.
35. Cázares-Delgadillo, J., Ganem-Rondero, A., Kalia, Y.N. 2011. Human growth hormone: New delivery systems, alternative routes of administration, and their pharmacological relevance. *European Journal of Pharmaceutics and Biopharmaceutics*. 78, 278–288.
36. Censi, R., Martino, P.D., Vermonden, T., Hennink, W.E. 2012. Hydrogels for protein delivery in tissue engineering. *Journal of Controlled Release*. 161, 680-692.
37. Chavda, H., Patel, C. 2010. Chitosan superporous hydrogel composite-based floating drug delivery system: a newer formulation approach. *Journal of Pharmacy and Bioallied Science*. 2, 123-134.
38. Chen, T., Oakley, D.M. 1995. Thermal analysis of proteins of pharmaceutical interest. *Thermochimica Acta*. 248, 229–244.
39. Chi, E.Y., Krishnan, S., Randolph, T.W., Carpenter, J.F. 2003. Physical stability of proteins in aqueous solution: mechanism and driving forces in non-native protein aggregation. *Pharmaceutical Research.* 20, 1325 – 1336.
40. Chiou, G.C. 1994. Systemic delivery of polypeptide drugs through ocular route, *Journal of Ocular Pharmacology*. 10, 93–99.
41. Çilek, A., Çelebi, N., Tirmaksiz, F., Tay, A. 2005. A lecithin-based microemulsion of rh-insulin with aprotinin for oral administration: investigation of hypoglycaemic effects in non-diabetic and STZ-induced diabetic rats. *International Journal of Pharmaceutics*. 298 (1), 176-185.
42. Clausen, A.E., Kast, C.E., Andreas, B.S. 2002. The role of glutathione in the permeation enhancing effect of thiolated polymers. *Pharmaceutical Research*. 19, 602–608.
43. Cornelius, V., Mitchell, J., Snowden, M. 2005. Polymeric films, a novel oral dosage form? *Industrial Pharmacy.* **7**, 6-8.

44. Cowie, J.M.G., Arrighi, V. 2008. *Polymers: chemistry and Physics of modern Materials*. 3rd Ed. CRC Press.
45. Cromwell, M.E.M., Hilario, E., Jacobson, F. 2006. Protein Aggregation and Bioprocessing. *The AAPS Journal*. 8 (66) (http://www.aapsj.org).
46. Crowe, L.M., Reid, D.S., Crowe, J.H. 1998. The role of vitrification in anhydrobiosis. *Annual Review of Physiology*. 60, 73-103.
47. Cui, F., He, C., He, M., Cui, T., Yin, L., Qian, F., Yin, C. 2008. Preparation and evaluation of ethylenediaminetetraacetic acid hydrogel films for the mucoadhesive transbuccal delivery of insulin. *Journal of Biomedical Materials Research part A*. DOI: 10.1002/jbm.a.32071. 1064-1071.
48. Dash, S., Murthy, P, N., Nath, L., Chowdhury, P. 2010. Kinetic modelling on drug release from controlled drug delivery systems. *Acta Poloniae Pharmaceutica – Drug Research.* 67 (3) 217 – 223.
49. Dashnau, J. L., Nucci, N.V., Sharp, K. A., Vanderkooi, J. M. 2006. Hydrogen Bonding and the Cryoprotective Properties of Glycerol/Water Mixtures. *Journal of Physical Chemistry* B. 110, 13670–13677.
50. De Campos, A.M., Diebold, Y., Carvalho, E.L., Sanchez, A., Alonso, M.J. 2004. Chitosan nanoparticles as new ocular drug delivery systems: in vitro stability, in vivo fate, and cellular toxicity. *Pharmaceutical Research*. 21, 803–810.
51. Deurloo, M.J., Hermens, W.A., Romeyn, S.G., Verhoef, J.C., Merkus, F.W. 1989. Absorption enhancement of intranasally administered insulin by sodium taurodihydrofusidate (STDHF) in rabbits and rats. *Pharmaceutical Research*. 6, 853-856.
52. Dixit, R.P., Puthli, S.P. 2009. Oral strip technology: Overview and future potential. *Journal of Controlled Release*. 139, 94-107.
53. Dodane, V., Amin, K. M., Merwin, J.R. 1999. Effect of chitosan on epithelial permeability and structure. *International Journal of Pharmaceutics*. 182, 21–32.
54. Dong, A., Prestrelski, S.J., Allison, S.D.S.D., Carpenter, J.F. 1995. Infrared spectroscopic studies of lyophilisation- and temperature-induced protein aggregation. *Journal of Pharmaceutical Sciences*. 84, 415–424.
55. Duchene, D., Touchard, F., Peppas, N.A. 1998. Pharmaceutical And Medical aspects of Bioadhesive system for drug administration. *Drug Development and Industrial Pharmacy*. 14, 283-381.

56. Engles, L. 2005. Review and application of serine protease inhibition in coronary artery bypass graft surgery. *American Journal of Health-System Pharmacy*. 62 (18), S9-14.

57. Eouani, C., Piccerelle, P., Prinderre, P Bourret, E., Joachim, J. 2001. In-vitro cpmparative study of buccal mucoadhesive performance of different polymeric films. *European Journal of Pharmaceutics and Biopharmaceutics*. 52, 45-55.

58. Ernst, O., Zor, T. 2010 Linearization of the Bradford Protein Assay. *Journal of Visualized Experiments*. DOI: 10.3791/1918. 1-6.

59. Estey, T., Kang, J., Schwendeman, S.P., Carpenter, J.F. 2006. BSA Degradation under Acidic Conditions: A Model for Protein Instability during Release from PLGA Delivery Systems. *Journal of pharmaceutical sciences*. 95 (7), 1626-1639.

60. Eyrich, V.A., Standley, D.M., Felts, A.K., Friesner, R.A. 1999. Protein tertiary structure prediction using a branch and bound algorithm. *Proteins: Structure, Function, and Genetics*. 35, 41–57.

61. Fasano, A., Uzzau, S. 1997. Modulation of intestinal tight junctions by Zonula occludens toxin permits enteral administration of insulin and other macromolecules in an animal model. *Journal of Clinical Investigations*. 99, 1158-1164.

62. Fefelova, N.A., Nurkeeva, Z.S., Muna, G.A., Khutoryanskiy, V.V. 2007. Mucoadhesive interactions of amphiphilic cationic copolymers based on [2-(methacryloyloxy)ethyl]trimethylammonium chloride. *International Journal of Pharmaceutics.* 339, 25–32.

63. Fernandez-Megia, E., Novoa-Carballal, R., Quinoa, E., Riguera, R. 2005. Optimal routine conditions for the determination of the degree of acetylation of chitosan by ^{1}HNMR. *Carbohydrate Polymer*. 61, 155-161.

64. Fetih, G., Ibrahim, M.A., Amin M.A. 2011. Design and Characterization of Transdermal films containing Ketorolac trimethamine. *International Journal of PharmTech Research.* 3 (1), 449-458.

65. Figueiras, A., Hombach, J., Veiga, F., Bernkop-Schnürch, A. 2009. In vitro evaluation of natural and methylated cyclodextrins as buccal permeation enhancing system for omeprazole delivery. *European Journal of Pharmaceutics and Biopharmaceutics*. 71, 339–345.

66. Ford, J.L., Mann, T.E. 2012, Fast-Scan DSC and its role in pharmaceutical physical form characterisation and selection. *Advanced Drug Delivery Reviews*. 64, 422-430.
67. Fox, K.C. 1995. Putting proteins under glass. *Science*.267, 1922-1923.
68. Franks, F. 1990. Freeze-drying: From empiricism to predictability. *Cryo-Letters*. 11, 93-110.
69. Franks, F. 1994. Long-term stabilization of biologicals. *Biotechnology*. 12, 253-256.
70. Freier, T., Koh, H.S., Kazazian, K., Shoichet, M.S. 2005. Controlling cell adhesion and degradation of chitosan films by *N*-acetylation. *Biomaterials*. 26, 5872–5878.
71. Friend, D.R. 2005. New Oral Delivery Systems for Treatment of Inflammatory Bowel Disease. *Advanced Drug Delivery Reviews*. 57, 247-255.
72. Gale, E.A.M. 2001. Two cheers for inhaled insulin. *Lancet*. 375, 324–325.
73. Gandhi, R.B., Robinson J.R. 1988. Bioadhesion in drug delivery. *Indian Journal of Pharmaceutical Sciences.* 50, 145–152.
74. Gelamo, E.L., Silva, C.H.T.P., Imasato, H., Tabak, M. 2002. Interaction of bovine (BSA) and human (HSA) serum albumins with ionic surfactants: spectroscopy and modelling. *Biochimica et Biophysica Acta*. 1594 84-99.
75. Gieseler, H. 2004. Product Morphology and drying behaviour delineated by a new Freeze-Drying Microbalance. *PhD Thesis*, University of Erlangen-nuemberg, Elangen, Germany.
76. Giovino, C., Ayensu, I., John Tetteh, J., Joshua S. Boateng, J.S. 2012. Development and characterisation of chitosan films impregnated with insulin loaded PEG-β-PLA nanoparticles (NPs): A potential approach for buccal delivery of macromolecules. *International Journal of Pharmaceutics*. 428, 143– 151.
77. Giunchedi, P., Juliano, C., Gavini, E., Cossu, M., Sorrenti, M. 2002. Formulation and in vivo evaluation of chlorhexidine buccal tablets prepared using drug-loaded chitosan microspheres. *European Journal Pharmaceutics and Biopharmaceuticals*. 53, 233–239.
78. Gorbach, V.I., Krasikova, I.N., Lukyanov, P.A., Loenko, Y.N., Soloveva, T.F., Ovood, Y.S., Deev, V.V., Pimenov, A.A. 1994. New glycolipids

(chitooligosaccharide derivatives) possessing immunostimulating and antitumor activities. *Carbohydrate Research*. 260, 73–82.

79. Grabovac, V., Foger, F., Bernkop-Schnürch, A. 2008. Design and *in vivo* evaluation of a patch delivery system for insulin based on thiolated polymers. *International Journal of Pharmaceutics.* 348. 169-174.
80. Grabovac, V., Guggi, D., Bernkop-Schnürch, A. 2005. Comparison of the mucoadhesive properties of various polymers. *Advanced Drug Delivery Reviews*. 57, 1713– 1723.
81. Grafstrom, R., Stead, A.H., Orrenius, S. 1980. Metabolism of extracellular glutathione in rat small-intestinal mucosa. *European Journal of Biochemistry*. 106, 571–577.
82. Greenfield, N.J. 1999. Application of circular dichroism in protein and peptide analysis. *Trends in analytical chemistry*. 18 (4), 236-244.
83. Gu, J. M., Robinson, J.R., Leung. S. 1998. Binding of acrylic polymers to mucin/epithelial surfaces; Structure-property-relationship. *Critical Reviews in Therapeutic Drug Carrier Systems*. 5, 21-67.
84. Guevara-Aguirre, J., Guevara, M., Saavedra, J., Mihic, M., Modi, P. 2004. Oral spray insulin in treatment of type 2 diabetes: a comparison of efficacy of the oral spray insulin (Oralin) with subcutaneous (SC) insulin injection, a proof of concept study. *Diabetes Metabolism Research and Reviews*. 20, 472-478.
85. Hamman, J.H., Schultz, C.M., Kotze, A.F., 2003. N-trimethyl chitosan chloride: optimum degree of quaternization for drug absorption enhancement across epithelial cells. *Drug Development and Industrial Pharmacy*. 29, 161-172.
86. Harris, D., Robinson, J.R. 1992. Drug delivery via the mucous membranes of the oral cavity. *Journal of Pharmaceutical Science*. 81, 1–10.
87. Hearnden, V., Sankar, V., Hull, K., Juras, D.V., Greenberg, M., Kerr, A.R., Lockhart, P.B., Patton, L.L., Porter, S., Thornhill, M.H. 2012. New developments and opportunities in oral mucosal drug delivery for local and systemic disease. *Advanced Drug Delivery Reviews.* 64, 16-28.
88. Henry, R.R., Mudaliar, S.R.D., Howland, W.C., Chu, N., Kim, D., An, B., Reinhardt, R.R. 2003. Inhaled insulin using the AREx insulin diabetes management system in healthy and asthmatic subjects. *Diabetes Care*. 26, 764–769.

89. Himmelmann, A., Jendle, J., Mellén, A., Petersen, A.H., Dahl, U.L., Wollmer, P. 2003.The impact of smoking on inhaled insulin. *Diabetes Care*. 26, 677–682.

90. Hommel, R., Kleber, H.P. 1990. Selective and rapid solubilisation of the microbial membrane enzyme aldehyde dehydrogenase. *Journal of Basic Microbiology*. 30 (4), 297-300.

91. Hoogstraate, A.J., Senel, S., Cullander, C., Verhoef, J., Junginger, H.E., Bodde, H.E. 1996. Effects of bile salts on transport rates and routes of FTIC-labelled compounds across porcine buccal epithelium in vitro. *Journal of Controlled Release.* 40, 211–221.

92. Hornof, M.D., Kast, C.E., Andreas, B.S. 2003. In vitro evaluation of the viscoelastic behaviour of chitosan – thioglycolic acid conjugates. *European Journal of Pharmaceutics and Biopharmaceuticals*. 55, 185–190.

93. Hua, Q., Jia, W., Weiss, M. A. 2011. Conformational dynamics of insulin. *Frontiers in Endocrinology*. 2 (48), 1-11.

94. Hubbell, J.A. 1995. Biomaterials in tissue engineering. *Biotechnology*, 13, 565-576.

95. ICH Guidance for Industry Q1A (R2): Stability testing of new Drug Substances and Products. FDA/CDER/CBER. November 2003.

96. Illum, L., Farraj, N.F., Davis, S.S. 1994. Chitosan as a novel nasal delivery system for peptide drugs. *Pharmaceutical Research*. 11, 1186–1189.

97. Illum, L., Jabbal-Gill, I., Hinchcliffe, M., Fisher, A.N., Davis, S.S. 2001. Chitosan as a novel nasal delivery system for vaccines. *Advanced Drug Delivery and Reviews*. 51, 81–96.

98. Jain, R., Pandey, A., and Pandeya, S.S. 2009. Mechanism of dissolution of delayed release formulation of diclofenac sodium. *Chemistry,* 18 (4), 131-138.

99. Janes, K.A., Calvo, P., Alonso, M.J. 2001. Polysaccharide colloidal particles as delivery systems for macromolecules. *Advanced Drug Delivery and Reviews*. 47, 83–97.

100. Jankowska, E., Stefanowicz, P., Sosnowska, M., Karpowicz, P., Radziszewska, K., Szewczuk, Z., Szymanska, A. 2012. Pressure as a denaturing agent in studies

of single-point mutants of an amyloidogenic protein human cystatin C. *Proteins: Structure, Function, and Bioinformatics*.80 (8), 1-9.

101. Jiang, G., Akers, M., Jain, M., Guo, J., Distler, A., Swift, R., Wadhwa, M., Jameel, F., Patro, S., Freud, E. 2007. Mechanistic studies of Glass Vial Breakage for Frozen Formulations. I. Vial breakage caused by crystallizable excipient mannitol. PDA. *Journal of Pharmaceutical Sciences and Technology*. 61 (6).

102. Jiang, S., Nail, S.L. 1998. Effect of process conditions on recovery of protein activity after freezing and freeze-drying. *European Journal of Pharmaceutics and Biopharmaceuticals*. 45, 249-257.

103. Jones, D.S., Lawlor, M.S., Woolfson, A.D. 2003. Rheological and mucoadhesive characterization of polymeric systems composed of poly (methylvinylether-co-maleic anhydride) and poly (vinylpyrrolidone), designed as platforms for topical drug delivery. *Journal of Pharmaceutical Science*. 92, 995-1007.

104. Juntapram, K., Praphairaksit, N., Siraleartmukul, K., Muangsin, N. 2012. Synthesis and characterisation of chitosan-homocysteine thiolactone as a mucoadhesive polymer. *Carbohydrate polymer*. 87, 2399-2408.

105. Kakihana, M., Kotaka, M., Okamoto, M. 1982. Infrared spectra of ^{13}C-substituted species of solid Sodium acetate at 80 K. *Journal of Physical Chemistry*. 86, 4385-4387.

106. Kan, K. S., Coleman, R. 1988. The calcium ionophore A23187 increases the tight-junctional permeability in rat liver. *Biochemistry Journal*. 256, 1039-1041.

107. Kang, G. D., & Song, S. 2008. Effect of chitosan on the release of protein from thermosensitive poly(organophosphazene) hydrogels. *International Journal of Pharmaceutics*. 349, 188–195.

108. Karbowiak, T., Hervet, H., Léger, L., Champion, D., Debeaufort, F., Voilley, A. 2006. Effect of plasticizers (water and glycerol) on the diffusion of a small molecule in iota-carrageenan biopolymer films for edible coating application. *Biomacromolecules.* 7, 2011-2019.

109. Kasper, J. C., Freiss, W. 2011. The freezing step in lyophilisation: Physico-chemical fundamentals, freezing methods and consequences on process

performance and quality attributes of biopharmaceutical. *European Journal of Pharmaceutics and Biopharmaceutics.* 78, 248–263.

110. Kast, C.E., Bernkop-Schnürch, A. 2001. Thiolated polymers –thiomers: development and in vitro evaluation of chitosan-thioglycolic acid conjugates. *Biomaterials.* 22, 2345–2352.

111. Kast, C.E., Valenta, C., Leopold, M., Bernkop-Schnürch, A. 2002. Design and in vitro evaluation of a novel bioadhesive vaginal drug delivery system for clotrimazole. *Journal of Controlled Release*. 81, 347–354.

112. Kelly, S.M., Jess, T.J., Price, N.C. 2005. How to study proteins by circular dichroism. *Biochimica et Biophysica Acta*. 1751, 119-139.

113. Khafagy, E., Morishita, M., Onuki, Y., Takayama, K. 2007. Current challenges in non-invasive insulin delivery systems: A comparative review. *Advanced Drug Delivery Reviews*. 59, 1521–1546.

114. Khan, T., Peh, K., Chang, H. 2000. Mechanical, bioadhesive strength and biological evaluations of chitosan films for wound dressing. *Journal of Pharmaceutical Sciences*. 3, 303–311.

115. Khrapunov, S. 2009. Circular dichroism has intrinsic limitations for protein secondary structure analysis. *Analytical Biochemistry*. 389, 174-176.

116. Khor, E., Lim, L.Y. 2003. Implantable applications of chitin and chitosan. *Biomaterials.* 24, 2339–2349.

117. Khutoryanskiy, V.V. 2007. Hydrogen-bonded interpolymer complexes as materials for pharmaceutical applications. *International Journal of Pharmaceutics*. 334, 15–26.

118. Khutoryanskiy, V.V. 2011. Advances in mucoadhesion and mucoadhesive polymers. *Macromolecular Bioscience*. 11, 748–764.

119. Kim, A. I., Akers, M. J., Nail, S. L. 1998. The physical state of mannitol after freeze-drying: effects of mannitol concentration, freezing rate, and a noncrystallizing cosolute. *Journal of Pharmaceutical Sciences.* 931-935.

120. Kissel, T., Werner, U. 1998. Nasal delivery of peptides, an in vitro cell culture model for the investigation of transport and metabolism in human nasal epithelium, *Journal of Controlled Release*. 53, 195–203.

121. Koschier, F., Kostrubsky, V., Toole, C., Gallo, M. A., 2011 In vitro effects of ethanol and mouth rinse on permeability in an oral buccal mucosal tissue construct. Food and Chemical Toxicology. doi:10.1016/j.fct.2011.06.018.

122. Kotze, A.F., Luessen, H.L., Thanou, M., Verhoef, J.C., De Boer, A.G., Juninger, H.E., Lehr, C.M. 1999. Chitosan and chitosan derivatives as absorption enhancers for peptide drugs across mucosal epithelia. In: Matiowitz, E., Chickering, D.E., Lehr, C.M. Eds. *Bioadhesive Drug Delivery Systems.* New York, NY: Marcel Dekker.

123. Kruger, N. 2008. The Bradford method for protein quantification In: Walker J.M., Ed. *The Protein Protocols Handbook*. Humana press Inc. Totowa, NJ.

124. Kulkarni, U., Mahalingam, R., Pather, I., Li, X., Jasti, B. 2010. Porcine buccal mucosa as *in vitro* model: effect of biological and experimental variables, *Journal of Pharmaceutical Sciences*. 99, 1265–1277.

125. Kumar, V., Aggarval, G., Choudhary, A. 2011. Buccal adhesive drug delivery – A novel technique. *International Journal of Pharmacy and Biological Sciences*. I (3), 89-102.

126. Langoth, N., Guggi, D., Pinter, Y., Bernkop-Schnürch, A. 2004. Thiolated Chitosan: In Vitro Evaluation of its Permeation Enhancing Properties. *Journal of Controlled Release*. 94, 177-86.

127. Langoth, N., Kahlbacher, H., Schoffmann, G., Schmerold, I., Schuh, M., Franz, S., Kurka, P., Bernkop-Schnürch, A. 2006. Thiolated Chitosans: Design and In vivo evaluation of a mucoadhesive Buccal Peptide drug delivery system. *Pharmaceutical Research.* 23 (3), 1-7.

128. Langoth, N., Kalbe, J., Bernkop-Schnürch, A. 2005. Development of a mucoadhesive and permeation enhancing buccal delivery system for PACAP (pituitary adenylate cyclise-activating polypeptide). *International Journal of Pharmaceutics.* 296, 103-111.

129. Lassmann-Vague, V., Raccah, D. 2006. Alternatives routes of insulin delivery. *Diabetes Metabolism*. 32, 513-522.

130. Lawlor, M.S., Jones, D.S., Woolfson, A.D. 1999. Mechanical and rheological characterisation of bioadhesive tetracycline-containing gels designed for the treatment of periodontal disease. *Journal of Pharmaceutics and Pharmacology*. 51, 78.

131. Lee, D., Zhang, W., Shirley, S. A., Kong, X., Hellermann, G. R., Lockey, R. F., Mohapatra, S.S. 2007. Thiolated chitosan/DNA nanocomplexes exhibit enhanced and sustained gene delivery. Pharmaceutical Research, 24 (1), 157–167.

132. Lee, J.W., Park. J.H., Robinson, J.R. 2000. Bioadhesive Dosage Form: The Next Generation. *Journal of Pharmaceutical Sciences.* 89 (17), 850-866.

133. Lee, M. K., Kim, M.Y., Kim, S., Lee, J. 2009. Cryoprotectants *for* freeze drying of drug nano-suspensions: effect of freezing rate. *Journal of Pharmaceutical Sciences.* 98, 4808-4817.

134. Lee, V. H. L., Yamamoto, A. 1989. Penetration and enzymatic barriers to peptide and protein absorption. *Advanced Drug Delivery Review.* 4, 171–207.

135. Lee, V.H. 1988. Enzymatic barriers to peptide and protein absorption. *Critical Reviews in Therapeutic Drug Carrier Systems*. 5, 69-97.

136. Lee, V. H., Yamamoto, A. Kompella, U. B. 1991. Mucosal penetration enhancers for facilitation of peptide and protein drug absorption. *Critical Reviews in Therapeutic Drug Carrier Systems*. 8, 91-192.

137. Leitner, V.M, Walker, G.F., Bernkop-Schnürch, A. 2003. Thiolated polymers: evidence for the formation of disulphide bonds with mucus glycoproteins. *European Journal of Pharmaceutics and Biopharmaceutics*. 56, 207–214.

138. Levine, M.J., Jones, P.C., Looms, R.E., Reddy, M.S., Al-Hashimi, I., Bergey, E.J. 1987. In: Mackenzie, I.C., Squier, C.A., Dablesteen (Eds.), *Oral Mucosal Diseases: Biology, Etiology and Therapy*, Laege-foreningens Folag, Copenhagen. 7–9.

139. Li, Z., Jia, G., Zhang, J., Zhao, Y., Lv, L., Ding, C., Zhang, X. 2010. Chitosan-graft-polyethylene with improved properties as a potential gene vector. *Carbohydrate polymer*. 80, 254-259.

140. Liao, X., Krishnamurthy, R., Suryanarayanan, R. 2007. Influence of processing conditions on the physical state of mannitol - implications in freeze-drying. *Pharmaceutical Research*. 370-376.

141. Liu, J. 2006. Physical Characterization of Pharmaceutical Formulations in Frozen and Freeze-Dried Solid States: Techniques and Applications in Freeze-Drying Development. *Pharmaceutical Development and Technology*. 11, 3-28.

142. Liu, W., Wang, D.Q., Nail, S. L. 2005. Freeze-Drying of Proteins from a Sucrose-Glycine Excipient System: Effect of Formulation Composition on the Initial Recovery of Protein Activity. *AAPS PharmSci Tech*; 6 (2) Article 23.

143. Lueben, H. L., Rentel, C. O., Kotze, A. F., Lehr, C. M., De Boer, A. G., Verhoef, J. C. And Junginger, H. E. 1997. Mucoadhesive polymers in peroral peptide drug delivery: Polycarbophil and chitosan are potent enhancers of peptide transport across intestinal mucosae in vitro. *Journal of Controlled Release* .45, 15-23.

144. Luessen, H.L., Leeuw, B.J.D., Langemeyer, M.W, Boer, A.G.D., Verhoef, J.C., Junginger, H.E. 1996. Mucoadhesive polymers in peroral peptide drug delivery. VI. Carbomer and chitosan improve the intestinal absorption of the peptide drug buserelin in vivo. *Pharmaceutical Research*. 13, 1668– 1672.

145. Luo, K., Yin, J., Khutoryanskaya, O.V., Khutoryanskiy, V.V. (2008). Mucoadhesive and elastic films based on blends of chitosan and hydroxyethyl cellulose. *Macromolecular Bioscience*. 8, 184-192.

146. Luthra, S. A., Hodge, I. M., Utz, M., Pikal M. J. 2008. Correlation of Annealing with Chemical stability in Lyophilized Pharmaceutical glasses. *Journal of Pharmaceutical sciences.* 97, 5240-5251.

147. Ma, Z., Yeoh, H.H., Lim, L.Y. 2002. Formulation pH modulates the interaction of insulin with chitosan nanoparticles. *Journal of Pharmaceutical Sciences*. 91, 1396–1404.

148. Madsen, F. And Peppas, N. A. 1999. Complexation graft copolymer networks: swelling properties, calcium binding and proteolytic enzyme inhibition. *Biomaterials* 20, 1701-1708.

149. Mathias, N.R., Hussain, M.A. 2010. Non-invasive Systemic Drug Delivery: Developability Considerations for Alternate Routes of Administration. *Journal of Pharmaceutical Sciences*. 99, 1-20.

150. Martins, A.M., Alves, C.M., Kasper, F.K., Mikosc, A.G., Reis, R.L. 2010. Responsive and in situ-forming chitosan scaffolds for bone tissue engineering applications: an overview of the last decade. *Journal of Material Chemistry*. 20, 1638–1645.

151. Maroni, A., Curto, M.D.D., Serratoni, M., Zema, L., Foppoli, A., Gazzaniga, A., Sangalli, M.E. 2009. Feasibility, stability and release performance of a time-dependent insulin delivery system intended for oral colon release. *European Journal of Pharmaceutics and Biopharmaceutics.* 72, 246-251.

152. Matsuki, M., Watanabe, T., Ogasawara, A., Mikami, T., Matsumoto, T. 2008. Inhibitory Mechanism of Melanin Synthesis by Glutathione. *Yakugaku Zasshi*. 128 (80), 1203-1207.

153. Matthews, K.H., Stevens, H.N.E., Auffret, A.D., Humphrey, H.M., Eccleston, G.M. 2005. Lyophilised wafers as a drug delivery system for wound healing containing methylcellulose as a viscosity modifier. *International Journal of Pharmaceutics.* 289, 51-62.

154. Matthews, K.H., Stevens, H.N.E., Auffret, A.D., Humphrey, M.J., Eccleston, G.M. 2003. Wafer for wounds. International Patent. Pfizer Ltd., WO 03,037,395, August 05.

155. Matthews, K.H., Stevens, H.N.E., Auffret, A.D., Humphrey, M.J., Eccleston, G.M. (2008). Formulation, stability and thermal analysis of lyophilised wound healing wafers containing an insoluble MMP-3 inhibitor and a non-ionic surfactant. *International Journal of Pharmaceutics*. 356, 110–120.

156. Mcinnes, F.J., O'mahony, B., Lindsay, B., Band, J., Wilson, C.G., Hodges, L.A., Stevens H.N.E. 2007. Nasal residence of insulin containing lyophilised nasal insert formulations, using gamma scintigraphy. *European Journal of Pharmaceutical Sciences.* 31, 25–31.

157. McNay, J.L.M., O'Connell, J.P., Fernandez, E.J. 2001. Protein unfolding during reversed-phase chromatography: II. Role of salt type and ionic strength, *Biotechnology and Bioengineering*. 76. 233-240.

158. Merkle, H.P. & Wolany, G. 1992. Buccal delivery for peptide drugs. *Journal of Controlled Release*. 21, 155-164.

159. Middleton, D. L., Leung, S. S., Robinson, J. R. 1990. Ocular Bioadhesive Delivery Systems: in *Bioadhesive Drug Delivery Systems*. Lenaerts, V., Gurny, R. Eds., CRC Press. 189-192.

160. Modi, P., Mihic, M. And Lewin, A. 2002. The evolving role of oral insulin in the treatment of diabetes using a novel RapidMist System. *Diabetes Metabolism and Research Reviews.* 18 (Suppl1), S38-42.

161. Moore, J.W., Flanner, H.H. 1996. Mathematical comparison of curves with an emphasis on in vitro dissolution profile. *Pharmaceutical Technology*. 20 (6), 64-74.

162. Morales, J.O., McConville, J.T. 2011. Manufacture and characterization of mucoadhesive buccal films. *European Journal of Pharmaceutics and Biopharmaceutics*. 77, 187–199.

163. Morishita, M., Morishita, I., Takayama, K., Machida, Y., Nagai, T. 1993. Site-dependent effect of aprotinin, sodium caprate, Na_2EDTA and sodium glycocholate on intestinal absorption of insulin. *Biological and Pharmaceutical Bulletin*. 16, 68-72.

164. Morishita, M., Peppas, N.A. 2006. Is the oral route possible for peptide and protein drug delivery? Drug discovery today. 11 (19/20), 905-910.

165. Morishita, M., Goto, T., Nakamura, K., Lowman, A.M., Takayama, K., Peppas, N.A. 2006. Novel oral insulin delivery systems based on complexation polymer hydrogels: single and multiple administration studies in type 1 and 2 diabetic rats. *Journal of Controlled Release*. 110, 587–594.

166. Mu, L., Feng, S. S. 2001. Fabrication, characterization and in vitro release of paclitaxel (Taxol®) loaded poly (lactic-co-glycolic acid) microspheres prepared by spray drying technique with lipid/cholesterol emulsifiers. *Journal of Controlled Release.* 76, 239-54.

167. Mukhopadhyay, P., Mishra, R., Rana, D., Kundu, P. 2012. Strategies for effective oral insulin delivery with modified chitosan nanoparticles: A review. *Progress in Polymer Science.* http://dx.doi.org/10.1016/j.progpolymsci.2012.04.004.

168. Mwale, F., Iordanova, M., Demers, C.N., Steffen, T., Roughley, P., Antoniuo, J. 2005. Biological evaluation of CS salts cross-linked to genipin as a cell scaffold for disk tissue engineering. *Tissue Engineering*. 11, 130–140.

169. Muzzarelli, R. A. A., Boudrant, J., Meyer, D., Manno, N., DeMarchis, M., Paoletti, M. G. 2012. Current views on fungal chitin/chitosan, human chitinases,

food preservation, glucans, pectins and inulin: A tribute to Henri Braconnot, precursor of the carbohydrate polymers science, on the chitin bicentennial. *Carbohydrate Polymers*. 87, 995–1012.

170. Nagahama, H., Maeda, H., Kashiki, T., Jayakumar, R., Furuike, T., & Tamura, H. 2009. Preparation and characterization of novel chitosan/gelatine membranes using chitosan hydrogel. *Carbohydrate Polymers*. 76 (2), 255–260.

171. Nagai, T. 1986. Topical mucosal adhesive dosage forms. *Medical Research Reviews*. 6, 227-242.

172. Nail, S. L., Gatlin L. A. 1992. Freeze Drying: Principles and Practices, in Pharmaceutical Dosage Forms: *Parenteral Medications*. (2), AVIS, *et al*., Eds., Marcel Dekker. 171, 174.

173. Nail, S. L., Schwegman, J. J., Kamp, V. 2000. Analytical Tools for Characterization of Frozen Systems in the Development of Freeze-Dried Pharmaceuticals. *American Pharmaceutical Review*. 3. 17-25.

174. Nicolazzo, J.A., Reed, B.L., Finnin, C. 2005. Buccal penetration enhancers—How do they really work? *Journal of Controlled Release* 105, 1 – 15.

175. Nielsen, H.M., Rassing, M.R. 2000. TR 146 cells grown on filters as a model of human buccal epithelium. V. Enzyme activity of the TR 146 cell culture model, human buccal epithelium and porcine buccal epithelium and permeability of Leuenkephalin. *International Journal of Pharmaceutics*. 200, 261–270.

176. Nochos, A., Douroumis, D., Bouropoulos, N. 2008. In vitro release of bovine serum albumin from alginate/HPMC hydrogel beads. *Carbohydrate Polymers*. 74, 451–457.

177. Oungbho, K., Muller, B. W. 1997. Chitosan sponges as sustained release drug carriers. *International Journal of Pharmaceutics*. 156, 229–237.

178. Park, H., Amiji, M., Park, K. 1989. Mucoadhesive hydrogels effective at neutral pH. *Proc. International Symposium on Controlled Release of Bioactive Materials*. 16, 217-218.

179. Park, K., Kwon, I.C., Park, K. 2011. Oral protein delivery: Current status and future prospect. *Reactive and Functional Polymers*. 71, 280–287.

180. Pastore, A., Piemonte, F., Locatelli, M., Russo, A.L., Gaeta, L.M., Tozzi, G., Federici, G. 2003. Determination of blood total, reduced, and oxidized glutathione in paediatric subjects. *Clinical Chemistry.* 47 (8), 1467-1469.

181. Patel, V.F., Liu, F., Brown, M.B. 2011. Advances in oral delivery. *Journal of Controlled Release*. Doi:10.1016/j. Jconrel.2011.01.27.

182. Patel, V.F., Liu, F., Brown, M.B. 2012. Modelling the oral cavity: In vitro and in vivo evaluation of buccal delivery systems. *Journal of Controlled Release*. 161, 746-756.

183. Patel, V.M., Prajapati, B.G., Patel M.M. 2007. Design and characterization of chitosan-containing Mucoadhesive buccal patches of propranolol hydrochloride. *Acta pharm.* 57, 61–72.

184. Payne, G.F., Chaubal, M.V., Barbari, T. 1996. Enzyme-catalyzed polymer modification: reaction of phenolic compounds with chitosan films. *Polymer*. 37, 4643-4648.

185. Peppas, N. A., Bury, P.A. 1985. Surface interfacial and molecular aspects of polymer bioadhesion on soft tissues. Journal of Controlled Release. 2, 257–275.

186. Peppas, N., A., Sahlin, J. J. 1996. Hydrogels as mucoadhesive and bioadhesive materials: a review. *Biomaterials*. 17, 1553–1561.

187. Perioli, L., Ambrogi, V., Pagano, C., Massetti, E., Rossi, C. 2011. New solid mucoadhesive systems for benzydamine vaginal administration. *Colloids and Surfaces B: Biointerfaces*, 84 (2), 413-420.

188. Peters Jr., T. (1985). Serum Albumin. *Adv. Protein Chem.*37; 161-245.

189. Pikal, M.J., 2002. Freeze Drying In: *Encyclopedia of Pharmaceutical Technology*, Marcel Dekker. New York. 1299-1326.

190. Pikal, M.J. 1990. Freeze-drying of proteins. Part II: formulation selection. *Biopharmaceutics*. 3 (8), 18-27.

191. Pompella, A., Visvikis, A., Paolicchi, A., De Tata, V., Casini, A.F. 2003. The changing faces of glutathione, a cellular protagonist. *Biochemical Pharmacology*. 66 (8), 1499-1503.

192. Poole, S., West, S. I. Walters, C. L. 1984. Protein-Protein Interactions: Their Importance in Foaming of Heterogeneous Protein Systems. *Journal of the Science of Food and Agriculture.* 35, 701-711.

193. Portero, A., Teijeiro-Osorio, D., Alonso, M.J., Remunan-Lopez, C. 2007. Development of chitosan sponges for buccal administration of insulin. *Carbohydrate Polymer*. 68, 617-625.

194. Prabaharan, M., Gong, S. 2008. Novel thiolated carboxymethyl chitosan-g-β-cyclodextrin as mucoadhesive hydrophobic drug delivery carriers. *Carbohydrate Polymer*. 73, 117–125.

195. Quiming, N.S. Vergel, R.B. Nicolas, M.G. Villanueva, J.A. 2005. Interaction of Bovine Serum Albumin and Metallothionein. *Journal of Health Science*. 51, 8-15.

196. Qin, C., Li, H., Xiao, Q., Liu, Y., Zhu, J. Du, Y. 2006. Water-solubility of chitosan and its antimicrobial activity. *Carbohydrate Polymer*. 63, 367–374.

197. Rabea, E.I., Badawy, M.E., Stevens, C.V., Smagghe, G., Steubaut, W. 2003. Chitosan as antimicrobial agent: applications and mode of action. *Biomacromolecules*. 4, 1457–1465.

198. Rahman, M.M., Hasan, S., Alam, M.A., Roy, S., Jha, M.K., Ahsan, M.Q., Rahman, H., 2011. Formulation and evaluation of Ranolazone sustained release matrix tablets using Eudragit and HPMC. *International Journal of Pharmaceutical and Biomedical Research.* 2 (1), 7-12.

199. Rai, V., Tan, H.S., Michniak-Kohn, B. 2011. Effect of surfactants and pH on naltrexone (NTX) permeation across buccal mucosa. *International Journal of Pharmaceutics*. 411, 92-97.

200. Rathbone, M.J., Ponchel, G., Ghazali, F.A. 1996. Systemic and oral mucosal drug delivery and delivery systems, In: M.J. Rathbone (Ed.), *Oral Mucosal Drug Delivery*. 74, Marcel Dekker Inc. New York. 241–284.

201. Read, R.C., Naylor, S.C., Potter, C.W., Bond, J., Jabbal-Gill., I., Fisher, A., Illum, L., Jennings, R. 2005. Effective nasal influenza vaccine delivery using chitosan. *Vaccine*. 23, 4367–4374.

202. Reseland, J. E., Holm, H., Jacobsen, M. B., Jenssen, T. G., Hanssen, L. E. 1996. Proteinase inhibitors induce selective stimulation of human trypsin and chymotrypsin secretion. *Journal of Nutrition*. 126, 634-642.

203. Rinaudo, M. 2006. Chitin and chitosan: Properties and applications. *Progress in Polymer Science*. 31, 603-632.

204. Robinson, J., R. 1990. Rationale of bioadhesion/ mucoadhesion. In: Bioadhesion Possibilities and Future Trends. Gurny, R., Junginger, H. E. Eds. *Wissenchaftliche verlag Gesellschaft*. Stuttgart.

205. Rodriguez-Spong, B., Price, C. P., Jayasankar, A., Matzger, A. J. & Rodriguez-Hornedo, N. 2004. General principles of pharmaceutical solid polymorphism: a supramolecular perspective. *Advanced Drug Delivery Reviews.* 56, 241-274.

206. Roldo, M., Hornof, M., Caliceti, P., Andreas, B.S. 2004. Mucoadhesive thiolated chitosans as platforms for oral controlled drug delivery: synthesis and in vitro evaluation. *European Journal of Pharmaceutics and Biopharmaceutics*. 57, 115-21.

207. Roy, S., Pal, K., Anis, A., Pramanik, K., Prabhakar, B. 2009. Polymers in Mucoadhesive Drug Delivery System: A Brief Note. *Designed Monomer and Polymers.* 12, 483- 495.

208. Roy, I., Gupta, M.N. 2004. Freeze–drying of proteins: some emerging concerns. *Biotechnology and Applied Biochemistry*. 39, 165–177.

209. Saboktakin, M. R., Tabatabaie, R. M., Maharramov, A., Ramazanov, M. A. 2011. Development and in vitro evaluation of thiolated chitosan—Poly (methacrylic-acid) nanoparticles as a local mucoadhesive delivery system. *International Journal of Biological Macromolecules*. 48, 403-407.

210. Sakkinen, M., Linna, A., Ojala, S., Jurjenson, H., Veski, P., Marvola, M. 2003. In vivo evaluation of matrix granules containing microcrystalline chitosan as a gel-forming excipient. *International Journal of Pharmaceutics*. 250 (1), 227-237.

211. Sakurai, K., Tanaka, H., Ogawa, N., Takahashi, T. 1997. *Journal of Macromolecular Science-Physics B.* 36, 703.

212. Schipper, N.G.M., Olsson, S., Hoogstraate, J.A., Boer, A.G.D., Varum, K.M., Artursson, P. 1997. Chitosans as absorption enhancers for poorly absorbable drugs. 2: Mechanism of absorption enhancement. *Pharmaceutical Research.* 14, 923–929.

213. Schipper, N.G.M., Varum, K.M., Stenberg, P., Ocklind, G., Lennernas, H., Artursson, P. 1999. Chitosans as absorption enhancers for poorly absorbable

drugs. 3: Influence of mucus on absorption enhancement. *European Journal of Pharmaceutical Sciences*. 8, 335–343.

214. Schwegman, J. J. 2009a. Basic cycle development techniques for lyophilized products. Technical Note from Website of ViRtis/FTS.

215. Schwegman, J. J. 2009b. Using Differential Scanning Calorimetry (DSC) for optimized lyophilisation cycle design. Technical Note from Website of ViRtis/FTS.

216. Seales, J.A. 2000. Heterogeneity Phenomenon in Pharmaceutical lyophilisation. PhD Thesis, University of Colorado, Boulder, CO.

217. Searles, J.A., Carpenter, J.F., Randolph, T.W. 2001a. Annealing to optimize the primary drying rate, reduce freezing-induced drying rate heterogeneity, and determine T(g)' in pharmaceutical lyophilisation. *Journal of Pharmaceutical Sciences*. 90, 872-887.

218. Searles J.A., Carpenter, J.F., Randolph, T.W., 2001b. The ice nucleation temperature determines the primary drying rate of lyophilisation for samples frozen on a temperature-controlled shelf. *Journal of Pharmaceutical Sciences.* 90, 860-871.

219. Senel, S., Hıncal, A. A. (2001). Drug permeation enhancement via buccal route: possibilities and limitations. *Journal of Controlled Release*. 72, 133–144.

220. Senel, S., Kremer, M.J., Kas, S., Wertz, P.W., Hincal, A.A., Squier, C.A. 2000. Enhancing effect of chitosan on peptide drug delivery across buccal mucosa. *Biomaterials*. 21. 2067-2071.

221. Shah, V.P., Tsong, Y., Sathe, P. 1998. In vitro dissolution profile comparison – statistics and analysis of the similarity factor f2. *Pharmaceutical Research*. 15, 889-896.

222. Shoaib, M.H., Sidiqi, S.A.S., Yousuf, R.I., Zaheer, K., Hanif, M., Rehana, S., Jabeen, S. 2010. Development and Evaluation of Hydrophilic Colloid of Famotidine Tablets. *AAPS PharmSciTech*. 11 (2).

223. Shoaib M.H., Tazeen, J., Merchant, H.A., Yousuf R.I. 2006. Evaluation of drug release kinetics from ibuprofen matrix tablets using HPMC**.** *Pakistan Journal of Pharmaceutical Science*. 19 (2), 119-124.

224. Silva, C.A., Nobre, T.M., Pavinatto, F.J Osvaldo N. Oliveira Jr., O.N. 2012 Interaction of chitosan and mucin in a biomembrane model environment. *Journal of Colloid and Interface Science.*376, 289–295.

225. Skoog, D.A. 2006. *Principles of Instrumental analysis*. 6th Ed. Thompsonbrooks/Cole: Belmont, CA.

226. Smart, J. D. 2005. The basics and underlying mechanisms of mucoadhesion. *Advanced Drug Delivery and Reviews*. 57, 1556-1568.

227. Smart, J. D. 1999. The role of water movement and polymer hydration in mucoadhesion. In: Bioadhesive Drug Delivery Systems: *Fundamentals, Novel Approaches and Development*. Mathiowitz, E., Chickering. D.E., Lehr, C. M. Eds. Marcel Decker. New York. 11-23.

228. Snyder, G.H., Reddy, M.K., Cennerazzo, M.J., Field, D. 1983. Use of local electrostatic environments of cysteines to enhance formation of a desired species in a reversible disulphide exchange reaction. *Biochimica et Biophysica Acta*. 749, 219-226.

229. Sogias, I.A., Williams, A.C., Khutoryanskiy, V.V. 2008. Why is Chitosan Mucoadhesive? *Biomacromolecules 9,* 1837–1842.

230. Sohi, H., Ahuja, A., Ahmad, F.J., Khar, R.K. 2010. Critical evaluation of permeation enhancers for oral mucosal drug delivery, *Drug Development and Industrial Pharmacy*. 36, 254–282.

231. Solomonidou, D., Cremer, K., Krumme, M., Kreuter, J. 2001. Effect of carbomer concentration and degree of neutralization on the mucoadhesive properties of polymer films. *Journal of Biomaterials and Scientific Polymers.* 12, 1191–1205.

232. Song, B., Wang, F., Guo, Y., Sang, Q., Liu, M., Li, D., Fang, W., Zhang, D. 2012. Protein–protein interaction network-based detection of functionally similar proteins within species. *Proteins: Structure, Function, and Bioinformatics.*80 (7), 1736-1743.

233. Sood, A., Panchagnula, R. 2003. Design of Controlled Release Delivery Systems Using a Modified Pharmacokinetic Approach: A Case Study for Drugs Having a Short Elimination Half-life and a Narrow Therapeutic Index. *International Journal of Pharmaceutics* 261, 27-41.

234. Spink, C.H. 2008. Differential Scanning Calorimetry. *Methods in Cell Biology*. 84. 115-141.

235. Squier, C.A., Finkelstein, M.W., 1989. In: A.R. Ten Cate (Ed). *Oral Histology, Development, Structure and Function*. C.V. Mosby, St. Louis. 345–385.

236. Squier, C.A., Wertz, P.W. 1996. Structure and function of the oral mucosa and implications for drug delivery. In: M.J. Rathbone (Ed.), *Oral Mucosal Drug Delivery*. Marcel Dekker, New York. 1–26.

237. Sreenivas, S.A., Pai, K.V. 2009. Synthesis of Thiolated Chitosans: promising polymers for prolonged mucoadhesive drug delivery. *International Journal of Pharmtech Research*. 1 (3), 670-678.

238. Staddon, J.M., Herrenknecht, K., Smales, C., Rubin, L.L. 1995. Evidence that tyrosine phosphorylation may increase tight junction permeability. *Journal of Cell Science*. 108, 609–619.

239. Steed, E., Balda, M.S., Matter, K. 2010. Dynamics and functions of tight junctions. *Trends in cell Biology*. 20 (3), 142-149.

240. Strambini, G. B., Gabelleiri, E. 1996. Proteins in Frozen Solutions: Evidence of Ice-Induced Partial Unfolding. *Biophysical Journal.* 70, 971-6.

241. Stratford, R. E, Lee, V. H. L. 1986. Aminopeptidase activity in homogenates of various absorptive mucosae m the albino rabbit: implications in peptide delivery. *International Journal of Pharmaceutics*. 30, 73-82.

242. Sudhakar, Y., Kuotsu, K., Bandyopadhyay A.K. 2006. Buccal bioadhesive drug delivery — A promising option for orally less efficient drugs. *Journal of Controlled Release.* 114, 15–40.

243. Szlachcic, A., Zakrzewska, M., Otlewski, J. 2011. Longer action means better drug: Tuning up protein therapeutics. *Biotechnology Advances*. DOI:10.1016/j.biotechadv.2011.03.005.

244. Takeuchi, H., Yamamoto, H., Kawashima, Y. 2001. Mucoadhesive nanoparticulate systems for peptide drug delivery. *Advanced Drug Delivery Reviews*. 47, 39–54.

245. Tamburic, S., Graig, D.Q.M. 1997. A comparison of different in vitro methods for measuring mucoadhesive performance. *European Journal of Pharmaceutics and Biopharmaceutics*. 44, 159-167.

246. Tattini, J.R.V., Parra, D. F., Polakiewicz, B., Pitombo, R. N.M. 2005. Effect of lyophilisation on the structure and phase changes of PEGylated-bovine serum albumin. *International Journal of Pharmaceutics*. 304, 124–134.

247. Thanou, M., Verhoef, J.C., Marbach, P., Junginger, H.E. 2000. Intestinal absorption of octreotide: N-trimethyl chitosan chloride (TMC) ameliorates the permeability and absorption properties of the somatostatin analogue in vitro and in vivo. *Journal of Pharmaceutical Sciences*. 89, 951-957.

248. Thirawong, N., Nunthanid, J., Puttipipatkhachorn S., Sriamornsak, P. 2007. Mucoadhesive properties of various pectins on gastrointestinal mucosa: An *in vitro* evaluation using texture analyser. *European Journal of Pharmaceutics and Biopharmaceutics*. 67, 132–140.

249. Thomsen, A. E., Jensen, H., Jorgensen, L., Weert, M., Østergaard J. 2008. Studies on human insulin adsorption kinetics at an organic-aqueous interface determined using a label-free electroanalytical approach. *Colloids and Surfaces B: Biointerfaces*. 63. 243-248.

250. Tiwari, D., Goldman, D., Sause, R., Madan, P.L. (1999). Evaluation of polyoxyethylene homopolymers for buccal bioadhesive drug delivery device formulations. *AAPS PharmSci.* 1, E13.

251. Tommaso, C, D., Como, C., Gurny, R., Möller, M. 2010. Investigations on the lyophilisation of MPEG–hexPLA micelle based pharmaceutical formulations. *European Journal of Pharmaceutical sciences*. 40, 38-47.

252. Tozaki, H., Odoriba. T., Okada, N., Fujita, T., Terabe, A., Suzuki, T., Okabe, S., Muranishi, S., Yamamoto, A. 2002. Chitosan capsules for colon-specific drug delivery: enhanced localization of 5-aminosalicylic acid in the large intestine accelerates healing of TNBS-induced colitis in rats. *Journal of Controlled Release*. 82, 51-61.

253. US Pharmacopeia. 2006. USP/NF General Chapter <788> Particulate Matter in Injections. In: U.S. Pharmacopeia, ed. *National Formulary, USP29-NF-24 (suppl 2).* Rockville, MD: USP.

254. Utracki, L.A. 1989. *Polymer alloys and blends: Thermodynamic and Rheology*. Hanser, Munich. 111-124.

255. Valenta, C., Kast, C.E., Harich, I.H., Bernkop-Schnürch, A. 2001. Development and in vitro evaluation of a mucoadhesive vaginal delivery system for progesterone. *Journal of Controlled Release*. 77, 323–332.

256. Vallee, A., Humblot, V., Methivier, C., Pradier, C. 2008. Glutathione adsorption from UHV to the liquid phase at various pH on gold and subsequent modification of protein interaction. *Surface and Intersurface analysis*. 40, 395-399.

257. Van Der Lubben, I.M., Verhoef, J.C., Borchard, G., Junginger, H.E., 2001a. Chitosan and its derivatives in mucosal drug and vaccine delivery. *European Journal of Pharmaceutical Sciences*. 14, 201–207.

258. Vandevord, P.J., Matthew, H.W., Desilva, S.P., Mayton, L., Wu, B., Wooley, P.H. 2002. Evaluation of the biocompatibility of a chitosan scaffold in mice. *Journal of Biomedical Materials and Research*. 59, 585–590.

259. Vashist, A., Gupta, Y.K., Ahmad, S. 2012. Interpenetrating biopolymer network based hydrogels for an effective drug delivery system. *Carbohydrate Polymer*. 87, 1433-1439.

260. Verheul, R.J., Slutter, B., Bal, S.M., Bouwstra, J.A., Jiskoot, W., Hennink, W. 2011. Covalently stabilized trimethyl chitosan-hyaluronic acid nanoparticles for nasal and intradermal vaccination. *Journal of controlled release*. 156, 46-52.

261. Veuillez, F., Kalia, Y.N., Jacques, Y., Deshusses, J., Buria, P. 2001. Factors and strategies for improving buccal absorption of peptides. *European Journal of Pharmaceutics and Biopharmaceutics.* 51, *93-109.*

262. Vives, M.A., Macian, M., Seguer, J., Infante, M.R., Vinardell, M.P. 1997. Irritancy potential produced by surfactants derived from lysine. *Toxicology in vitro.* 11, 779-783.

263. Walker, G.F., Langoth, N., Bernkop-Schnürch, A. 2002. Peptidase activity on the surface of the porcine buccal mucosa. *International Journal of Pharmaceutics*. 233, 141-147.

264. Wang, B., Tchessalov, S. W., Pikal, M.J. 2009. Impact of sucrose level on storage stability of *proteins* in *freeze*-dried solids: I. Correlation of *protein*-sugar interaction with native structure preservation. *Journal of Pharmaceutical Sciences*. 98 (9), 3131-3144.

265. Wang W. 2000. Lyophilisation and development of solid protein pharmaceuticals. *International Journal of Pharmaceuticals*. 203, 1-60.

266. Ward, K., Gaster, T., Wood, R. 2008. Freeze drying Technology. *Biopharma Technology Ltd*. Lulu. C19.8-C19.22.

267. Warne, N.W. 2011. Development of high concentration protein biopharmaceuticals: The use of platform approaches in formulation development. *European Journal of Pharmaceutics and Biopharmaceutics*. 78, 208–212.

268. Waxler, B., Rabito, S.F. 2003. Aprotinin: a serine protease inhibitor with therapeutic actions: its interaction with ACE inhibitors. *Current Pharmaceutical Design*. 9 (9), 777-87.

269. Wood, K.M., Stone, G.M., Peppas, N.A. 2010. The effect of complexation hydrogels on insulin transport in intestinal epithelial cell models. *Acta Biomaterialia*. 6, 48–56.

270. Wood S. P., Blundell T. L. 1975. The Relation of Conformation and Association of Insulin to Receptor Binding; X-Ray and Circular-Dichroism Studies on Bovine and Hystricomorph Insulins. *European Journal of Biochemistry*. 55, 531-542.

271. Woodley, J. 2001. Bioadhesion: New Possibilities for Drug Administration. *Clinical Pharmacokinetics*. 40, 77-84.

272. Wu, J., Su, Z., Ma, G. 2006. A thermo- and pH-sensitive hydrogel composed of quaternized chitosan/glycerophosphate. *International Journal of Pharmaceutics*. 315, 1–11.

273. Wu, S. 1982 Formation of adhesive bond; Polymer Interface and Adhesion. Marcel Dekker Inc. New York. 359-447.

274. Wu, Z.M., Zhang, X.G., Zheng, C. Li, C.X., Zhang, S.M., Dong, R.N., Yu, D.M. 2009. Disulphide-crosslinked chitosan hydrogel for cell viability and controlled protein release. *European Journal of Pharmaceutical Sciences* 37, 198–206.

275. Xu, Y., Du, Y. 2003. Effect of molecular structure of chitosan on protein delivery properties of chitosan nanoparticles. *International Journal of Pharmaceutics*. 250, 215–226.

276. Xu, Y., Zhan C., Fan L., Wang L., Zheng H. 2007. Preparation of dual crosslinked alginate–chitosan blend gel beads and in vitro controlled release in oral site-specific drug delivery system. *International Journal of Pharmaceutics*. 336, 329–337.

277. Yang, L., Hsiao, W.W., Chen, P., 2001. Chitosan-cellulose composite membrane for affinity purification of biopolymers and immunoadsorption. *Journal Membrane Science*. 5084, 1–13.

278. Yu, A. S.L. Cheng, M.H., Angelow, S., Gunzel, D., Kanzawa, S.A., Schneeberger, E.E., Fromm**,** M., Coalson, R. D. 2009**.** Molecular Basis for Cation Selectivity in Claudin-2–based Paracellular Pores: Identification of an Electrostatic Interaction Site. *The Journal of General Physiology*. 133, 111-127.

279. Yu, W., Lin, J., Liu, X., Xie, H., Zhao, W., Ma, X. 2010. Quantitative characterization of membrane formation process of alginate-chitosan microcapsules by GPC. *Journal of Membrane science.* 346, 296-301.

280. Zalewska, A., Zwierz, K., Kowski, K., Gindzieñski, A. 2000 Structure and biosynthesis of human salivary mucins. *Acta Biochimica Polonica*. 47. 1067–1079.

281. Zhang, D., Xie, Y., Mrozek, M.F., Ortiz, C., Davisson, V.J., Ben-Amotz, D. 2003. Raman detection of proteomic analytes. *Analytical Chemistry.* 75, 5703–5709.

282. Zhang, L., Liu, L., Qian, Y., Chen, Y. 2008. The effects of cryoprotectants on the freeze-drying *of* ibuprofen-loaded solid lipid microparticles (SLM). *European Journal of Pharmaceutics and Biopharmaceutics*. 69, 750-759.

283. Zhang, X. G., Teng, D. Y., Wu, Z. M., Wang, X. 2008. PEG-grafted chitosan nanoparticles as injectable carrier for sustained protein release. *Journal of Materials Science: Materials in Medicine*. 19, 3525-353.

284. Zhu, H., Damodaran, S. 1994. Effects of Calcium and Magnesium Ions on aggregation of Whey Protein Isolate and its effect on foaming properties. *Journal of Agriculture and Food Chemistry*. 42, 856-862.

285. Zor, T., Selinger, Z. 1996. Linearization of the Bradford protein assay increases its sensitivity: theoretical and experimental studies. *Analytical Biochemistry*. 236, 302-308.

286. www.purdue.edu/rem/rs/sem.htm

287. http://thermoscientific.com

288. http://www2.chemistry.msu.edu/faculty/reusch/VirtTxtJml/Spectrpy/nmr/nmr1.htm

289. http://www4.mpbio.com/ecom/docs/proddata.nsf/(webtds2)/190779

290. http://www4.nau.edu/microanalysis/Microprobe-SEM/Instrumentation.html (26/06/2012)

291. http://www.bruker-axs.com/d8_advance.html

292. http://www.bmrb.wisc.edu/metabolomics/mol_summary/?molName=D_mannitol

293. http://www.bmrb.wisc.edu/metabolomics/mol_summary/?molName=GLY

294. http://www.fda.gov/downloads/Drugs/GuidanceComplianceRegulatoryInformation/Guidances/ucm070237.pdf

295. http://www.nuance.northwestern.edu/KeckII/Instruments/FT-IR/keck-ii%20pages1.html

296. http://www.mattek.com/pages/ 05/07/2012

297. http://www.mattek.com/pages/products/epiairway/ (b) (05/07/2012)

298. http://www.mitegen.com/technotes/salt_for_micrort.pdf (30/01/2012)

299. http://www.mpbio.com/detailed_info.php?family_key=02194840

300. http://www.permegear.com/franz01.gif

301. https://www.photophysics.com/chirascan_plus.php.

302. http://www.sigmaaldrich.com/life-science/metabolomics/enzyme-explorer/aprotinin-monograph.html

303. http://www.sigmaaldrich.com/catalog/product/sigma/16005?lang=en&region=GB

304. http://www.tainstruments.com

CHAPTER NINE

APPENDIX

APPENDIX A: List of Publications

1. Ayensu, I., Boateng, J.S. 2012. Development and evaluation of lyophilized thiolated-chitosan wafers for buccal delivery of protein. *Journal of Science and Technology*. 32 (2), 11-17.
2. Ayensu, I., Mitchell, J.C., Boateng, J.S. 2012. Effect of membrane dialysis on characteristics of lyophilised chitosan wafers for potential buccal delivery of proteins. *International Journal of Biological Macromolecules*. 50, 905– 909.
3. Ayensu, I., Mitchell, J.C., Boateng, J.S. 2012. In vitro characterisation of chitosan based xerogels for potential buccal delivery of proteins. *Carbohydrate Polymers*. 89, 935– 941.
4. Giovino, C., Ayensu, I., John Tetteh, J., Joshua S. Boateng, J.S. 2012. Development and characterisation of chitosan films impregnated with insulin loaded PEG-β-PLA nanoparticles (NPs): A potential approach for buccal delivery of macromolecules. *International Journal of Pharmaceutics*. 428, 143– 151.
5. Ayensu, I., Mitchell, J.C., Boateng, J.S. 2011. Development and physico-mechanical characterisation of lyophilised chitosan wafers as potential protein drug delivery systems via the buccal mucosa. *Colloids and Surfaces B: Biointerfaces*. 91, 258– 265.
6. Ayensu, I., Mitchell, J.C., Boateng, J.S. 2011. Formulation and evaluation of lyophilised thiolated chitosan wafers for buccal mucosal delivery of proteins. *The AAPS Journal*, 13 (S2). M1144-M1144.
7. Ayensu, I., Mitchell, J.C., Boateng, J.S. 2010. Freeze-dried thiolated chitosan formulations for protein delivery via the buccal mucosa. *Journal of Pharmacy and Pharmacology*. 62 (10), 1273-1274.
8. Ayensu, I., Mitchell, J.C., Boateng, J.S. 2010. Novel lyophilisation cycle development of chitosan based formulations for buccal delivery using paracetamol as model drug. *The AAPS Journal*. 12 (S2), W4170- W4170.

APPENDIX B: Manuscripts in preparation

1. Development characterisation of laminated thiolated chitosan-based lyophilised xerogels for potential buccal delivery of macromolecules.

2. Effect of protease enzyme inhibitors on mucoadhesion and release kinetics of macromolecules from laminated thiolated-chitosan freeze-dried xerogels.

3. *In-vitro* permeation studies of insulin using sheep buccal tissue and EpiOral^{TM} buccal tissue construct.

APPENDIX C: Abstracts and posters from conference proceedings

1. Accepted abstract for poster presentation - AAPS 2012

Abstract I.D. AM-12-01660

Evaluation of enzyme inhibitors on laminated thiolated chitosan xerogels for buccal delivery of insulin

I. Ayensu[1], J.C. Mitchell[1], J.S. Boateng[1]

[1] School of Science, University of Greenwich, Central Avenue, Chatham Maritime, Kent, UK, ME4 4TB

j.s.boateng@gre.ac.uk

Purpose: This research aims to evaluate the effect of different enzyme inhibitors (EI) on the physical characteristics of lyophilised chitosan-thioglycolic acid (TG-chitosan) based xerogels as a novel system for buccal mucosa delivery of insulin (INS).

Method: TG-chitosan was prepared via amide conjugation of chitosan and thioglycolic acid, characterised by Ellman's reaction and the molecular weight (MW) monitored by gel permeation chromatography (GPC). 1g each of formulated TG-chitosan gels (Table 1) was added onto already dried impervious ethylcellulose (EC) films (laminate) in moulds and lyophilised. The laminated lyophilised xerogels were characterised by attenuated total reflectance-Fourier transform infra red spectroscopy (ATR-FT-IR), circular dichroism (CD), *in-vitro* drug release in 0.1M PBS (pH 7.4) using Franz-type diffusion cell and mucoadhesion with a texture analyser. The effect of different EI (aprotinin and glutathione) on mucoadhesion and release characteristics, were investigated.

Results: Lyophilised TG-chitosan xerogels attached onto EC films contained Brij 35 which acted as a permeation enhancer while mannitol and glycerol served as cryoprotectant and plasticizer respectively. The EC backing was to ensure one directional release of INS. The released INS was conformationally stable by ATR-FT-IR and CD analyses. 10 mg of glutathione was deemed optimum from preliminary evaluation with varying amounts of glutathione. Statistically significant difference ($p < 0.01$) was observed between the stickiness of formulations B and C (Fig.1). There was however, no statistically significant differences ($p > 0.05$), in work of adhesion and cohesion between all the formulations. Formulation B showed improved mucoadhesion properties compared to formulations A and C. Fig. 2 shows the biphasic % release profiles of INS from the various formulations with initial burst release resulting from drug adsorbed on polymer surface. Slow release of INS in the second phase was due to INS-TG-chitosan interaction. Furthermore, possible interaction between glutathione and INS led to statistical significant difference ($p = 0.01$) between the % release from formulations B and C. Release of INS from formulation A containing aprotinin was not significantly different from that of control formulation, C.

Conclusion: Aprotinin showed no significant effect on characteristics of TG-chitosan xerogels while glutathione improved *in vitro* mucoadhesion but with limited INS release.

2. Accepted abstract for podium and poster presentation - APS 2012 (UKPHARMSCI)

Abstract number: 42

Development of laminated thiolated chitosan-based lyophilised xerogels for potential buccal delivery of macromolecules.

I. Ayensu, J.C. Mitchell, J.S. Boateng
School of Science, University of Greenwich at Medway, Chatham Maritime, ME4 4TB, UK.
ai19@gre.ac.uk

INTRODUCTION

Mucosal routes including the buccal membrane offer a potential for the delivery of proteins. However, due to size exclusion at epithelial barriers, salivary washout and peptidase activity, the buccal route may still be limited in its potential for protein delivery. This project is aimed at preparing a delivery system using chitosan thioglycolic acid (TG-chitosan) as the polymer matrix for potential buccal mucosa delivery of protein macromolecules. The effect of glutathione (GSH) as an enzyme inhibitor on xerogel characteristics was also evaluated.

MATERIALS AND METHOD

Conjugation and characterisation of chitosan and thioglycolic acid to obtain TG-chitosan were performed as previously described [1]. 2g each of formulated gels (Table 1) were added unto dried hydrophobic ethyl cellulose (EC) films (backing membrane) in moulds and lyophilised [2].

Table 1. Formulation components

Component	Formulations (mg)	
	Formulation A	Formulation B
TG-chitosan	100	100
Mannitol	10	10
Glycerol	10	10
Brij 35	10	10
Glutathione	0	10
BSA	50	50

The laminated lyophilised xerogels were characterised for surface morphology by SEM, swelling capacity (%) with or without reducing agent dithiothreitol (DTT), mucoadhesion using texture analysis (TA) and *in-vitro* drug release in 0.1M PBS (pH 6.8) using Franz-type diffusion cell.

RESULTS AND DISCUSSION

Flexible and tough xerogels with mannitol as cryoprotectant, glycerol as plasticizer and Brij 35 as permeation enhancer have been prepared. Statistically significant differences ($p < 0.05$) were observed between the % swelling capacity with or without DTT in formulation A. This indicates that disulphide formation drives the swelling capacity of formulation A but not B (Table 2).

Table 2. Formulations % swelling capacities and TA properties

Samples	Swelling capacity (%)		Texture Analysis (*In vitro* mucoadhesion)		
	With DTT	Without DTT	PAF (N)	TWA (mJ)	Cohesiveness (mm)
Formulation A	1086.8 ± 5.1	480.0 ±18.2	3.8 ± 0.5	13.2 ± 3.0	9.6 ± 3.3
Formulation B	849.3 ± 32.6	912.5 ±25.1	5.7 ± 0.9	19.4 ± 3.7	10.4 ± 3.2

Improved mucoadhesion properties were achieved with the use of GSH (Table 2). To ensure unidirectional release of BSA, an impervious backing membrane (EC film) was employed (Fig 1). Drug release was facilitated by the porous polymeric network of the xerogels (Fig 1) due to the increased surface area of dispersed drug.

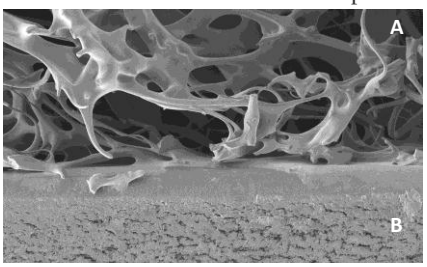

Fig. 1 SEM image of xerogel (A) on EC backing membrane (B)

The initial BSA burst release (Fig. 2) was due to drug molecules adsorbed on the xerogel surface and high initial loading of BSA.

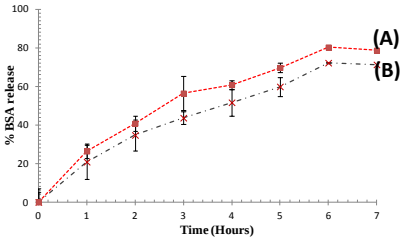

Fig. 2. BSA release from formulations (A) and (B).

A subsequent prolonged release period ensued due to BSA-TG-chitosan complexation. A slow diffusion of entrapped protein from hydrated xerogels therefore occurred. At pH 6.8, however, BSA (isoelectric point around 5) is adsorbed by GSH and disulphide formation in TG-chitosan limits TG-chitosan-BSA complexation leading to higher release of BSA from the TG-chitosan xerogels containing no GSH.

CONCLUSION

Laminated lyophilised TG-chitosan based xerogel for potential protein delivery via buccal mucosa has been developed that incorporates improved mucoadhesion, permeation enhancing and enzyme inhibition properties.

ACKNOWLEDGEMENT

This research is being funded by the Commonwealth Scholarship Commission, London, UK.

REFERENCES

[1] M.R. Saboktakina, R.M. Tabatabaiea, A. Maharramovb, M.A. Ramazanov. "Development and in vitro evaluation of thiolated chitosan—Poly(methacrylic-acid) nanoparticles as a local mucoadhesive delivery system". *Int. J. Bio. Macromol*. **48**, (2011) 403-407.

[2] I. Ayensu, J.C. Mitchell, J.S. Boateng. "Development and physico-mechanical characterisation of lyophilised chitosan wafers as potential protein drug delivery systems via the buccal mucosa". *Colloids. Surf. B: Biointerfaces.* 91, 258-265.

3. Accepted abstract for poster presentation - APS 2012 (UKPharmaSci)

Abstract number: 60

In-vitro permeation studies of insulin using lamb buccal tissue and EpiOral™ buccal tissue construct

I. Ayensu, J.C. Mitchell, J.S. Boateng
School of Science, University of Greenwich at Medway, Chatham Maritime, ME4 4TB, UK.
ai19@gre.ac.uk

INTRODUCTION

Protein drug delivery presents a number of challenges including cost, injection site injury, patient non-compliance and GIT enzyme degradation. Alternate non-invasive routes of delivery such as the buccal membrane have been investigated to overcome these challenges. The route may still be limited in its potential for protein delivery and mucoadhesive polymers, permeation enhancers and enzyme inhibitors (EI) have been employed to improve drug permeation. This study evaluates the permeability of insulin through lamb buccal tissue and EpiOral™ buccal tissue construct. The effect of an EI (aprotinin) on permeation using chitosan thioglycolic acid (TG-chitosan) as the polymer matrix was investigated.

MATERIALS AND METHODS

TG-chitosan was synthesized via amidation, purified and sulfhydryl groups immobilised on chitosan was estimated as previously described [1]. The average molecular weights (Mw) of chitosan and TG-chitosan were monitored with gel permeation chromatography (GPC). 1g each of formulation gels (Table 1) was overlaid on dried impervious ethyl cellulose (EC) films in moulds and lyophilised [2].

Table 1. Formulation components

Component	Formulations (mg)	
	Formulation A	Formulation B
TG-chitosan	100	100
Mannitol	10	10
Glycerol	10	10
Brij 35	10	10
Aprotinin	5	0
Insulin	15	15

Conformational stability of insulin in the xerogels was determined by far-UV circular dichroism (CD). *In-vitro* insulin permeability studies was carried using freshly excised lamb buccal tissue mounted on a Franz-type diffusion cell and EpiOral™ buccal tissue constructs, cultured on the surface of tissue inserts. Tissue viability was examined by 3-[4,5-dimethylthiazol-2-yl] 2,5-diphenyltetrazolium bromide (MTT). The effect of aprotinin on permeation was evaluated.

RESULTS AND DISCUSSION

Stable TG-chitosan xerogels containing insulin, glycerol (plasticizer) and mannitol (cryoprotectant) with enhanced mucoadhesion characteristics, enzyme inhibition (aprotinin) and permeation enhancing (Brij 35) properties have been prepared. Hydrophilic EC laminate ensured unidirectional release of insulin unto mucosal surface. The released insulin was conformationally stable via CD determination.

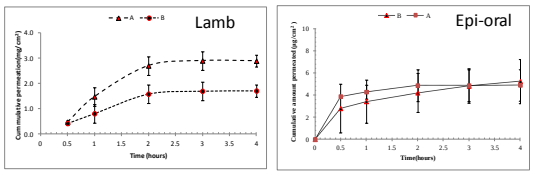

Fig 1. Permeation of insulin released from formulations A and B.

Enhanced permeation was observed with formulation A, containing aprotinin as EI in lamb buccal tissue (Fig.1) with a permeation coefficient of 0.33 cm^2/hr compared to 0.19 cm^2/hr for formulation B. No significant difference in permeation coefficient of formulations was observed with EpiOral™ tissue (Table 2)

Table 2. Permeation coefficients of insulin through both tissues

	Buccal tissue			
	Lamb		Epi-oral	
	A	B	A	B
Permeation coefficient (cm^2 /hr)	0.33	0.19	0.04	0.04

Permeation correlation between lamb and EpiOral™ tissues was however, better in the formulation containing aprotinin (Fig. 2) compared to formulation without the EI.

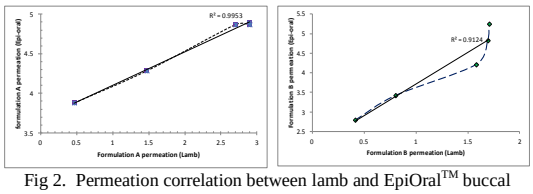

Fig 2. Permeation correlation between lamb and EpiOral™ buccal tissues.

Tissues were deemed viable at the end of the permeation studies.

CONCLUSION

The inclusion of aprotinin in TG-chitosan xerogels improved insulin permeation in lamb buccal tissue and correlated with permeation through the EpiOral™ buccal tissue construct.

ACKNOWLEDGEMENT

This research is being funded by the Commonwealth Scholarship Commission, London, UK.

REFERENCES

[1] A. Bernkop-Schnurch, D. Guggi, Y. Pinter. "Thiolated chitosans: development & in vitro evaluation of a mucoadhesive, permeation enhancing oral drug delivery system" *J. Control. Rel.*, **94** (2004)177-186.

[2] I. Ayensu, J.C. Mitchell, J.S. Boateng. "Development and physico-mechanical characterisation of lyophilised chitosan wafers as potential protein drug delivery systems via the buccal mucosa". *Colloids. Surf. B: Biointerfaces.* 91, 258-265.

4. Abstract # 43 awarded podium and poster presentation - UKPharmSci 2011

Characterisation and evaluation of lyophilised chitosan (CS) wafers for protein delivery via the buccal mucosa

I. Ayensu, J. C. Mitchell, J.S. Boateng
School of Science, University of Greenwich at Medway, Chatham Maritime, ME4 4TB, UK.
ai19@gre.ac.uk

Introduction

The buccal mucosa offers a potential portal for the delivery of proteins due to its large surface area, rich vascularisation and minimal peptidase activities. Chitosan (CS) has been developed as a suitable matrix for the controlled release of protein/peptide drugs over the last two decades [1]. It has been identified to deliver proteins/peptides across the buccal mucosa because of its mucoadhesive, penetration enhancing and peptidase inhibition properties. This project aims to formulate lyophilised chitosan wafers for protein delivery via the buccal mucosa and to evaluate the effect of annealing on the characteristics of the protein loaded wafers

Materials and methods

Preparation and characterization of chitosan wafer

500mg of medium molecular weight chitosan was dissolved in 50ml of 1% v/v acetic acid and the pH adjusted to 6 ± 0.1 with 5M NaOH. The resulting gel was dialysed according to a slightly modified method reported in literature [2] against different aqueous media. 6.5g of the dialysed gel, loaded with BSA as a model protein drug in a 2:1 CS:BSA ratio and 6.5mg each of plasticizer (glycerol) and cryoprotectant (D-mannitol) was lyophilised (**Fig. 1**) with or without an annealing process.

Fig. 1. Lyophilisation cycles

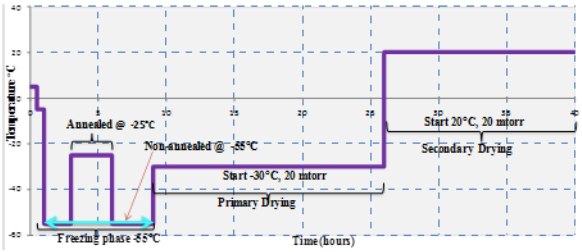

The lyophilized products were evaluated for drug loading capacity, moisture content by TGA, % swelling capacity and surface morphology by SEM. *In-vitro* mucoadhesion measurements of Peak Adhesive Force-**PAF**, Total Work of Adhesion-**TWA** and Cohesiveness was determined by gelatine equilibrated with 2% mucin solution as mucosal substrate, and % drug release (0.1M PBS, pH = 6.8) by Bradford's assay.

Results and Discussion

Physico-mechanical characterisation of CS-BSA wafer

Table 1. Characterisation of CS-BSA wafers

Formulation	Drug loading % (n=4, mean± SD)	Moisture content % (n=4, mean± SD)	Swelling capacity % (n=4, mean± SD)*
Annealed/CS-BSA	91.6 ± 4.0	1.8 ± 0.7	1110 ± 23.3
Non-Annealed/CS-BSA	90.5 ± 4	2.2 ± 0.2	800 ± 21.4

*Measurements performed in PBS pH 6.8 after 7 hours

Table 1 summarises the characteristics of the lyophilised wafers. High drug loading capacities were obtained for both wafers with the annealed wafers showing slightly lower residual moisture content as a result of large ice crystals that enhanced rapid sublimation. Statistically significant difference ($p < 0.05$) was observed between the % swelling capacities.

Fig. 2. Wafer morphology: SEM

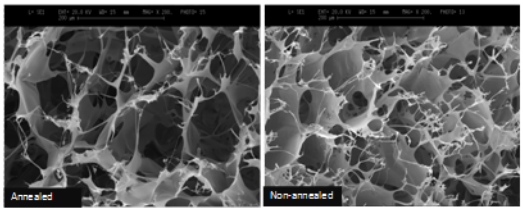

The annealed CS-BSA wafers formed a porous network of larger pore with closer size distribution than the non-annealed wafers (Fig. 2). The annealing process led to growth of both solute crystals and ice crystals which resulted in the larger pores.

Fig. 3. Mucoadhesive properties

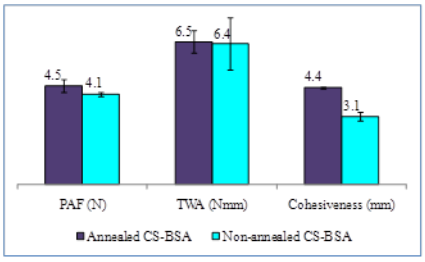

The minor discrepancies between the PAF and TWA and the significant difference ($p < 0.05$) between the cohesiveness (Fig. 3) of the annealed and non- annealed wafers were due to variation in the stability of wafer micro-porous structure.

The variation in the performance of the wafers with respect to swelling capacity, *in-vitro* mucoadhesion properties and release characteristics, could be attributed to differences in pore size and distribution of the annealed and non-annealed wafers.

Fig. 4. *In vitro* release studies

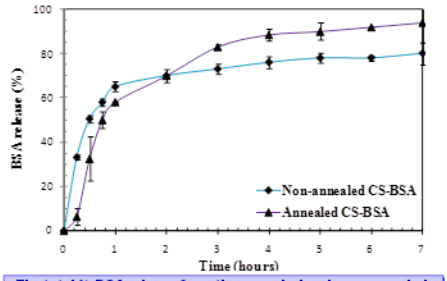

The total % BSA release from the annealed and non-annealed wafers were 91.5 ± 3.7 % and 80.1 ± 4.9 % respectively (Fig. 4). This difference was also statistically significant ($p < 0.05$) though both wafers exhibited a controlled release typical of chitosan based formulations

Conclusion

A stable lyophilised chitosan based system for potential protein delivery via buccal mucosa has been developed. Annealing impacted on the swelling capacity, mucoadhesion properties, drug release and surface morphology.

References

[1] K. Jones, P. Calvo, M. Alonso. 2001. Polysaccharide colloidal particles as delivery systems for macromolecules. Adv Drug Deliv Rev. 47, 83–97

[2] A. Bernkop-Schnurch, D. Guggi, and Y. Pinter. 2004. Thiolated chitosans: development and in vitro evaluation of a mucoadhesive, permeation enhancing oral drug delivery system. J. Control. Rel. 94: 177-186.

Acknowledgments

This research is being supported by the Commonwealth Scholarship Commission, UK. The authors are grateful to Dr Ian Slipper for the SEM images.

5. Abstract # 59 awarded Poster presentation – UKPharmSci 2011

Development and characterisation of lyophilised chitosan wafers: effect of membrane dialysis.

I. Ayensu, J. C. Mitchell, J.S. Boateng
School of Science, University of Greenwich at Medway, Chatham Maritime, ME4 4TB, UK.
ai19@gre.ac.uk

Introduction

Chitosan (CS) has been developed as an appropriate delivery system for protein drugs over the past two decades and been identified for buccal mucosa delivery due to its enzyme inhibitory, mucoadhesive and penetration enhancing characteristics [1]. Its solubility in aqueous media is however limited but may be improved by protonation of the primary amino group. This project aims to evaluate the effect of membrane dialysis on the development and characteristics of lyophilised CS wafers for delivery of proteins via the buccal mucosa.

Materials and methods

Fig.1 illustrates the preparation of chitosan gel dialysed by a modified method [2] against 5 mM HCl five (5) times, replacing the dialysate medium 8 hourly. 6.5 g of the dialysed gel was loaded with BSA in a 1:2 BSA:CS ratio and 6.5mg each of plasticizer (glycerol) and cryoprotectant (D-mannitol) and lyophilised. The process was repeated, excluding dialysis. The lyophilized wafers were evaluated for phase separation with DSC, crystalline structures by XRD, *in-vitro* mucoadhesion (peak adhesive force-PAF; total work of adhesion-TWA and cohesiveness) using gelatine equilibrated with 2% mucin solution as mucosal substrate, drug loading capacity and % drug release (0.1M PBS, pH 6.8) by Bradford's assay.

Fig.1 Preparation of chitosan gels for lyophilisation

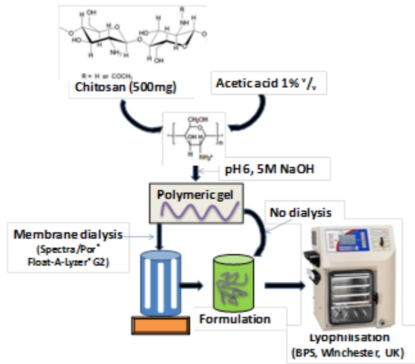

Results and Discussion

Fig 2. DSC thermograms of (a) dialysed and (b) undialysed wafers

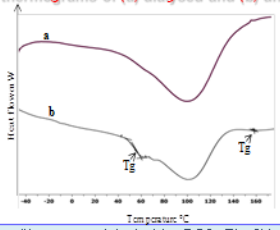

Multiple glass-transitions were detected by DSC (Fig 2b) after lyophilisation, indicating possible phase separation of protein in the undialysed CS-BSA wafer and/or metastable crystalline structures. No glass-transition was observed for the dialysed CS-BSA wafer (Fig 2a).

Fig 4. Mucoadhesion properties

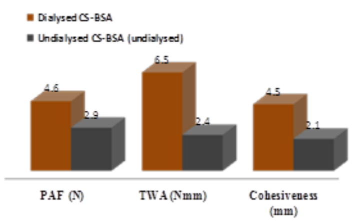

Fig 4 shows the *in-vitro* mucoadhesion characteristics of the wafers. Statistically significant differences ($p < 0.05$) were observed between the PAF, TWA and the cohesiveness of the wafers.

Fig. 3 XRD transmission diffractograms of BSA wafers

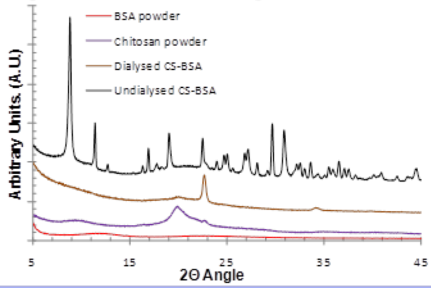

The XRD diffractogram in fig 3 showed crystalline sodium acetate for the undialysed CS-BSA wafer instead of an amorphous structure observed for the dialysed CS-BSA wafer.

Fig 5. *In vitro* release studies

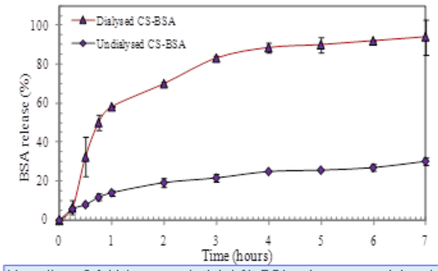

More than 3-fold increase in total % BSA release was determined from the dialysed wafer compared to the undialysed wafer (Fig 5). Competitive hydration rate and suppression of release by crystalline Sodium acetate could have accounted for this observation.

Percent drug loading capacities of 91.8 ± 4.2 % and 54.0 ± 5.4 % were observed for the dialysed and undialysed wafers respectively.. The differences in the performances of the wafers with respect to the examined characterisations could be attributed to the presence of excess acetic acid and crystalline sodium acetate which impacted negatively on the desired lyophilised quality of the undialysed wafers. The process of dialysis removes all excess acetic acid and the formed sodium acetate, thereby allowing for optimum drug loading, subsequent *in vitro* release and improved mucoadhesive properties.

Conclusion

Lyophilised chitosan based wafers have been developed for potential protein delivery via the buccal mucosa. Exhaustive dialysis as a process step is vital in achieving wafers with desired characteristics.

References

[1] S. Senel, G. Ikinci, S. Kas, A. Yousefi-Rad, M. F. Sargon, A. A. Hincal. "Chitosan films and hydrogels of chlorhexidine gluconate for oral mucosal delivery". *Int. J. Pharm.* 193,(2000) 197-203.
[2] M. R. Saboktakin, R. M. Tabatabaie, A. Maharramovb, M. A. Ramazanov "Development and in vitro evaluation of thiolated chitosan—Poly(methacrylic-acid) nanoparticles as a local mucoadhesive delivery system". *Int. J. Bio. Macromole.* 48, (2011)403-407.

Acknowledgments

This research is being supported by the Commonwealth Scholarship Commission, UK. The authors are grateful to Dr Ian Slipper for the XRD diffractograms

6. Published abstract M1144 (2011). *AAPS Journal*, 13 (S2)

Formulation and evaluation of lyophilised thiolated chitosan wafers for buccal mucosa delivery of proteins

M1144

I. Ayensu[1], J.C. Mitchell,[1] J.S. Boateng[1]
[1] University of Greenwich, School of Science, Chatham Maritime, Kent, UK, ME4 4TB
ai19@.gre.ac.uk

Objectives

1. To prepare lyophilised protein loaded chitosan-4 thioglycolic acid (CS-TGA) wafers
2. To evaluate the effect of annealing on the characteristics of the wafers for buccal mucosa delivery.

Materials and methods

- Synthesis, purification and sulfhydryl immobilization determination of CS-TGA(Fig 1).

- 6.5 g of 1 % w/v dialysed gel loaded with BSA as a model protein drug in a 2:1 CS-TGA: BSA ratio and 6.5 mg each of plasticizer (glycerol) and cryoprotectant (D-mannitol) was lyophilised based on a cycle developed with DSC (Fig. 2) with or without an annealing process.

Fig. 1 Synthesis, formulation & lyophilization

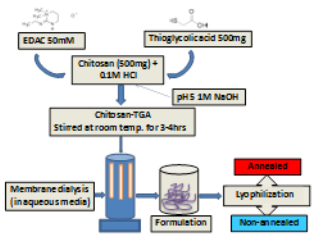

Fig. 2 Lyophilization cycles

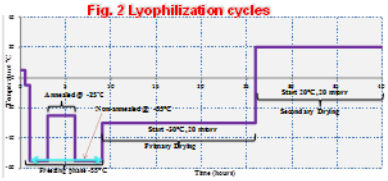

Lyophilized products were evaluated for surface morphology by SEM, drug loading capacity by Bradford's assay, % swelling ratio and % drug release in 0.1M PBS (pH = 6.8), texture analysis (*in-vitro* mucoadhesion using gelatine equilibrated with 2 % mucin solution as mucosal substrate) and moisture content by TGA.

Results and Discussion

Table 1. Characterisation of CS-BSA wafers

Formulation	Drug loading % (n=4, mean±SD)	Moisture content % (n=4, mean±SD)	Swelling capacity % (n=4, mean±SD)
Annealed CSTGA-BSA	94.6 ± 1.6	1.8 ± 0.1	482 ± 23.3
Non-Annealed CSTGA-BSA	88.8 ± 4.0	1.8 ± 0.4	434 ± 21.4

Fig. 4 *In vitro* release studies

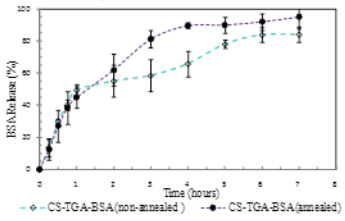

Table 1 summarises the characteristics of the lyophilised wafers. High drug loading capacities were obtained for both wafers with the annealed wafers showing higher loading. Residual moisture content was adequate due to large ice crystals that enhanced rapid sublimation. Statistically significant difference ($p < 0.003$) was however, observed between the % swelling capacities of the wafers.

The wafers obtained were of uniform mass and texture, elegant in appearance, flexible and tough with no visible cracks. The SEM micrographs (Fig. 3) showed wafers with porous interconnecting network of polymeric sponge-like circular pores, with closer pore size distribution which allowed for higher drug loading as well as release.

The cumulative % BSA release from the annealed and non-annealed wafers were 95.2 ± 7.3 % and 84.1 ± 4.9 % respectively (Fig. 4) This difference was also statistically significant ($p < 0.05$) though both wafers exhibited a controlled release profile typical of chitosan based formulations

The significant differences ($p < 0.05$) observed between the peak adhesive force-PAF, total work of adhesion-TWA and the cohesiveness (Fig. 5) of the annealed and non-annealed wafers were due to variation in the stability of water micro-porous structure.

The optimised characteristics make the annealed wafers suitable for easy application and potentially patient compliance. Work is underway investigating ex-vivo permeation as well as protein stability within the wafer by bio-analytical techniques.

Conclusion

A stable thiolated chitosan based system for potential protein delivery via buccal mucosa has been developed. Annealing, plasticisation and cryoprotection helped achieve lyophilised protein loaded chitosan-thioglycolic acid wafer with desired characteristics.

Fig. 3 Wafer morphology: SEM

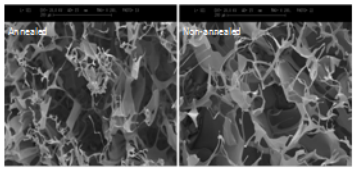

Fig. 5 Mucoadhesion properties

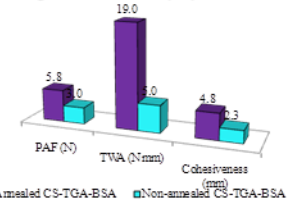

7. Published abstract # 42. *Journal of Pharmacy and Pharmacology/APS 2010*. 62 (10).

Freeze dried thiolated chitosan formulations for protein delivery via the buccal mucosa

I. Ayensu, J.C. Mitchell, J.S. Boateng.
School of Science, University of Greenwich at Medway, Chatham Maritime, Kent, UK, ME4 4TB

Introduction

The buccal mucosa has received increased attention in recent years for the delivery of protein and peptide based drugs, as an alternative to the currently used parenteral route [1]. Protein transport across the mucosa is limited by molecular size, hydrophobicity and low permeability of the membrane. However, thiolated chitosan derivatives have been identified for protein/peptide delivery across the buccal mucosa because of their mucoadhesive, penetration enhancing and peptidase inhibition properties [2]. This project aims to develop freeze dried thiolated chitosan formulations for protein drug delivery via the buccal mucosa and to determine the effectiveness of cryoprotection and annealing on the stability of the drug.

Materials & Methods

Chitosan-4-thiobutylamidine (C-TBA) was synthesized, purified and thiol content determined according to a method reported in literature by Langoth. *et. al., (2006)* [3]. Matrix formulations with C-TBA incorporating glutathione as enzyme inhibitor, glycerol as plasticizer, mannitol as cryoprotectant and bovine serum albumin (BSA) as a model protein drug [Table 1] were freeze-dried using a Virtis Advantage Freeze Dryer (Winchester, UK). A novel lyophilisation cycle incorporating an annealing process was developed based on preliminary thermal characterization by DSC.
The process involved freeze treatment from room temperature to -55°C (2 hours), annealing to -35°C (2 hours) and finally freezing back to -55°C (2 hours). The effect of the annealing process and cryoprotectant on the stability of the freeze dried protein formulation was evaluated using SEM, XRD and Raman spectroscopy.

Table 1. Matrix Formulations

	Form. A (mg/mL)	Form. B (mg/mL)	Form. C (mg/mL)
C-TBA	10.0	10.0	10.0
Glutathione	0.5	0.5	0.5
Glycerol	1.0	1.0	1.0
Mannitol	1.0	-	1.0
BSA	5.0	5.0	-

Results & Discussion

The thermal events observed from the DSC characterization of the formulation components were used to select the annealing temperature.
The annealing process employed during the freezing stage prevented premature crystallisation of mannitol and led to the growth of both solute crystals and ice crystals. These resulted in faster water vapour transport, shorter primary drying time and elegant porous wafers with high water absorption capacity.
In addition to acting as plasticizer, glycerol allowed the formulation to swell instead of instant disintegration when it came in contact with dissolution medium.
A high magnification SEM (Fig 1) showed porous, flexible and non brittle freeze dried wafers with wool-like spongy network which were morphologically stable.

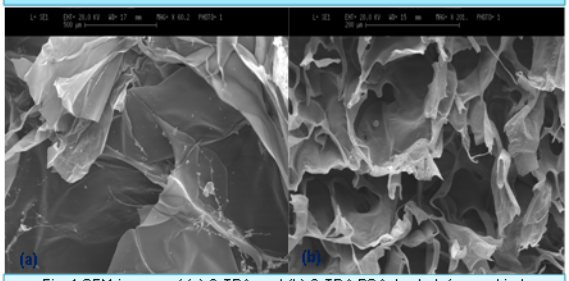

Fig. 1 SEM images of (a) C-TBA and (b) C-TBA-BSA loaded freeze-dried formulations

In fig.2, the XRD patterns in the 2θ range of 5-40° show the reduced intensity characteristic peaks of chitosan around 2θ = 10° and 20°. However the appearance of peaks around 2θ = 25° of the annealed freeze dried C-TBA-BSA and C-TBA formulations indicate the existence of amorphous structures, predicating the stability of the model protein drug (BSA) formulated with the cryoprotectant mannitol.

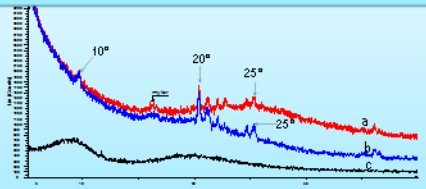

Fig. 2 XRD of BSA loaded freeze-dried formulation: (a) C-TBA-BSA (b) C-TBA and (c) BSA

The Raman vibrational spectra (Fig. 3) displayed the characteristic amide I (1653cm-1) band indicative of secondary structure with high α-helical content in the control BSA and the lyophilised C-BSA formulations. No significant changes in the stability of the model drug were observed in the annealed formulation. Further research is underway to determine the release profile and storage stability of the novel freeze dried protein formulations

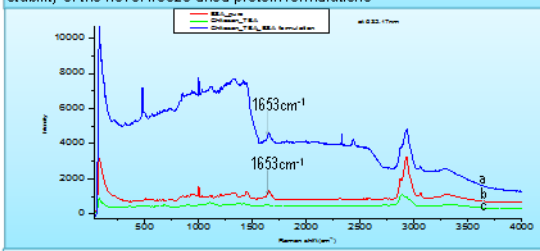

Fig. 3 Raman spectra of (a) C-TBA-BSA loaded freeze-dried wafer (b) Native BSA and (c) C-TBA wafer

Conclusion

A stable thiolated chitosan based system for potential protein delivery via buccal mucosa has been developed. Annealing and cryoprotection helped stabilise the freeze dried chitosan-4-thiobutylamidine protein formulation

Acknowledgments

This research is being supported by the Commonwealth Scholarship Commission, UK. The authors are grateful to Dr Ian Slipper for the SEM/ XRD determinations and Rajitha Hanarasinghe for the Raman data acquisition,

References

[1] Y. Sudhakar, K. Kuotsu, A.K. Bandyopadhyay. "Buccal bioadhesive drug delivery - A promising option for orally less efficient drugs". *J. Control. Rel.* **114**, (2006) 15–402.
[2] A. Bernkop-Schnurch, D. Guggi, Y. Pinter. Thiolated chitosans: development and in vitro evaluation of a mucoadhesive, permeation enhancing oral drug delivery system. *J. Control. Rel* **94**, (2004) 177-186.
[3] N. Langoth, H. Kahlbacher, G. Schoffmann, I. Schmerold, M Schuh, S. Franz, P. Kurka, A. Bernkop-Schnurch. Thiolated chitosans: design and *in vivo* evaluation of a mucoadhesive buccal peptide drug delivery system. *Pharm. Res* **23**, (2006) 573-579.

Contact details

Isaac Ayensu
School of Science (Grenville Building)
University of Greenwich at Medway

Central Avenue	**Tel: 020-8331-7570**
Chatham Maritime	**Fax: 020-8331-9805**
Kent, ME4 4TB	**E-mail: ai19.gre.ac.uk**

8. Published abstract W1470 (2010). *The AAPS Journal.* 12 (S2).

Novel lyophilization cycle development of chitosan based formulation for buccal delivery using paracetamol as a model drug

I. Ayensu[1], J.C. Mitchell,[1] J.S. Boateng[1]
[1] University of Greenwich, School of Science, Chatham Maritime, Kent, UK, ME4 4TB
j.s.boateng@gre.ac.uk

Purpose: To develop freeze dried chitosan formulations for buccal mucosa delivery and to determine the effects of plasticization and annealing on their physical properties.

Method: 1g of chitosan (medium molecular weight) was dissolved in 50ml of 1% acetic acid and the pH adjusted to 6.5 with 5M NaOH added drop wise. 50ml solutions comprising mannitol (10%) as cryoprotectant, glycerol (0-50%) as plasticizer and paracetamol (10%) as a model drug in deionised water were added to give homogeneous gels (1%) and stirred continuously at room temperature (1hour). The resulting gels were freeze-dried in a Virtis Advantage Freeze Dryer. Preliminary thermal characterization by DSC informed the selection of annealing temperature for the novel lyophilization cycle development. The process involved freeze treatment from room temperature to -55°C (2 hours), annealing to -35°C (2 hours) and finally freezing back to -55°C (2 hours). The wafers obtained were evaluated for flexibility, toughness, brittleness, residual water content by TGA and weighing on an analytical balance, micro-structure characterisation by SEM and hydration behaviour in dissolution medium.

Results: Unplasticised wafers were brittle, easily broken along fractured surface (fig. 1a) and instantaneously disintegrated upon contact with dissolution medium whiles high content plasticized wafers collapsed during lyophilization. Optimized concentration of glycerol (10%) however produced flexible, tough and non-brittle wafers (fig. 1b). Annealing facilitated the removal of stresses and softened crystallisable materials thereby improving toughness and reducing brittleness. The mean ($\pm$ *s.d*) residual water content of optimized wafers by TGA and weighing methods was 1.9% ($\pm$ 0.18) which is consistent with literature optimum range of 1.7% to 4%. The SEM evaluation showed micrographs of plasticized and annealed wafers with porous network which were morphologically stable (fig. 2).

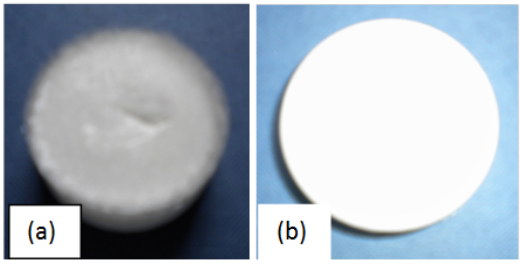

Figure 1 Digital photographs of chitosan wafers

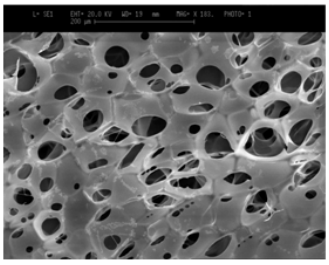

Figure 2 SEM of freeze-dried chitosan wafer.

In addition to plasticizing, glycerol allowed the formulation to swell instead of instantly disintegrating when in contact with dissolution medium. Work is underway for investigating the muco-adhesive properties of the freeze-dried chitosan wafers and drug stability within the formulation.

Conclusion: Stable freeze-dried chitosan wafers have been developed. Plasticization and annealing helped to achieve the desirable physical characteristics of these wafers.